UNIVERSIDAD DE SANTIAGO DE COMPOSTELA

FACULTAD DE FARMACIA

Departamento de Farmacia y Tecnología Farmacéutica

Lentes de contacto y sistemas trampa sintetizados por moldeado molecular para captura selectiva y liberación controlada de moléculas activas

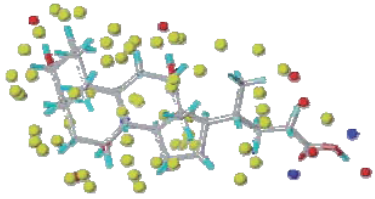

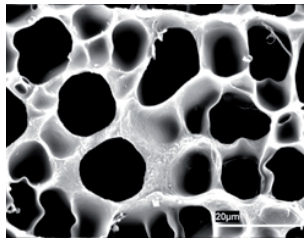

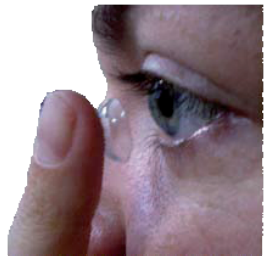

Fernando Yáñez Gómez

Santiago de Compostela, 2010

Llegado este momento, no puedo dejar pasar la oportunidad de expresar mi más sincero y profundo agradecimiento a todas y cada una de las personas que me han ayudado, apoyado y animado durante estos años para que esta Tesis Doctoral pasara de ser un sueño a convertirse en una realidad.

Me gustaría mostrar mi especial agradecimiento a mis directores de Tesis, *Carmen Alvarez Lorenzo y Angel Concheiro Nine*, quienes con su constante apoyo, dedicación, paciencia, buenos consejos y especial sentido del humor, me han ayudado en la realización de este trabajo. No puedo más que mostrarles admiración y agradecimiento.

Al profesor *Ramón Martínez Pacheco* le agradezco sus valiosos consejos y su apoyo incondicional durante estos años, al profesor *José Luis Gómez Amoza* su proximidad, su buena disposición para ayudarme y su inestimable contribución al análisis de los datos, y al profesor *Francisco Otero Espinar* que me haya iniciado en el apasionante mundo de la Tecnología Farmacéutica mostrándome siempre su amistad desinteresada.

Al resto de profesores del Departamento de Tecnología Farmacéutica, *Begoña, Loli, Carmucha y Alejandro*, quienes se mostraron permanentemente accesibles ante cualquier duda o problema que me surgiera durante estos últimos cuatro años, y especialmente, a *Chelo, Mariana, Pepe y Juan*, que contribuyen a crear un excelente ambiente de trabajo.

Me gustaría hacer una especial mención a *Rafael Barreiro, Marcos Mayo, Felipe Alvarez, Carmen Rodríguez-Tenreiro y Ana Rodríguez*, que me ayudaron en mis inicios en el laboratorio en la realización de la tesina y me brindaron su amistad dentro y fuera del laboratorio.

A mis compañeros del Departamento de Tecnología Farmacéutica, con los que he compartido innumerables horas en el laboratorio que, gracias a ellos, siempre han sido llevaderas y que, por una razón o por otra nunca olvidaré, *Manolo, Luis, Laura, Fabio, Eva, Fani, Maria José, Julia, Marga, Magdalena, Fernando, Andreza, Mariajo, Clara, Bárbara, Álvaro, Elena, Ana Puga, Lourdes, Alberto, Norberto, Luis y Maria José*. Mención especial merecen mis compañeras de sala, *Ana Rey, Lidia y Patricia*, que durante estos últimos años han compartido numerosas horas a mi lado, alegrándome cada día con sus conversaciones, comentarios y, sobre todo, amistad.

Al personal de los Servicios Generales de la Universidad de Santiago de Compostela (CACTUS), especialmente, a *Ramiro, Merche, Raquel y Maria José* del Servicio de Microscopía Electrónica, a los que tuve que recurrir en numerosas ocasiones y que, siempre se esforzaron y me atendieron con la mejor de las sonrisas.

Me gustaría agradecer también, tanto por el trato personal como por la atención científica recibida durante mis meses de estancia en el extranjero a lo largo del período de realización de esta Tesis, a todos los integrantes de los distintos centros en los que he estado, especialmente, a *Stefaan De Smedt* y *Koen Raemdonck* del Department of Pharmaceutics de la Universidad de Gante (Bélgica), a *Sergey Pilestky* e *Iva Chianella* del HealthCare Center de la Universidad de Cranfield (Reino Unido), y a *Herminio De Sousa, Mara Braga y Joao Maia* del Departamento de Ingeniería Química de la Universidad de Coimbra (Portugal).

A todos los estudiantes ERASMUS y de doctorado que han pasado por nuestro laboratorio durante estos años y que han contribuido a mi enriquecimiento personal y profesional.

A mi amigo y compañero *Vicente Yaziji*, por estos años de convivencia y amistad.

A mis compañeros de la Residencia Universitaria Tte. General Barroso, especialmente a *Jose, Santi, Chis y Gonzalo*, que me brindaron su compañerismo y amistad y con los que comparto infinidad de anécdotas que no podré olvidar a lo largo de mi vida.

A mis amigos, *Miki, Luís, Pepote, Sergio, Juan, María del Mar, Caty y Lluch* quienes han estado conmigo desde nuestros inicios en el Colegio y que, a pesar de la distancia que nos separa, continúan estándolo.

A *Marta*, que siempre ha estado a mi lado en este último año, escuchándome, comprendiéndome y ayudándome a seguir hacia delante, con un constante e incondicional apoyo.

A mi familia, mi *Abuela Pilar* y mi *Abuela Lina*, mis tíos *Marta, Ricardo, Charo, Luís, María, Belén, Paco, Lola, Jorge, Mar y Juan Carlos*, mis primos, *Ricardo, Luís, Carlos, Bea, Carola, Jorge, Loreto y Pablo*, por sus constantes muestras de cariño y afecto durante todos estos años en Galicia.

A mis padres, *José y Bea*, a los que les debo absolutamente todo en esta vida, y a mis hermanos, *Jose*, *Santi* y *Beiña*, que siempre me han apoyado y ayudado en la consecución de mis metas.

Finalmente, quiero dejar constancia de mi agradecimiento al MICINN por la concesión de una beca de FPI que me ha permitido realizar mi Tesis Doctoral y disfrutar de tres estancias en centros de investigación extranjeros.

A todos, **MUCHAS GRACIAS !!**

CARMEN ALVAREZ LORENZO, PROFESORA TITULAR, Y ANGEL CONCHEIRO NINE, CATEDRÁTICO DE FARMACIA Y TECNOLOGÍA FARMACÉUTICA, DE LA UNIVERSIDAD DE SANTIAGO DE COMPOSTELA,

INFORMAMOS: Que la presente memoria titulada "Lentes de contacto y sistemas trampa sintetizados por moldeado molecular para captura selectiva y liberación controlada de moléculas activas" ha sido realizada por el Licenciado en Farmacia D. Fernando Yánez Gómez bajo nuestra dirección en el Departamento de Farmacia y Tecnología Farmacéutica y, hallándose concluída, autorizamos su presentación a fin de que pueda ser juzgada por el tribunal correspondiente.

Y, para que conste, expedimos y firmamos el present informe en Santiago de Compostela a 15 de Junio de 2010.

C. Alvarez Lorenzo A. Concheiro Nine

ÍNDICE

Introducción

1. INTRODUCCIÓN

1.1. Administración tópica ocular de fármacos

Además de los problemas de visión que se manifiestan cuando la córnea y el cristalino no son capaces de enfocar la imagen en la retina, en las estructuras oculares se pueden producir lesiones y enfermedades diversas que están relacionadas con procesos infecciosos, alérgicos, vasculares o degenerativos y que requieren tratamiento farmacológico (Reddy y Ganesan, 1996; Myles y col., 2005).

Las barreras anatómicas y los mecanismos de defensa del ojo dificultan el acceso de los fármacos a los tejidos diana cuando se administran por vía sistémica o por vía tópica (Kearns y Williams, 2009; Velpandian, 2009). La eficacia de la administración sistémica se ve limitada por la barrera hemato-ocular (sangre-humor acuoso, sangre-retina y sangre-humor vítreo) y sólo conduce a buenos

resultados en procesos que afectan al segmento posterior (humor vítreo, esclerótida, mácula, retina y nervio óptico) (Plazonnet y col. 2003; Gaudana y col., 2009). La aplicación tópica de fármacos o, en situaciones de especial gravedad, la administración periocular o intraocular (intracameral o intravítrea) permite tratar patologías que afectan a estructuras del segmento anterior como la pupila, la córnea, el iris, el cuerpo ciliar, el humor acuoso y el cristalino (Lang, 1995; Sander y col., 2003; Hughes y col., 2005; Kearns y Williams, 2009).

Por vía tópica se administran de manera cómoda, eficaz y segura antimicrobianos, antivirales, beta-bloqueantes adrenérgicos, mióticos, midriáticos, anestésicos locales, antiinflamatorios y antialérgicos. El fármaco, una vez aplicado sobre la superficie del ojo, pasa a través de la córnea hacia el humor acuoso y desencadena la respuesta terapéutica, o bien atraviesa la conjuntiva dando lugar a una absorción que es mayoritariamente "improductiva" (figura 1.1). La cantidad de fármaco que penetra en la córnea depende de la permeabilidad del epitelio, del tiempo de permanencia en el área precorneal y de la dinámica del fluido lacrimal (Zhu y Chauhan, 2005). Las bombas de eflujo pueden interferir negativamente en la absorción (Gaudana y col., 2009). Cuando se acude al procedimiento habitual de administración de gotas oftálmicas, se vierten 30 µL en cada aplicación. Como consecuencia del parpadeo, el ojo sólo puede alojar unos 10 µL de fluido lacrimal (Plazonnet y col., 2003), que se renuevan cada minuto en un 10-20%, lo que conduce a que la disolución de fármaco se elimine rápidamente del área precorneal (Tomlinson y Khanal, 2005). Este eficaz drenaje nasolacrimal es determinante para que se produzca una considerable absorción sistémica (Robinson, 1989). En su conjunto, la incidencia de estos mecanismos determina que la penetración en las estructuras oculares se limite al 1-10% de la dosis (Singh y Shah, 1999). Por ejemplo, cuando la pilocarpina se administra en forma de colirio, la eliminación del área precorneal es 100 veces más rápida que la penetración del fármaco a través de la cornea (Robinson, 1989). Para paliar este

inconveniente se suelen efectuar dos aplicaciones de pequeño volumen (5-10 μL) separadas por un intervalo de 5 minutos, reproduciendo esta secuencia varias veces al día durante todo el tratamiento (Wilson, 2004). Esta administración en pulsos tiene el inconveniente de que da lugar a importantes fluctuaciones en la concentración ocular de fármaco, con los consiguientes riesgos de que se manifiesten efectos colaterales. Por lo tanto, el diseño de sistemas de liberación que proporcionen una adecuada biodisponibilidad ocular y que resulten cómodos y seguros para los pacientes sigue representando un importante desafío y constituye un área de investigación de indudable interés (Reddy y Ganesan, 1996; Felt y col., 2002; Plazonnet y col., 2003; Myles y col., 2005).

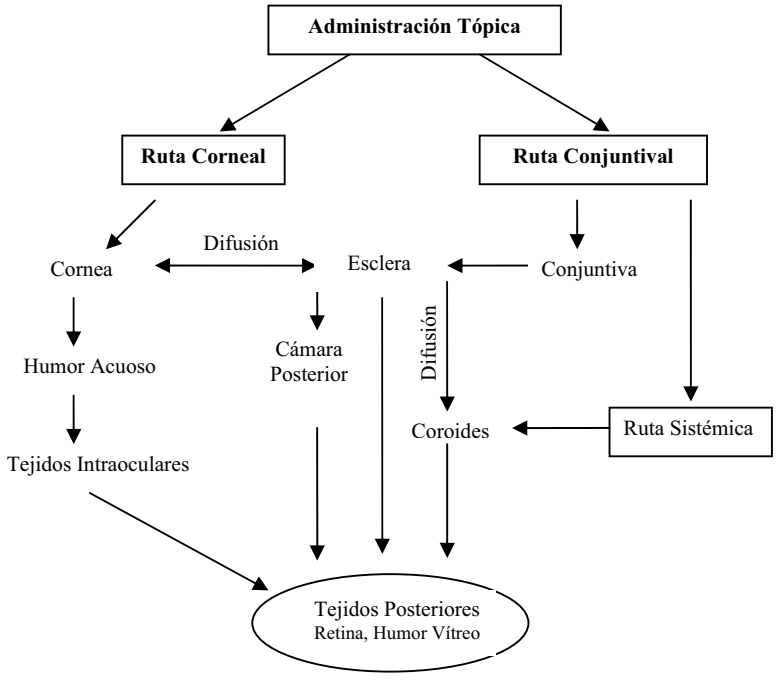

***Figura 1.1**. Rutas de penetración de los fármacos que se administran por vía tópica ocular (Hughes y col., 2005).*

1.2. Prolongación de la permanencia de los fármacos en el área precorneal: aproximaciones tecnológicas

Para incrementar el tiempo de permanencia del fármaco en el área precorneal y mejorar la biodisponibilidad ocular, se puede acudir al uso de disoluciones viscosas mucoadhesivas, dispersiones coloidales o insertos poliméricos (Felt y col., 2002; Davis y col., 2004; Ludwig, 2005; Mainardes y col., 2005; Mundada y Avari, 2009; Nagarwal y col., 2009). Aunque no resulta fácil llegar a conclusiones claras a partir de la información disponible, dada la dificultad que encierra comparar datos obtenidos por procedimientos de evaluación que no están estandarizados, parece claro que algunos de estos sistemas aportan mejoras significativas (Aqil, 2006).

La viscosidad de las lágrimas oscila entre 1.05 y 5.97 cPs (Pandit y col., 1999) y se ha observado que el tiempo de contacto corneal de las disoluciones oftálmicas se incrementa progresivamente a medida que la viscosidad aumenta hasta 20 cPs. Por encima de este valor, el estímulo de los reflejos de lagrimeo y parpadeo restaura rápidamente la viscosidad original (Wilson, 2004). Las mejoras en la biodisponibilidad ocular que se producen como consecuencia del incremento del tiempo de permanencia de la formulación en el área precorneal, permiten reducir la frecuencia de dosificación. Como agentes viscosizantes se pueden utilizar polímeros biocompatibles, como el alcohol polivinílico (PVA), la polivinilpirrolidona (PVP), el polietilenglicol (PEG), el ácido poliacrílico (PAA) y diversos derivados de la celulosa (Sintzel y col., 1996; Pandit y col., 1999; Felt y col., 2002; Davis y col., 2004; Ludwig, 2005; Aqil, 2006). También se ha propuesto el uso de otros polímeros que dan lugar a disoluciones que adquieren consistencia semisólida cuando entran en contacto con la superficie del ojo, y que combinan una fácil administración con un tiempo prolongado de permanencia en al área precorneal. La gelificación *in situ* es el resultado de los cambios en la conformación de las cadenas del polímero producidas como respuesta a

modificaciones de la temperatura, el pH o la concentración de iones en el área precorneal (Vadnere y col., 1984; Zignani y col., 1995; Kaur y Kanwar, 2002; Sultana y col., 2004). Tomando esta idea como punto de partida, se han desarrollado formulaciones a base de goma gelano y alginatos para cesión sostenida de timolol (Timoptic®; Schenker y Silver, 2000) y de PAA y éteres de celulosa para prolongar la liberación de ofloxacino (Srividya y col., 2001). Algunos de estos polímeros son capaces, además, de interaccionar con la mucina conjuntival estableciendo enlaces no covalentes. De esta manera, se prolonga el tiempo contacto de la formulación con la superficie corneal hasta que se renueva de la capa de mucina. Los polímeros con grupos ácido carboxílico, hidroxilo, amida o sulfato pueden interaccionar electrostáticamente o por puentes de hidrógeno con las glucoproteínas del fluido lacrimal. En los últimos años, se han publicado numerosas revisiones sobre materiales mucoadhesivos y su aplicación como componentes de sistemas de liberación ocular de fármacos, en las que se analizan en profundidad sus ventajas y sus limitaciones (Herrero-Vanrell y col., 2000; Ludwig, 2005; Mayol y col., 2008; Shen y col., 2009). El mayor inconveniente de las formas mucoadhesivas es el efecto de visión borrosa y la sensación de pegajosidad que producen.

También se puede incrementar el tiempo de permanencia en el área precorneal administrando los fármacos en suspensión. Tras la instilación, las micropartículas se retienen en el saco conjuntival y el fármaco se disuelve lentamente en el fluido lacrimal (Zimmer y Kreuter, 1995). Para que no se produzca sensación de cuerpo extraño ni irritación ocular, el tamaño de las partículas no debe superar las 10 μm. Los liposomas, las nanopartículas, las nanocápsulas y las microesferas han recibido también una considerable atención (Calvo y col., 1996; Gavini y col., 2004; Budai y col., 2007; Liu y col., 2008; Sahoo y col., 2008; Barbu y col., 2009; Civiale y col., 2009; Li y col., 2009; Nagarwal y col., 2009). Los liposomas promueven el contacto con el epitelio y mejoran la penetración transcorneal

(Ebrahim y col., 2005; Mainardes y col., 2005). Las nanopartículas y las nanocápsulas pueden penetrar en la cornea y liberar el fármaco en el humor acuoso (Alonso, 2004; Diebold y col., 2007). Los niosomas -partículas esféricas de 0,1-2 μm de diámetro con una cavidad central acuosa rodeada por una o más capas de lípidos anfifílicos- y las nanoemulsiones resultan fáciles de preparar y son más estables (Kaur y Kanwar, 2002; Vandamme, 2002; Aggarwal y Kaur, 2005; Chan y col., 2007; Kapoor y Chauhan, 2008). En su conjunto estos sistemas ofrecen interesantes perspectivas, pero su desarrollo se ve limitado por la complejidad de los procedimientos de elaboración y por su inestabilidad frente a la esterilización (Felt y col., 2002).

Los implantes sólidos o semisólidos responden al objetivo de combinar una dosificación exacta con una liberación prolongada. El tamaño y la forma deben ser apropiados para que se puedan colocar bajo el párpado inferior o, más raramente, bajo el párpado superior o sobre la cornea. Se suelen clasificar en tres categorías: solubles, bioerosionables e insolubles (Felt y col., 2002). La cesión del fármaco desde los implantes solubles tiene lugar en dos etapas: i) penetración del fluido lacrimal en el sistema y liberación rápida del fármaco y ii) liberación lenta, una vez que se forma una película superficial de gel. Si los componentes se solubilizan rápidamente se puede producir un efecto de visión borrosa (Weyenberg y col., 2004). Las vendas de colágeno escleral porcino o de tejido coriónico bovino (Willoughby y col., 2002) y los minicomprimidos que se preparan por moldeado, extrusión o compresión de mezclas fármaco-polímero (Verestiuc y col., 2006) son ejemplos de insertos solubles. Los polímeros bioerosionables (derivados de gelatina reticulada, poliésteres o PLA) se utilizan para preparar implantes que actúan como reservorios de fármaco libre o unido a través de enlaces lábiles (Heller, 2005; Kim y col., 2008). La velocidad de cesión se regula por la degradación del polímero o por la rotura de los enlaces fármaco-polímero. Los perfiles de cesión que se consiguen con los insertos biodegradables

suelen ser muy variables, debido a la influencia de las condiciones del entorno fisiológico sobre la erosión. Los insertos de 60 y 700 μg de dexametasona Surodex® (Seah y col., 2005) y Posurdex® (Kuppermann y col., 2007) a base de PLGA forman parte de este grupo. El primer inserto insoluble que llegó al mercado fue el Ocusert®, diseñado para liberar pilocarpina durante 7 días. Otros implantes insolubles son el Vitrasert® (Bourges y col., 2006) constituido por polímeros de EVA y PVA que controlan la liberación de ganciclovir, y el Retisert® (Jaffe y col., 2006) constituido por PVA y silicona, que se comercializó para tratar la uveitis crónica no infecciosa con fluocinolona. A pesar de su indudable atractivo, la utilidad de los insertos insolubles se ve limitada por la incomodidad de su manejo, la sensación de cuerpo extraño que producen y la frecuente expulsión accidental (Sintzel y col., 1996). Estos inconvenientes se pueden evitar acudiendo al uso de lentes de contacto medicadas.

1.3. Lentes de contacto como dispositivos terapéuticos

Desde que Leonardo Da Vinci construyó, en el siglo XVI, el primer dispositivo considerado como precursor de las lentes de contacto, se llevaron a cabo numerosos intentos para adaptar lentes al ojo humano con el fin de proteger su superficie y corregir la ametropía, que no fructificaron hasta bien entrado el siglo XX (Munoa-Roiz y Aramendia-Salvador, 2006). Para construir las primeras lentes se utilizó el vidrio, que impide el intercambio natural de oxígeno y nutrientes y no puede permanecer sobre la córnea más allá de unos cuantos minutos, por lo que se hizo necesario buscar materiales alternativos. La generalización del uso de las lentes de contacto sólo fue posible una vez que se dispuso de materiales, como el polimetil metacrilato, PMMA, sintetizado en 1936, y el poli (2-hidroxietil metacrilato), PHEMA, sintetizado en 1954 (Witcherle y Lim, 1960; McMahon y Zadnik, 2000; Munoa-Roiz y Aramendia-Salvador, 2006). Estos materiales combinan una elevada claridad óptica y unas buenas

propiedades mecánicas con una baja densidad y una suficiente permeabilidad al oxígeno (Nicolson y Vogt, 2001; Yamauchi, 2001). Dado que las lentes de contacto están consideradas por las agencias regulatorias como productos sanitarios, los materiales que se utilizan en su fabricación tienen que responder a estrictos estándares de calidad y seguridad, relacionados con propiedades como la biocompatibilidad, la resistencia mecánica, la transparencia a la luz y la tendencia a adsorber componentes del fluido lacrimal. Además, tienen que ser adaptables a los procedimientos de fabricación industrial y dar lugar a lentes fáciles de manejar e insertar.

En función de la composición química y las propiedades físicas, las lentes de contacto se clasifican en dos grandes grupos: hidrofílicas ("filcon") e hidrofóbicas ("focon") (tabla 1.1). Las lentes de contacto duras hidrofóbicas presentan una excelente transparencia, pero su bajo contenido en agua (< 10% p/p) determina que un porcentaje significativo de usuarios las toleren mal. Las lentes de contacto blandas son hidrogeles flexibles y pueden absorber grandes cantidades de agua (> 35% p/p) en la que se puede disolver el oxígeno y difundir hacia la córnea. La excelente biocompatibilidad de algunas lentes de contacto blandas hizo posible que, a finales de los años 70 del pasado siglo, se aprobase su uso para periodos de tiempo más prolongados (7 días). El desarrollo en 1979 de lentes duras altamente permeables sólo fue posible cuando se introdujeron nuevos materiales siliconados que evitan la hipoxia inducida por las lentes durante el tiempo que el usuario permanece con los ojos cerrados (McMahon y Zadnik, 2000; Nicolson y Vogt, 2001). La silicona presenta una elevada permeabilidad al oxígeno debido al elevado volumen molecular del grupo -$Si(CH_3)_2$-O- y a la movilidad de las cadenas que forman el entramado polimérico (Tighe, 2000; Nicolson y Vogt, 2001). Sin embargo, el elastómero de silicona es muy hidrofóbico (si no está tratado en su superficie) y sus propiedades mecánicas son deficientes. Para conseguir lentes de contacto con alta permeabilidad al oxígeno, los iones y el agua

se combinaron elastómeros de silicona con monómeros más hidrofílicos como HEMA, N-vinilpirrolidona (NVP) o ácido metacrílico (MAA), que además hacen más fácil el movimiento de las lentes sobre el ojo (Nicolson y Vogt, 2001; Donshik, 2003).

Clasificación	Grupo	Descripción	Ejemplos (Polímeros y nombre comercial)
Hidrofílica	I	No iónica[a], bajo contenido en agua	Crofilcon A (MMA-GMA; CSI® 38), Lotrafilcon A (DMAA-silicona; Focus®, Night & Day), Polimacon (HEMA-NVP-CMA; Optima® FW y Plano T)
	II	No iónica[a], alto contenido en agua	Afilcon A (HEMA-NVP-CMA; SoftLens® 66), Omafilcon (HEMA-fosforilcolina; Pronuclear Compatibles®)
	III	Iónica[b], bajo contenido en agua	Balafilcon A (silicona-NVP; PureVision®)
	IV	Iónica[b], alto contenido en agua	Etafilcon A (HEMA-MAA; Acuvue®2), metafilcon (HEMA-MAA; Kontour®55), vifilcon A (HEMA-MAA-NVP; Focus® Monthly)
Hidrofóbica	I	Sin silicona y sin fluor	Porofocon A (CAB; RX56), arfocon (t-butilestireno; Airlens)
	II	Con silicona y sin fluor	Pasifocon (Acrilato de silicona; Boston® II y Boston® IV)
	III	Con silicona y con fluor	Itrafluorocon A(FSC;Equalens®), tisilfocon A (FSC; Menicon ZTM), paflucon (FSC; Fluoroperm®), flusifocon (FSC; Fluorex®), enflucon B (FSC; Boston® IV)
	IV	Con fluor y sin silicona	Fluorofocon A (PPFE; fluoropolímero 3M)

[a] Grado de ionización <1% a pH 7,2; [b] Grado de ionización >1% a pH 7,2

CAB = acetato butirato de celulosa; **CMA** = ciclohexilmetacrilato; **DMAA** = N,N-dimetilacrilamida; **FSC** = acrilato de fluorosiloxano; **GMA** = glicerol metacrilato; **HEMA** = hidroxietilmetacrilato; **MAA** = ácido metacrílico; **MMA** = metil metacrilato; **NVP** = N-vinil pirrolidona; **PPFE** = poliperfluoroeter.

Tabla 1.1. *Clasificación de las lentes de contacto (FDA 1994). Todas las lentes que se citan están comercializadas o se han ensayado para uso terapéutico (Shah y col., 2003; Karlgard y col. 2003b).*

El número de personas que utilizan de manera habitual lentes de contacto se ha estimado recientemente en 125 millones (82% lentes de contacto blandas, 16% lentes duras permeables al oxígeno y 2% lentes duras convencionales), y se espera que en pocos años llegue a superar al de usuarios de gafas (Hiratani y col., 2002; Barr, 2005).

Aunque las lentes de contacto se usan principalmente para corregir problemas de visión, sus aplicaciones en terapéutica están cobrando un interés creciente. De hecho, la FDA las clasifica en función de su uso previsto en los grupos siguientes: i) no terapéuticas para la corrección de la ametropia, afaquia y presbicia; ii) de uso especial para el tratamiento del queratocono; y iii) terapéuticas para el tratamiento de una amplia variedad de enfermedades oftálmicas refractarias a otras terapias (Shah y col., 2003).

Los objetivos que se persiguen con el uso de lentes de contacto terapéuticas son muy diversos: aliviar el dolor ocular, promover la curación de heridas corneales, proporcionar protección y apoyo mecánico, mantener la hidratación del epitelio corneal y controlar la cesión de fármacos (Lim y col., 2001; Kanpolat y Ucakhan, 2003; Mely, 2004; Bendoriene y Vogt, 2006; Steele, 2006; DeNaeyer, 2008). Se cuenta con abundante información sobre la utilidad de las lentes para cubrir las cuatro primeras aplicaciones (McMahon y Zadnik, 2000; Lim y col., 2001; Kanpolat y Ucakhan, 2003; Shah y col., 2003; Mely, 2004; Silbert, 2006), pero su uso como sistemas de liberación de medicamentos es poco frecuente aunque ya se dispone de información que demuestra su potencial terapéutico (Krejci y col., 1975; Silbert, 1996; Zegans y col., 2002; Donshik, 2003; Wong y col., 2003; Gulsen y Chauhan, 2004; Mely, 2004; Dart y col., 2008; Gaudana y col., 2009; Stapleton y col., 2008; Xinming y col., 2008; Kearns y Williams, 2009; Martin y col., 2009; Por y col., 2009).

1.3.1. Lentes de contacto convencionales como sistemas de liberación de medicamentos.

1.3.1.1. Interés terapéutico

En 1886, Galezowski utilizó discos de gelatina cargados con cocaína para prevenir las complicaciones asociadas a la cirugía de cataratas (Galezowski, 1886; Mely, 2004) pero la primera prueba relevante de la utilidad de las lentes de contacto como sistemas de liberación de medicamentos no se produjo hasta después de la introducción del pHEMA (Sedlacek, 1965; Gasset y Kaufman, 1970). Las lentes comerciales se pueden cargar con fármacos i) por inmersión en una disolución concentrada de fármaco (Sedlacek, 1965; Waltman y Kaufman, 1970; Hillman, 1974; Ruben y Watkins, 1975; Marmion y Jain, 1976; Hehl y col., 1999; Peterson y col., 2006; Schrader y col., 2006), ii) vertiendo un pequeño volumen de la disolución de fármaco en su concavidad inmediatamente antes de colocarlas en el ojo, o iii) instilando gotas de colirio sobre su superficie una vez insertadas (Hull y col., 1974; Matoba y McCulley, 1985; Jain, 1988; Rootman y col., 1992; Sano y col., 1996; Rubinstein y Evans, 1997; Bourlais y col., 1998). El fármaco incorporado a las lentillas por cualquiera de estos procedimientos se cede al fluido lacrimal post-lente y permanece retenido entre la córnea y la lente durante un periodo de tiempo relativamente prolongado (figura 1.2). La superficie externa se seca entre sucesivos parpadeos, lo que determina que la cantidad de fármaco que difunde al fluido lacrimal sea cinco veces inferior que la que se cede hacia el epitelio corneal (Li y Chauhan, 2006). Esto explica que con las lentes de contacto medicadas se consigan mejoras muy notables en la biodisponibilidad ocular y en la respuesta farmacológica (Waltman y Kaufman, 1970; Hull y col., 1974; Matoba y McCulley, 1985; Vandorselaer y col., 2001) y que resulten eficaces en ciertas situaciones clínicas (inflamación del segmento anterior del ojo, glaucoma de ángulo cerrado, infecciones) en las que se requieren concentraciones

intraoculares elevadas. En algunos casos, el uso de lentes de contacto medicadas permite incluso reducir la dosis terapéutica (Li y Chauhan, 2006).

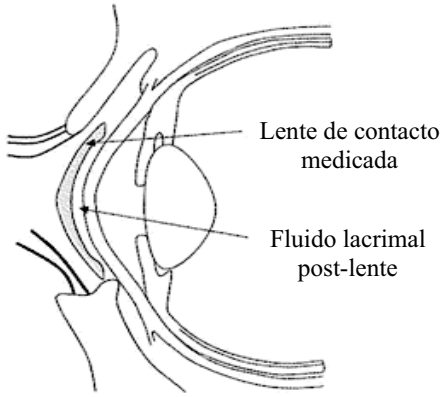

***Figura 1.2**. Cesión de un fármaco a partir de una lente de contacto medicada. El fármaco difunde desde el entramado polimérico y alcanza el fluido lacrimal post-lente, desde el que penetra en la córnea.*

1.3.1.2. Carga y cesión de fármacos

Los fármacos penetran en las lentes hidrofílicas a una velocidad dependiente del tamaño de malla de la red polimérica (que está condicionado a su vez por el grado de reticulación y el contenido en agua), del tamaño de la molécula del fármaco y de la concentración en la disolución de carga (Refojo y col., 1983). En general, la captación de fármaco por lentes de contacto aumenta a medida que transcurre el tiempo de inmersión, alcanzando un máximo al cabo de 30-60 minutos, si bien en algunos casos, pueden ser necesarias 24 horas para que se alcance la saturación (400-500 μg de pilocarpina en lentes Sauflon) (Podos y col., 1972; Hillman, 1974; Hsiue y col., 2001). La distribución uniforme del fármaco en el seno del entramado polimérico es determinante para la eficacia de la lente como sistema de liberación. Si está homogéneamente distribuido, se puede conseguir que la lente actúe como reservorio, reponiendo fármaco hacia la superficie a medida que se va cediendo, con lo que el proceso resulta más

sostenido y reproducible (Jain, 1988; Warlen y col., 1992; Lesher y Gunderson, 1993; Karlgard y col., 2003; Dracopoulos y col., 2005; Winterton y col., 2007). Esto explica las mejoras que se consiguen instilando colirios de pilocarpina y diclofenaco sobre lentes convencionales ya insertadas (Kaufman y col., 1971; Salz y col., 1994). La aplicación de lentes de contacto precargadas por inmersión en disoluciones de agentes antimicrobianos (antifúngicos, aminoglucósidos y fluoroquinolonas) también da lugar a mejoras muy importantes en la biodisponibilidad ocular, lo que convierte esta práctica en una alternativa a la inyección subconjuntival (Jain, 1988; Hehl y col., 1999; Tian y col., 2001a, 2001b; Pinilla-Lozano y col., 2006a, 2006b; Anderson y col., 2009). En un estudio llevado a cabo en pacientes sometidos a cirugía de cataratas, casi todos los pacientes a los que se prescribió el uso de lentes de contacto cargadas con ofloxacino o ciprofloxacino durante 4-5 horas antes de la operación, presentaron en el momento de la intervención concentraciones de fármaco en humor acuoso superiores a la concentración mínima inhibitoria ($MIC_{90\%}$) del *Staphylococcus epidermidis* (Hehl y col., 1999). Cuando se aplicó el protocolo convencional de administración de colirios, sólo el 65% de los pacientes tratados con ofloxacino y el 41% de los tratados con ciprofloxacino alcanzaron niveles similares de fármaco. No se observaron erosiones corneales durante la utilización de las lentes, por lo que los buenos resultados obtenidos se justifican por el papel de las lentes como reservorio y por los incrementos en la hidratación y la permeabilidad epitelial derivados de la ligera hipoxia corneal que producen.

En un estudio reciente, se evaluó la capacidad de carga y cesión de ciprofloxacino a partir de seis variedades de lentes de silicona: Balafilcon A (PureVision, Bausch & Lomb), Comfilcon A (Biofinity, CooperVision,), Galifilcon A (Acuvue Advance, Johnson & Johnson), Lotrafilcon A (Night and Day, CIBA Vision), Lotrafilcon B (O2Optix, CIBA Vision) y Senofilcon A (Acuvue OASYS, Johnson & Johnson) y de tres lentes de contacto blandas:

Alfafilcon A (SoftLens 66, Bausch & Lomb), Etafilcon A (Acuvue2, Johnson & Johnson) y Polimacon (SoftLens38, Bausch & Lomb) (Hui y col., 2008). Las lentes se cargaron por inmersión en una disolución de fármaco al 0,3 % (pH 4) alcanzándose el equilibrio en 3 horas. A pH 7,4 todas las lentes, salvo las Etafilcon A y Polimacon que requirieron 25 minutos, cedieron la totalidad del fármaco cargado al cabo de 10-15 minutos. También se observó que las lentes blandas cargaron y cedieron cantidades de ciprofloxacino sensiblemente mayores que las lentes de silicona. Las lentes Etafilcon A mostraron una ligera precipitación durante la carga de ciprofloxacino y una completa opacificación tras el ensayo de cesión. También se observaron fenómenos de precipitación en las lentes Alfafilcón A y Polimacon cuando se encontraban en el medio de cesión. Las restantes se mantuvieron transparentes hasta el final del ensayo. Dado que la MIC_{90} de la mayoría de los patógenos oculares se sitúa entre $2{,}5 \cdot 10^{-4}$ y $3{,}2 \cdot 10^{-2}$ mg/ml (Oliveira y col., 2007), para alcanzar concentraciones eficaces frente a los patógenos más resistentes cada lente debe ser capaz de ceder 0,064 mg (Hui y col., 2008). Por lo tanto, los perfiles de cesión resutaron adecuados para tratar la infección en todos los casos salvo en el de las lentes Lotrafilcon A, Lotrafilcon B, Senofilcon A y Comfilcon A (tabla 1.2). Estos resultados coinciden con los obtenidos previamente por Karlgard y col. (2003).

Lente	Monómeros	Recubrimiento superficial	Fármaco cargado en 120 min (mg/lente)	Fármaco cedido en 1440 min(%)
Alfafilcon A	HEMA + NVP	No	0,32±0,24	56,2
Balafilcon A	NVP + TPVC + NVA + PBVC	Oxidación con plasma	0,39±0,36	20,0
Comfilcon A	FM0411M + HOB + IBM + M3U + NVP + TAIC + VMA	No	0,89±0,06	6,7
Etafilcon A	HEMA + MA	No	1,51±0,14	27,8
Galifilcon A	mPDMS + DMA + EGDMA + HEMA + silicona + PVP	Agente humectante interno (PVP)	0,57±0,12	12,5
Lotrafilcon A	DMA + TRIS + silicona	Capa hidrofílica de 25 nm obtenida por oxidación con plasma	0,79±0,19	2,0
Lotrafilcon B	DMA + TRIS + silicona	Capa hidrofílica de 25 nm obtenida por oxidación con plasma	0,75±0,16	6,3
Polimacon	HEMA	No	0,72±0,13	37,5
Senofilcon A	mPDMS + DMA + HEMA + silicona + PVP	Agente humectante interno (PVP)	1,29±0,13	4,4

***Tabla 1.2**. Carga y cesión de ciprofloxacino en lentes de silicona y en lentes blandas. DMA, N,N-dimethylacrylamida; EGDMA, etileneglicoldimethacrilato; FM0411M, α–metacriloiloxietil iminocarboxietiloxipropilpoli (dimetilsiloxi)-butildimetilsilano; HEMA, 2-hidroxietilmetacrilato; HOB, 2-hidroxibutil metacrilato; IBM, isobornilmetacrilato; MA, ácido metacrilico; mPDMS, polidimetilsiloxano monofuncional; NVP, N-vinil pirrolidona; TEGDMA, tetraetilenglicoldimethacrilato; TPVC, tris-(trimetilsiloxisilil) propilvinilcarbamato; TRIS, trimetilsiloxisilano; M3U, α ωbis (methacriloiloxietiliminocarboxietiloxipropil)-poli(dimetilsiloxano)-poli(trifluoropropilmetilsiloxano)-poly(ω-methoxi-poli(etileneglicol)propil metilsiloxano); NVA, N-vinil aminoacido; PBVC, polidimetilsiloxi disililbutanol bisvinil carbamato; PC, fosforilcolina; PVP, polivinil pirrolidona; TAIC, 1,3,5-triallil-1,3,5-triazina-2,4,6(1H,3H,5H)-triona; VMA, N-vinil-N-metilacetamida (Hui y col., 2008).*

También se evaluó la capacidad para cargar glucocorticoides de lentes de silicona (Lotrafilcon A, Lotrafilcon B, Balafilcon A, Senofilcon A, Galifilcon A y Comfilcon A) y de lentes blandas (Polimacon, Alfafilcon A y Etafilcon A) (Boone

y col., 2009). La cantidad de fármaco incorporado y el tiempo necesario para completar la carga por inmersión en una disolución de dexametasona al 0,1% (tabla 1.3) resultaron ser muy diferentes dependiendo de la composición de la lente. Por otra parte, mientras que con las lentes Etafilcon A, Galifilcon A, Alfafilcon A, Balafilcon A y Comfilcon A la cesión se completó en la primera hora del ensayo, las lentes Lotrafilcon A, Polimacon y Lotrafilcon B mostraron cierta capacidad para controlar el proceso. Estos resultados indican que es posible modular la carga y la cesión del fármaco seleccionando convenientemente los monómeros y aplicando un tratamiento superficial a las lentes.

Lente	**Carga de fármaco**		**Cesión de fármaco**		
	µg/lente	Tiempo (min)	µg/lente	Tiempo (min)	% cedido
Alfafilcon A	118 ± 10	10	64,8 ± 1,3	30	56 ± 2
Balafilcon A	50 ± 3	90	32,0 ± 0,5	50	65 ± 4
Comfilcon A	39 ± 4	15	26,1 ± 0,6	20	67 ± 9
Etafilcon A	37 ± 4	180	30,5 ± 0,3	30	84 ± 9
Galifilcon A	34 ± 6	60	27,9 ± 0,7	40	77 ± 8
Lotrafilcon A	102 ± 11	240-1440	11,3 ± 0,2	1440	11 ± 1
Lotrafilcon B	38 ± 5	300-1440	22,1 ± 0,6	1440	59 ± 7
Polimacon	67 ± 8	150	28,3 ± 1,0	300	42 ± 5
Senofilcon A	56 ± 6	120	21,1 ± 0,4	1440	44 ± 5

Tabla 1.3. *Carga y cesión de dexametasona en lentes de silicona y convencionales (Boone y col., 2009).*

Recientemente se ha evaluado el efecto de la incorporación de vitamina E (10-74%) en la matriz de lentes de contacto blandas, por inmersión en una disolución etanólica, sobre la velocidad de cesión de fármacos cargados posteriormente por inmersión en disoluciones de los mismos (Peng y col., 2010). Debido a su carácter hidrofóbico, la vitamina E ejerce un efecto barrera que dificulta la difusión de

timolol, dexametasona y fluconazol a través de la red polimérica, haciendo que la liberación se produzca más lentamente en las lentes Galifilcon (NIGHT&DAY™), Senofilcon A (ACUVUE® ADVANCE™), Lotrafilcon A (ACUVUE® OASIS™), Lotrafilcon B (O_2OPTIX™) y Balafilcon A (PureVision™) (figura 1.3). La vitamina E dio lugar a un incremento en el diámetro de las lentes (6,5 % para un 30% de carga) y redujo la permeabilidad al oxígeno hasta un 40% tras cargar un 74%. Por otro lado, la vitamina E se mostró como un filtro eficaz frente a la radiación ultravioleta, por lo que las lentes que la incorporan, también pueden ser útiles para reducir los efectos nocivos de esta radiación sobre la córnea.

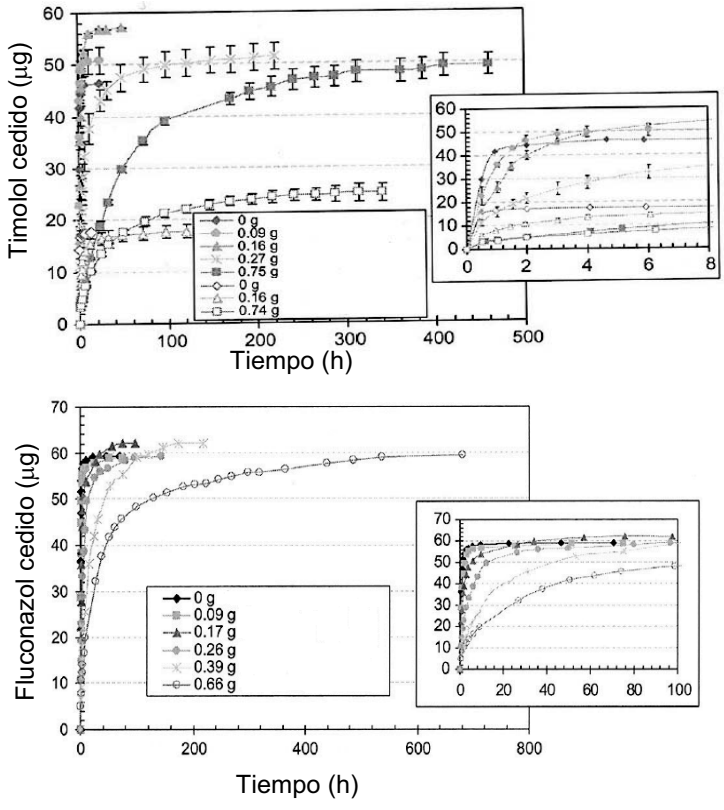

Figura 1.3. *Perfiles de cesión de timolol y fluconazol a partir de las lentes de contacto NIGHT&DAY™ cargadas con distintas cantidades de vitamina E (Peng y col., 2010).*

La baja afinidad de las lentes de contacto por la mayoría de los fármacos constituye un obstáculo muy importante para que su uso como sistemas de liberación se llegue a generalizar (Momose y col., 1997; Karlgard y col., 2003). Por ejemplo, las lentes de PHEMA tienen una capacidad de carga de cloranfenicol, adrenalina y pilocarpina similar a la del cristalino de una persona sana (Heyrman y col., 1989; Chapman y col., 1992). Por lo tanto, si la carga se efectúa por inmersión en una disolución concentrada, sólo una pequeña parte del fármaco disuelto se incorpora a la lente y el resto se pierde. Incluso cuando la carga es suficiente para alcanzar niveles terapéuticos en las estructuras oculares, la liberación suele ser demasiado rápida para que se mantengan niveles eficaces durante periodos de tiempo suficientemente largos (Krejci y col., 1975; Weiner, 1994; McMahon y Zadnik, 2000; Karlgard y col., 2003). También hay que tener en cuenta que el contacto prolongado de ciertos fármacos con la córnea puede exacerbar sus efectos adversos a nivel tópico (Silbert, 1996).

Para incrementar la carga y mejorar el control de la cesión, se ensayó el uso de lentes más gruesas. Con lentes de PHEMA de 0,7-1,3 mm se puede sostener la cesión de fluoresceína, tetraciclina y cloranfenicol durante 24 horas (Krejci, 1971; Krejci y col.; 1971). También se consigue controlar la cesión de dietilenotriamina, tetraacetato de etilendiamina disodio y de hidrocloruro de cisteína y reducir a la mitad el tiempo del tratamiento de quemaduras y úlceras, comparativamente con la terapia ocular clásica (Krejci y col., 1975). Sin embargo, en la práctica la posibilidad de incrementar el espesor se ve limitada por la necesidad de satisfacer unos requerimientos mínimos de permeabilidad al oxígeno y también por razones de comodidad.

El contenido en agua desempeña un papel fundamental en la carga cuando no se establecen interacciones específicas entre el fármaco y la red polimérica. La fase acuosa de la lente se encuentra en equilibrio con la disolución de carga, por lo que la concentración de fármaco en ambas es la misma (Wajs y Meslard, 1986).

Por lo tanto, la cantidad cargada es proporcional al volumen de fase acuosa en el hidrogel, tal como se muestra en la siguiente expresión (Kim y col., 1992):

$$Fármaco\ en\ fase\ acuosa\ \left(\text{p/p hidrogel seco}\right) = \left(Vs/Wp\right)\cdot C_o \qquad \text{(Ec. 1.1)}$$

en la que *Vs* representa el volumen de fase acuosa en el hidrogel, *Wp* el peso de hidrogel seco y C_0 la concentración de fármaco en la disolución de carga. Esto explica que, al instilar gotas de tobramicina sobre lentes Permalens® que contienen un 71% de agua, se consigan niveles más altos y prolongados de fármaco en tejido corneal que si se utilizan lentes terapéuticas Plano T® con un 38,6% de agua. No obstante, para cargas similares, las lentes con un contenido en agua más bajo sostienen más eficazmente la cesión (Lesher y Gunderson, 1993).

La permeabilidad al oxígeno de las lentes de contacto hidrofílicas también se incrementa con el contenido en agua de acuerdo con la expresión (Kuenzler y McGee, 1995; Lloyd y col., 2001):

$$Dk = 2{,}00\cdot 10^{-11}\exp^{(0{,}041\cdot Vs)} \qquad \text{(Ec. 1.2)}$$

Para conseguir lentes de contacto blandas con contenidos elevados en agua (hasta el 80%) se copolimeriza HEMA con monómeros más hidrofílicos, como NVP, N,N-dimetil acrilamida (DMAA) o MAA. Por su parte, las lentes de silicona hidrofóbicas presentan una elevada permeabilidad al oxígeno y un bajo contenido en agua. Al aumentar éste, la permeabilidad se reduce exponencialmente (Lloyd y col., 2001). Este comportamiento limita su utilidad como reservorio de fármacos.

En ausencia de mecanismos específicos de retención, la carga del hidrogel y la cesión tienen lugar de forma casi inmediata siguiendo las leyes de la difusión. En condiciones *sink*, la velocidad de cesión viene dada por (Wajs y Meslard, 1986):

$$dM/dt = 8\,DM_{\infty}/l^2\ \exp^{\left(-\pi^2 Dt/l^2\right)} \qquad \text{(Ec. 1.3)}$$

En esta expresión, M_∞ representa la cantidad total de fármaco cedido, l es el espesor de la lente y D el coeficiente de difusión del fármaco, que se mantiene constante si no se producen cambios en el grado de hinchamiento.

Para un fármaco y una lente en particular, el tiempo necesario para la difusión disminuye a medida que se incrementa el contenido de agua. Por otra parte, el tiempo de difusión es más corto cuanto más bajo es el peso molecular del fármaco (Wajs y Meslard, 1986). A este respecto, resultan muy ilustrativos los datos de incorporación de cromolin sódico, ketorolaco trometamina, dexametasona sódica y fumarato de ketotifeno a lentes de contacto de silicona (Lotrafilcon y Balafilcon) y de PHEMA (Etafilcon, Alfafilcon, Polimacon, Vifilcon y Omafilcon) (tabla 1.4) (Karlgard y col., 2003). La carga y la cesión *in vitro* de los tres primeros fármacos, de peso molecular bajo, se completó en menos de 1 hora independientemente de la composición de la lente, tal como se describió previamente para lentes Vifilcon, Etafilcon y Polimacon con cromolin sódico, ciprofloxacino, idoxuridina, pilocarpina y prednisolona (Lesher y Gunderson, 1993). La captación y la cesión de fumarato de ketotifeno fueron más lentas, completándose en 2 horas, debido a que la baja solubilidad del fármaco en agua (0,01 mg/ml) obligó a efectuar la carga con disoluciones muy diluidas.

El cromolín sódico fue el fármaco que mostró una incorporación más eficaz debido a la elevada concentración de la disolución de carga. La dexametasona fosfato sódico se incorporó a las lentes en muy pequeña cantidad, debido a su

elevada hidrofília. Los hidrogeles de PHEMA con grupos ionizables en su estructura cargaron cantidades elevadas de fumarato de ketotifeno y de ketorolaco trometina. En medio tampón borato salino sólo se cedió una pequeña proporción del fármaco cargado (12% cromolin sódico, 1,5-28% ketorolaco trometamina y 4-16% fumarato de ketotifeno), lo que apunta al establecimiento de uniones irreversibles entre los fármacos y el entramado polimérico.

Fármaco (concentración de carga)	Propiedades de las lentes	Carga (μg/lente)	Cesión (μg/lente)
Cromolyn sodium (20 mg/ml)	Iónica vs No iónica	7548 vs 8126	390 vs 522
	Silicona vs hidrogel de PHEMA	7811 vs 7906	338 vs 517
	Alto vs bajo contenido en agua	8066 vs 8126	552 vs 349
Fumarato de ketotifeno (0,20 mg/ml)	Iónica vs No iónica	198 vs 123	103 vs 77
	Silicona vs hidrogel de PHEMA	128 vs 166	84 vs 89
	Alto vs bajo contenido en agua	170 vs 135	90 vs 85
Ketorolaco trometamina (0,30 mg/ml)	Iónica vs No iónica	103 vs 99	17 vs 20
	Silicona vs hidrogel de PHEMA	85 vs 106	13 vs 21
	Alto vs bajo contenido en agua	108 vs 90	20 vs 16
Fosfato de dexametasona sódica (0,845 mg/ml)	Iónica vs No iónica	67 vs 68	NA
	Silicona vs hidrogel de PHEMA	57 vs 71	NA
	Alto vs bajo contenido en agua	74 vs 57	NA

NA = No disponible; **PHEMA** = poli(2-hidroxietilmetacrilato)

Tabla 1.4. *Carga y cesión de algunos fármacos en lentes de contacto comerciales (Kargard y col., 2003).*

También se cargaron lentes de silicona con maleato de timolol, dexametasona y acetato de dexametasona (Kim y col., 2008). Las lentes se prepararon haciendo reaccionar N,N-dimetilacrilamida (DMA) con metacriloxipropil tris(trimetilsiloxil)silano (TRIS) y bis-α,o-(metacriloxipropil) polidimetilsiloxano. También se incorporó 1-vinil-2-pirrolidona (NVP) para aumentar la capacidad de captación de agua y EGDMA como agente reticulante. Ajustando la proporción de los monómeros se consiguió sostener la cesión durante periodos de tiempo comprendidos entre 20 días y 3 meses.

1.4. Lentes de contacto modificadas para carga y liberación controlada de fármacos

En los últimos años, ha resurgido el interés por la búsqueda de procedimientos eficaces para mejorar las prestaciones de las lentes de contacto como sistemas de liberación de medicamentos, tomando como base los avances en el conocimiento de los mecanismos implicados en los procesos de cesión de solutos a partir de hidrogeles y las posibilidades abiertas por las nuevas tecnologías para mejorar la carga y el control de la cesión.

En la cesión de un fármaco a partir de un sistema polimérico intervienen mecanismos de hinchamiento, difusión y biodegradación (Langer, 1980). En el caso de las lentes de contacto no se puede regular la liberación actuando sobre el grado de hinchamiento, puesto que las dimensiones no se deben modificar para que se mantenga la funcionalidad óptica. Por el contrario, se han aplicado con éxito las aproximaciones basadas en el control de la liberación mediante difusión o la rotura de enlaces químicos (figura 1.4) que se comentan a continuación: i) inmovilización química reversible de fármacos en el hidrogel a través de enlaces lábiles; ii) incorporación de sistemas coloidales cargados con el fármaco a la superficie o a la matriz de las lentes; iii) incorporación de comonómeros funcionales capaces de interaccionar directamente con el fármaco, y iv) moldeado molecular (*molecular imprinting*). En todos los casos, el sistema final debe mantener la permeabilidad al oxígeno, la hidrofilia y las propiedades ópticas, mecánicas y morfológicas que requiere una lente de contacto.

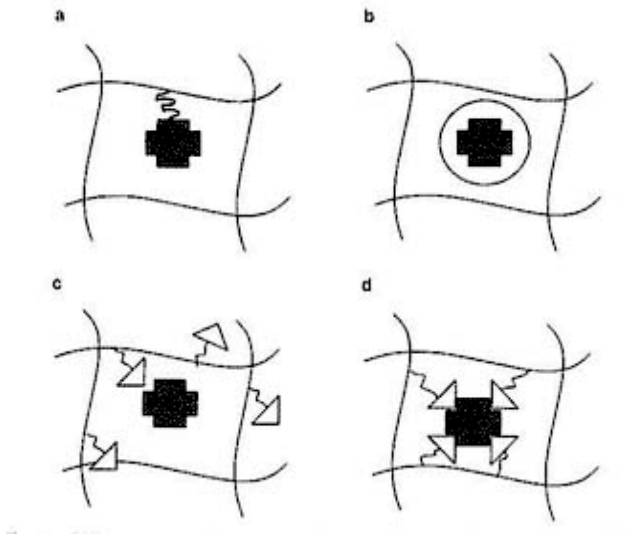

***Figura 1.4**. Mecanismos de retención de fármacos en lentes de contacto: (a) fijado mediante enlaces lábiles; (b) incorporado a sistemas coloidales; (c) unido no covalentemente a ciertos grupos funcionales y (d) interaccionando con cavidades creadas mediante moldeado molecular.*

1.4.1. Inmovilización de fármacos mediante enlaces covalentes lábiles

Esta aproximación consiste en unir el fármaco a las redes de polímero a través de un espaciador, que regula la hidrofilia local y la cinética de hidrólisis química o enzimática responsable de la liberación del fármaco a velocidad constante (Wajs y Meslard, 1986). Para que la técnica resulte útil es necesario que la rotura de los enlaces se produzca más lentamente que la difusión del fármaco. Las lentes se preparan en dos etapas: i) funcionalización del fármaco con un grupo polimerizable unido a un espaciador; y ii) copolimerización con monómeros adecuados para producir lentes de contacto blandas.

Para obtener lentes cargadas con indometacina, se hizo reaccionar este fármaco con metacrilamida fenol y se formaron derivados polimerizables con MMA y NVP, o HEMA y NVP. La composición de las lentes condiciona la entrada del medio acuoso y, consecuentemente, la velocidad de hidrólisis de los enlaces éster que inmovilizan al fármaco (figura 1.5). Las lentes cedieron *in vitro*

entre 5 y 30 μg/día (Vairon y col., 1992). Al cabo de 24 horas se alcanzó en tejido corneal de conejo una concentración media de fármaco de 1 μg/g, que se mantuvo constante durante 7 días (Vairon y col., 1992). Los perfiles de cesión de fármaco fueron similares a los que se consiguieron administrando en forma de colirio una dosis 100 veces superior. La velocidad de cesión se incrementó sensiblemente con la incorporación a la red polimérica del monómero hidrofílico MAA (Vairon y col., 1992).

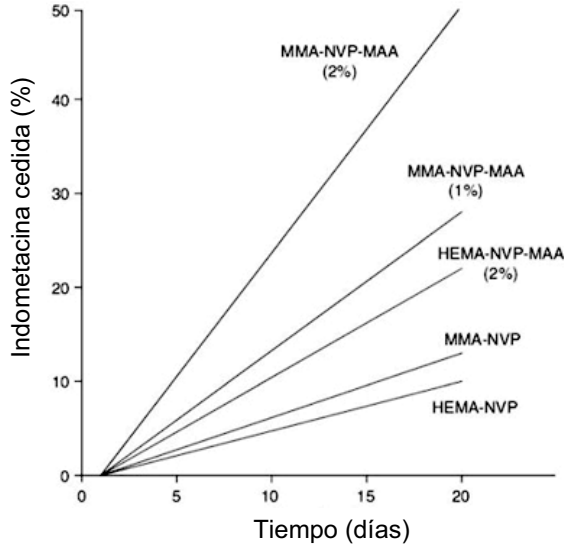

Figura 1.5. *Perfiles de cesión de indometacina en tampón fosfato de pH 7 a partir de hidrogeles de MMA-co-NVP y HEMA-co-NVP preparados con diferentes proporciones de MAA y que contienen el fármaco unido a través de enlaces éster. HEMA = hidroxietilmetacrilato; MAA = ácido metacrílico; MMA = metilmetacrilato; NVP = N-vinilpirrolidona (Vairon y col., 1992).*

1.4.2. Lentes de contacto con partículas coloidales en dispersión o en superficie

Recientemente, se ha abordado el desarrollo de lentes de contacto con el fármaco encapsulado en estructuras coloidales (gotas nanométricas, micelas, vesículas o partículas) que se dispersan en la mezcla monomérica antes de su polimerización (Gulsen y Chauhan, 2005; Chow y Yan, 2006). Si el tamaño de las

partículas es suficientemente pequeño y se incorporan al sistema en proporción baja, las lentes mantienen la transparencia. Una vez que la lente se coloca en el ojo, las nanoestructuras deben liberar el fármaco para que difunda a través de la lente y alcance el fluido lacrimal post-lente, de manera que se mantengan niveles sostenidos en la superficie corneal durante periodos de tiempo prolongados. Gulsen y Chauhan (2004, 2005) han desarrollado lentes de este tipo dispersando gotículas de una microemulsión de fase interna oleosa y fase externa acuosa (10-20 nm) en hidrogeles de PHEMA. Se utilizaron cuatro tipos de dispersiones isotrópicas con lidocaína disuelta en la fase oleosa (tabla 1.5). A dos de estas dispersiones se les añadió octadeciltrimetoxisilano, que se acumula en la interfase aceite/agua y da lugar a una cubierta de sílice. Para obtener las lentes, las microemulsiones (7,4 ml) se mezclaron con HEMA (10 ml) y con el reticulante etilenglicol dimetacrilato (EGDMA) (0,037 ml). La polimerización se llevó a cabo a 60ºC durante 24 horas en moldes de 0,2 mm a 1,2 mm de espesor. También se sintetizaron hidrogeles control de 1,25 mm de grosor reemplazando la microemulsión por el mismo volumen de agua y se cargaron sumergiéndolos en una disolución acuosa de lidocaína.

La opacidad de los hidrogeles de tipo 1 y 2 (tabla 1.5) causada por la agregación de las gotículas de emulsión una vez que se desorbió el Tween 80®, los hizo inadecuadas como lentes. Los hidrogeles preparados con Brij® 97, que es menos soluble en las disoluciones del monómero HEMA, sólo mostraron una ligera pérdida de transparencia. En los hidrogeles de tipo 4 se observó una distribución irregular. Las gotículas se fueron concentrando en la fase no polimerizada a medida que se formó el entramado polimérico hasta ser atrapadas por le hidrogel cuando el medio se hizo muy viscoso (Gulsen y Chauhan, 2004, 2005).

Hidrogel	Composición de la microemulsión			Transmitancia
	Fase oleosa	**Fase acuosa**	**Tensoactivo**	**(% a 600 nm)**
Tipo 1	Aceite de Canola	NaCl al 2%	Tween 80® y Panodan® SDK	4,4
Tipo 2	Aceite de Canola	NaCl al 2%	Tween 80®, Panodan® SDK y OTMS	19
Tipo 3	Hexadecano	Agua	Brij® 97	65,6
Tipo 4	Hexadecano	Agua	Brij® 97 y OTMS	79

OTMS = Octadeciltrimetoxisilano

Tabla 1.5. *Composición y transparencia óptica de lentes de pHEMA (1 mm de espesor) con microemulsiones de lidocaína (Gulsen y Chauhan, 2005).*

Los perfiles de liberación de lidocaína mostraron un *burst* del 30-50% de la dosis, que corresponde al fármaco adsorbido sobre la superficie de la lente y al fármaco libre en el hidrogel (figura 1.6). Ni la densidad de reticulación ni el espesor de las lentes afectaron a la velocidad de cesión del fármaco remanente, lo que indica que después del *burst*, las gotículas ubicadas en la matriz polimérica controlan la liberación. Las dificultades más importantes que plantea esta aproximación son el ajuste de la composición de la microemulsión a los requerimientos de cada fármaco concreto y la estabilización de las gotículas. Este último aspecto es esencial para conseguir que se mantengan las propiedades ópticas de los hidrogeles.

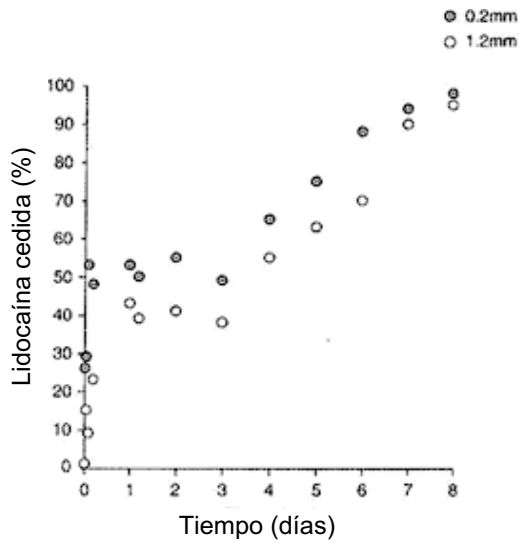

Figura 1.6. *Perfiles de cesión de lidocaína a partir de hidrogeles tipo 4 con diferente espesor (ver tabla 1.5). La carga inicial de fármaco fue 1,2 mg de lidocaína/ g de hidrogel (Gulsen y Chauhan, 2005).*

Aplicando un procedimiento similar al anterior, se dispersaron liposomas de dimiristoil fosfatidilcolina cargados con lidocaína en hidrogeles de PHEMA de 1 mm de espesor (Gulsen y col., 2005). Los liposomas pueden cargar fármacos hidrofóbicos en las bicapas lipídicas concéntricas, o fármacos hidrofílicos en las capas acuosas. En las condiciones en las que transcurre la polimerización, los liposomas se mantuvieron estables y no se alteró la transparencia de los hidrogeles. Para maximizar la carga sin deteriorar las propiedades ópticas de las lentes, la dispersión acuosa de liposomas se añade a la mezcla de polimerización en una proporción igual al contenido en agua del hidrogel cuando se encuentra completamente hinchado (aproximadamente 40%) (Gulsen y Chauhan, 2006). La capacidad de incorporación de fármaco se puede mejorar incrementando el contenido en lípidos de los liposomas. Una vez cedido el 15-30% de la dosis en las primeras 24 horas, la liberación se sostuvo durante más de una semana debido a la lenta difusión del fármaco a través de las capas lipídicas de las vesículas. Para prevenir la descarga prematura, hay que almacenar los hidrogeles en un tampón

saturado con el fármaco, lo que supone un inconveniente importante en la práctica.

También se han desarrollado lentes de PHEMA con microemulsiones de timolol (Li y col., 2007) y ciclosporina A (Kapoor y Chauhan, 2008) aplicando el procedimiento que se esquematiza en la figura 1.7. La velocidad de cesión de ciclosporina fue sensiblemente inferior a la que se observó con hidrogeles control de PHEMA (figura 1.8).

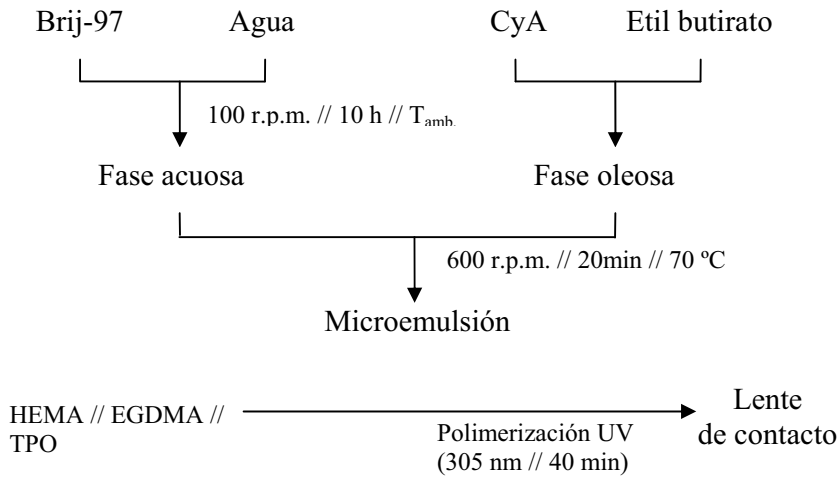

Figura 1.7. *Esquema del proceso de preparación de hidrogeles de pHEMA con microemulsiones de ciclosporina en la matriz polimérica.*

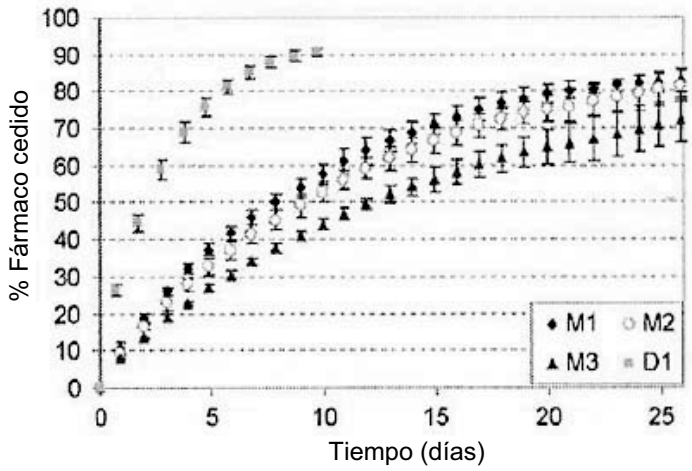

Figura 1.8. *Perfiles de cesión de ciclosporina A a partir de hidrogeles con microemulsiones preparadas con distintas cantidades de tensoactivos en su estructura (M1= 1, M2= 1,5, M3= 2 g de Brij 97) y de un hidrogel control (D1) sin tensoactivo (Kapoor y Chauhan, 2008).*

Para evaluar los efectos de los tensoactivos sobre la cesión, se sintetizaron nuevos hidrogeles incorporando micelas en su matriz, de acuerdo con el procedimiento que se esquematiza en la figura 1.9 (Kapoor y col., 2009).

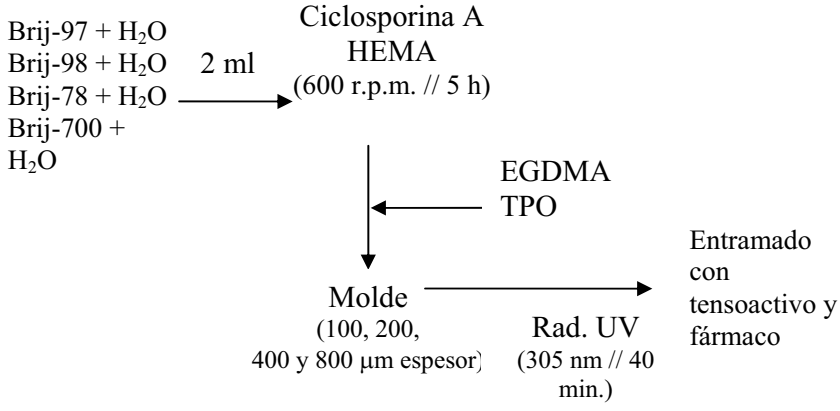

Figura 1.9. *Preparación de lentes de contacto con micelas en su matriz.*

La naturaleza y la proporción de tensoactivo, determinan la velocidad de cesión del fármaco a partir de este tipo de sistemas. A medida que se incrementa

la longitud de la cadena hidrofóbica del tensoactivo, aumenta la afinidad de la ciclosporina A por las micelas (figura 1.10). Una ventaja adicional de los tensoactivos es que promueven la captación de agua por el hidrogel, con lo que las lentillas se hacen más permeables al oxígeno y resultan más cómodas para el usuario.

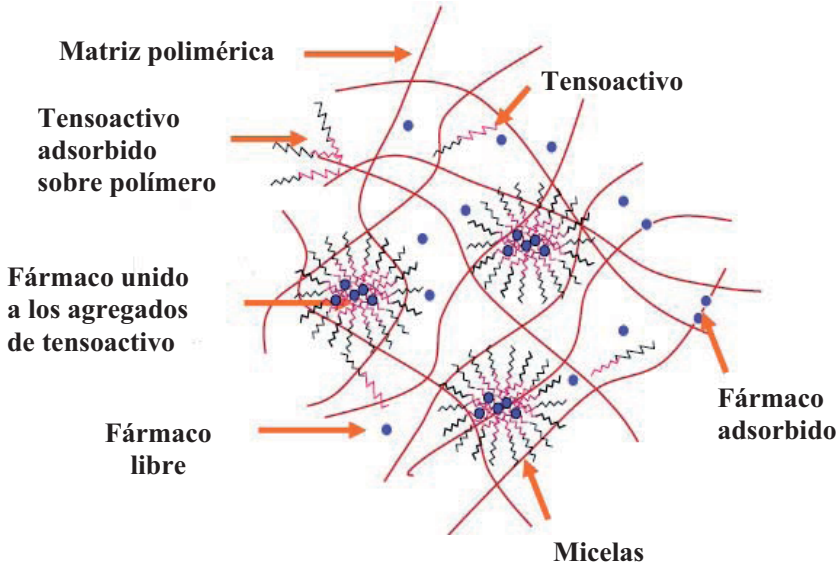

Figura 1.10. *Estructura de un hidrogel con micelas poliméricas cargadas de fármaco y fármaco libre (Kapoor y col., 2009).*

La incorporación de Brij a la estructura polimérica permitió quintuplicar el tiempo necesario para completar la cesión en comparación con los hidrogeles control (sintetizados sin tensoactivo), lo que prueba que el fármaco se distribuye preferentemente en las micelas (figura 1.11).

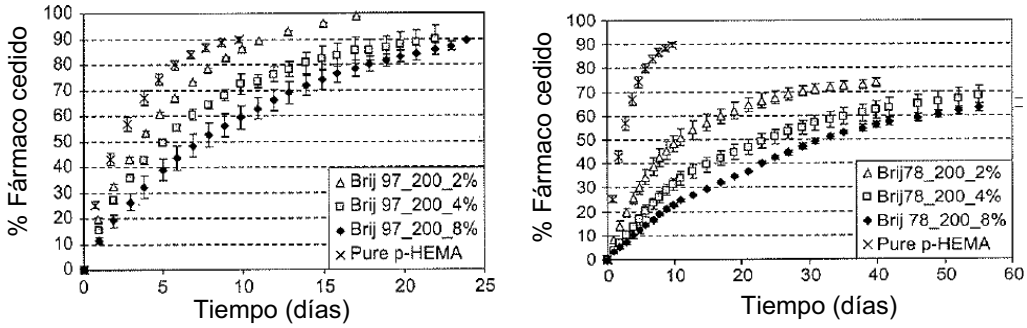

Figura 1.11. *Efecto de la proporción de Brij sobre la cesión de ciclosporina A a partir de lentes de contacto de pHEMA con micelas de fármaco (200 μm de espesor) en medio tampón fosfato salino (Kapoor y col., 2009).*

Las partículas coloidales también se pueden fijar sobre la superficie de la estructura polimérica. Así, se han desarrollado lentes con liposomas adsorbidos en su superficie y cargados de levofloxacino para la prevención y el tratamiento de la queratitis y otras infecciones oculares (Danion y col., 2007b). Los liposomas se incorporaron a las lentes por recubrimiento en multicapa (Danion y col., 2007a, 2007b). Para favorecer la adsorción de los liposomas, las lentes se sumergieron sucesivamente en una disolución de disuccimidilcarbonato, otra de polietilenimina (PEI) y una tercera de N-hidroxisuccinimida-polietilenglicol-biotina (NHS-PEG-biotina) suplementada con N-hidroxisuccinimida (NHS) y 1-etil-3-(3-dimetilaminopropil) carbodiimida (EDC). Una vez recubiertas con PEG-biotina se mantuvieron en una disolución de neutravidina en tampón HEPES 10mM a pH 7,4 durante 24 horas. Por último, las lentes se incubaron en una suspensión de lípidos para promover la formación de una monocapa de liposomas (figura 1.12).

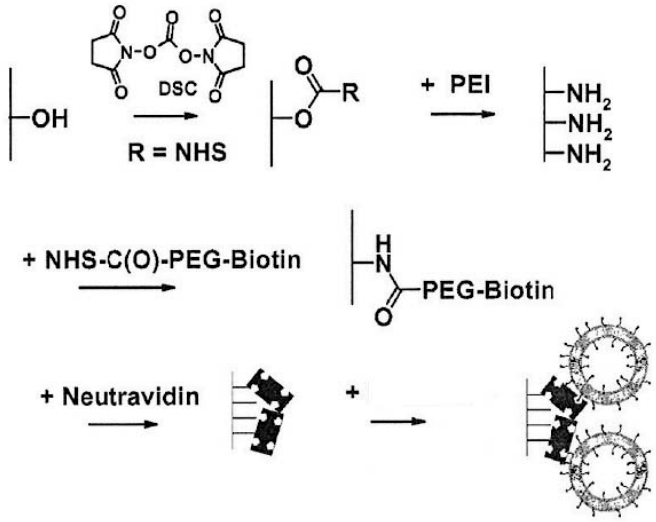

Figura 1.12. *Esquema del procedimiento aplicado para recubrir lentes de contacto con liposomas (Danion y col., 2007b).*

Se ensayaron lentes recubiertas con una, dos o cinco capas de liposomas, obteniéndose perfiles de cesión bifásicos de levofloxacino. En una primera etapa se cede rápidamente el principio activo incorporado por adsorción. En la segunda fase, el fármaco incorporado a los liposomas se libera por difusión. El control de la cesión se va haciendo más eficaz a medida que se incrementa el número de capas de liposomas sobre la superficie de la lente. Por este procedimiento se ha conseguido inhibir el crecimiento *in vitro* de *S. aureus* utilizando levofloxacino.

1.4.3. Lentes de contacto blandas con grupos funcionales capaces de interaccionar con fármacos específicos

Para incrementar la capacidad de carga y el control de la cesión se pueden incorporar al entramado de las lentes, grupos o estructuras funcionales que interaccionen específica y reversiblemente con los fármacos de interés (Uchida y col., 2003; Sato y col., 2005). Para seleccionar los monómeros y establecer su proporción hay que tener en cuenta la necesidad de que se mantengan las

dimensiones y las propiedades mecánicas de las lentes, y de que se produzcan interacciones intensas con las proteínas en las condiciones de pH, temperatura y presión osmótica del fluido lacrimal (Lord y col., 2006). Partiendo de esta idea, se han desarrollado lentes de contacto de HEMA con comonómeros ionizables que captan/liberan fármacos mediante reacciones de intercambio iónico (Uchida y col., 2003; Sato y col., 2005). Cuando la lente se sumerge en una disolución de un fármaco ionizable o protonizable, éste puede interaccionar con los grupos de carga opuesta presentes en la estructura de la lente. Una vez en el ojo, el fármaco se liberará por intercambio con los iones Cl^- o Na^+ del fluido lacrimal. Por este procedimiento se prepararon geles con cloruro de metacrilamida propiltrimetilamonio (MAPTAC) o con fosfato de 2-metacriloxietil (MOEP) para cargar azuleno -un antialérgico utilizado en el tratamiento de la conjuntivitis- o nafazolina, un fármaco que se utiliza para aliviar la congestión ocular, respectivamente (Uchida y col., 2003). Los hidrogeles de poli(HEMA-co-MAPTAC) se contraen al neutralizarse con el azuleno las cargas positivas del entramado y se expanden en una disolución de NaCl debido a que el intercambio iónico con el fármaco da lugar a repulsiones entre los grupos catiónicos de la red polimérica. Los cambios de volumen se minimizaron incorporando comonómeros aniónicos (MAA o MOEP) que reducen la carga neta positiva del entramado (tabla 1.6). Para conseguir una mayor eficacia de carga de nafazolina y un mejor control de la liberación, manteniendo las dimensiones de las lentes, se prepararon hidrogeles de poli (HEMA-co-MOEP-co-MAm) con MOEP y MAm en proporciones comprendidas entre el 0,05 y el 0,6 mol% (figura 1.13) (Sato y col., 2005). El MAm contribuye a la estabilización de los complejos fármaco-fosfato y, a medida que el fármaco se va liberando, los grupos amina del MAm neutralizan parcialmente los grupos fosfato del MOEP, con lo que se atenúan las fuerzas de repulsión y se restringe el hinchamiento del hidrogel.

MAPTAC (mmol)	MAA (mmol)	MOEP (mmol)	Fármaco cargado (%)[a]	Diámetro (mm)	
				Antes de la cesión	Después de la cesión
10	-	-	105	14,8	Deformación de la lente
10	10	-	0,61	14,1	14,1
10	7,5	-	2,03	14,2	14,3
10	5,0	-	11,7	14,5	14,7
10	2,5	-	30,4	14,8	15,1
10	-	10	7,4	13,3	13,3
10	-	7,5	32,4	13,4	13,4
10	-	5,0	38,4	13,7	13,8
10	-	2,5	48,9	14,1	14,2

HEMA = hidroxietilmetacrilato; **MAA** = ácido metacrílico;
MAPTAC = metacrilamida de propiltrimetilamonio; **MOEP** = 2- metacriloxietil fosfato

Tabla 1.6. *Composición de lentes de contacto de poli(HEMA-co-MAPTAC-comonómero aniónico) y dimensiones de las lentes antes y después de ceder azuleno in vitro (Uchida y col., 2003).[a] El porcentaje de azuleno incorporado se calculó como: [azuleno incorporado (mmol)/MAPTAC (mmol)]x100.*

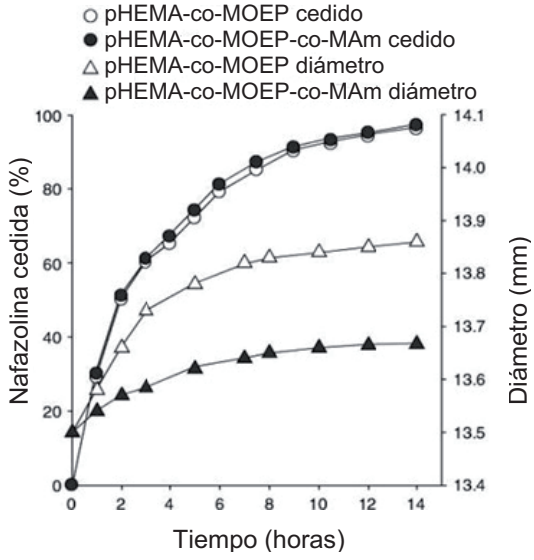

Figura 1.13. *Perfiles de cesión de nafazolina en NaCl al 0,9% y evolución del diámetro de lentes de poli(HEMA-co-MOEP) o poli(HEMA-co-MOEP-co-MAm). Los hidrogeles de poli(HEMA-co-MOEP-coMAm) cargaron 1,5 veces la cantidad de nafazolina incorporada por los hidrogeles de poli(HEMA-co-MOEP) (Sato y col., 2005).*

La copolimerización de HEMA con acrilamida (AAm) permitió modular el grado de hinchamiento e incrementar la capacidad de los hidrogeles para cargar

cloranfenicol. Los hidrogeles con más AAm fueron los que cargaron más fármaco, pero también los que lo cedieron más rápidamente (Li y Cui, 2008). La incorporación de 4-vinilpiridina (4-VP) y/o N-(3-aminopropil)metacrilamida (APMA) a los entramados permitió mejorar la capacidad de carga de ibuprofeno (10 veces) y de diclofenaco (20 veces) sin modificar las propiedades viscoelásticas del material, lo que abre la posibilidad de adaptar los perfiles de liberación a requerimientos específicos ajustando la proporción entre ambos monómeros (Andrade-Vivero y col., 2007).

La búsqueda de estructuras capaces de crear en el hidrogel microambientes que favorezcan el alojamiento del fármaco, sin que ello suponga un deterioro para su funcionalidad como correctores de la visión ni para su biocompatibilidad, llevó a introducir ciclodextrinas en los entramados de pHEMA, utilizando dos aproximaciones: (i) preparación de monómeros acrílicos de ciclodextrina y posterior copolimerización y (ii) funcionalización de hidrogeles preformados con ciclodextrinas colgantes (figura 1.14) (Alvarez-Lorenzo y col., 2010).

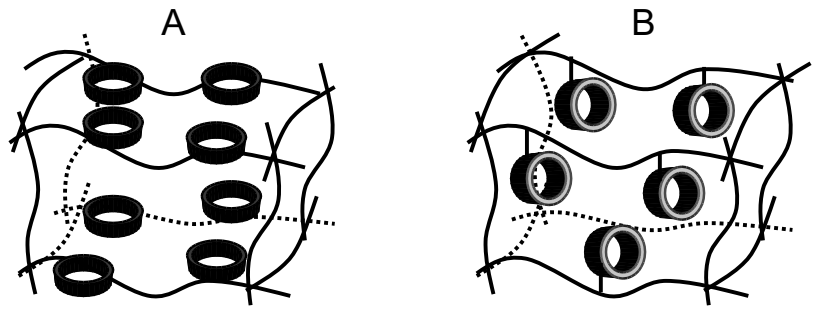

Figura 1.14. *Esquema de un hidrogel obtenido por (A) copolimerización de monómeros de ciclodextrina y (B) funcionalización de un entramado preformado por anclaje de ciclodextrinas.*

La copolimerización de un monómero permetacrilado de β-ciclodextrina dio lugar a hidrogeles capaces de cargar y controlar la cesión de hidrocortisona y acetazolamida (Rosa dos Santos y col., 2008), si bien la incorporación del

monómero de β-ciclodextrina causa un notable incremento en la rigidez del entramado (figura 1.13 A). Por otra parte, copolimerizando monómeros de β-ciclodextrina con HEMA (Xu y col., 2010) se obtuvieron hidrogeles que cargaron eficazmente puerarina -un β-bloqueante de origen natural efectivo en el tratamiento del glaucoma- y controlaron su cesión.

La postfuncionalización de los entramados permite mantener las propiedades mecánicas y otras características que son críticas para la funcionalidad de los hidrogeles de pHEMA como lentes de contacto, al tiempo que los dota de una elevada afinidad por fármacos que forman complejos de inclusión, como el diclofenaco (Rosa dos Santos y col., 2009). Para hacer posible el anclaje de las unidades de ciclodextrina, se procedió en primer lugar a copolimerizar HEMA con glicidilmetacrilato (GMA) y, a continuación, se hicieron reaccionar los grupos epóxido del GMA con los grupos hidroxilo de la ciclodextrina. Cada ciclodextrina se ancla a través de 2-3 enlaces éter. Las ciclodextrinas ancladas mejoran las propiedades de deslizamiento del hidrogel, reduciendo en un 50% el coeficiente de fricción, y multiplican por quince la capacidad de carga de diclofenaco. Además, los hidrogeles controlan la cesión de diclofenaco en fluido lacrimal y no se descargan prematuramente cuando se almacenan durante un mes en un líquido comercial de conservación de lentes de contacto (figura 1.15).

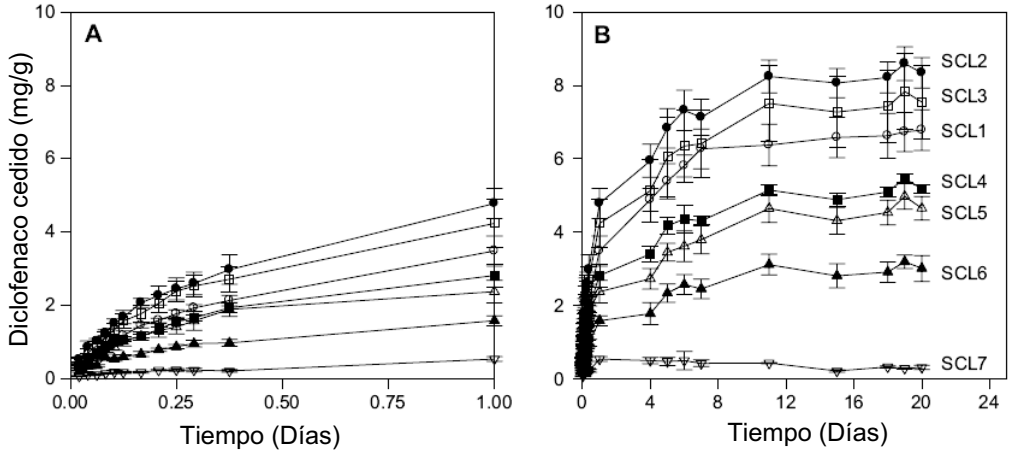

Figura 1.15. *Perfiles de cesión de diclofenaco a partir de hidrogeles con β-ciclodextrinas colgantes, durante uno (A) y veinte días (B) (Rosa dos Santos y col., 2009).*

1.4.4. Lentes de contacto preparadas por moldeado molecular (molecular imprinting)

1.4.4.1. Moldeado molecular

La eficacia de las interacciones entre los grupos funcionales de la lente y un fármaco determinado se puede mejorar considerablemente si se optimiza su distribución espacial en la red polimérica. Una aproximación útil para dotar de capacidad de reconocimiento molecular específico a materiales altamente reticulados y consecuentemente, muy rígidos es el moldeado molecular, denominado en la bibliografía anglosajona "molecular imprinting". Esta técnica consiste en sintetizar el polímero en presencia de la sustancia que debe reconocer específicamente, de manera que pueda actuar como molde durante la polimerización (Maeda y Bartsch, 1998; Ramström y Ansell, 1998). Para controlar la secuencia y la distribución espacial de los monómeros funcionales, éstos deben ser capaces de interaccionar con la molécula molde antes de la polimerización, a través de enlaces covalentes reversibles (Wulff, 1995; Wulff y

Biffis, 2001) o de interacciones no covalentes, tales como enlaces iónicos, hidrofóbico o por puentes de hidrógeno (Arshady y Mosbach, 1981; Sellergren B., 2001). La polimerización hace permanente la distribución de los monómeros y, cuando se retira el fármaco del entramado polimérico, las cavidades formadas en la estructura del hidrogel mantienen su capacidad para interaccionar con las moléculas molde si de nuevo entran en contacto con ellas (Allender y col., 1999).

Una mera polimerización en presencia del fármaco no asegura el efecto *imprinting*. Si la relación molar fármaco:monómero funcional no es la apropiada (Anderson y col., 1999) o si los complejos se disocian durante la polimerización (Mayes y Whitcombe, 2005), los monómeros funcionales se distribuirán aleatoriamente en la red como ocurre en ausencia de fármaco. Para que no se disocien los complejos monómero funcional-molécula molde, hay que llevar a cabo la polimerización en un medio adecuado y a la temperatura más baja posible (Ramström y Ansell, 1998; Mayes y Whitcombe, 2005).

Los polímeros *imprinted* altamente reticulados son materiales rígidos que se usan en la extracción de moléculas a partir de matrices complejas, como fases estacionarias en separaciones cromatográficas, como componentes de sensores y reactivos de inmunoensayo y como catalizadores (Kandimalla y Ju, 2004; Hillberg y col., 2005). En los últimos años, la técnica de moldeado molecular está recibiendo una creciente atención en el campo de los sistemas de liberación de medicamentos (Allender y col., 2000; Byrne y col., 2002; Alvarez-Lorenzo y Concheiro, 2004; Hilt y Byrne, 2004; Alvarez-Lorenzo y Concheiro, 2005, 2006, 2008; Cunliffe y col., 2005; Van Nostrum, 2005).

1.4.4.2. Optimización de la capacidad de carga de las lentes de contacto aplicando técnicas de moldeado molecular

Para aplicar las técnicas de moldeado molecular al desarrollo de lentes de contacto blandas hay que tomar en consideración los siguientes aspectos: i) el fármaco ha de ser estable en las condiciones de síntesis del hidrogel y formar complejos con los monómeros funcionales; ii) los monómeros funcionales se tienen que elegir entre un número limitado de monómeros con potencial capacidad de interacción con el fármaco y que no alteren las propiedades ópticas ni la biocompatibilidad de la lente; iii) la densidad de reticulación debe ser la adecuada para proporcionar a los hidrogeles las propiedades mecánicas requeridas. Este es un factor crítico, debido a que las cavidades *imprinted* tienen que tener una estructura suficientemente estable como para mantener su conformación en ausencia de la molécula molde y, al mismo tiempo, el material tiene que ser suficientemente flexible para que se pueda utilizar como lente de contacto. Los sistemas *imprinted* convencionales contienen entre un 50 y un 90% de agente reticulante, lo que dota a las cavidades de una gran estabilidad y les confiere una gran resistencia mecánica (Sibrian-Vazquez y Spivak, 2003), pero su excesiva rigidez hace que no se puedan utilizar como lentes blandas. En las lentes de contacto blandas, la proporción de reticulante no debe sobrepasar el 10 mol%. Por lo tanto, es esencial diseñar correctamente el hidrogel para conseguir un balance adecuado entre las propiedades mecánicas y la estabilidad de las cavidades *imprinted*; y iv) el disolvente se debe seleccionar de modo que no interfiera ni compita con las moléculas molde en la interacción con los monómeros funcionales, reduciendo la afinidad y la selectividad de la red polimérica. En general, los polímeros *imprinted* convencionales se sintetizan en medios orgánicos, que facilitan la formación de estructuras macroporosas con cavidades fácilmente accesibles. En el caso de las lentes de contacto, se prefiere utilizar los monómeros en estado líquido evitando el uso de disolventes.

El hinchamiento de la red polimérica en los líquidos de conservación de las lentes o en el fluido lacrimal podría distorsionar la estructura de las cavidades *imprinted*. Sólo las que cuentan con una alta afinidad pueden memorizar las características estructurales del fármaco y experimentar un ajuste inducido en su presencia, recuperando la conformación que tenían inmediatamente después de la polimerización (Alvarez-Lorenzo y col., 2002; Hiratani y Alvarez-Lorenzo, 2002 2003, 2004; Hiratani y col., 2005a, 2005b). De esta manera, los hidrogeles *imprinted* poco reticulados mimetizan la capacidad de reconocimiento de ciertas biomacromoléculas (por ejemplo, receptores, enzimas, anticuerpos) (Ito y col., 2003).

Tomando como base ciertos principios biomiméticos, se puede dotar a las lentes de contacto de una afinidad elevada, de manera que sean capaces de cargar el fármaco y sostener su cesión. Para hacer más eficiente el desarrollo de los materiales imprinted y reducir los costes de tiempo y material que implican los clásicos ensayos de prueba y error, se puede establecer *a priori* la estequiometría de los complejos fármaco:monómero funcional mediante técnicas analíticas como la resonancia magnética nuclear, la espectroscopía UV o la microcalorimetría isotérmica (Fish y col., 2005; McStay y col., 2005; Molinelli y col., 2005; O´Mahony y col., 2005) o aplicando procedimientos de modelización molecular (Piletska y col., 2004, 2005; Karim y col., 2005). Hasta el momento la investigación sobre lentes de contacto blandas *imprinted* se ha centrado en dos grupos terapéuticos -los antagonistas β-adrenérgicos (timolol) y los antihistamínicos (ketotifen)- y un aditivo, el ácido hialurónico, para hacerlas más confortables.

1.4.4.3. Lentes de contacto blandas *imprinted* con timolol

Las lentes de contacto blandas cargadas con timolol responden al objetivo de reducir la absorción no productiva y disminuir los efectos secundarios. La permeabilidad de la conjuntiva a este β-bloqueante es alta y similar a la de la córnea (Ahmed y col., 1987, 1989) por lo que, cuando se administra en forma de gotas oftálmicas, la mayor parte de la dosis accede a la circulación general y puede inducir efectos secundarios graves a nivel cardiovascular y pulmonar (Nelson y col., 1986). Por otra parte, la estructura del timolol es particularmente adecuada para preparar sistemas *imprinting*, puesto que ofrece numerosos lugares para interaccionar con los monómeros funcionales a través de enlaces iónicos y de puentes de hidrógeno y no interfiere en la polimerización ni en la transparencia de las lentes (Alvarez-Lorenzo y col., 2002). Se prepararon hidrogeles de pHEMA no *imprinted* (convencionales) e *imprinted* (sintetizados en presencia de timolol 23 mM) de 0.7 mm de espesor con una densidad de reticulación muy baja (0.128 mol%), usando ácido metacrílico (MAA) o metilmetacrilato (MMA) como monómeros funcionales en un intervalo de concentración de 0 a 5,12 mol% (Alvarez-Lorenzo y col., 2002). Una vez polimerizados, los hidrogeles se lavaron por inmersión en agua hirviendo durante 3 minutos. Sólo el 30% de la dosis de timolol se perdió durante la ebullición. Esta etapa se puede evitar puesto que es previsible que la polimerización sea completa y no se esperan monómeros residuales. Los hidrogeles *imprinted* sostuvieron la cesión durante varias horas, dependiendo la velocidad de liberación de la naturaleza de los comonómeros funcionales y de las características del medio de cesión (NaCl 0.9% de pH 5,5, tampón fosfato de pH 7,4 o fluido lacrimal artificial de pH 8) (figura 1.16). Los hidrogeles más hidrofóbicos preparados con MMA dieron lugar a la velocidad de liberación más lenta. Una vez cedido el fármaco, los hidrogeles *imprinted* preparados con la proporción más baja de MAA (100 mmol/L) recargaron 3 veces más timolol que los hidrogeles no *imprinted*.

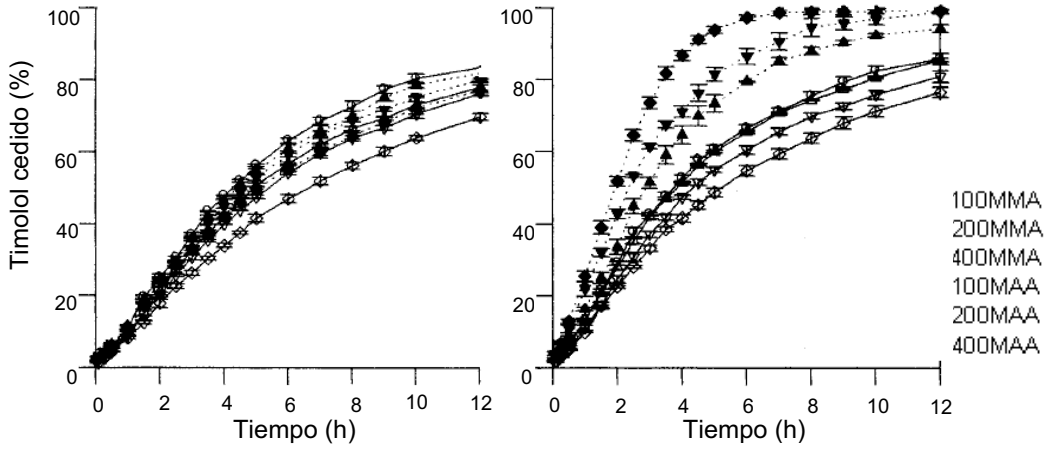

Figura 1.16. *Cesión de timolol en (a) NaCl al 0,9% (pH 5,5) y (b) fluido lacrimal artificial (pH 8) a partir de hidrogeles obtenidos por copolimerización de 2-hidroxietil metacrilato (HEMA) con metil metacrilato (MMA) o ácido metacrílico (MAA) en presencia de maleato de timolol. Para preparar las lentes se utilizaron concentraciones de MMA y MAA 100, 200 y 400 mmol/L (Alvarez-Lorenzo y col., 2002).*

En estudios adicionales llevados a cabo con lentes *imprinted* de HEMA o N,N-dietil acrilamida (DEAA) conteniendo diferentes proporciones de MAA (1,28-5,12 %mol) y agente reticulante EGDMA (0,32-8,34 %mol) se observó que se requiere un mínimo de 0,9 %mol EGDMA para incrementar la capacidad de carga y mejorar el control de la cesión con respecto a las lentes convencionales. Las lentes imprinted podrían cargar una cantidad efectiva de timolol, sostener su cesión en fluido lacrimal durante más de 12 horas y recargar otra dosis durante la noche, encontrándose listas para su uso al día siguiente (Alvarez-Lorenzo y col., 2002; Hiratani y col., 2002).

Para evaluar el efecto de la composición monomérica del esqueleto del entramado, se fijó la proporción de monómero funcional (MAA, 100 mmol/L) y de agente reticulante (EGDMA, 140 mmol/L) (tabla 1.7; Hiratani y Alvarez-Lorenzo, 2003). Las lentes de 0.3 mm se prepararon por irradiación con luz UV en presencia de maleato de timolol (25 mM). La afinidad de las lentes por el

fármaco en medio acuoso a 37ºC se ordenó de la manera siguiente: lente B > lente D > lente C > lente A. El efecto *imprinting* más marcado (es decir, el mayor incremento relativo en la afinidad total respecto de los sistemas no *imprinted*) se observó con los dos últimos tipos de lente. Estos resultados indican que las mejoras en la afinidad que aporta la aplicación de esta técnica son más evidentes cuando la intensidad de las interacciones fármaco-polímero no es muy alta.

Lentes	**Monómeros (%mol)**							**K (mol^{-1})**	
	DEAA	HEMA	MMA	SiMA	DMAA	MAA	EGDMA	No Imprinted	Imprinted
A	96,84					1,29	1,87	49 (6)	123 (5)
B		97,10				1,18	1,72	203 (6)	232 (14)
C			47,94		49,55	1,02	1,49	122 (55)	92 (15)
D				17,87	78,17	1,62	2,35	170 (7)	144 (1)

DEAA = N,N-dietil acrilamida; **DMAA** = N,N-dimetil acrilamida;
EGDMA = etilenglicol dimetacrilato; **HEMA** = 2-hidroxietil metacrilato;
MAA = ácido metacrílico; **MMA** = metilmetacrilato;
SiMA = 1-(tristrimetilsiloxisililpropil)metacrilato

Tabla 1.7. *Proporciones de monómero estructural, monómero funcional MAA y agente reticulante EGDMA usadas en la preparación de lentes imprinted de 0,3 mm de espesor y valores de la constante de afinidad por el timolol (Hiratani y Álvarez-Lorenzo, 2003).*

Con las lentes se obtuvieron perfiles de cesión sostenida en NaCl al 0,9% durante 2-8 horas (Hiratani y Alvarez-Lorenzo, 2003). Los coeficientes de difusión del fármaco a través de las lentes *imprinted* fueron 2,2 x 10^{-9} cm^2/s para las lentes de DEAA, 9,9 x 10^{-9} cm^2/s para las lentes de HEMA, 66,5 x 10^{-9} cm^2/s para las lentes de MMA-DMAA, y 71,3 x 10^{-9} cm^2/s para las lentes de SiMA-DMAA. Estos valores confirman que las moléculas de timolol abandonan más fácilmente los hidrogeles hidrofílicos con menor afinidad (MMA-DMAA y SiMA-DMAA).

En un estudio llevado a cabo en conejos con lentes ultrafinas de DEAA (14 mm de diámetro y 0,08 mm de espesor) se puso de manifiesto la aptitud de los

hidrogeles *imprinted* para controlar *in vivo* la cesión de timolol. Los niveles de timolol en fluido lacrimal se monitorizaron tras la inserción de lentes *imprinted* (con una carga de fármaco de 34 μg) y de lentes no *imprinted* (cargados con 20 μg de fármaco) y de la instilación de gotas de timolol de 0,068% (dosis total 34 μg) o 0,25% (dosis total 125 μg) (figura 1.17; Hiratani y col., 2005a).

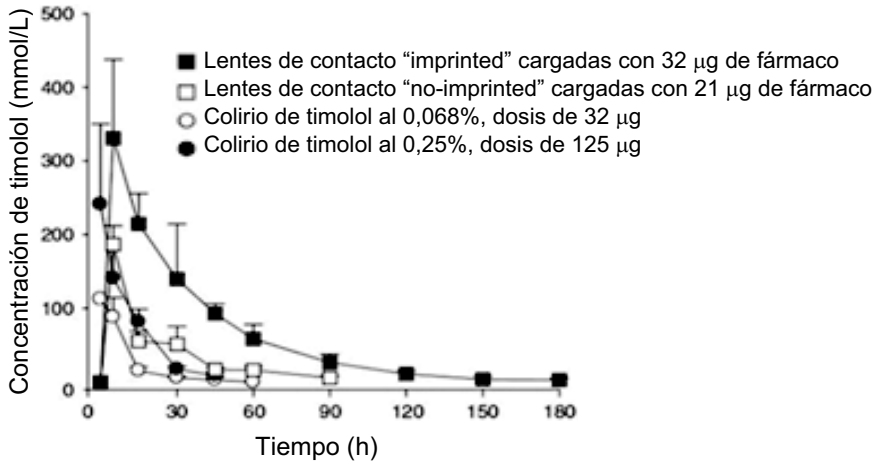

***Figura 1.17**.- Evolución de la concentración de timolol en el fluido lacrimal tras la inserción de lentes imprinted o no imprinted pre-sumergidas en una disolución de fármacoo, o la instilación de un colirio en conejos (Hiratani y col., 2005a).*

Las lentes *imprinted* sostuvieron la cesión durante 180 minutos, en contraste con los 90 minutos que requirieron las no *imprinted* para completar el proceso. Con los dos tipos de lentes se alcanzaron los niveles oculares máximos a los 5 minutos, decayendo a continuación monoexponencialmente. Con independencia de la concentración de la disolución, el timolol aplicado en forma de gotas se eliminó del ojo en menos de una hora. El valor del área bajo la curva concentración en fluido lacrimal *vs.* tiempo (AUC) fue 3,3 y 8,7 veces mayor para las lentes de contacto imprinted que para las no *imprinted* y las gotas, respectivamente. No se encontraron diferencias entre las lentes no *imprinted* y los

colirios comerciales. Por lo tanto, la capacidad de las lentes de contacto blandas para sostener los niveles de fármaco en el fluido lacrimal fue proporcional a su capacidad de carga. Estos resultados indican que las lentes previenen la eliminación precorneal, de manera que se requiere una dosis mucho más reducida para alcanzar niveles terapéuticos que si se utilizan colirios.

Finalmente, se analizó la influencia de la relación molar timolol: monómero funcional sobre la eficacia del imprinting, utilizando lentes con DMAA y SiMA (50:50 v/v) como monómeros principales, MAA como monómero funcional y EGDMA como agente reticulante (Hiratani y col., 2005b). La velocidad de cesión de timolol se redujo fuertemente al incrementar la relación molar MAA:timolol desde 4:1 a 16:1. Las lentes de 0,3 mm de espesor preparadas con una relación molar timolol:MAA 1:16 mostraron coeficientes de difusión de fármaco dos órdenes de magnitud más bajos que los obtenidos con los hidrogeles no imprinted. Esta influencia tan marcada de la relación timolol:MAA se explica por la diferente conformación de las cavidades *imprinted* (Anderson y col., 1999; Mayes y Whitcombe, 2005). Relaciones timolol:MAA altas dan lugar a cavidades *imprinted* con un número de unidades MAA insuficiente para satisfacer la capacidad de interacción del fármaco. Estos sitios de unión muestran una baja afinidad por el timolol que, en consecuencia, se puede ceder más fácilmente. A medida que la cantidad relativa de timolol se reduce, hay más unidades de MAA disponibles para agruparse durante la síntesis y formar cavidades imprinted con más puntos de unión y, por lo tanto, más eficientes; cada cavidad tiene una estructura más perfecta y su afinidad por el timolol retrasa el proceso de cesión. (figura 1.18).

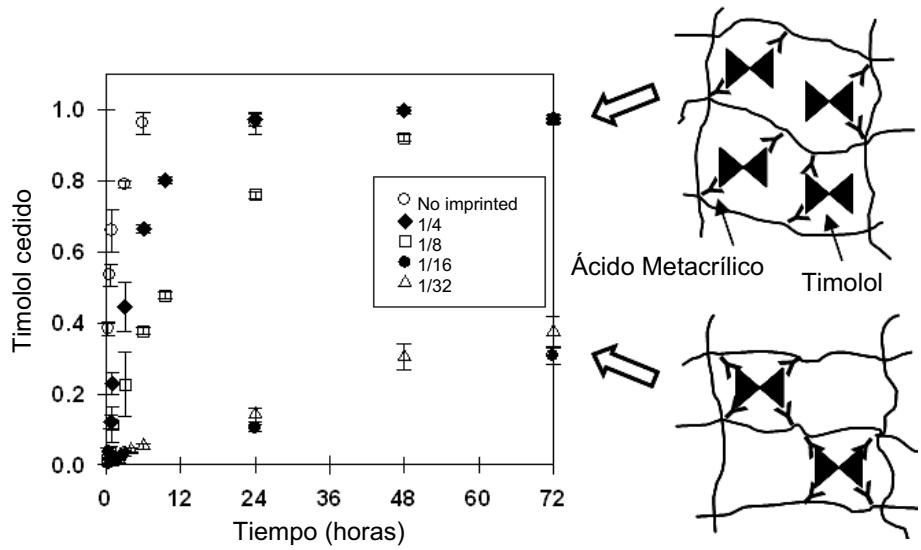

Figura 1.18. *Perfiles de cesión de timolol (fracción de dosis) en NaCl 0,9% a partir de lentes imprinted y no imprinted preparadas con ácido metacrílico (MAA, 400 mmol/L), etilenglicol dimetacrilato (EGDMA, 600 mmol/L), N,N-dimetil acrilamida (DEAA), y 1-(tristrimetilsiloxisililpropil)metacrilato (SiMA). La relación molar timolol:monómero funcional (1:4, 1:8, etc.) determina la afinidad por el fármaco de los hidrogeles imprinted. Con una pequeña porción de timolol en el medio de polimerización, se puede crear cavidades con un gran número de puntos de unión y una elevada afinidad que controla eficazmente la cesión (Hiratani y col., 2005b).*

1.4.4.4. Lentes de contacto blandas *imprinted* con ketotifeno

Para diseñar lentes de contacto imprinted con el antihistamínico fumarato de ketotifeno, se siguió una aproximación denominada moldeado configuracional biomimético (CBIP) (Hilt y Byrne, 2004; Venkatesh y col., 2005, 2007). Para ello, se seleccionaron monómeros funcionales (HEMA, AA, NVP y Am) similares a los grupos químicos del receptor H1 de la histamina (ácido aspártico, lisina, arginina y tirosina) buscando mimetizar las interacciones no covalentes que son responsables del acoplamiento de la histamina con su receptor fisiológico (figura 1.19). La hipótesis de partida fue que, si los antihistamínicos tienen afinidad por el receptor H1, un hidrogel que presente una funcionalidad química

similar deberá captar el antihistamínico, incrementar la carga y dar lugar a una cinética de cesión sostenida.

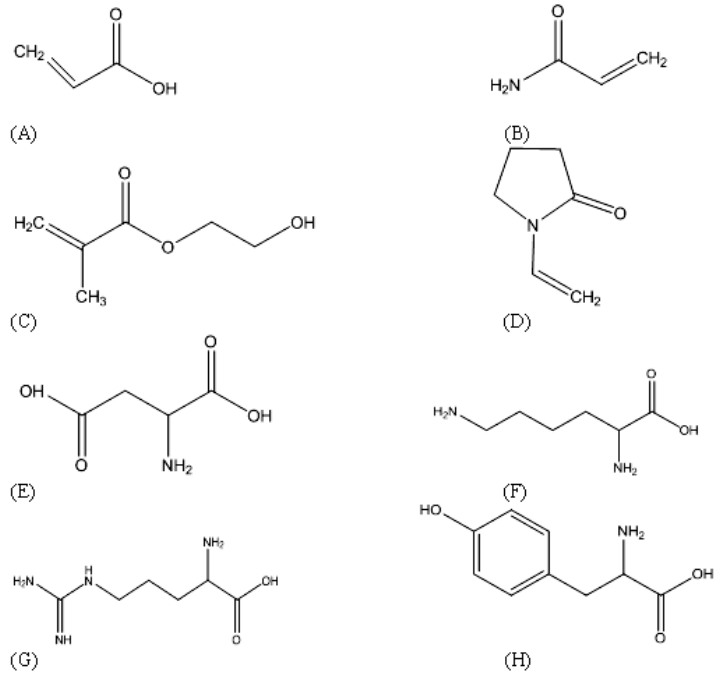

Figura 1.19. *Estructura de los monómeros usados en la síntesis de los hidrogeles por moldeado configuracional biomimético, y de los aminoácidos que conforman el lugar activo del receptor H1 de la histamina; (A) Ácido Acrílico (AAc), (B) Acrilamida (Am), (C) 2-Hidroxietilmetacrilato (HEMA), (D) N-vinil pirrolidona, (E) Ácido Aspártico, (F) Lisina, (G) Arginina, (H) Tirosina.*

Las lentes se prepararon por fotopolimerización partiendo de HEMA (92% mol), agente reticulante PEG200DMA (5% mol), y monómeros funcionales (AA, AM y/o NVP 3% mol). Los análisis de fotocalorimetría diferencial de barrido evidenciaron que el ordenamiento de los monómeros previo a la polimerización que induce la presencia de fumarato de ketotifeno, restringe determinadas configuraciones monoméricas, el movimiento de los radicales libres y la propagación de las cadenas. Estas restricciones reducen la velocidad de polimerización, lo que hace que los receptores del fármaco que se forman en la red polimérica sean más perfectos. No se observaron diferencias en el grado de

hinchamiento ni en las propiedades mecánicas y ópticas de los entramados *imprinted* y no *imprinted* (Venkatesh y col., 2007). La formulación más biomimética, poli(AA-co-AM-co-NVP-co-HEMA-co-PEG200DMA), mostró una carga seis veces mayor que los hidrogeles control y tres veces superior a la de los entramados con uno o dos monómeros funcionales. En medio salino, se observó cesión sostenida de fármaco durante dos días. El perfil de cesión en fluido lacrimal con lisozima, un medio más mimético con el fisiológico, se prolongó durante cuatro días (figura 1.20).

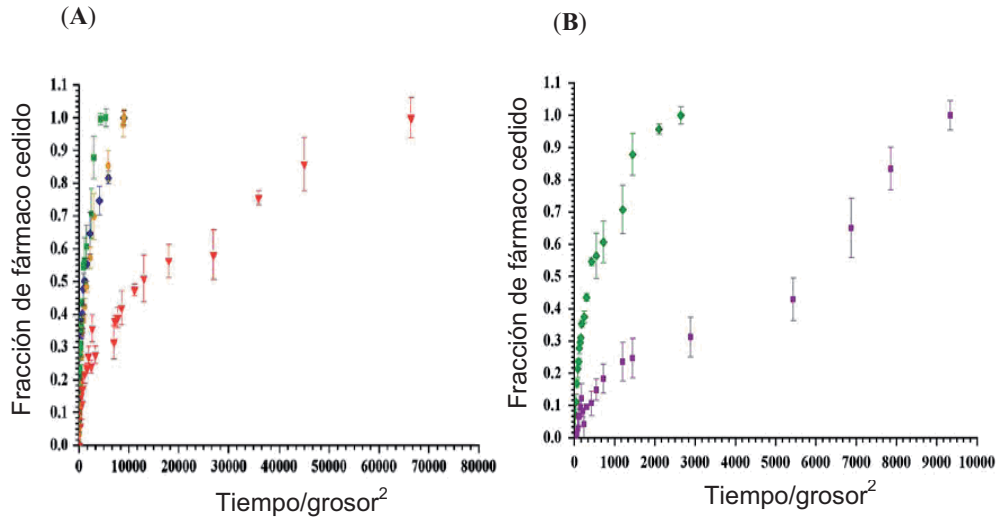

***Figura 1.20**. (A) Cesión de ketotifeno en fluido lacrimal a 25 ºC a partir de lentes de contacto preparadas por copolimerización de HEMA con PEG200DMA y con AM (linea naranja), AA (línea azul), AA-co-AM (línea verde) o NVP-co-AA-co-AM (línea roja). (**B**) Cesión de ketotifeno a partir de hidrogeles de poli(AA-co-AM-co-HEMA-co-PEG200DMA) en fluido lacrimal en presencia o en ausencia de lisozima (1 mg/ml) (Venkatesh y col., 2007).*

Un estudio más profundo de estos hidrogeles reveló que los coeficientes de reparto del fármaco fueron, al menos, dos veces superiores en los hidrogeles *imprinted* que en los hidrogeles control. Los hidrogeles *imprinted* de poli(AA-co-AM-co-NVP-co-HEMA-co-PEG200DMA) mostraron un coeficiente de difusión de fármaco de $5.57 \cdot 10^{-10}$ cm^2/s, inferior en un factor de 9, 7.2 y 13.8 a los

observados en hidrogeles *imprinted* de poli(AA-co-HEMA-co-PEG200DMA), poli(AM-co-HEMA-co-PEG200DMA) y poli(AA-co-AM-co-HEMA-co-PEG200DMA), respectivamente (Venkatesh y col., 2008) (figura 1.20).

Los estudios de cesión, que se llevaron a cabo en un dispositivo que simula la velocidad de flujo (3 μL/min) y el volumen del líquido lacrimal en el ojo, confirmaron la mayor eficacia de los hidrogeles *imprinted* con múltiples monómeros funcionales. Bajo condiciones *sink*, las lentes *imprinted* mostraron una cinética de cesión Fickiana (dependiente de la concentración) con coeficientes de difusión comprendidos entre $4.04 \cdot 10^{-9}$ y $5.57 \cdot 10^{-10}$ cm^2/s. Con el entramado *imprinted* más funcionalizado se observó, como promedio, un coeficiente de difusión diez veces más pequeño que con el hidrogel menos funcionalizado, cediéndose el fármaco durante cinco días a velocidad decreciente. En cambio, bajo condiciones de flujo fisiológico, la velocidad de cesión se mantuvo constante durante 3.5 días, liberándose una dosis terapéuticamente relevante de acuerdo con una cinética de orden cero. En su conjunto, estos resultados sugieren que los dispositivos de microflujo podrían ser útiles para predecir la velocidad de cesión de fármacos en condiciones fisiológicas a partir de lentes medicadas (Ali y col., 2007)

1.4.4.5. Lentes de contacto con ácido hialurónico

La queratoconjuntivitis sicca, comúnmente conocida como síndrome del ojo seco, es una patología en la que la conjuntiva y la córnea no están bien lubrificadas (Berkow y col., 1997). Cuando se deteriora la homeostasis del film lacrimal, como consecuencia de un aporte insuficiente, una pérdida excesiva o una composición anómala del fluido lacrimal, su capacidad para proteger el epitelio de la superficie ocular disminuye. En consecuencia, el síndrome del ojo seco comprende epiteliopatía de la superficie ocular, hiperosmolaridad, inestabilidad

del film e irritación e inflamación ocular más o menos intensa (Lemp, 1995). Esta patología afecta al 10-20% de la población adulta y su prevalencia alcanza al 70% de los usuarios de las lentes de contacto (Johnson y Murphy, 2004; Maruyama y col., 2004; Glasson y col., 2006). Aunque la prevención y el tratamiento del síndrome del ojo seco requiere una aproximación global (Johnson y Murphy, 2004), se ha comprobado que la aplicación de gotas de disoluciones de polímeros hidrofílicos puede servir para estabilizar el film lacrimal reduciendo la fricción con los tejidos oculares y facilitando la expulsión de cuerpos extraños y para lubrificar las lentes de contacto.

Para los demulcentes que se utilizan como componentes de gotas oftálmicas y lágrimas artificiales, a una concentración comprendida entre el 0.1 y el 2%, la FDA (2009) establece la siguiente clasificación: i) derivados celulósicos: carboximetilcelulosa sódica, hidroxietil celulosa, hipromelosa y metilcelulosa; ii) dextrano 70; iii) gelatina; iv) polioles líquidos: glicerina, polietilenglicol 300, polietilenglicol 400, polisorbato 80, propilenglicol; v) alcohol polivinílico (PVA); y vi) polivinil pirrolidona (povidona). Los llamados "ingredientes de comfort" constituyen otro grupo de sustancias que se utilizan para aliviar molestias oculares. Una de ellas es el ácido hialurónico, un polímero natural que tiene una alta capacidad de retención de agua y da lugar a disoluciones viscoelásticas que permanecen sobre la superficie ocular durante periodos de tiempo más prolongados que las disoluciones de demulcentes (Szczotka-Flynn, 2006).

Desde hace algunos años se han empezado a incorporar polímeros hidrofílicos a la estructura de las lentes de contacto blandas con el objetivo de recubrirlas con una capa que amortigüe y suavice el contacto con la superficie ocular y con el párpado (Peterson y col., 2006; Schwarz y Nick, 2006). Ya se encuentran en el mercado lentes con PVA y PVP para mejorar la humectabilidad y la comodidad

de los usuarios; por ejemplo, Focus Dailies con AquaRelease de CIBA Vision, Inc. y 1-Day Acuvue Moist de Vistakon (Peterson y col., 2006; Nichols y Nichols, 2007; Winterton y col., 2007). Recientemente, se ha inmovilizado ácido hialurónico en lentes de contacto de HEMA (Van Beek y col., 2008a) y de silicona (Van Beek y col., 2008b) para prevenir la adsorción de proteínas.

La tecnología de moldeado molecular se ha utilizado para preparar lentes de contacto cargadas con ácido hialurónico (Ali y Byrne, 2009). Los monómeros funcionales se seleccionaron teniendo en cuenta la estructura de aminoácidos del receptor del ácido hialurónico (la proteína CD44): AM por su grupo amida que se asemeja al de la asparagina, NVP por presentar una capacidad para formar puentes de hidrógeno similar a la de la tirosina y 2-(dietilamino)etil metacrilato (DEAEM) porque cuenta con un grupo con carga positiva, al igual que la arginina o la lisina. Para preparar los hidrogeles, se adicionó ácido hialurónico a una disolución monomérica de Nelfilcon A (1g) con proporciones variables de AM, NVP y DEAEM. Los hidrogeles preparados con 0.125% p/p de monómeros funcionales proporcionaron una amplia variedad de velocidades de cesión dependiendo de la naturaleza de los monómeros y de la relación en que se incorporaron (figura 1.21). Los cambios en el coeficiente de difusión del fármaco se explican por la existencia de puntos de unión múltiples en el entramado y no por cambios estructurales en la malla. Además, por encima de una cierta proporción de monómeros funcionales, la cesión se puede ver completamente impedida, consecuencia de la fortaleza de las uniones.

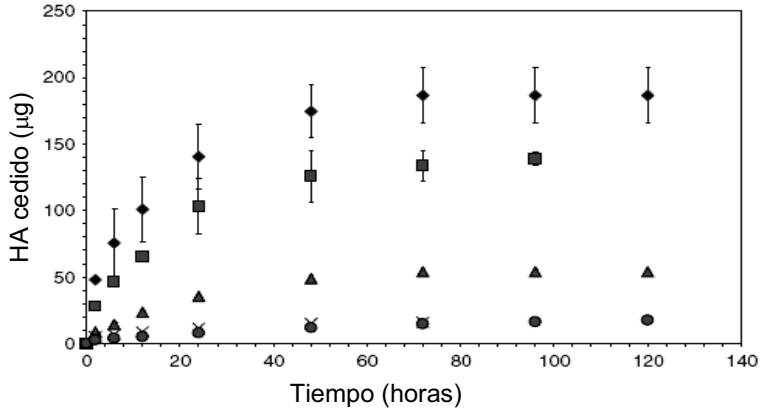

Figura 1.21. *Perfiles de cesión de ácido hialurónico a partir de lentes Nelfilcon imprinted preparadas sin monómero funcional en su estructura (♦) o con distintas proporciones de monómeros funcionales AM:NVP:DEAEM 1:1:0 (▪), 1:1:2 (▲), y 0:0:1 (×) al 0.125% o 1:1:2 (•) al 0.25% (Ali y Byrne, 2009).*

1.5. Impregnación de lentes de contacto con fármacos utilizando CO_2 supercrítico

En los últimos años se están evaluando las posibilidades que ofrecen las técnicas de impregnación con fluidos supercríticos (SSI) para incorporar fármacos en materiales poliméricos diversos (de Sousa y col., 2006; Duarte y col., 2007; Braga y col., 2008a, 2008b; Natu y col., 2008). La técnica de SSI utiliza un disolvente supercrítico, generalmente dioxido de carbono (CO_2) puro o mezclado con cosolventes, como agente solubilizante del fármaco. El fluido supercrítico actúa al mismo tiempo como solvatante y plastificante de la matriz polimérica, incrementando el volumen libre y facilitando la difusión del fármaco (Bertucco y Vetter, 2001). De esta manera se consigue que el fármaco penetre en el entramado y que, cuando el sistema se despresuriza, quede retenido en o sobre el polímero (Kikic y col., 2003; Kemmere y Meyer, 2005).

Un fluido supercrítico (FSC) se encuentra en condiciones de temperatura y presión por encima del punto crítico (figura 1.22) y combina propiedades típicas

de los gases (elevada difusividad) y de los líquidos (capacidad disolvente) (Tabla 1.8). Por encima del punto crítico no se produce licuación al aumentar la presión, ni ebullición al elevar la temperatura. El poder disolvente de los fluidos supercríticos depende directamente de su densidad, que se incrementa al aumentar la presión y la temperatura (Luque de Castro y col., 1993).

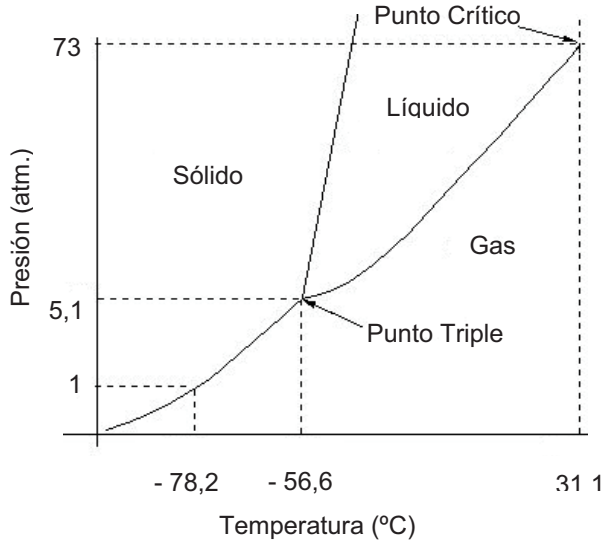

Figura 1.22. *Diagrama de fases del dióxido de carbono.*

Propiedad	Gas	FSC	Líquido
Densidad (kg/m^3)	1	100-8010	1000
Viscosidad (cP)	0,01	0,05-0,1	0,5-1,0
Disfusividad (mm^2/s)	1-10	0,01-0,1	0,001

Tabla 1.8. *Valores característicos de algunas propiedades de los fluidos supercríticos (FSC), en comparación con los de los gases y los líquidos.*

En la tabla 1.9 se resumen las propiedades de algunos disolventes que se utilizan en estado supercrítico para distintas aplicaciones.

FLUIDO	Temperatura crítica (ºC)	Presión crítica (bar)	Densidad crítica (g/cm^3)	Densidad a 400 bar (g/cm^3)	Densidad en estado líquido (g/cm^3)
Xe	16,6	58,4	1,10	2,30	3,08
CHF_3	25,9	46,9	0,52	-	1,51
CO_2	31,3	72,9	0,47	0,96	0,93
N_2O	36,5	72,5	0,45	0,94	0,91
SF_6	45,5	37,1	0,74	1,61	1,91
CCl_2F_2	111,8	40,7	0,56	1,12	1,53
NH_3	132,5	122,5	0,24	0,40	0,60
Butano	152,0	37,5	0,23	0,50	0,58
Pentano	196,6	33,3	0,23	0,51	0,75

Tabla 1.9. *Propiedades físicas de algunos fluidos supercríticos.*

En comparación con los disolventes convencionales, los FSCs presentan importantes ventajas: i) facilitan la transferencia de materia; ii) presentan mayor capacidad solubilizante de compuestos orgánicos; iii) sus propiedades se pueden modular modificando la presión y la temperatura dentro de la zona supercrítica; iv) ofrecen mejores prestaciones a temperaturas bajas; y v) producen menor impacto medioambiental y son más seguros. Los FSCs se utilizan ampliamente como agentes de extracción. Por una simple descompresión se consigue que el FSC pase al estado gaseoso, produciéndose la precipitación de la sustancia extraída, que se recupera fácilmente. El disolvente también se recupera y se puede reutilizar.

El CO_2 se produce en la respiración de los animales y las plantas y en los procesos de combustión y es un componente natural del aire. Por lo tanto, desde el punto de vista de la llamada "química verde" o química respetuosa con el medio ambiente, el CO_2 resulta especialmente atractivo. Aunque se puede separar del aire, en la práctica casi todo el CO_2 que se utiliza comercialmente se obtiene como

subproducto en la síntesis del amoníaco (Weissermel y Arpe, 1997). Sus condiciones de punto crítico se alcanzan a presiones y temperaturas más bajas que para los demás FSCs. Todo ello lo convierte en una opción relativamente barata, eficaz, segura y muy adecuada para las industrias alimentaria y farmacéutica (Srivastava y col., 2003; Brown y col., 2008). El mayor inconveniente radica en que debido a su baja constante dieléctrica es necesario combinarlo con cosolventes, como el agua o el etanol, para disolver compuestos polares. Además, por su carácter de base débil puede reaccionar con algunas sustancias.

En tecnología farmacéutica, el CO_2 supercrítico ha encontrado interesantes aplicaciones en la ingeniería de nanopartículas de fármacos y excipientes y para la optimización de sistemas de liberación de medicamentos (Kawashima and York, 2008). También se está ensayando en la impregnación (*supercritical solvent impregnation* (SSI) de productos sanitarios de naturaleza polimérica, con el fin de dotarlos de funcionalidad como sistemas de liberación de fármacos (Kazarian, 2000; Elvassore y Kikic, 2001; Kikic y Vecchione, 2003; Fleming y Kazarian, 2005; Braga y col., 2008a, b). Este procedimiento ofrece la posibilidad de incorporar fármacos hidrofóbicos, modulando la carga y la profundidad de penetración mediante el control de la temperatura y de la presión (de las que depende la densidad del disolvente), del tiempo de impregnación y de la velocidad de despresurización. El proceso de impregnación raramente altera las propiedades químicas, físicas y mecánicas de las matrices, pero la penetración de las moléculas de fármaco puede favorecer un reordenamiento de las cadenas de polímero y dar lugar a la creación de cavidades de tamaño idóneo para el fármaco (Kazarian, 2000; Kazarian y Chan, 2003; Kikic y col., 2003; Kikic y Vecchione, 2003; Fleming y col., 2005; Fleming y Kazarian, 2005; Kazarian, 2005; Braga y col., 2008 a, b).

En el campo de la administración ocular de medicamentos, la impregnación con fluidos supercríticos se ha aplicado a la preparación de partículas y dendrímeros cargados con cortisona y retinol (Westesen y col., 1997), ibuprofeno (Kazarian y Martirosyan, 2002; Braga y col., 2008a), pilocarpina (Vandamme y Brobeck, 2005), indometacina (Gong y col., 2006), maleato de timolol y flurbiprofeno (Braga y col., 2008a). Recientemente, se ha publicado una primera prueba de la utilidad de la tecnología del CO_2 supercrítico para impregnar lentes intraoculares con flurbiprofen (Duarte y col., 2008) y lentes de contacto blandas comerciales con acetazolamida y maleato de timolol (Costa y col., 2010).

1.6. Aspectos regulatorios: Las lentes de contacto medicadas como productos combinados

Se consideran productos de combinación las asociaciones físicas o químicas de un fármaco con un dispositivo, de un fármaco con un agente biológico o de un dispositivo con un fármaco y un agente biológico; por ejemplo, un anticuerpo monoclonal conjugado con un fármaco, un catéter recubierto con un agente antimicrobiano o una prótesis recubierta con factores de crecimiento. Cuando el producto se comercializa con los componentes separados, éstos se pueden presentar juntos en el mismo envase o bien en envases diferentes con etiquetas en las que se indique explícitamente que deben ser usados de manera conjunta (Lauritsen y Nguyen, 2009).

La OCP (Oficina de Productos Combinados; *http://www.fda.gov/CombinationProducts/default.htm*) de la FDA es la unidad que se encarga de la clasificación de las solicitudes de aprobación de productos de combinación, asignando la competencia primaria al CDER (Center for Drug Evaluation and Research), al CBER (Center for Biologics Evaluation and Research), o al CDRH (Center for Devices and Radiological Health) (figura 1.23).

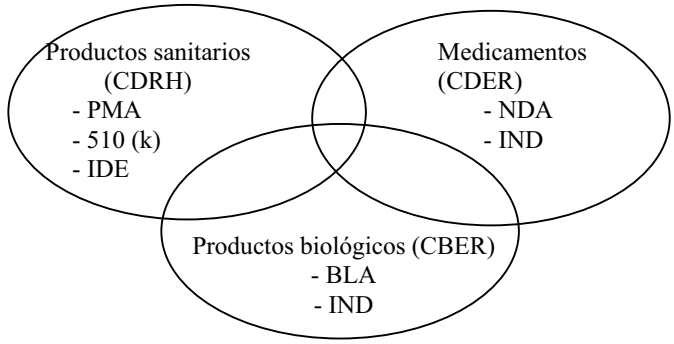

Figura 1.23. *Centros de regulación de la FDA y sus subdivisiones. La autorización del uso de un producto sanitario se puede solicitar por tres vías: solicitud de aprobación con datos clínicos (PMA, premarket approval) para productos sanitarios de Clase III que son susceptibles de causar enfermedades o lesiones; notificación de entrada en mercado (510 (k)) en la que se informa a la agencia regulatoria con 90 días de antelación de la comercialización de un producto sanitario de Clase I o II; o autorización para ensayo clínico (IDE: Investigational device exemption). La autorización para administrar un nuevo medicamento se puede solicitar por dos vías: NDA (new drug application) para comercializarlo o IND (investigational new drug) para llevar a cabo ensayos clínicos. En el caso de los productos biológicos, se puede solicitar la comercialización a través de una BLA (Biologics Licensing Application) o su ensayo clínico a través de un IND (Lauritsen y Nguyen, 2009).*

Dado que los productos combinados están compuestos por dos o más productos regulados (producto biológico, producto sanitario y/o medicamento), cada parte proporciona un modo de acción característico, con lo que tienen más de un modo de acción. La asignación de un producto combinado a uno u otro centro se lleva a cabo basándose en el principal modo de acción del producto (PMOA). La FDA define este concepto como el medio por el que el producto alcanza el efecto o la acción terapéutica prevista, que puede ser el diagnóstico, la curación, el tratamiento o la prevención de alguna enfermedad o un efecto sobre la estructura o sobre una función del cuerpo. La tramitación de los productos combinados cuyo PMOA se debe al fármaco se asigna al CDER, si se debe al producto sanitario al CDRH, y si se debe a un producto biológico al CBER. Aunque todos los centros trabajan conjuntamente en el proceso de aprobación, una vez designado el

responsable, el producto combinado se tiene que ajustar en el modelo de solicitud de comercialización a lo establecido con carácter general en ese centro.

Las lentes de contacto medicadas, al estar constituidas por un producto sanitario con un fármaco embebido en su matriz o anclado en su superficie, reciben la consideración regulatoria de "producto combinado" (FDA) o de "combinación de producto sanitario con una sustancia auxiliar medicinal o con una formulación medicinal" (EMEA). El efecto terapéutico principal se debe al fármaco incorporado en la estructura del dispositivo, si bien éste último juega un papel muy importante en el control de la cesión de la sustancia activa. Además, las lentes de contacto medicadas desempeñan una función propia de un producto sanitario. Si se van a utilizar exclusivamente como dispositivos desde el que se cede el fármaco, todo el sistema se considera como un medicamento y la tramitación de su autorización corresponde al CDER. Si además de actuar como sistema de liberación del fármaco, la lente actúa como correctora de la visión, recibe la consideración de producto combinado y su solicitud de aprobación podrá ser tramitada por el CDER o el CDRH (Novack, 2009). En el caso de que la patente del fármaco esté caducada, la documentación puede tomar como base la investigación clínica o preclínica que se haya llevado a cabo para registrar el producto innovador del fármaco en cuestión. Sin embargo, se requerirá previsiblemente una investigación preclínica adicional en relación con aspectos como la seguridad local, la farmacocinética y la eficacia del fármaco incorporado a la lente medicada.

Planteamiento y objetivos

2. PLANTEAMIENTO Y OBJETIVOS

De la información recogida en el apartado anterior se deduce que las lentes de contacto se han revelado en los últimos años como interesantes plataformas para la liberación controlada de fármacos y macromoléculas terapéuticas destinadas al tratamiento de las patologías que afectan al segmento anterior del ojo. Entre las distintas aproximaciones utilizadas para dotar a las lentes de contacto de capacidad para cargar dosis terapéuticas y cederlas de manera sostenida, el moldeado molecular o "molecular imprinting" se presenta como una técnica que, aunque incipiente en este campo, puede ofrecer prestaciones muy prometedoras. Este procedimiento no requiere cambios importantes en la composición de las lentes -muy condicionada por los requerimientos de citocompatibilidad, transparencia óptica, permeabilidad al oxígeno y propiedades mecánicas- ni la formulación del fármaco en estructuras coloidales, que constituye un elemento

adicional de complejidad en el proceso de síntesis de las lentes. Se pretende lograr un reordenamiento de los monómeros y de las cadenas de polímero que haga posible que se aloje una cantidad suficiente de fármaco en el entramado y que se establezcan interacciones que promuevan una mejor retención de éste cuando la lente se aplica en el ojo. Sin embargo, este planteamiento entra en conflicto con los requerimientos de flexibilidad. El bajo grado de reticulación necesario para que se mantengan las propiedades mecánicas propias de las lentes blandas, determina que las cavidades imprinted creadas durante la síntesis en presencia de la molécula molde presenten una estabilidad física limitada. Para soslayar este importante inconveniente y lograr que la conformación de la cavidad se memorice en el entramado, de forma que aunque se altere se pueda recuperar en presencia del fármaco, es necesario crear cavidades lo más adaptadas que sea posible al tamaño y los grupos químicos del fármaco. Por ello, es muy importante que la naturaleza del monómero funcional se ajuste a las características del fármaco y que la estequiometría fármaco/monómero funcional sea la más adecuada. En general, el cribado y la optimización de los entramados imprinted se viene abordando por procedimientos empíricos de prueba y error, que requieren un importante consumo de reactivos y tiempo y que no garantizan que se llegue a alcanzar el óptimo.

El objetivo genérico de este trabajo de Tesis Doctoral es profundizar en el conocimiento de los factores que condicionan la formación de entramados poliméricos con capacidad para reconocer fármacos o sustancias activas (incluyendo demulcentes) y avanzar en la aplicación de técnicas analíticas y computacionales que permitan abordar el diseño de sistemas imprinted sobre bases racionales. De acuerdo con este planteamiento, un objetivo parcial es evaluar la utilidad de la microcalorimetría isotérmica (ITC) y de la modelización *in silico* para identificar los monómeros funcionales más adecuados y la relación fármaco molde/monómero funcional óptima para sintetizar los entramados. Un

segundo objetivo, directamente relacionado con el desarrollo de lentes de contacto interpenetradas con polímeros demulcentes, fue delimitar el efecto de la porosidad de los entramados sobre la velocidad de cesión del demulcente y el coeficiente de fricción de las lentes. También se planteó un estudio dirigido a establecer la incidencia de la porosidad sobre la permeabilidad a los microorganismos de los hidrogeles acrílicos, un aspecto muy relevante en relación con los problemas de colonización microbiana de la córnea asociados al uso de lentes de contacto blandas y también para una posible aplicación de los hidrogeles acrílicos como apósitos en el tratamiento de úlceras y heridas.

Un objetivo adicional del trabajo fue evaluar las posibilidades que ofrece la impregnación con fluidos supercríticos como procedimiento de incorporación de fármacos a lentes preformadas y también como técnica de post-imprinting, es decir, de creación de cavidades imprinted en lentes de contacto comerciales. El procedimiento convencional de moldeado molecular requiere la incorporación del fármaco en el momento de la síntesis de las lentillas y, por lo tanto, cada lentilla se tiene que diseñar para un fármaco concreto. Por ello, resulta de gran interés la puesta a punto de procedimientos más versátiles que permitan transformar "bajo demanda" lentes comerciales en lentes medicadas con el fármaco que se requiera para una aplicación terapéutica concreta. La solubilización de un fármaco en un fluido en estado supercrítico, capaz de hinchar la estructura de la lentilla y provocar el reordenamiento de sus cadenas para alojar las moléculas del fármaco, debe dar lugar, cuando el fluido se retire por despresurización, al depósito de las partículas del fármaco en la estructura de la lente. Esto podría constituir un procedimiento rápido de carga de fármacos en lentes comerciales. Además, la hipótesis de trabajo es que, una vez que se extraiga el fármaco, es posible que la microestructura de la lentilla haya quedado "marcada" por su presencia, de manera que si vuelve a entrar en contacto con él, por ejemplo por inmersión en una disolución acuosa, es previsible que pueda alojar el fármaco en una cuantía

mayor que las lentes que no hayan sido sometidas previamente a impregnación. De esta manera se obtendría un efecto imprinting en la lente preformada (post-imprinting).

De acuerdo con este planteamiento, el trabajo se ha planificado en las siguientes etapas:

- Desarrollo de lentes de contacto imprinted con norfloxacino y con timolol utilizando la ITC como técnica de cribado de monómeros y de establecimiento de la relación monómero funcional/fármaco óptima.
- Preparación de lentes de contacto con el demulcente polivinilpirrolidona (PVP) interpenetrado en su estructura y evaluación del efecto del peso molecular del polímero y de la proporción de polímero y de agua sobre las propiedades de fricción de las lentes y sobre la velocidad de cesión de la PVP. También se ha estudiado el efecto del agua sobre la porosidad del entramado y se ha evaluado la repercusión de las diferencias en porosidad sobre la permeabilidad de los hidrogeles a los microorganismos.
- Síntesis de entramados imprinted para sales biliares utilizando la modelización computacional como herramienta de cribado de monómeros con afinidad por moléculas específicas y evaluación de los entramados obtenidos como sistemas trampa de ácido cólico. Para ello se construyeron las isotermas de adsorción en modo estático y dinámico y se analizaron utilizando distintos modelos matemáticos.
- Puesta a punto de la tecnología de fluidos supercríticos para cargar lentes de contacto comerciales (Hilafilcon B, Bausch & Lomb) con flurbiprofeno y evaluación del efecto imprinted producido por impregnaciones sucesivas, con el fin de mejorar las prestaciones de las lentes de contacto blandas que se utilizan para corregir defectos de visión como lentes medicadas.

Publicaciones

3. PUBLICACIONES

3.1. Ocular drug delivery from molecularly imprinted contact lenses

Journal of Drug Delivery Science and Technology. En prensa.

Ocular drug delivery from molecularly imprinted contact lenses

Carmen Alvarez-Lorenzo, Fernando Yañez* and *Angel Concheiro*

Departamento de Farmacia y Tecnologia Farmaceutica, Facultad de Farmacia,

Universidad de Santiago de Compostela, 15782-Santiago de Compostela, Spain.

*Corresponding author. E-mail: carmen.alvarez.lorenzo@usc.es

Abstract

Soft contact lenses (SCL) are particularly attractive as drug delivery devices capable of overcoming some limitations of conventional ophthalmic formulations. Although the main use of commercially-available SCL is for correcting ametropia problems, they may also uptake some drugs and release them into the postlens lachrymal fluid, minimizing the clearance and the sorption through the conjunctiva. Novel approaches to enhance the capability of SCL to load drugs and to control the release may make these optical devices to behave as advanced drug delivery systems, fulfilling the requirements of both chronic and acute ocular diseases. Among those approaches, the application of the molecular imprinting technology during SCL manufacture enables the creation in the lens structure of imprinted pockets that memorize the spatial features and bonding preferences of the drug and provide the lens with a high affinity for a given drug. Imprinted SCL could prolong the permanence of the drug in the precorneal area and provide sustained drug levels, increasing ocular bioavailability and avoiding systemic side-effects. In this review, the potential and the advantages/drawbacks of drug-imprinted SCL are critically analyzed and examples of the application of the molecular imprinting technology to β-adrenergic antagonist, antimicrobials, antihistamines and ocular comfort ingredients are shown.

Key words: *soft contact lens - molecular imprinting technology – sustained delivery – drug-eluting device - timolol – norfloxacin – ketotifen – hyaluronic acid.*

1. Ocular topical treatment: general issues

The eye structures can suffer lesions and diseases of varied origin, namely infections and allergic, vascular and degenerative processes [1,2]. Systemic treatments have to face the efficiency of the blood-ocular barriers (blood-aqueous humour, blood-retine, and blood-vitreous humour) against drug penetration [3,4]. Even administering high drug doses, systemic delivery only helps in the treatment of diseases affecting posterior segment of the eye [5]. Direct administration of drugs through topical or, in some severe cases, periocular or intraocular (intracameral or intravitreal) routes has become the main

way of managing ocular disorders affecting the anterior segment of the eye [1,6,7]. Topical treatments combine patient convenience and sufficient safety and efficiency for routinely administration of antimicrobials, antivirals, β-adrenergic blocking agents, miotics, mydriatics, local anesthetics, and anti-inflammatory and antialergic-antihistaminic drugs. Ocular surface disorders, such as dry eye syndrome, require specific topic treatments. Excellent reviews on drug delivery onto the eye can be found elsewhere [8,9]. The following paragraphs seek for highlighting the role of relevant variables that affect the success of conventional ophthalmic formulations but that could be managed, at least partially, by using soft contact lenses (SCL) as ocular drug delivery systems.

After topical administration, the drug may pass through the cornea to the aqueous humour and exert the therapeutic effect, or may be absorbed through the conjunctiva leading to an absorption that it is mostly unproductive [10,11]. The amount of drug that penetrates into the cornea depends on the permeability of the epithelium, the time of permanence of the drug in the precorneal area, and the dynamics of the lachrymal fluid [12]. Drug efflux pumps may also interfere in the absorption [5]. A typical ophthalmic dropper delivers 30 μL, but when blinking occurs the eye can only hold about 10 μL of tear fluid [1]. Additionally, the normal human tear turnover, 10-20% per minute, facilitates the removal of the remaining drug solution from the conjunctival cul-de-sac [13]. Therefore, most of the administered drug is rapidly lost through nasolachrymal drainage, which contributes to important systemic absorption [14], while the fraction of dose that penetrates into the ocular structures is limited to 1-10% [15]. To overcome these limitations, a small volume (ideally 5 to 10 μL) [16] of extremely concentrated solution should be instilled twice within 5 minutes interval, and this sequence reproduced several times a day [17]. This pulsate type of dosing has the drawback of giving rise to extreme fluctuations in ocular level, which increases the risk of untoward side effects.

To prolong the permanence of the drug in the precorneal area and, consequently, to enhance the ocular bioavailability, different types of systems, such as polymeric viscous/mucoadhesive solutions and semisolid formulations, colloidal systems, and inserts, are receiving a great deal of attention [6,18-22]. Ophthalmic solid or semisolid inserts have been envisioned as dosage forms able to provide accurate dosing and

prolonged delivery, and thus to increase the ocular bioavailability [8,20]. Despite the remarkable therapeutic advantages of the inserts, the difficulties of handling, the foreign body sensation, and the high risk of accidental expulsion still limit their practical use. Most of these drawbacks could be overcome, without losing the control release performance, by the use of drug-loaded SCLs.

More than 40 years ago, Sedlacek [23] and Kaufman and coworkers [24] envisioned contact lenses as reservoirs that could slowly release a previously loaded drug. Immersion in aqueous solutions of concentrated drug was the first loading method tested [25-28]. Another way consisted of placing the drug solution in the concavity of the lenses before placed on the eye, or of the instillation of the eye drops on their surface after insertion [29-32]. As shown in recent studies, the drug is released from the contact lens to the post-lens tear film, between the cornea and the lens, where it can remain for long time. During the time interval between blinking the external surface of the lens becomes dry. This causes that the amount of drug that diffuses towards the corneal epithelium is *ca.* 5 times greater than the amount released to the lachrymal fluid that bathes its external surface [33]. This explains why drug pre-soaked or eye-drop splashed contact lenses can improve both ocular bioavailability and pharmacological response, compared to conventional eye drops administration [25,30,31,34]. Therefore, SCLs may be particularly convenient for clinical conditions requiring a high intraocular concentration of drug, such as anterior segment inflammations, angle closure glaucoma or infections. In some cases, drug delivery by contact lenses can even lead to a decrease of the dose required to attain the desired therapeutic effect [32]. The possibility of both correcting the vision and acting as a drug delivery system is expected to remarkably enhance the benefits of SCLs.

2. Therapeutic soft contac lenses

2.1. Background

Development of contact lenses as medical devices for vision correction was possible due to advances in the synthesis and polymerization of acrylic polymers, such as poly(methyl methacrylate) (PMMA) in 1936, and especially of poly(2-hydroxyethyl methacrylate) (PHEMA) in 1954 [35-37]. These materials combine the high optical

clarity of glass with a lower density and better mechanical properties and served as starting point for designing polymers with optimized features for contact lenses [38,39] (Table 1). Oxygen permeability, mechanical strength, optical clarity, resistance to deposition of tear film components, comfort, and easiness of manufacture and of handling and insertion are critical aspects regarding the safety and performance of contact lenses [39,40]. Hydrophobic hard contact lenses have excellent transparency, but their low content in water (<10% w/w) makes the wearer have the sensation of a foreign-body in the eye. Thus, the improvements offered by the more comfortable and oxygen permeable hydrophilic SCLs explain why their use is widespread nowadays. SCLs are flexible slightly cross-linked hydrogels that can absorb and retain large amounts of water (> 35% w/w), in which the oxygen can dissolve and diffuse towards the cornea. In the 1980´s gas-permeable hard lenses appeared in the market as materials with greater oxygen permeability, maintaining the optical clarity and the easiness of handling of hard lenses.[36,39,41] Nowadays, high gas-permeable contact lenses combine silicon elastomer (responsible for the oxygen permeability) with more hydrophilic monomers such as HEMA, N-vinylpyrrolidone (NVP) or methacrylic acid (MAA), for enhancing ions and water permeability and facilitating the on-eye movement of the contact lens [39,42]. The number of people who regularly wear contact lenses (currently *ca.* 125 million people all over the World) is exponentially increasing and it is expected to supersede traditional pairs of glasses [43,44].

Classification	Group	Description	Examples: Material (polymer composition; Brand name)
Hydrophilic	I	Non ionic[a], low water content	Crofilcon A (MMA-GMA; CSI 38), Lotrafilcon A (DMA-siloxane macromer; Focus Night & Day), Polymacon (HEMA-NVP-CMA; Optima FW and Plano T)
	II	Non-ionic[a], high water content	Alphafilcon A (HEMA-NVP-CMA; Soflens 66); Omalfilcon (HEMA-phosphorylcholine; Proclear Compatibles)
	III	Ionic[b], low water content	Balafilcon A (Siloxane macromer-NVP; Pure Vision)
	IV	Ionic[b], high water content	Etafilcon A (HEMA-MA; Acuvue-2), Methafilcon (HEMA-MA ; Kontour 55), Vasurfilcon A (NVP-MMA-AMA-UVAM; Precision UV^{TM}); Vifilcon A (HEMA-MA-NVP; Focus Monthly)
Hydrophobic	I	Without silicon and fluorine	Porofocon A (CAB; RX56), Arfocon (t-butyl styrene; Airlens)
	II	With silicon but not fluorine	Pasifocon (silicone acrylate; Boston II and IV)
	III	With silicon and fluorine	Itafluorocon A (FSC; Equalens), Tisilfocon A (FSC; Menicon Z), Paflucon (FSC; Fluoroperm), Flusifocon (FSC; Fluorex), Enflucon B (FSC; Boston EO)
	IV	With fluorine but not silicon	Fluorofocon A (PPFE; 3M Fluoropolymer)

Table 1. *Classification of contact lenses according to the FDA [40]. All contact lenses shown as examples of the hydrophilic ones are available for therapeutic use or have been used in an off-label manner as therapeutic lenses.*
a: having an ionic content of <1% mole fraction at pH 7.2; b: having an ionic content of >1% mole fraction at pH 7.2.
MMA: methyl methacrylate; GMA: glycerol methacrylate; DMA: N,N´-dimethyl acrylamide; HEMA: hydroxyethyl methacrylate; NVP: N-vinyl pyrrolidone; CMA: cyclohexyl methacrylate; MA: methacrylic acid; AMA: allyl methacrylate; UVAM: ultraviolet absorbing monomer; CAB: cellulose acetate butyrate; FSC: fluoro-siloxane acrylate; PPFE: polyperfluoroether.

FDA classifies contact lenses according to the intended uses as: (1) non-therapeutic contact lenses, e.g. for correction of refractive ametropia, aphakia, and presbyopia; (2) specialized use contact lenses, e.g. for the treatment of keratoconus; and (3) therapeutic contact lenses which have proved to be an effective tool in the management of a wide variety of ophthalmic disorders refractory to other treatment modalities [45]. The aims of

therapeutic contact lenses wear are quite diverse, i.e., relief of ocular pain, promotion of corneal healing, mechanical protection and support, maintenance of corneal epithelial hydration, and drug delivery [46-51]. The use of contact lenses as drug delivery devices, although still infrequent, is attracting a growing attention in the last few years [52-54].

2.1. Conventional contact lenses as drug delivery systems

The feasibility of using drug-loaded soft contact lenses depends on whether the drug and the hydrogel material can be matched so that the lens uptakes a sufficient quantity of drug and releases it in a controlled fashion. Drug uptake by a contact lens depends on both structural features and loading conditions [53]. It has been recently reported that hydrophilic drugs scarcely adsorb on SCL. Cationic substances show some affinity to anionic and hydrated methacrylic acid-based SCL (lens type IV, see Table 1), anionic drugs mainly interact with nonionic and hydrated NVP-based SCL (lens type II), and nonionic substances adsorb on hydrophobic silicone-based lenses (lens type III) [55]. Water content and thickness of the lens, the molecular weight of the drug, and the concentration and time the lens remains in the drug solution strongly determine the rate at which drug penetrates and the total amount loaded [56]. Commercially available lenses require 30 to 60 minutes to approach the maximum uptake, although 24 h may be required to reach equilibrium [26,57,58]. Drug equilibration throughout the lens can remarkably determine the performance as delivery device; when the drug diffuses out from the surface layers, they can be replenished from the deeper part which acts as a reservoir making a more sustained and reproducible release possible [32,59].

Polymacon and alphafilcon A lenses (see Table 1 for lens composition) saturated with ciprofloxacin by immersion in a commercial eye-drop solution for one hour led to remarkably greater drug levels in both cornea (8.03 and 6.43 μg, respectively) and aqueous humour (0.361 and 0.240 μg, respectively) than the direct application of the eye drops (0.45 μg in cornea and 0.007 μg in aqueous humor) [60,61]. Etafilcon A (1-Day Acuvue) lenses, when loaded by immersion in eye-drop solutions, provided higher concentrations of antifungals, aminoglycosides and fluoroquinolones in aqueous humour

than when the eye drops were directly instilled [62-64]. In a study carried out with patients that required cataract extraction, all who preoperatively worn for 4-5 h ofloxacin-loaded lenses and the 92% who worn ciprofloxacin-loaded lenses had aqueous humour concentrations above the MIC_{90} of *Staphylococcus epidermidis* at the beginning of the surgery [64]. The proportion of patients who reached similar levels using the conventional protocol for eye drops instillation was of only the 65% in the case of ofloxacin and the 41% for ciprofloxacin. Since no corneal erosions were observed during the wearing, these findings could be attributed to the reservoir function of the lenses and to a slight hypoxic effect on the cornea which enhanced hydration and epithelial permeability. Recently, vasurfilcon A and etafilcon A lenses loaded with timolol maleate or birmonidine tartrate, respectively, were involved in a short clinical study to evaluate their potential for controlling intraocular pressure (IOP) in patients suffering glaucoma. The results evidenced that 30-min wearing lenses, previously loaded with low amounts of drug, rendered adequate IOP levels [65].

Regarding structural features, an increase in lens thickness or in water content may result in a higher load of drug. For example, thick PHEMA lenses (0.7-1.3 mm) sustained the release of fluorescein, tetracycline or chloramphenicol up to 24 h [66-68] and have been shown useful in the delivery of diethylenetriamine (DETA) or disodium ethylenediamine tetraacetate (EDTA) for the treatment of severe acid and lime burns, or of cystein hydrochloride for the treatment of corneal burns and ulcers [51]. In comparison with classical ocular therapy, the use of drug-loaded thick-lenses shortened the period of treatment by half. However, the practical possibilities of increasing the thickness of the lenses are limited not only by comfort reasons but also by the requirements of oxygen permeability (which inversely correlated to the thickness) [39]. On the other hand, the aqueous phase of the SCL is the only place available to host drugs that do not specifically interact with the network. At equilibrium, the drug concentration in the aqueous phase of the hydrogel equals to that in the loading solution [69]. Thus, the higher the content in water and the aqueous solubility of the drug, the greater the amount of drug that can be loaded [70]. This explains that, for example, high water content (71%) Permalens lenses provide greater tobramycin concentrations in corneal tissue when the antibiotic is instilled on the lens, and for longer periods of time, than low water content (38.6%) Plano T

therapeutic lenses [31]; although the sustaining of the release is in general more efficient from low water content lenses [59]. Oppositely to SCL, high permeable silicone-based lenses showed an exponential decrease in oxygen permeability as the water content raises [71], which limits their potential as drug reservoirs. Several comparative studies about the uptake and release performance of silicon-based and PHEMA-based commercial contact lenses have been recently reported elsewhere [72,73].

The main drawback for a general use of SCL as drug delivery systems is their poor affinity for most drugs [74]; for example, PHEMA lenses load amounts of chloramphenicol, epinephrine and pilocarpine similar to those taken up by the intact human crystalline lenses [75,76]. Thus, the lenses generally provide only one-tenth of the aqueous humour concentration that can be achieved when eye drops are used [75-77]. On the other hand, when the loading is carried out by immersion in a concentrated drug solution, most drug is not loaded but wasted. Drug-loading may also cause conformational changes and discoloration of the lenses, damaging their optical properties. In the few cases in which the loading can be enough for therapeutic purposes, the major limitation lies in the fact that the release occurs far too quickly to maintain therapeutic levels in the ocular structures for long enough periods of time [36,51,72,77]. More infrequently, drug-loaded SCL can lead to an excessive contact time between drug and cornea, exacerbating the topical drug side effects [52].

The performance of the drug-loaded lenses described above is mostly constrained by the fact that the drug passively diffuses through the aqueous phase of the network without interacting with the polymeric structure. This causes a limitation in both the amount loaded and the control of the release, which is deficient in the absence of mechanisms of drug retention in the hydrogel [72]. Over the last few years, a better understanding of the mechanisms involved in the release of solutes from hydrogels and the application of new technologies for a better loading and release behavior has led to a revival of the interest of drug-eluting SCLs. The following approaches are being explored to improve the performance of SCLs as drug delivery devices: i) chemically-reversible immobilization of drugs through labile bonds [69,78, 79]; ii) incorporation of drug-loaded colloidal systems

into the lens [80-84]; iii) copolymerization with functional monomers able to interact directly with the drug [85-87]; and iv) molecular imprinting [53,54,88]. Of course, in all cases, the final system should maintain the oxygen permeability, the hydrophilicity, and the optical, morphological and mechanical properties required for SCLs. Furthermore, too strong and irreversible binding of the drug has to be avoided [85]; otherwise the lens would not release the drug. General reviews on the peculiarities and the advantages/limitations of each approach can be found elsewhere [5,8,53,54,69]. The present review specifically focuses on the peculiarities of the molecular imprinting approach and the state-of-art of drug-imprinted SCLs.

3. Molecularly-imprinted contact lenses

3.1. Molecular imprinting technology

Monomers possessing chemical groups able to interact with a given drug may remarkably raise the affinity of SCLs to the drug; such monomers are named "functional". The interaction should be enough to increase the drug partition coefficient between the polymeric network and the loading solution and, thus, to drive the drug uptake. It has to be kept in mind that the list of monomers approved for preparing SCL is quite limited and, consequently, the possibilities of using the most suitable monomer to interact with a certain drug become restricted [86,87,89]. Furthermore, the proportion of functional monomers should be the result of a compromise between the achievement of the functionality as drug vehicles and the maintenance of the dimensions of the lens under the pH, temperature or osmotic pressure conditions which the lens has to face up during handling and wearing.

Molecular imprinting technology pursues the optimization of the spatial distribution of the functional monomers in order to achieve the maximum efficiency of the interactions between the drug and the polymeric network. This technology, which uses the target molecules (in our case the drug) as templates during polymerization, has been progressively developed along the last forty years as a tool for endowing rigid highly cross-linked polymeric systems with the ability to recognize target species [90]. The traditional conception of molecular imprinting is to engrave the drug structure on the

polymer network by creating “tailored-active sites” or “imprinted pockets” with the size and the most suitable chemical groups to interact with the drug [91]. The template molecules are added to the monomers solution (including backbone monomers, functional monomers and cross-linker) and allowed to arrange as a function of their affinity before polymerization [92]. The sequence and the spatial arrangement of the monomers is fixed upon polymerization (Figure 1). The molecular-scale regions with higher affinity for the drug (i.e., monomers surrounding the drug molecules during polymerization) are expected to reveal, upon washing out the drug molecules that served as templates, “imprinted pockets” or receptors that memorize the spatial features and bonding preferences of the template. If so, when the polymer network comes again into contact with the target molecules, they are efficiently accommodated into the high affinity cavities.

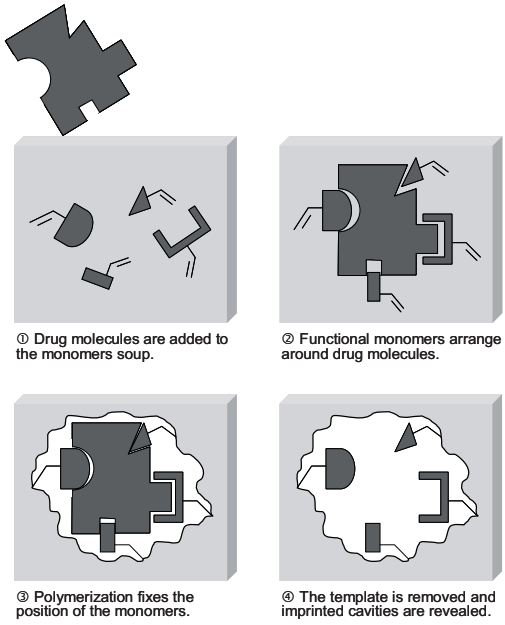

Figure 1. *Scheme of the molecular imprinting process for obtaining hydrogels with high affinity for the template drug.*

There are two main approaches to regulate the functional monomer/template association previous to the polymerization: i) the pre-organized or covalent approach; and ii) self-assembly or non-covalent approach. In the pre-organized or covalent approach, the

template is covalently bound to the monomers prior to polymerization [92-93]. The bonds are reversibly broken after the synthesis of the networks to form the imprinted cavities. In the self-assembly or non-covalent approach, the template molecules and functional monomers arrange themselves, prior to polymerization, to form stable and soluble complexes of appropriate stoichiometry by non-covalent or metal coordination interactions [94-96]. In this case, multiple-point interactions between a template molecule and various functional monomers are required to form strong complexes. In general, the non-covalent imprinting protocol enables more versatile combinations of templates and monomers, and provides faster bond association and dissociation kinetics than the covalent imprinting approach [6]. In either case, the preparation of conventional molecularly imprinted polymers (MIPs) requires the co-polymerization of the functional monomer-template complexes with high proportions of cross-linking agents in a porogen solvent, and the subsequent removal of the template molecules, in order to reveal the recognition cavities complementary in shape and functionality to the template molecules (i.e., specific receptors) [96].

Simple polymerization in the presence of a drug (chemically stable enough to endure the polymerization conditions) does not ensure an imprinting effect. The success of the imprinting strongly depends on the stability and solubility of the functional monomers-target assemblies during polymerization. If the molar ratio in the complex is not appropriate [97] or if the assemblies dissociate to some extent during polymerization [98], the functional monomers would be far apart from both the template and each other, resulting in a small difference between imprinted and non-imprinted (conventional) networks. The polymerization should be carried out at the lowest temperature possible to shift the equilibrium toward the formation of target-monomers complexes [91,98]. From this point of view, polymerization by UV irradiation at room temperature would be preferable, compared to heating, whenever the template remains stable.

Highly cross-linked MIPs are being shown useful in selectively rebinding the target molecules from mixtures of chemical species, and thus have aroused interest to a wide range of applications, including solid phase extraction, environment remediation, chromatography, sensors, immunoassay or artificial catalyse [99-101]. In the last few

years, the molecular imprinting technique has also received increasing attention in the drug delivery field as a way to obtain affinity-regulated and feed-back controlled drug release [88, 102-109].

3 2. Molecularly imprinted contact lenses

A distinguishing key feature of SCLs is their much lower cross-linking density, compared to the polymer networks to which molecular imprinting is routinely applied. Conventional imprinting is like to engrave the structure of the template drug molecule in a rigid plastic [110]. By contrast, flexibility is a priority property of SCLs and, thus, the cross-linker should not be above 10 mol% (or carefully chosen to enable flexibility at greater proportions [88]). This may cause a detriment in the physical stability of the imprinted cavities. Swelling of the network in the lens preservation fluids or in the lachrymal fluid is likely to distort the structure of the imprinted pockets. T. Tanaka´s group pioneered the application of molecular imprinting technology in hydrogels, realizing that only high affinity cavities can memorize the structural features of the drug and undergo an "induced fit" in presence of the drug recovering the same conformation as upon polymerization [111-116]. In such a way loosely cross-linked imprinted hydrogels try to mimic the recognition capacity of certain biomacromolecules (e.g. receptors, enzymes, antibodies). Natural evolution has determined the unique details of protein´s native state, such as its shape and charge distribution, that enable it to recognize and interact with specific molecules [117]. Based on biomimetic principles, SCLs endowed with such high affinity imprinted pockets are expected to be able to load the drug and, subsequently, to sustain the release.

Another critical point is the solvent used to prepare the monomers and template solution. The solvent should not interfere or compete with the target molecules for the interactions with the functional monomers. Conventional MIPs are synthesized using organic solvents to give a macroporous structure that enables the access of the target molecules to the receptors. In the case of SCLs, it would be preferable to avoid the use of solvents, taking advantage of the liquid state of the main monomers. Therefore, a highly precise design of imprinted SCLs is mandatory to achieve an optimum balance between

the mechanical properties required for the ocular application and the stability of the imprinted cavities in the lens structure required for drug affinity and selectivity.

Research on drug-imprinted SCLs has focused so far on three therapeutic groups, namely β-adrenergic antagonists (timolol), antimicrobials (norfloxacin), and antihistamines (ketotifen), and two comfort ingredients (polyvinylpyrrolidone and hyaluronic acid). Figure 2 depicts the structure of these template molecules. Only non-covalent imprinting techniques have been applied until now.

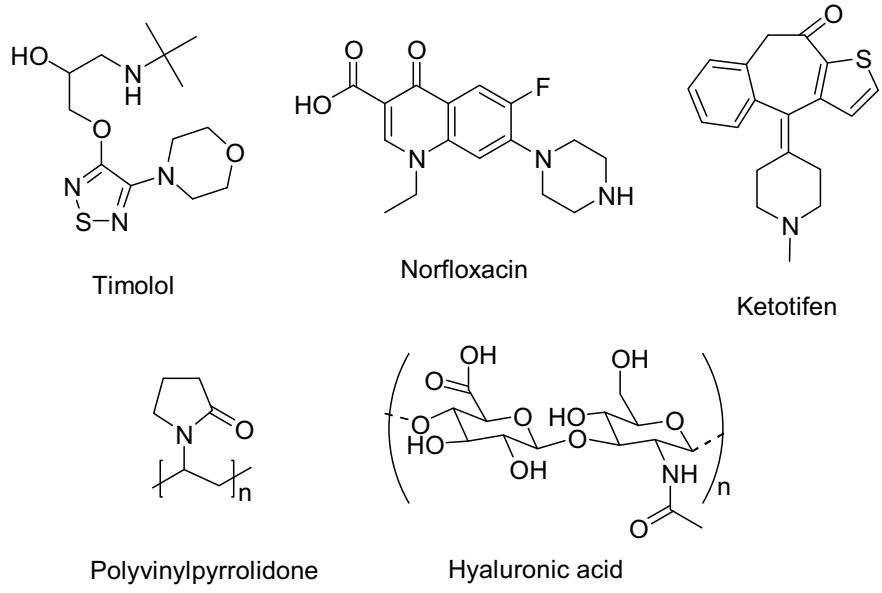

Figure 2. *Structure of drugs and comfort ingredients tested as templates for creating molecularly imprinted SCL.*

3.2.1. Timolol-imprinted SCL

Glaucoma is a multifactorial optic neuropathy that, although asymptomatic in its earlier stages, may lead to irreversible blindness. Thus, an active search for improving the efficacy of the topical medications is being carried out [118]. Timolol is a beta-adrenergic

blocking agent widely used for the treatment of glaucoma. Nevertheless, the permeability of the conjunctiva to timolol is very significant and similar to that of the cornea [119]. Consequently, upon topical delivery through ophtalmic drops, most timolol dose is absorbed into the blood stream and can induce severe cardiovascular and pulmonary side effects [120]. Timolol-loaded SCLs aim to reduce the non-productive absorption and to minimize the side effects. On the other hand, timolol structure is particularly suitable for providing imprinted systems since it offers multiple sites for interacting with functional monomers through ionic and hydrogen bonds [110]. Timolol does not interfere in the polymerization process and the hydrogels are optically clear and, once wet, show adequate mechanical properties. Therefore, a comprehensive study of the incidence of the nature of the functional monomer and the backbone monomer, the degree of cross-linking and the drug:functional monomers ratio on the loading and release performance of the lenses was carried out by our group.

As a first step, non-imprinted (conventional) and imprinted (synthesized in the presence of 23 mM drug) PHEMA hydrogels with particularly low cross-linking density (0.128 mol%) and 0.7 mm thickness were prepared using as functional monomers methacrylic acid (MAA) or methyl methacrylate (MMA) in a concentration range of 0 to 5.12 mol% [111]. Once polymerized, the hydrogels were cleaned by immersion in boiling water for 3 minutes. Although only 30% timolol was lost during boiling, this step can be avoided if the polymerization is complete and no residual monomers are expected [121]. The imprinted hydrogels were able to sustain the release of the remaining drug for several hours; the release rate being greatly determined by the nature of the functional comonomers and the characteristics of the release medium (0.9% NaCl solution pH 5.5, phosphate buffer pH 7.4, or artificial lachrymal fluid pH 8) (Figure 3). Despite presenting a similar ionic strength, the differences in the nature of the ions and on pH of the medium profoundly conditioned the uptake of water by the hydrogels and the strength of the interactions of the drug molecules with the functional groups. At pH >7, most MAA groups are ionized (cross-linked polyMAA has an apparent pKa that rises from 6 to 9 with increasing ionization [122]) and the hydrophilicity of the hydrogels raises, while the ability to interact with the drug through hydrogen or hydrophobic bonds decreases and,

therefore, the drug release rate is speeded up. By contrast, the more hydrophobic hydrogels prepared with MMA showed a slower release rate because timolol finds it more difficult to move from the hydrophobic network into the aqueous environment. Once the drug was released, the imprinted PHEMA hydrogels prepared with the lowest MAA proportion were able to reload 3 times more timolol than the non-imprinted hydrogels, from a pH 5.5 drug solution; showing a release rate similar to that upon polymerization.

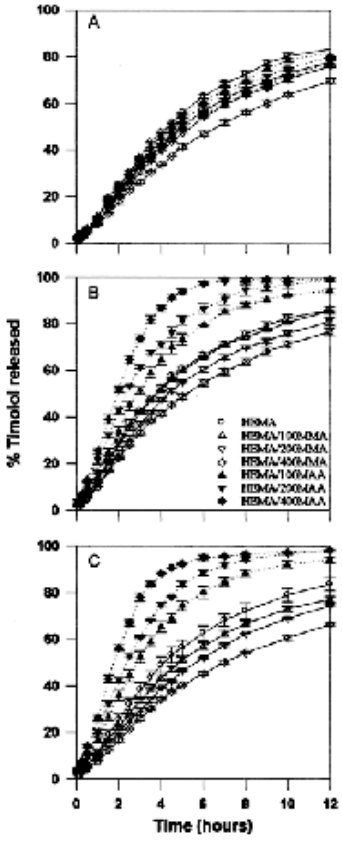

Figure 3. *Timolol release at 37°C from imprinted hydrogels (A) in 0.9% NaCl solution (pH 5.5), (B) in phosphate buffer (pH 7.4), and (C) in artificial lachrymal fluid (pH 8). The legend for all plots is the same as in plot B (open symbols, HEMA hydrogels only or with MMA; full symbols, HEMA hydrogels with MAA). Reproduced from [111] with permission of Wiley.*

Further studies with imprinted lenses based on HEMA or N,N-diethyl acrylamide (DEAA), and synthesized with different proportions of MAA (1.28-5.12 mol%) and cross-linker EGDMA (0.32-8.34 mol%), revealed that a minimum of 0.9 mol% EGDMA was required to achieve remarkably greater loading (one order of magnitude) compared to the non-imprinted lenses, although DEAA-based lenses sustained the release disregarded

being imprinted or not [112]. The imprinted lenses could load a therapeutic dose of timolol, sustain its release in lachrymal fluid for more than 12 h and reload another dose overnight, being ready for use the next day [111,112].

In order to generalize the applicability of the molecular imprinting technology to manufacture therapeutic SCLs, the influence of the backbone monomers was analyzed keeping the proportions of the functional monomer (MAA, 100 mM) and cross-linker (EGDMA, 140 mM) constant (Table 2) [114]. Four backbone compositions were chosen: i) N,N-diethylacrylamide (DEAA), ii) 2-hydroxyethylmethacrylate (HEMA), iii) 1-(tristrimethyl-siloxysilylpropyl)-methacrylate (SiMA) and N,N-dimethylacrylamide (DMAA) 50:50 v/v, and iv) MMA:DMAA 50:50 v/v solutions. Lenses of 0.3-mm thickness were prepared by UV irradiation in the presence of timolol maleate (25 mM). The backbone monomers remarkably determined the glass transition temperature, the equilibrium water content and the drug loading and release properties. Drug sorption isotherms in water at 37 ºC revealed that the overall affinity of the lenses for timolol ranked in the order HEMA>SiMA-DMAA>MMA-DMAA>DEAA. The highest imprinting effect, i.e., the greatest relative increase in overall affinity respect to non-imprinted systems, was obtained for the last two systems which contain the backbone monomers with lower affinity for timolol [114]. In the hydrated non-imprinted lenses, MAA groups are too far apart to form binding sites for timolol. By contrast, the imprinting procedure provides cavities made of groups of MAA spaced close together and considerably increases the loading capacity. All lenses showed sustained release in 0.9% NaCl solution over 2-8 hours (Figure 4). Timolol diffusion coefficients through the imprinted lenses were 2.2×10^{-9} cm^2/s for DEAA-based lenses, 9.9×10^{-9} cm^2/s for HEMA-based lenses, 66.5×10^{-9} cm^2/s for MMA–DMAA-based lenses, and 71.3×10^{-9} cm^2/s for SiMA–DMAA-based lenses. These values confirmed that timolol molecules move out easier from hydrophilic networks that possess low affinity for the drug (i.e. MMA-DMAA and SiMA-DMAA).

Lens		Monomers						
		DEAA	HEMA	MMA	SiMA	DMAA	MAA	EGDMA
A	mL	4					0.034	0.105
	mol	30.17					0.401	0.583
	mol%	96.84					1.29	1.87
B	mL		4				0.034	0.105
	mol		32.92				0.401	0.583
	mol%		97.10				1.18	1.72
C	mL			2		2	0.034	0.105
	mol			18.78		19.41	0.401	0.583
	mol%			47.94		49.55	1.02	1.49
D	mL				2	2	0.034	0.105
	mol				4.44	19.41	0.401	0.583
	mol%				17.87	78.17	1.62	2.35

Table 2. *Composition of the timolol-imprinted SCL prepared with different backbone monomers. Reproduced from [114] with permission of Elsevier.*

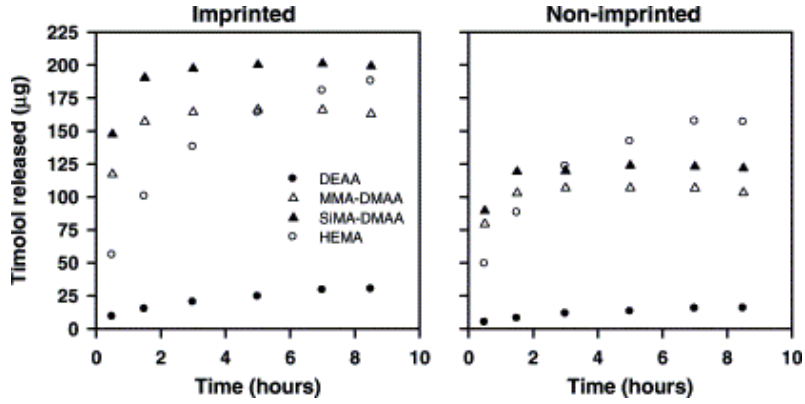

Figure 4. *Timolol release in 0.9% NaCl solution at 37°C from reload imprinted and non-imprinted lenses made with different backbone monomers. Drug diffusion coefficients through the imprinted lenses were 2.2×10^{-9} cm^2/s for DEAA systems, 9.9×10^{-9} cm^2/s for HEMA systems, 66.5×10^{-9} cm^2/s for MMA–DMAA systems, and 71.3×10^{-9} cm^2/s for SiMA–DMAA systems. Reproduced from [114] with permission of Elsevier.*

Ultrathin DEAA-based lenses (14 mm diameter and 0.08 mm center thickness) evidenced the suitability of the imprinted networks for controlled timolol delivery *in vivo*. Timolol levels in rabbits´ lachrymal fluid were monitored after the insertion of imprinted lenses (34 □g drug) and non-imprinted lenses (20 µg drug) and after the instillation of

timolol eye-drop solutions of 0.068% (total dose 34 μg) or of 0.25% (commercial solution, total dose 125 μg) (Figure 5) [115]. The imprinted lenses were able to maintain the timolol release for 180 min, compared to the 90 min of the non-imprinted lenses. Both displayed the maximum ocular level at around 5 min, followed by a monoexponential decay. Irrespective of the initial concentration, timolol applied as drops was flushed out of the eye in less than 60 min. Furthermore, the area under the timolol concentration-time curve (AUC) was 3.3-fold and 8.7-fold greater for imprinted contact lenses than non-imprinted ones and eyedrops, respectively. The capability of SCL to sustain the drug levels in the tear fluid was proportional to the amount of drug loaded. These results indicate that imprinted SCLs reduce the precorneal elimination of the drug compared to the eyedrops and, in consequence, much smaller amount of drug is needed to achieve the desired therapeutic levels.

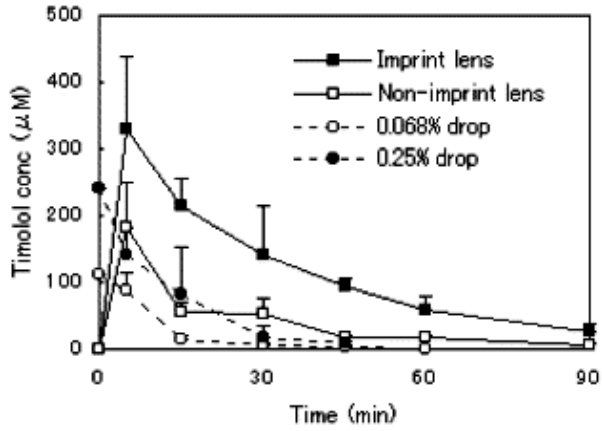

Figure 5. *Timolol tear fluid concentration-time profiles after application of presoaked imprinted and non-imprinted contact lenses and instillation of eyedrops. The doses were 34 μg for imprinted contact lens, 21 μg for non-imprinted contact lens, 34 μg for 0.068% timolol eyedrop, and 125 μg for 0.25% timolol eyedrop. Each point represents the mean±S.D. (n=3–5). Reproduced from [115] with permission of Elsevier.*

Finally, the influence of timolol/functional monomer molar ratio was analyzed in detail using lenses prepared with DMAA and tris(trimethylsiloxy)silylpropyl methacrylate (TRIS) (50:50 v/v) as backbone monomers, and MAA and EGDMA as functional monomer and cross-linker, respectively [116]. Timolol release rate strongly

decreased by increasing the MAA:timolol ratio in the gel recipe from 4:1 to 16:1. Lenses (0.3 mm thickness) prepared with timolol:MAA 1:16 mole ratio showed drug diffusion coefficients two orders of magnitude lower than those obtained with non-imprinted hydrogels. This considerable influence of the timolol:MAA ratio is related to differences in conformation of the imprinted cavities [97,98]. Large timolol:MAA ratios lead to imprinted pockets with insufficient MAA units to fulfil the interaction capacity of the drug. Such binding sites show weak affinity for timolol and deliver it quite easily. Oppositely, as the relative amount of timolol decreases, more MAA units are available to gather during synthesis to form efficient imprinted cavities with greater multiple-point binding constants. Each binding site is more perfectly constructed and its affinity for timolol delays the release process.

3.2.2. Norfloxacin-imprinted SCL

Ocular infections are relatively frequent and its treatment requires the instillation of eye-drops each 30-120 min during the first days [123]. Additionally, the use of SCLs itself promotes the biofilm formation and notably enhances the risk of ocular infections [124-126]. Therefore, the improvement of antibiotic loading and release properties of SCLs, maintaining their utility to correct ametropia problems, is of a paramount practical importance. Norfloxacin is a fluorquinolone with a broad–spectrum activity against Gram+ and Gram- bacteria, including *P. aeruginosa*, *S. aureus* and *E. coli* [127], that shows relatively good intra-corneal and intra-cameral penetration.

Norfloxacin structure makes the drug suitable to interact simultaneously with various functional monomers. It possesses a carboxylic acid (pKa_1= 6.34 ±0.06) and an amino group (pKa_2= 8.75 ±0.07), which can electrostatically interact with ionized groups of other molecules, and an aromatic ring that can establish hydrophobic interactions. Norfloxacin-imprinted lenses were designed applying analytical tools that enable to predict the optimum template/functional monomer ratio before polymerization. The study of the interactions between monomers and template molecules using NMR, UV spectrophotometry or isothermal titration calorimetry (ITC) [128-131] is gaining interest

as a way to obtain accurate information for creating imprinted networks, avoiding the time and material expenses of trial/error assays.

Preliminarily, two functional monomers were tested: i) 4-vinyl pyridine, which is a weak base (pK_b = 8.5; [132]) with affinity for acid groups and also able to interact with aromatic groups through π-π stacking, and ii) acrylic acid (AA) (pK_a = 4.5) that can potentially interact with protonizable amino groups or with hydrogen bond acceptor groups. Hydrogels prepared with these monomers revealed that only AA exhibits affinity for norfloxacin. Then, the interactions between norfloxacin and AA in HEMA solution were deeper evaluated by ITC, titrating the AA solution (0.50 M, 0.290 ml) onto the drug solution (0.01M, 1.439 ml) [133]. A strong exothermic interaction with an inflexion point at norfloxacin:AA 1:1 molar ratio was observed (Figure 6). The addition of greater amounts of AA resulted in a progressively lower change in enthalpy, and the binding finally saturated at 1:4 molar ratio. This ratio was considered as the most adequate to create high-affinity receptors in the lens structure.

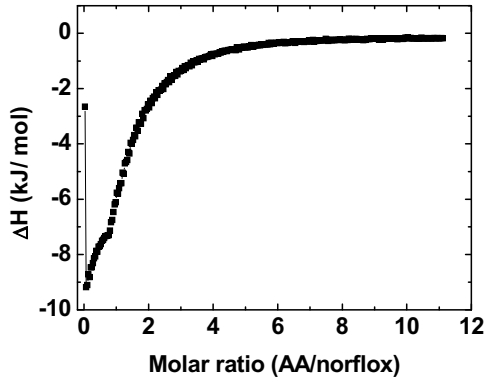

Figure 6. *ITC titration at 298 K of norfloxacin (NRF) 0.01 M with AA 0.50 M in HEMA solution. Reproduced from [133] with permission of Elsevier.*

To experimentally confirm the ITC predictions, PHEMA-based hydrogels were synthesized using norfloxacin:AA molar ratios ranging from 1:2 to 1:16, at two fixed AA total concentrations; the cross-linker molar concentration being 1.6 times that of AA. Control (non-imprinted) hydrogels were prepared similarly but with the omission of

norfloxacin. All hydrogels showed a similar degree of swelling (55%) and, once hydrated, presented adequate optical and viscoelastic properties. After immersion in norfloxacin solution of various concentrations, imprinted hydrogels loaded greater amounts of drug than the non-imprinted ones. Furthermore, imprinted hydrogels synthesized using norfloxacin:AA 1:3 and 1:4 molar ratios released the drug at a rate 3.5-times lower than non-imprinted hydrogels (Figure 7). These results confirmed the interest of ITC for the optimization of the structure of the imprinted cavities and evidenced the potential of norfloxacin-imprinted SCL as 24-hours controlled release devices. Hydrogels of various AA contents and thicknesses synthesized using the norfloxacin:AA 1:4 molar ratio exhibited similar loading/release behavior, proving the robustness of the imprinting technique developed.

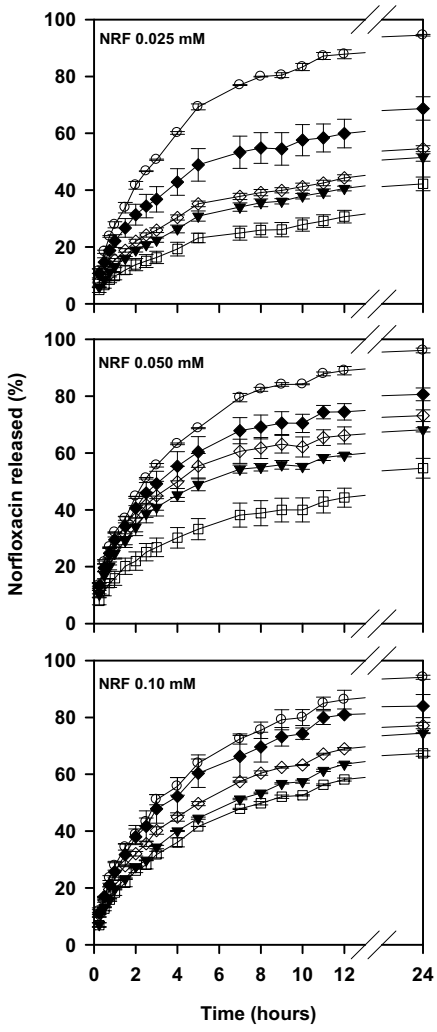

Figure 7. *NRF release profiles in lachrymal fluid from PHEMA hydrogels synthesized with AA 200 mM and EGDMA 160 mM using different NRF:AA molar ratios; zero, i.e. non-imprinted hydrogels (○), 1:16 (♦), 1:10 (◊), 1:6 (▼), and 1:4 (□). The hydrogels (thickness 0.4 mm) were previously loaded by immersion in 0.025 mM, 0.050 mM or 0.10 mM NRF solutions (n=3). Reproduced from [133] with permission of Elsevier.*

3.2.3. Ketotifen-imprinted SCL

Seasonal and perennial allergic conjunctivitis have a high prevalence; wearing of SCL itself may contribute to induce or exacerbate the symptoms. Topical antihistamines with multiple actions (mast cell stabilization, and antiinflammatory and antihistaminic actions) are considered as the best treatment option, thanks to their rapid action, safety and convenience of use [134]. Byrne et al. group have designed imprinted SCL with the

antihistamic drug ketotifen fumarate according to rational principles. They chose the functional monomers that are more similar to the chemical groups present in histamine H1-receptor, in order to mime the non-covalent interactions responsible for the docking of the antihistamine in the physiological receptor [135]. HEMA, AA, NVP and acrylamide (AM) were selected as monomers taking into account that residues such as aspartic acid, lysine, arginine and tyrosine form the active site in the H_1-receptor. The guiding hypothesis was that if antihistamines have high affinity for the H_1-receptor, a hydrogel with similar chemical functionality would bind the antihistamine tightly, increase loading, and show delayed release kinetics. The hydrogels were prepared by photopolymerization starting from 5 mol% cross-linker (polyethylene glycol 200 dimethacrylate, PEG200DMA) and 95 mol% functional monomers (92 mol% HEMA and 3 mol% other functional monomers) [136].

Differential scanning photocalorimetry analysis evidenced that the pre-polymerization arrangement of the monomers induced by the presence of the template molecules, ketotifen fumarate, constrains certain monomer configurations and leads to physical restrictions on free radical and propagating chain diffusional motion. Such constrains to the movement lowers the rate of polymerization; the slower the polymerization rate, the more perfect the drug receptors formed in the polymer network. Nevertheless, no differences in swelling degree, mechanical or optical properties between imprinted and non-imprinted networks were observed [135]. The most biomimetic formulation, poly(AA-*co*-AM-*co*-NVP-*co*-HEMA-*co*-PEG200DMA), demonstrated six times enhanced loading over the control network and three times enhanced loading over the networks containing one or two functional monomers. Sustained delivery of therapeutically relevant concentrations of drug was observed over 2 days in salt aqueous solution. Interestingly the release profile in artificial lachrymal fluid containing lysozyme was even remarkably slower (sustained for 4 days), suggesting that *in vivo* the delivery should be extended for several days (Figure 8).

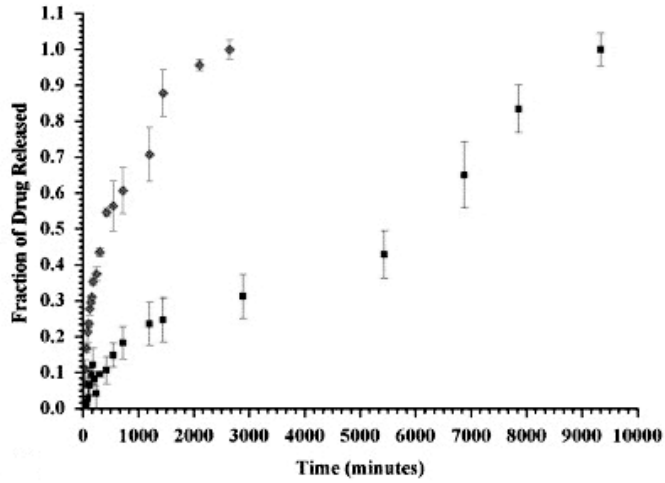

Figure 8. *Ketotifen release profiles from a poly(AA-co-AM-co-HEMA-co-PEG200DMA) network in artificial lachrymal fluid without (grey diamonds) and with lysozyme (black squares). Reproduced from [135] with permission of Elsevier.*

A deeper study of these hydrogels revealed that the drug partition coefficients for the imprinted networks were at least two times greater that for the control networks. The partition coefficients were 5.65, 7.13, 18.06 and 45.05 for poly(AA-co-HEMA-PEG200DMA), poly(AM-co-HEMA-PEG200DMA), poly(AA-co-AM-co-HEMA-PEG200DMA) and poly(AA-co-AM-co-NVP-HEMA-PEG200DMA) networks, respectively, when the hydrogels were placed in ketotifen fumarate aqueous solutions (0.4 mg/mL). Poly(AA-co-AM-co-NVP-co-HEMA-PEG200DMA) imprinted networks exhibited a ketotifen fumarate diffusion coefficient of $5.57 \cdot 10^{-10} cm^2/s$, which was a factor of 9, 7.2, and 13.8 less than poly(AA-co-HEMA-PEG200DMA), poly(AM-co-HEMA-PEG200DMA), and poly(AA-co-AM-co-HEMA-PEG200DMA) imprinted networks, respectively [137]. Thus, the imprinted lenses are endowed with an outstanding ability to sustain ketotifen release.

Dynamic *in vitro* drug release studies using a novel microfluidic device that simulates the flow rate (3 μL/min), tear volume and tear composition of the eye, confirmed the

improved performance of the imprinted hydrogels possessing multiple functional monomers. Under infinite sink conditions, imprinted SCLs showed Fickian (concentration dependent, Figure 9) release kinetics with diffusion coefficients ranging from $4.04 \cdot 10^{-9}$ to $5.57 \cdot 10^{-10}$ cm^2/s.

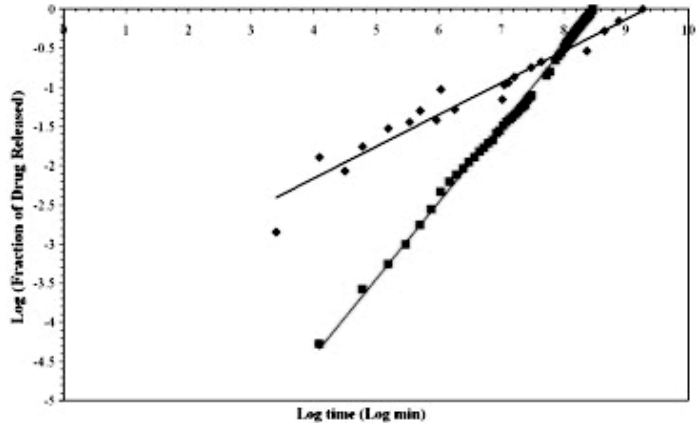

Figure 9. *Zero-order release of ketotifen for imprinted lenses in physiological flow. The slope yields n, where n − 1 is the order of release, for the infinite sink method (diamonds, n = 0.406 ± 0.022) and the physiological flow case utilizing the microfluidic device (squares, n = 0.981 ± 0.006, zero-order) for poly(AA-co-AM-co-NVP-co-HEMA-co-PEG200DMA) networks. Reproduced from [138] with permission of Elsevier.*

The highest functionalized imprinted network exhibited a diffusion coefficient averaging ten times smaller than less functionalized hydrogels and released drug for over 5 days with 3 distinct rates of release. On the other hand, under physiological volumetric flow rates, the release rate was constant for 3.5 days delivering a therapeutically relevant dosage according to zero-order release kinetics (Figure 8). The zero-order release is achieved by reducing the concentration gradient through the accumulation of ketotifen in the slow moving fluid at simulated physiological tear turnover rates. Therefore, micro/nanofluidic devices may be useful for predicting drug release rates from drug-loaded SCL under physiologic-like conditions [138].

3.2.3. Comfort ingredient-imprinted SCL

Dry eye syndrome encompasses a heterogeneous group of ocular surface disorders characterized by abnormal tear film, which causes inadequate ocular lubrication [139]. When the homeostasis of the tear film is lost due to insufficient supply, excessive loss or anomalous composition of tears, its ability to protect the ocular surface epithelium decreases. As a consequence, dry eye syndrome involves ocular surface epitheliopathy, tear hyperosmolality, unstable pre-ocular tear film, and more or less intense inflammation and ocular irritation [140]. This syndrome affects to 10-20% in adult population [139], but the prevalence rises up to the 70% of contact lenses wearers [141].

Although the prevention and management of DES requires a global approach [139], it has been observed that drops of hydrophilic polymers may act as tear film stabilizer, lubricating the lens, reducing the friction with the ocular tissues and washing out foreign bodies. There are six main categories of ophthalmic demulcents established by the FDA, which can be found in ophthalmic drops and artificial tears in concentrations ranging 0.1 to 2% [142]: (a) Cellulose derivatives: carboxymethylcellulose sodium, hydroxyethyl cellulose, hypromellose, methylcellulose; (b) Dextran 70; (c) Gelatin; (d) Polyols, liquid: glycerin, polyethylene glycol 300, polyethylene glycol 400, polysorbate 80, propylene glycol; (e) Polyvinyl alcohol; (f) Polyvinyl pyrrolidone (povidone). An advanced group of substances for the soothe of the ocular surface, named as “comfort-ingredients”, includes hyaluronic acid. This naturally-occurring polymer possesses a high ability to retain water, leading to viscoelastic solutions that remain for longer periods of time on the ocular surface, and has already shown to promote wound healing [143].

Few years ago, hydrophilic polymers began to be incorporated to the SCL structure with the aim of wrapping the lens with a cushion-like layer, softening the contact with the eye and the lid [144,145]. For example, polyvinyl alcohol (PVA) can be found in some already commercialized SCLs with the purpose of enhancing wettability and wearer comfort [145,146]. An additional feature of the polymer-loaded SCLs is that could sustain the release of the hydrophilic polymer for the whole period of time most disposable lenses are used (one week). Compared to artificial tears that are intermittently applied, a sustained delivery from SCLs may resemble better the lubrication role of

natural tears. In this sense, we carried out an study aimed to prepare PHEMA-based SCL containing AA, as functional monomer able to interact with polyvinyl pyrrolidone (PVP). It is well known that AA strongly interacts with PVP through electrostatic and hydrogen bond interactions [147]. The demulcent agent was added to the prepolymerization mixture for enabling the formation of a semi-interpenetrating network [148]. PVP has been shown efficient as lubricating and soothing component in ocular anti-allergy eye drops [149]. The incidence of composition variables, such as molecular weight and proportion of PVP or volume of water added to the lens monomeric solution, on PVP release rate and frictional properties of the lenses was characterized in detail [148]. The hydrogels rapidly released a portion of PVP in the first 24 hours and then the release was more sustained; at the 9^{th} day they still kept unreleased more than 80% PVP. The release profiles were well fitted to a square-root kinetics, which means that diffusion is the main mechanism involved in the release. The amounts of PVP released by the hydrogels in the first 24 hours were in the range of those delivered by conventional ophthalmic solution. It is expected that the sustained delivery from the lens and the prolonged time of permanence in the post-lens lachrymal fluid could greatly enhance both the amount and the residence time of PVP in the ocular surface, as found for drug-loaded SCLs. Furthermore, up to 10-fold decrease in the friction coefficient values were recorded for PVP-loaded hydrogels compared to control hydrogels. It should be noticed that PVP loading by conventional hydrogels and by PVP-imprinted hydrogels was not evaluated because the difficulty to completely remove the PVP used as template from the PVP-imprinted hydrogels. Thus, the imprinting effect could not be tested.

Just recently the molecular imprinting technology has been applied to prepare hyaluronic acid-loaded SCLs [150]. Hyaluronic acid consists of repeating units of glucuronic acid and N-acetylglucosamine. Taking into account the amino acid structure of the binding receptor in the human body (the hyaluronic acid binding protein CD44), the following functional monomers were chosen: AM because its amide group resembles that of asparagine, NVP due to a hydrogen bonding capability similar to that of tyrosine, and 2-(diethylamino)ethyl methacrylate (DEAEM) because it bears a positively charged group like arginine or lysine. To prepare the hydrogels, hyaluronic acid (6.5 mg) was added to nelfilcon A monomeric solution (1 g) containing variable proportions of AM,

NVP and DEAEM. Hydrogels prepared with 0.125% by mass of functional monomers provided a wide range of release rates depending on the nature and ratio of the functional monomers. The changes in drug diffusion coefficient were related to the presence of multiple binding points in the network and not to structural changes of the mesh. Furthermore, beyond certain proportion of functional monomers the delivery can be even completely prevented, evidencing the strength of the binding.

4. Conclusions

The molecular imprinting technology aims to endow polymeric networks with binding sites that recognize specific molecules and regulate their uptake and release according to their affinity. The research carried out up until now shows that this technology is an interesting tool for the design and synthesis of SCLs with performance as drug delivery systems. Drug-loaded SCLs provide higher and more sustained ocular drug levels than conventional ophthalmic formulations. The imprinted networks may be tailored to uptake sufficient amounts of therapeutic substances and to adjust their release kinetics as a function of clinical needs. The knowledge about the stoichiometry, the strength and the stability of the drug-functional monomers complexes, both during the lens synthesis and in the aqueous precorneal environment, is expected to provide rational basis for the design of efficient drug-imprinted SCLs. In addition to the use of analytical techniques, the application of biomimetic principles may serve as a guide for optimizing the performance of the recognition, mimicking the way Nature does in the physiological drug-receptors.

Acknowlegements

This work was supported by MICINN and FEDER (SAF2008-01679), and the Xunta de Galicia (PGIDT07CSA002203PR), Spain. F. Yañez is grateful to MICINN for a FPI grant.

References

1. Reddy I.K., Ganesan M.G.- Ocular therapeutics and drug delivery: an overview.- In: Ocular therapeutics and drug delivery, Reddy I.K., Ed., Technomic Publishing Co., Lancaster, Pennsylvania, 1996, pp. 3-29.

2. Myles M.E., Neumann D.M., Hill J.M.- Recent progress in ocular drug delivery for posterior segment disease: Emphasis on transscleral iontophoresis.- Adv. Drug Del. Rev., 57, 2063-2079, 2005.

3. Gunda S., Hariharan S., Mandava N., Mitra A.K.- Barriers in ocular drug delivery.- In: Ocular transporters in ophthalmic diseases and drug delivery, Tombran-Tink J., Barnstable C.J., Eds. Humana Press, Totowa NJ, 2008, pp. 399-413.

4. Barar J., Javadzadeh A.R., Omidi Y.- Ocular novel drug delivery: impacts of membranes and barriers.- Expert Opin. Drug Del., 5, 567-581, 2008.

5. Gaudana T., Jwala J., Boddu S.H.S., Mitra A.S.- Recent perspectives in ocular drug delivery.- Pharm. Res., 26, 1197-1216, 2009.

6. Mainardes R.M., Urban M.C.C., Cinto P.O., Khalil N.M., Chaud M.V., Evangelista R.C., Daflon Gremiao M.P.- Colloidal carriers for ophthalmic drug delivery.- Current Drug Targets, 6, 363-371, 2005.

7. Bejjani R., Benezra D., Cohen H., Rieger J., Andrieu C., Jeanny J.C., Gollomb G., Behar-Cohen F.F.- Nanoparticles for gene delivery to retinal pigment epithelial cells.- Molec. Vision, 11, 124-132, 2005.

8. Kearns V.R., Williams R.L.- Drug delivery systems for the eye.- Expert Rev. Med. Devices, 6, 277-290, 2009.

9. Velpandian T.- Intraocular penetration of antimicrobials agents in ophthalmic infections and drug delivery strategies.- Expert Opin. Drug Deliv., 6, 255-270, 2009.

10. Davies N.M.- Biopharmaceutical considerations in topical ocular drug delivery.- Clin. Exp. Pharmacol. P., 27, 558-562, 2000.

11. Hughes P.M., Olejnik O., Chang-Lin J.E., Wilson C.G.- Topical and systemic drug delivery to the posterior segments.- Adv. Drug Del. Rev., 57, 2010-2032, 2005.

12. Zhu H., Chauhan A.- A mathematical model for ocular tear and solute balance.- Curr. Eye Res., 30, 841-854, 2005.

13. Tomlinson A., Khanal S.- Assessment of tear film dynamics: Quantification approach.- Ocular Surf., 3, 81-95, 2005.

14. Robinson J.R.- Ocular drug delivery mechanism of corneal drug transport and mucoadhesive delivery systems.- STP Pharma. Sci., 5, 839-846, 1989.

15. Singh C.P., Shah D.O.- Surface chemical aspects of ocular drug delivery systems.- In: Ocular therapeutics and drug delivery, Reddy I.K., Ed. Technomic Publishing Co., Lancaster, Pennsylvania, 1996, pp. 31-49.

16. Keister J.C., Cooper E.R., Missel P.J., Lang J.C., Hager D.F.- Limits on optimizing ocular drug delivery.- J. Pharm. Sci., 80, 50-53, 1991.

17. Wilson C.G.- Topical drug delivery in the eye.- Exp. Eye Res., 78, 737-743, 2004.

18. Mundada A.S., Avari J.G.- *In situ* gelling polymers in ocular drug delivery systems: a review.- Crit. Rev. Ther. Drug Carrier Syst., 26, 85-118, 2009.

19. Nagarwal R.C., Kant S.; Singh P.N., Maiti P., Pandit J.K.- Polymeric nanoparticulate system: A potential approach for ocular drug delivery.- J. Control. Release, 136, 2-13, 2009.

20. Felt O., Einmahl S., Gurny R., Furrer P., Baeyens V.- Polymeric systems for ophthalmic drug delivery.- In: Polymeric Biomaterials, Dumitriu S. Ed. Marcel Dekker Inc., New York 2002, pp.377-421.

21. Davis J.L., Gilger B.C., Robinson M.R.- Novel approaches to ocular drug delivery.- Current Opin. Molecular Ther., 6, 195-205, 2004.

22. Ludwig A.- The use of mucoadhesive polymers in ocular drug delivery.- Adv. Drug Del. Rev., 57, 1595-1639, 2005.

23. Sedlacek J.- Possibilities of application of eye drugs with the aid of gel-contact lenses.- Cs. Oftal., 21, 509-512, 1965.

24. Gasset A., Kaufman H.E.- Therapeutic uses of hydrophilic contact lenses.- Am. J. Ophtalmol., 69, 252-259, 1970.

25. Waltman S.R., Kaufman H.E.- Use of hydrophilic contact lenses to increase ocular penetration of topical drugs.- Inv. Ophthalmol., 9, 250-255, 1970.

26. Hillman J.S. -Management of acute glaucoma with pilocarpine-soaked hydrophilic lens.- Brit. J. Ophthalmol., 58, 674-679, 1974.

27. Ruben M., Watkins R.- Pilocarpine dispensation for soft hydrophilic contact-lens.- Brit. J. Ophthalmol., 59, 455-458, 1975.

28. Marmion V.J., Jain M.R.- Role of soft contact-lenses and delivery of drugs.- Trans. Ophthalmol. Soc. UK, 96, 319-321, 1976.

29. Rubinstein M.P., Evans J.E.- Therapeutic contact lenses and eyedrops- is there a problem?.- Cont. Lens Anterior Eye, 20, 9-11, 1997.

30. Hull D.S., Edelhauser H.F., Hyndiuk R.A.- Ocular penetration of prednisolone and hydrophilic contact-lens.- Arch. Ophthalmol., 92, 413-416, 1974.

31. Matoba A.Y., McCulley J.P.- The effect of therapeutic soft contact-lenses on antibiotic delivery to the cornea.- Ophthalmology, 92, 97-99, 1985.

32. Jain M.R.- Drug delivery through soft contact-lenses.- Brit. J. Ophthalmol., 72, 150-154, 1988.

33. Li C.C., Chauhan A.- Modeling ophthalmic drug delivery by soaked contact lenses.- Ind. Eng. Chem. Res., 45, 3718-3734, 2006.

34. Vandorselaer T., Youssfi H., Caspers-Valu L.E., Dumont P., Vauthier L.- Treatment of traumatic corneal abrasion with contact lens associated with topical nonsteroid anti-inflammatory drug (NSAID) and antibiotic: a safe, effective, and comfortable solution.- J. Fr. Ophtalmol., 24, 1025-1033, 2001.

35. Witcherle O., Lim D.- Hydrophilic gels for biological use.- Nature, 185, 117-118, 1960.

36. McMahon T.T., Zadnik K.- Twenty-five years of contact lenses.- Cornea, 19, 730-740, 2000.

37. Kopecek J.- Hydrogels: from soft contact lenses and implants to self-assembled nanomaterials.- J. Polym. Sci. Part A: Polym. Chem., 47, 5929-5946, 2009.

38. Yamauchi A.- Soft contact lenses.- In: Osada Y, Kajiwara K, editors. Gels Handbook, vol. 3. San Diego: Academic Press, 2001, pp. 166-179.

39. Nicolson P.C, Vogt J.- Soft contact lens polymers: an evolution.- Biomaterials, 22, 3273-3283, 2001.

40. FDA. Premarket Notification (510(k))-Guidance Document for Daily Wear Contact Lenses.- http://www.fda.gov/cdrh/ode/conta.html, accessed December 2009.

41. Tighe B.- Silicone hydrogel materials: how do they work?.- In: Silicone Hydrogels, Sweeney D.F. Ed. Butterworth Heinemann, Oxford, 2000, pp.1-27.

42. Donshik P.C.- Extended wear contact lenses.- Ophtalmol. Clin. N. Am., 16, 79-83, 2003.

43. Hiratani H., Nakajima T., Yamamoto K.J.- The state and prospect of contact lenses.- Jpn. Soc. Biomater., 20, 221-227, 2002.

44. Barr J.- 2004 Annual Report.- Contact Lens Spectrum. January, 2005.

45. Shah C., Raj S., Foulks G.N.- The evolution in therapeutic contact lenses.- Ophtalmol. Clin. N. Am., 16, 95-101, 2003.

46. DeNaeyer G.W.- Exploring the therapeutic applications of contact lenses.- New O.D. December, 11-15, 2008.

47. Lim L., Tan D.T.H., Chan W.K.- Therapeutic use of Bausch & Lomb Pure Vision contact lenses.- CLAO J., 27, 179-185, 2001.

48. Kanpolat A., Ucakhan O. -Therapeutic use of Focus Night & Day contact lenses.- Cornea, 22, 726-734, 2003.

49. Mely R.- Therapeutic and cosmetic indications of Lotrafilcon. A silicone hydrogel extended-wear lenses.- Ophthalmologica, 218, 33-38, 2004.

50. Bendoriene J., Vogt U.- Therapeutic use of silicone hydrogel contact lenses in children.- Eye Contact Lens., 32, 104-108, 2006.

51. Krejci L., Brettschneider I., Praus R.- Hydrophilic gel contact lenses as a new drug delivery system in ophtalmology and as a therapeutic bandage lenses.- Act. Univ. Carol. Med., 21, 387-396, 1975.

52. Silbert J.A.- A review of therapeutic agents and contact lens wear.- J. Am. Optom. Assoc., 67, 165-172, 1996.

53. Alvarez-Lorenzo C., Hiratani H., Concheiro A.- Contact lenses for drug delivery: achieving sustained release with nivel systems.- Am. J. Drug Deliv., 4, 131-151, 2006.

54. Xinming L., Yingde C., Lloyd A.W., Mikhalovsky S.V., Sandeman S.R., Howel C.A., Liewen L.- Polymeric hydrogels for novel contact lens-based ophthalmic drug delivery systems: A review.- Cont. Lens Anterior Eye, 31, 57-64, 2008.

55. Tabuchi N., Watanabe T., Hattori M., Sakai K., Sakai H., Abe M.- Adsorption of actives in ophthalmological drugs for over-the-counter on soft contact lens surfaces.- J. Oleo Sci., 58, 43-52, 2009.

56. Refojo M.F., Leong F.L., Chan I.M., Tolentino F.I.- Absorption and release of antibiotics by a hydrophilic implant for scleral buckling.- Retina, 3, 45-49, 1983.

57. Podos S.M., Becker B., Asseff C.F., Harstein J.- Pilocarpine therapy with soft contact lenses.- Am. J. Ophtalmol., 73, 336-341, 1972.

58. Schultz C.L., Poling T.R., Mint J.O.- A medical device/drug delivery system for treatment of glaucoma.- Clin. Exp. Optom., 92, 343-348, 2009.

59. Lesher G.A., Gunderson G.G.- Continuous drug-delivery through the use of disposable contact-lenses.- Optometry Vision Sci., 70, 1012-1018, 1993.

60. Pinilla Lozano I., Polo Llorens V., Larrosa Poves J.M., Pérez Oliván S., Izaguirre L., Gorricho J.- Medium-water-content contact lenses ciprofloxacin saturation: differences between exposure times.- Rev. Esp. Contact. 1998; http://www.oftalmo.com/sec/98-tomo-2/Ind-98-2.htm, accessed December 2009.

61. Pinilla Lozano I., Larrosa Poves J.M., Pérez Oliván S., Polo Llorens V., Izaguirre L., Navascues J.- Quinolones intraocular penetration depending on therapeutic contact lens wear.- Rev. Esp. Contact. 1998; http://www.oftalmo.com/sec/98-tomo-2/Ind-98-2.htm, accessed December 2009.

62. Tian X., Iwatsu M., Kanai A.- Disposable 1-Day Acuvue® contact lenses for the delivery of lomefloxacin to rabbits' eyes.- CLAO J., 27, 209-215, 2001.

63. Tian X., Iwatsu M., Sado K., Kanai A.- Studies on the uptake and release of fluoroquinolones by disposable contact lenses.- CLAO J., 27, 216-220, 2001.

64. Hehl E.M., Beck R., Luthard K., Guthoff R., Drewelow B. -Improved penetration of aminoglycosides and fluoroquinolones into the aqueous humour of patients by means of Acuvue contact lenses.- Eur. J. Clin. Pharmacol., 55, 317-323, 1999.

65. Schultz C.L., Poling T.R., Mint J.O.- A medical device/drug delivery system for treatment of glaucoma.- Clin. Exp. Optom., 92, 343-348, 2009.

66. Krejci L.- Therapeutic use of scleral gel contact lenses.- Cs. Oftal., 27, 104-109, 1971.

67. Krejci L., Brettschneider I., Praus R.- Comparative study of fluorescein release from various types of therapeutic hydrophilic gel contact lenses.- Cs. Oftal., 27, 285-91, 1971.

68. Praus R., Brettschneider I., Havranek M., Krejci L.- Penetration of radioactive sulphate and glucose from hydrophilic gel contact lenses into the eye of rabbit.- Ophthal. Res., 6, 291-300, 1974.

69. Wajs G., Meslard J.C.- Release of therapeutic agents from contact lenses.- Crit. Rev. Ther. Drug, 2, 275-289, 1986.

70. Kim S.W., Bae Y.H., Okano T.- Hydrogels: swelling, drug loading, and release.- Pharm. Res., 9, 283-290, 1992.

71. Lloyd A.W., Faragher R.G.A., Denyer S.P.- Ocular biomaterials and implants.- Biomaterials, 22, 769-785, 2001.

72. Karlgard C.C.S., Wong N.S., Jones L.W., Moresoli C.- In vitro uptake and release studies of ocular pharmaceutical agents by silicon-containing and p-HEMA hydrogel contact lens materials.- Int. J. Pharm., 257, 141-151, 2003.

73. Boone A., Hui A., Jones L.- Uptake and release of dexamethasone phosphate from silicon hydrogel and group I, II and IV hydrogel contact lenses.- Eye & Contact Lens, 5, 260-267, 2009.

74. Momose T., Ito N., Kanai A., Watanabe Y., Shibata M.- Adsorption of levocabastine eye drops by soft contact lenses and its effects in rabbit eyes.- CLAO J., 23, 96-99, 1997.

75. Heyrman T.P., McDermott M.L., Ubels J.L., Edelhauser H.F.- Drug uptake and release by a hydrogel intraocular-lens and the human crystalline lens.- J. Cataract. Refr. Surg., 15, 169-175, 1989.

76. Chapman J.M., Cheeks L., Green K.- Drug-interaction with intraocular lenses of different materials.- J. Cataract. Refr. Surg., 18, 456-459, 1992.

77. Weiner A.L.- Polymeric site-specific pharmacotherapy.- In: Polymeric drug delivery systems for the eye, A.J. Domb Ed., Wiley, Chichester, 1994, pp. 315-346.

78. Vairon J.P., Yean L., Meslard J.C., Subira F., Bunel C.- Immobilisation reversible sur polymers et liberation controlee. Application aux lentilles corneennes reservoirs de medicaments.- L´actualité Chimique, Septembre-Octobre, 330-335, 1992.

79. Anne D., Heidi B., Yves M., Patrick V.- Fabrication and characterization of contact lenses bearing surface-immobilized layers of intact liposomes.- J. Biomed. Mater. Res. A, 80A, 41–51, 2007.

80. Gulsen D., Chauhan A.- Ophthalmic drug delivery through contact lenses.- Invest. Ophthalmol. Vis. Sci., 45, 2342-2347, 2004.

81. Gulsen D., Chauhan A.- Dispersion of microemulsion drops in HEMA hydrogel: a potential ophthalmic drug delivery vehicle.- Int. J. Pharm., 292, 95-117, 2005.

82. Gulsen D., Li C.C., Chauhan A.- Dispersion of DMPC liposomes in contact lenses for ophthalmic drug delivery.- Current Eye Res., 30, 1071-1080, 2005.

83. Gulsen D., Chauhan A.- Effect of water content on transparency, swelling, lidocaine diffusion in p-HEMA gels.- J. Membr. Sci., 269, 35-48, 2006.

84. Kapoor Y, Chauhan A.- Ophthalmic delivery of Cyclosporine A from Brij-97 microemulsion and surfactant-laden p-HEMA hydrogels.- Int. J. Pharm., 361, 222-229, 2008.

85. Miranda M.N., Garcia-Castineiras S.- Effects of pH and some common topical ophthalmic medications on the contact lens permalens.- CLAO J., 9, 43-48, 1983.

86. Uchida R., Sato T., Tanigawa H., Uno K.- Azulene incorporation and release by hydrogel containing methacrylamide propyltrimethylammonium chloride, and its application to soft contact lens.- J. Control. Rel., 92, 259-264, 2003.

87. Sato T., Uchida R., Tanigawa H., Uno K., Murakami A.- Application of polymer gels containing side-chain phosphate groups to drug-delivery contact lenses.- J. Appl. Polym. Sci., 98, 731-735, 2005.

88. Byrne M.E., Salian V.- Molecular imprinting within hydrogels II. Progress and analysis of the field.- Int. J. Pharm., 364, 188-212, 2008.

89. Lord M.S., Stenzel M.H., Simmons A., Milthorpe B.K.- Lysozyme interaction with poly(HEMA)-based hydrogel.- Biomaterials, 27, 1341-1345, 2006.

90. Maeda M., Bartsch R.A.- Molecular and Ionic Recognition with Imprinted Polymers: A brief overview.- In: Molecular and Ionic Recognition with Imprinted Polymers, Barstch R.A., Maeda M., Eds. ACS Symposium Series 703, American Chemical Society, Washington DC 1998, pp 1-8.

91. Ramström O., Ansell R.J.- Molecular imprinting technology: challenges and prospects for the future.- Chirality, 10, 195-209, 1998.

92. Wulff G., Biffis A.- Molecularly imprinting with covalent or stoichiometric non-covalent interactions.- In: Molecularly Imprinted Polymers, Sellergren B. Ed., Elsevier, Amsterdam 2001, pp 71-111.

93. Wulff G.- Molecular imprinting in cross-linked materials with the aid of molecular templates- a way towards artificial antibodies.- Angew. Chem. Int. Ed. Engl., 34, 1812-1832, 1995.

94. Arshady R, Mosbach K.- Synthesis of substrate-selective polymers by host-guest polymerization.- Makromol. Chem., 182, 687-692, 1981.

95. Hall A.J., Emgenbroich M., Sellergren B.- Templates in Chemistry II- Top Curr. Chem., 249, 317-349, 2005.

96. Hillberg A.L., Brain K.R., Allender C.J.- Molecular imprinted polymer sensors: Implications for therapeutics.- Adv. Drug Del. Rev., 57, 1875-1889, 2005.

97. Andersson H.S., Karlsson J.G., Piletsky S.A., Koch-Schmidt A.C., Mosbach K., Nicholls I.A.- Study of the nature of recognition in molecularly imprinted polymers. Influence of monomer-template ratio and sample load on retention and selectivity.- J. Chromatog. A, 848, 39-49, 1999.

98. Mayes A.G., Whitcombe M.J.- Synthetic strategies for the generation of molecularly imprinted organic polymers.- Adv. Drug Del. Rev., 57, 1742-1778, 2005.

99. Kandimalla V.B., Ju H.X.- Molecular imprinting: a dynamic technique for diverse applications in analytical chemistry.- Anal. Bioanal. Chem., 380, 587-605, 2004.

100. Pichon V., Chapuis-Hugon F.- Role of molecularly imprinted polymers for selective determination of environmental pollutants. A review.- Anal. Chim. Acta, 622, 48-61, 2008.

101. Haginaka J.- Molecularly imprinted polymers as affinity-based separation media for sample preparation.- J. Sep. Sci., 32, 1548-1565, 2009.

102. Allender C.J., Richardson C., Woodhouse B., Heard C.M., Brain K.R.- Pharmaceutical applications for molecularly imprinted polymers.- Int. J. Pharm., 195, 39-43, 2000.

103. Byrne M.E., Park K., Peppas N.A.- Molecular imprinting within hydrogels.- Adv. Drug Del. Rev., 54, 149-161, 2002.

104. Alvarez-Lorenzo C., Concheiro A.- Molecularly imprinted polymers for drug delivery.- J. Chromatogr. B, 804, 231-245, 2004.

105. Hilt J.Z., Byrne M.E.- Configurational biomimesis in drug delivery: molecular imprinting of biologically significant molecules.- Adv. Drug Del. Rev., 56, 1599-1620, 2004.

106. Kryscio D.R., Peppas N.A.- Mimicking biological delivery through feed back-controlled drug release systems based on molecular imprinting.- AICHE J., 55, 1311-1324, 2009.

107. Cunliffe D., Kirby A., Alexander C.- Molecularly imprinted drug delivery systems.- Adv. Drug Del. Rev., 57, 1836-1853, 2005.

108. Alvarez-Lorenzo C., Concheiro A.- Molecularly imprinted gels and nano- and microparticles. Manufacture and applications.- In: Smart Nano and Microparticulates, Arshady R, Kono K, Eds. MML Series Vol. 7. Kentus Books, London 2005, pp. 279-336.

109. Alvarez-Lorenzo C., Concheiro A.- Molecularly imprinted materials as advanced excipients for drug delivery systems.- In: Biotechnology Annual Review, Vol. 12, El-Gewely MR, Ed. Elsevier, Amsterdam, 2006, pp. 225-268.

110. Sibrian-Vazquez M., Spivak D.A.- Improving the strategy and performance of molecularly imprinted polymers using cross-linking functional monomers.- J. Org. Chem., 68, 9604-9611, 2003.

111. Alvarez-Lorenzo C., Hiratani H., Gómez-Amoza J.L., Martinez-Pacheco R., Souto C., Concheiro A.- Soft contact lenses capable of sustained delivery of timolol.- J. Pharm. Sci., 91, 2182-2192, 2002.

112. Hiratani H., Alvarez-Lorenzo C.- Timolol uptake and release by imprinted soft contact lenses made of N,N-diethylacrylamide and methacrylic acid.- J. Control. Release, 83, 223-230, 2002.

113. Hiratani H, Alvarez-Lorenzo C.- Process for production of hydrogel material enhanced in the intake of drugs and permitting sustained release of drugs.- WO03090805, November 6, 2003.

114. Hiratani H., Alvarez-Lorenzo C.- The nature of backbone monomers determines the performance of imprinted soft contact lenses as timolol drug delivery systems.- Biomaterials, 25, 1105-1113, 2003.

115. Hiratani H., Fujiwara A., Tamiya Y., Mizutani Y., Alvarez-Lorenzo C.- Ocular release of timolol from molecularly imprinted soft contact lenses.- Biomaterials, 26, 1293-1298, 2005.

116. Hiratani H., Mizutani Y., Alvarez-Lorenzo C.- Controlling drug release from imprinted hydrogels by modifying the characteristics of the imprinted cavities.- Macromol. Biosci., 5, 728–733, 2005.

117. Kenji Ito, Jeffrey Chuang, Carmen Alvarez-Lorenzo, Tsuyoshi Watanabe, Nozomi Ando, Alexander Yu. Grosberg.- Multiple point adsorption in a heteropolymer gel and the Tanaka approach to imprinting: experiment and theory.- Progr. Polym. Sci., 28, 1489-1515, 2003.

118. Tsai J.C., Kanner E.M.- Current and emerging medical therapies for glaucoma.- Expert Opin. Emerg. Drugs, 10, 109-118, 2005.

119. Reichl S.- Cell culture models of the human cornea: a comparative evaluation of their usefulness to determine ocular drug absorption in-vitro.- J. Pharm. Pharmacol., 60, 299-307, 2008.

120. Nelson W.L., Fraunfelder F.T., Sills J.M., Arrowsmith J.B., Kuritsky J.N. - Adverse respiratory and cardiovascular events attributed to timolol ophthalmic solution, 1978-1985.- Am. J. Ophthalmol., 102, 606-611, 1986.

121. Andrzejewska E.- Photopolymerization kinetics of multifunctional monomers.- Prog. Polym. Sci., 26, 605-665, 2001.

122. Sellergren B., Shea K.J.- Correlation between solute retention and a theoretical ion-exchange model using imprinted polymers.- J. Chromatogr. A, 654,17–28, 1993.

123. Martindale.- The Complete Drug Reference- 32nd ed., Parfitt K. Ed., Pharmaceutical Press, London, 1999, p. 233.

124. Wong T., Ormonde S., Gamble G., McGhee C.N.J.- Severe infective keratitis leading to hospital admission in New Zealand- Brit. J. Ophthalmol., 87, 1103-1108, 2003.

125. Zegans M.E., Becker H.I., Budzik J., O'Toole G.- The role of bacterial biofilms in ocular infections- DNA Cell. Biol., 21, 415-420, 2002.

126. Mely R.- Therapeutic and cosmetic indications of Lotrafilcon: A silicone hydrogel extended-wear lenses- Ophthalmologica, 218, 33-38, 2004.

127. Kim M.N., Lim A.H., Yoon J.S.- Antibacterial activity of polymers with norfloxacin moieties against native and norfloxacin-tolerance-induced bacteria- J. Appl. Polym. Sci., 96, 936-943, 2005.

128. Molinelli A., O'Mahony J., Nolan K., Smyth M.R., Jakusch M., Mizaikoff B.- Analyzing the mechanisms of selectivity in biomimetic self-assemblies via IR and NMR spectroscopy of prepolymerization solutions and molecular dynamics simulations.- Anal. Chem., 77, 5196-5204, 2005.

129. McStay D., Al-Obaidi A.H., Hoskins R., Quinn P.J.- Raman spectroscopy of molecularly imprinted polymers.- J. Opt. A: Pure Appl. Opt., 7, S340-S345, 2005.

130. Fish W.P., Ferreira J., Sheardy R.D., Snow N.H., O'Brien T.P.- Rational design of an imprinted polymer: maximizing selectivity by optimizing the monomer-template ratio of a cinchonidine MIP, prior to polymerization, using microcalorimetry.- J. Liquid Chromatogr. Related Techn., 28, 1-15, 2005.

131. Nicholls I.A., Andersson H.S., Charlton C., Henschel H., Karlsson B.C.G., Karlsson J.G., O'Mahony J., Rosengren A.M., Rosengren K.J., Wikman S.- Theoretical and computational strategies for rational molecularly imprinted polymer design.- Biosens. Bioelectron. 25, 543-552, 2009.

132. Mika A.M., Childs R.F.- Acid/base properties of poly(4-vinylpyridine) anchored within microporous membranes.- J. Membr. Sci., 152, 129-140, 1999.

133. Alvarez-Lorenzo C., Yañez F., Barreiro-Iglesias R., Concheiro A.- Imprinted PHEMA soft contact lenses as norfloxacin delivery systems.- J. Control. Release, 113, 236-244, 2006.

134. del Cuvillo A., Sastre J., Montoro J., Jauregui I., Davila I., Ferrer M., Bartra J., Mullol J., Valero A. -Allergic conjunctivitis and H1 antihistamines.- J. Investig. Allergol. Clin. Immunol. 19, 11-18, 2009.

135. Venkatesh S., Sizemore S.P., Byrne M.E..- Biomimetic hydrogels for enhanced loading and extended release of ocular therapeutics.- Biomaterials, 28, 717-724, 2007.

136. Venkatesh S., Sizemore S.P., Byrne M.E..- Biomimetic recognitive polymer networks for ocular delivery of anti-histamines.- Mater. Res. Soc. Symp. Proc., 897E, 2006.

137. Venkatesh S., Saha J., Pass S., Byrne M.E.- Transport and structural analysis of molecular imprinted hydrogels for controlled drug delivery.- Eur. J. Pharm. Biopharm., 69, 852-860, 2008.

138. Ali M., Horikawa S., Venkatesh S., Saha J., Pass S., Hong J.W., Byrne M.E.- Zero-order therapeutic release from imprinted hydrogel contact lenses within in vitro physiological ocular tear flow.- J. Control. Release, 124, 154-162, 2007.

139. Johnson M.E., Murphy P.J.- Changes in the tear film and ocular surface from dry eye syndrome- Prog. Retin Eye Res., 23, 449-474, 2004.

140. Lemp M.A.- Report of the National Eye Institute/Industry workshop on clinical trials in dry eyes.- CLAO J., 21, 221-232, 1995.

141. Maruyama K., Yokoi N., Takehisa Y., Kinoshita S.- Effect of environmental conditions on tear dynamics in soft contact lens wearers.- Invest. Ophthalmol. Vis. Sci., 45, 2563-2568, 2004.

142. FDA -Ophthalmic demulcents.- Part 349.12. Subheading of Ophthalmic Drug Products For Over-the-Counter Human Use. 21CFR349, 2009. http://ecfr.gpoaccess.gov/cgi/t/text/textidx?c=ecfr&rgn=div5&view=text&node=21:5.0.1.1.23&idno=21

143. Szczotka-Flynn L.- Chemical properties of contact lens rewetters- Contact Lens Spectrum, April 2006.

144. Schwarz S., Nick J.- Effectiveness of lubricating daily disposable lenses with different additives.- Optician, 231, 22-26, 2006.

145. Peterson R.C., Wolffsohn J.S., Nick J., Winterton L., Lally J.- Clinical performance of daily disposable soft contact lenses using sustained release technology.- Contact Lens Ant. Eye, 29, 127-134, 2006.

146. Winterton L.C., Lally J.M., Sentell K.B., Chapoy L.L.- The elution of poly(vinyl alcohol) from a contact lens: the realization of a time release moisturizing agent/artificial tear.- J. Biomed. Mater. Res. B Appl. Biomater., 80 B, 424-432, 2007.

147. Vasheghani B., Rajabi F.H., Ahmadi M.H., Gholehzadeh A.- Effect of ionic strength of the solution of some hydrogen-bonded interpolymer complexes on the stability and thermodynamic parameters.- Polimery, 54, 261-265, 2009.

148. Yanez F., Concheiro A., Alvarez-Lorenzo C.- Macromolecule release and smoothness of semi-interpenetrating PVP-pHEMA networks for comfortable soft contact lenses.- Eur. J. Pharm. Biopharm., 69, 1094-1103, 2008.

149. Abelson M.B., Anderson R.- Demystifying Demulcents.- Review of Ophtalmology,13, 2006. http://www.revophth.com/index.asp?page=1_13162.htm.

150. Ali M., Byrne M.E.- Controlled release of high molecular weight hyaluronic acid from molecularly imprinted hydrogel contact lenses.- Pharm. Res., 26, 714-726, 2009.

3.2. Imprinted soft contact lenses as norfloxacin delivery systems

Journal of Controlled Release **113**, 236–244 (2006).

Available online at www.sciencedirect.com
SCIENCE DIRECT®
Journal of Controlled Release 113 (2006) 236–244
journal of controlled release
www.elsevier.com/locate/jconrel

Imprinted soft contact lenses as norfloxacin delivery systems

Carmen Alvarez-Lorenzo *, Fernando Yañez, Rafael Barreiro-Iglesias, Angel Concheiro

Departamento de Farmacia y Tecnología Farmacéutica, Facultad de Farmacia, Universidad de Santiago de Compostela, 15782–Santiago de Compostela, Spain

Received 3 April 2006; accepted 4 May 2006
Available online 20 May 2006

Abstract

Soft contact lenses are receiving an increasing attention not only for correcting mild ametropia but also as drug delivery devices. To provide poly(hydroxyethyl methacrylate), PHEMA, lenses with the ability to load norfloxacin (NRF) and to control its release, functional monomers were carefully chosen and then spatially ordered applying the molecular imprinting technology. Isothermal titration calorimetry (ITC) studies revealed that maximum binding interaction between NRF and acrylic acid (AA) occurs at a 1:1, and that the process saturates at 1:4 molar ratio. Hydrogels were synthesized using different NRF:AA molar ratios (1:2 to 1:16), at two fix AA total concentrations (100 and 200 mM), and using moulds of different thicknesses (0.4 and 0.9 mm). The cross-linker molar concentration was 1.6 times that of AA. Control (non-imprinted) hydrogels were prepared similarly but with the omission of NRF. All hydrogels showed a similar degree of swelling (55%) and, once hydrated, presented adequate optical and viscoelastic properties. After immersion in 0.025, 0.050 and 0.10 mM drug solutions, imprinted hydrogels loaded greater amounts of NRF than the non-imprinted ones. Imprinted hydrogels synthesized using NRF:AA 1:3 and 1:4 molar ratios showed the greatest ability to control the release process, sustaining it for more than 24 h. These results prove that ITC is a useful tool for the optimization of the structure of the imprinted cavities in order to obtain efficient therapeutic soft contact lenses.

Keywords: Soft contact lenses; Ocular controlled release; Molecular imprinting; ITC; Template:functional monomer ratio

1. Introduction

The success of the therapy with antibiotics strongly depends on achieving enough drug concentration in the infected area for a sufficient period of time. Systemic delivery generally does not allow these aims to be accomplished when the infection affects poorly irrigated areas, such as ocular and bone structures [1,2]. In these cases, antibiotics have to be locally applied using appropriate devices [3,4]. The ocular bioavailability of drugs instilled on the corneal surface is usually limited to the 1–10% of the dose owing to the intense draining effect of blinking and lachrymal fluid removal [5]. Thus instillation has to be frequently repeated, providing pulse-type concentration profiles. An important fraction of the dose can be unproductively absorbed through the conjunctiva and/or swept through the nasolachrymal conduct, and then systemically absorbed, with the consequent risk of side effects. Several approaches have been proposed to obtain more sustained profiles, such as the addition of thickening, in situ gel or bioadhesive polymers, or the use of inserts [6–8]. Nevertheless, much effort is still needed to avoid the sticking and blurring effects and the foreign body sensation of most of them.

The use of soft contact lenses as drug delivery devices may produce a miracle of therapeutic opportunities. Since the development of poly(hydroxyethyl methacrylate), PHEMA, hydrogels as soft contact lenses by Wicherle and Lim in 1961, important efforts have been made to use them as drug vehicles for both chronic (e.g. glaucoma) and acute (e.g. infections or inflammatory process) diseases [9–13]. The high content in water of PHEMA hydrogel enables the uptake of some drugs by simple immersion in concentrated solutions or direct instillation of eye-drops [9,14,15]. Once applied on the eye, the drug preferentially diffuses towards the postlens lachrymal fluid (i.e. that in between the lens and the cornea). Since the exchange of this fluid is quite poor, the permanence time of the drug on the corneal surface is significantly increased compared to delivery by eye-drops [16]. Thus, the ocular bioavalability could be remarkably enhanced [17]. However, the success of this approach is restricted to few drugs, since most drugs passively

* Corresponding author. Fax: +34 981547148.
E-mail address: ffrusdog@usc.es (C. Alvarez-Lorenzo).

0168-3659/$ - see front matter © 2006 Elsevier B.V. All rights reserved.
doi:10.1016/j.jconrel.2006.05.003

diffuse through the aqueous phase of the lens network without interacting effectively. This limits both the amount loaded and the ability to control the release, which are deficient in the absence of mechanisms of drug retention in the hydrogel. As well as the drug uptake being generally rapid, a burst release is observed [18–20].

In order to overcome these limitations, the chemically-reversible immobilization of drugs in the lens through labile bonds [21], the incorporation of drug-loaded colloidal structures into the lens [22,23], or the copolymerization with functional groups able to interact directly with the drug [24,25] are being evaluated. In the first two approaches the lens is forcedly loaded during synthesis by the covalent binding of the drug to polymerizable compounds or by dispersing drug microemulsions or liposomes; the control of the release being carried out, respectively, by the hydrolysis of the labile bonds or by the delivery from the colloidal structures. Their main drawbacks are related still to the reduced possibilities of modulating drug release and to the stability of the drug and of the colloidal structures. The third approach aims at increasing the drug affinity of the lens network through the introduction of monomers (functional monomers) able to establish non-covalent interactions with the drug. If the lenses are synthesized following the traditional polymerization methods, a random distribution of functional monomers is obtained. To optimize the spatial distribution of the monomers and, therefore, the likelihood of creating efficient binding points for the drug, the molecular imprinting technology has been recently adapted to the synthesis of contact lenses as timolol dosage forms [26–30]. This technique consists of adding the drug to the monomers solution to allow the functional ones to arrange themselves around the drug molecules according to their interaction capability. The polymerization and cross-linking fix such spatial sequence and, after the removal of the template molecules, recognition cavities complementary in shape and functionality (i.e. specific receptors) to the drug are obtained. In addition to the interest in the analytical field, imprinted materials have enormous potential for a better performance of drug dosage forms [31–36].

The distinctive safety, optical and mechanical characteristics of the lenses, which restrict the number of suitable functional monomers and the degree of cross-linking (<10%-mol), demand a particularly careful design of the molecular imprinting procedure [30]. The affinity for the drug has to be maximized to compensate the lower physical stability of the cavities in the imprinted lenses, if compared with those of the traditional rigid imprinted systems. Therefore, knowledge about the stoichiometry, strength and stability of the drug-functional monomers complexes, both during the lens synthesis and in the aqueous loading and release environments, is required for an efficient performance. The aim of this work is to develop, following a rational design, contact lenses able to load and to release norfloxacin in a sustained way. Ocular infections are relatively frequent and its treatment requires the instillation of eye-drops each 30–120 min during the first days [37]. Additionally, the use of soft contact lenses itself promotes the biofilm formation and notably enhances the risk of ocular infections [38–41]. Therefore, the improvement of antibiotic loading and release properties of soft contact lenses, maintaining their utility to correct ametropia problems, is of a paramount practical importance. Norfloxacin is a fluorquinolone with a broad-spectrum activity against Gram+ and Gram− bacteria, including *P. aeruginosa*, *S. aureus* and *E. coli* [42], that shows relatively good intra-corneal and intra-cameral penetration. The work was carried out in the following steps: i) selection of the functional monomers taking into account chemical (interaction with the drug) and biocompatibility criteria; ii) characterization in detail of the drug:functional monomer complexation by isothermal titration calorimetry (ITC) [43]; and iii) synthesis of lenses with various template:functional monomer ratios to evaluate the effect of this variable on the loading and release behaviour on the basis of the ITC data.

2. Materials and methods

2.1. Materials

Ophthalmic grade 2-hydroxyethyl methacrylate (HEMA) was supplied by Merck (Germany); 2,2′-azo-bis(isobutyronitrile) (AIBN), acrylic acid (AA), 4-vinyl pyridine (VP), ethyleneglycol dimethacrylate (EGDMA), norfloxacin (NRF) and timolol maleate (TM) by Sigma-Aldrich (Spain). Ultrapure water obtained by reverse osmosis (resistivity > 18.2 MΩ cm; MilliQ®, Millipore Spain) was used.

2.2. Synthesis of non-imprinted hydrogels

EGDMA cross-linker (80 mM equivalent to 1 mol%) and different amounts of AA or VP functional monomers (0, 50, 100 and 200 mM, i.e. ranging from 0 to 2.5 mol%) were dissolved in HEMA (6 ml, 96.5–99.0 mol%). After addition of AIBN initiator (10 mM), each monomers solution was immediately injected into a mould constituted by two glass plates covered internally with a polypropylene sheet and separated by a silicone frame 0.9 mm wide [26]. The moulds were then placed in an oven for 12 h at 50 °C followed by 24 h at 70 °C. After polymerization, each gel was immersed in boiling water for 15 min to remove unreacted monomers and to facilitate the cut of discs 10 mm in diameter. The discs were immersed in NaCl 10 mM for 1 week, replacing the medium each 12 h, then in HCl 10 mM for 1 d and in water for 1 d more. Finally, the discs were dried at 40 °C for 48 h. Samples of all hydrogels were characterized as follows in Section 2.4.

2.3. Design and synthesis of molecularly imprinted hydrogels

2.3.1. Calorimetric titration of NRF with AA

The interactions between NRF and AA in HEMA solution were evaluated by ITC (VP-ITC MicroCal Inc., Northampton, MA). The experiments were carried out by duplicate (reproducibility within ±5%) at 25 °C, titrating the AA solution (0.50 M, 0.290 ml) onto the NRF solution (0.01 M, 1.439 ml). The binding experiment involved sequential additions of 1 μl aliquots of the AA solution in the reaction cell under continuous stirring at 280 rpm. Control experiments were carried out under identical

conditions to obtain the heats of dilution and mixing involved in the injection of AA solution into the HEMA medium. The net reaction enthalpy was obtained by subtracting the dilution enthalpies from the apparent titration enthalpies.

2.3.2. Synthesis of imprinted hydrogels

Two sets of imprinted PHEMA hydrogels (0.9 mm thickness) were prepared using a procedure similar to that described in Section 2.2., with the following compositions: a) AA 100 mM (1.25 mol%) and EGDMA 160 mM (2 mol%); or b) AA 200 mM (2.4 mol%) and EGDMA 320 mM (3.9 mol%). To each of these solutions, NRF was added to have NRF:AA molar ratios of 1:2 to 1:16. Control hydrogels were prepared without NRF, or neither NRF nor AA. Boiling, washing and drying were carried out as described above. The hydrogels containing AA 200 mM were also prepared with a 0.4 mm thickness.

2.4. Hydrogels characterization

2.4.1. Infrared spectroscopy

The IR spectra of dried discs were recorded over the range 400–4000 cm^{-1}, in a Bruker IFS 66V FT-IR spectrometer (Germany), using the potassium bromide pellet technique.

2.4.2. Differential scanning calorimetry (DSC)

Thermal characterization of 4–6 mg samples of dried discs in aluminium crucibles was performed heating from 30 °C to 200 °C, then cooling to 0 °C and finally heating again up to 200 °C, at a rate of 20 °C/min, in a DSC Q-100 apparatus (TA Instruments, UK) equipped with a refrigerated cooling accessory. Nitrogen was used as purge gas at a flow rate of 50 ml/min. The calorimeter was calibrated for cell constant and temperature using indium (melting point 156.61 °C, enthalpy of fusion 28.71 J/g), and for heat capacity using sapphire standards. Tg is reported as the midpoint of the glass transition.

2.4.3. Swelling in water

The weight of each gel type at the dry state and after reaching equilibrium in water was measured in triplicate, at 25 °C. The water content, Q, was calculated as follows:

$$Q = (\mathrm{Ws}-\mathrm{Wd}) \times 100/\mathrm{Ws} \quad (1)$$

where Ws is the weight in the swollen state and Wd is the weight in the dry state.

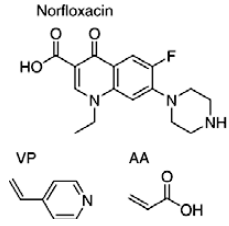

Fig. 1. Structure of norfloxacin and of the functional monomers evaluated (VP: 4-vinyl pyridine; AA: acrylic acid).

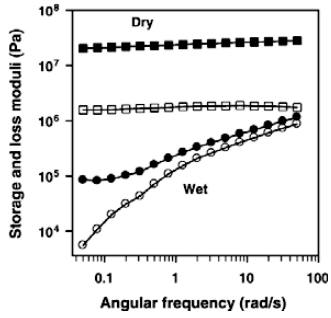

Fig. 2. Dependence of the storage (G', full symbols) and loss (G'', open symbols) moduli on the angular frequency for wet and dried PHEMA hydrogels copolymerized with AA 100 mM.

2.4.4. Viscoelastic properties

The storage or elastic (G') and the loss or viscous (G'') moduli of each lens when dry and when fully swollen were evaluated in triplicate at 25 °C, applying 0.5% strain and angular frequencies of 0.05–50 rad/s in a Rheolyst AR1000N rheometer (TA Instruments, UK) equipped with an AR2500 data analyzer, an environmental test chamber and a solid torsion kit. The sample was fixed between two clamps separated 6±0.5 mm. Additionally, the temperature dependence of G', G'', and $\tan\delta(=G''/G')$ of dry discs was recorded for an angular frequency of 1 rad/s by measuring these parameters while increasing the temperature from 25 to 200 °C at a rate of 3 °C/min.

2.4.5. NRF loading

Dried discs were placed in 0.025 mM, 0.050 mM or 0.100 mM NRF aqueous solutions (10 ml). Samples were allowed to equilibrate at 25 °C protected from light. The amount of NRF loaded by each gel was calculated as the difference between the initial and final concentrations in the surrounding solution, determined by UV spectrophotometry at 273 nm (HP Agilent, Germany).

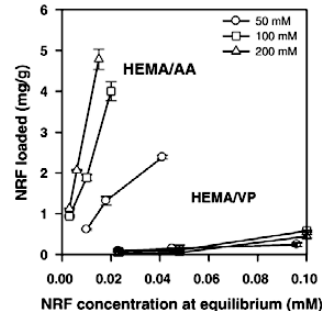

Fig. 3. NRF sorption isotherms for non-imprinted PHEMA hydrogels copolymerized with different proportions of AA or VP.

Table 1
Amount of NRF loaded (mg/g of dried gel) by non-imprinted PHEMA hydrogels cross-linked with EGDMA 80 mM and prepared with different proportions of VP or AA

PHEMA hydrogels	NRF loading solution (mM)		
	0.025	0.05	0.010
No comonomer	0.005 (0.001)	0.009 (0.002)	0.018 (0.002)
VP50	0.088 (0.014)	0.146 (0.007)	0.241 (0.045)
VP100	0.074 (0.065)	0.106 (0.062)	0.579 (0.025)
VP200	0.029 (0.030)	0.048 (0.029)	0.447 (0.045)
AA50	0.668 (0.118)	1.315 (0.104)	2.384 (0.045)
AA100	0.942 (0.020)	1.883 (0.077)	4.003 (0.232)
AA200	1.129 (0.018)	2.067 (0.013)	4.786 (0.247)

Mean values (standard deviations in brackets; $n=3$).

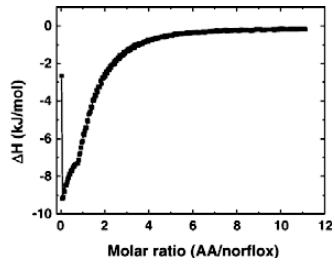

Fig. 5. ITC titration at 298 K of NRF 0.01 M with AA 0.50 M in HEMA solution.

2.4.6. Timolol loading

Dried discs were placed in a 0.050 mM timolol maleate aqueous solution (10 ml) for several days at 25 °C. The amount of drug loaded by each gel was calculated as the difference between the initial and final concentrations in the surrounding solution, which were determined by UV spectrophotometry at 294 nm (HP Agilent, Germany).

2.4.7. NRF release

NRF loaded hydrogels were rinsed with water and placed in 10–15 ml of artificial lachrymal fluid (6.78 g/l NaCl, 2.18 g/l $NaHCO_3$, 1.38 g/l KCl, 0.084 g/l $CaCl_2 \cdot 2H_2O$, pH 8) at 37 °C for 1 week. The experiments were carried out in triplicate under sink conditions. Samples of the solution (1 ml) were withdrawn at regular intervals and returned to the vial immediately after their NRF concentration was measured spectrophotometrically at 273 nm. The Higuchi equation [44] was fitted to the release profiles from 10 up to 70% drug released. The statistical comparison of release rates, K_H, was made using the non-parametric Kruskal–Wallis analysis (Statgraphics Plus 5.1), which is an adequate procedure for testing the equality of means in the one factor analysis of variance when the experimenter wishes to avoid the assumption that the samples were selected from normal populations, followed by Multiple Range Test [45].

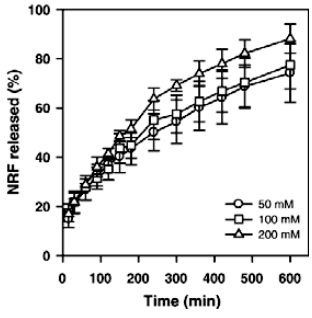

Fig. 4. NRF release profiles in lachrymal fluid from non-imprinted PHEMA hydrogels copolymerized with different proportions of AA, after being loaded in 0.1 mM NRF solution ($n=3$).

3. Results and discussion

The NRF structure makes the drug potentially able to interact simultaneously with various functional monomers, which is a main requirement for the achievement of imprinted networks. It has two ionisable groups: a carboxylic acid ($pK_{a_1}=6.34\pm0.06$) and an amino group ($pK_{a_2}=8.75\pm0.07$) [37] that can electrostatically interact with ionized groups of other molecules (Fig. 1). Additionally, it can also interact through hydrogen bonds or establish hydrophobic interactions through the aromatic ring. This has prompted us to choose VP and AA as possible functional monomers (Fig. 1). AA is a weak acid ($pK_a=4.5$) that could interact with the protonizable amino groups or with hydrogen bond acceptor groups; whilst VP is a weak base ($pK_b=8.5$; [46]) with affinity for acid groups and also able to interact with the aromatic group through π–π stacking.

3.1. Non-imprinted hydrogels: preliminary studies

In order to carry out a first screening of the suitability of AA or VP as functional monomers, conventional (i.e. non-imprinted) hydrogels were prepared with different proportions for each

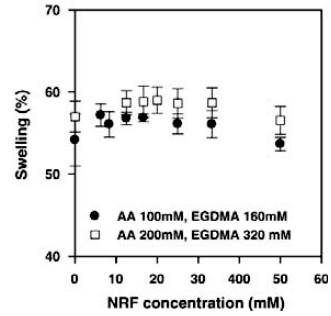

Fig. 6. Influence of the NRF concentration used to prepare imprinted PHEMA hydrogels on their ability to swell in water ($n=3$).

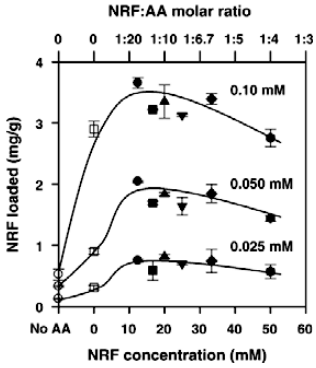

Fig. 7. NRF loaded by PHEMA hydrogels synthesized with AA 200 mM and EGDMA 320 mM using different NRF:AA molar ratios (upper *X*-scale). The lower *X*-scale represents the NRF concentration in the monomers solution during synthesis (imprinted: full symbols; non-imprinted: open squares). NRF concentrations of the solutions used for loading are shown on the plots. The open circles on the *Y*-axis represent the amount loaded by non-imprinted PHEMA hydrogels that do not contain AA. Lines are only a guide for the eye ($n=3$).

of them. After boiling in water, which is a common procedure for removal of unreacted species and sterilization of contact lenses, their properties as contact lenses and as drug delivery devices were evaluated.

For all the hydrogels, the completion of polymerization was shown by their FTIR spectra, not featuring bands at 1638 cm^{-1} and 950 cm^{-1} that are characteristic of unreacted C═C double bonds. This ensures good chemical compatibility and lack of cellular toxicity. The dry discs also showed a high transmittance at 600 nm (>90%) and a glass-to-rubber transition at 120–130 °C, which is in agreement with the values previously reported for PHEMA networks [47]. Fig. 2 shows the dependence of the elastic, G', and viscous, G'', moduli of PHEMA-AA hydrogels on angular frequency at 25 °C; the pattern being similar for all the hydrogels. The dried discs were rigid and fragile and had G' and G'' values almost three orders of magnitude greater than once swollen in water. The G' and G'' values of fully swollen hydrogels were slightly dependent on angular frequency, which is characteristic of a well-structured polymer network, and in the range considered appropriate for obtaining physically resistant but comfortable lenses [48]. PHEMA hydrogels containing AA showed slightly greater rates and degrees of swelling ($Q=60\pm 5\%$) than those prepared with VP ($Q=55\pm5\%$), owing to the more hydrophilic character of the former. Water uptake was well fitted by the square-root kinetics ($r^2>0.97$), which indicates that the process is mainly driven by Fickian diffusion. The slopes of the water uptake plots for both the hydrogels prepared with AA ($4.7\pm0.2\%\ s^{-0.5}$) or with VP ($4.0\pm0.1\%\ s^{-0.5}$) demonstrate that water molecules easily penetrate into the network. Therefore, any of these hydrogels fulfil the requirements for use as contact lenses.

Once immersed in NRF solutions, PHEMA-AA hydrogels showed a remarkably greater affinity for the drug than PHEMA-VP hydrogels (Fig. 3; Table 1), being able to absorb most of the drug initially present in the loading solution (ca. 90% by PHEMA-AA 200 mM). Although the presence of any of the functional monomers enhanced the loading capacity of PHEMA hydrogels, only those copolymerized with AA 100 mM or 200 mM were able to load amounts of drug similar or above to 0.18 mg/disc. This dose matches up with the total amount of drug ocularly available each 24 h when instilled as eye-drops, supposing that 2 drops of 25 μl of 0.3% solution were instilled each hour, and that 5% of the instilled dose was effectively absorbed through the cornea. These results highlight the role of AA in the loading of the drug by the hydrogels, probably because its electrostatic attraction for the amino groups and the hydrogen bonding interactions with various groups of the drug. The affinity of the PHEMA-AA hydrogels for the drug is also shown in the sustained release pattern obtained when immersed in artificial lachrymal fluid (Fig. 4). Hydrogels prepared with AA 200 mM showed a slightly greater release rate owing to their greater swelling in the release medium.

3.2. Imprinted hydrogels

According to the preliminary results AA was chosen as functional monomer to apply the molecular imprinting technology. NRF is highly photosensitive and, therefore, UV-photopolymerization could not be applied. By contrast, it is stable at the temperature used for thermal polymerization [49]. Additionally, it dissolves easily in HEMA.

For a successful imprinting, the cross-linking proportion has to be above that of the functional monomer [50] and adequate template: functional monomer molar ratios have to be used [51]. Therefore, EGDMA 160 mM or 320 mM was chosen to prepare imprinted PHEMA hydrogels containing AA 100 mM or 200 mM, respectively. To characterize the complexation of NRF with AA, ITC studies were carried out using an AA concentration low enough to minimize the self-association of this monomer [43].

Table 2
Amount of NRF loaded (AL; mg/g of gel) by imprinted PHEMA hydrogels prepared with NRF:AA 1:3 to 1:6 molar ratios and different thicknesses

PHEMA Hydrogels	NRF loading solution (mM)					
	0.025		0.050		0.010	
	AL	I_F	AL	I_F	AL	I_F
AA 100 (0.9 mm)	0.79 (0.06)	1.70–2.10	1.62 (0.14)	1.41–1.70	3.00 (0.19)	0.85–1.00
AA 200 (0.9 mm)	1.01 (0.04)	1.86–2.41	1.84 (0.13)	1.60–2.05	3.32 (0.20)	0.95–1.17
AA 200 (0.4 mm)	1.60 (0.12)	2.06–2.46	3.21 (0.21)	1.42–1.80	5.89 (0.56)	0.99–1.13

The imprinted factor ranges ($I_F=AL_{MIP}/AL_{NIP}$) are also shown. Mean values (standard deviations in brackets; $n=3$).

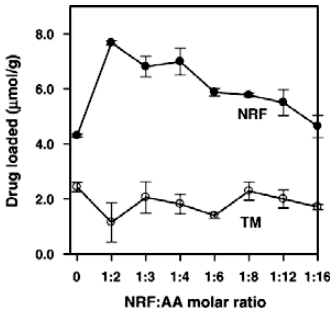

Fig. 8. Amounts of timolol (TM) and norfloxacin (NRF) loaded by immersion in 0.05 mM drug solutions of PHEMA hydrogels synthesized with AA 100 mM and EGDMA 160 mM using different NRF:AA molar ratios. Lines are only a guide for the eye ($n=3$).

Nevertheless, the small dilution enthalpies were subtracted from the raw enthalpy data obtained during the titration. The corrected calorimetric profile of the titration of 0.01 M NRF solution with 0.5 M AA solution in HEMA medium (Fig. 5) revealed a strong exothermic interaction. There was an inflexion point at a NRF:AA 1:1 molar ratio and the addition of greater amounts of AA caused a progressively lower change in enthalpy. The binding saturates at 1:4 molar ratio. This ratio should be adequate to create receptors in the lens structure with a high affinity for NRF. If a lower proportion of AA is used, the NRF binding capability cannot be completely fulfilled; if the proportion of AA is greater, some AA can randomly distribute within the network as in the case of the non-imprinted lenses. To elucidate the practical importance of the NRF:AA molar ratio on the loading and controlled release properties of the PHEMA lenses, these were prepared with the following compositions: i) 100 mM AA, 160 mM EGDMA and NRF:AA molar ratios of 1:2, 1:3, 1:4, 1:6, 1:8, 1:12 and 1:16; and ii) 200 mM AA, 320 mM EGDMA and NRF:AA molar ratios of 1:4, 1:6, 1:8, 1:10, 1:12 and 1:16. Additionally, non-imprinted hydrogels were prepared without adding NRF.

Once the drug was removed, the imprinted hydrogels were transparent, and showed an appearance and viscoelastic properties similar to those of the non-imprinted hydrogels. FT-IR spectra confirmed the absence of residual monomers. The swelling behaviour was neither affected by the synthesis of the hydrogels in the presence of the drug (Fig. 6).

When reloaded in NRF solutions of low concentration, imprinted hydrogels were able to uptake significantly greater NRF amounts than the non-imprinted ones. Fig. 7 shows the loading ability of the different PHEMA hydrogels prepared with AA 200 mM, after removal of the drug used in the synthesis, and also of PHEMA hydrogels prepared without comonomer (data on the *Y*-axis). Once immersed in the most diluted NRF solution (0.025 mM), the difference in amount of NRF loaded by imprinted and non-imprinted hydrogels was maximum. When there are few NRF molecules in the solution surrounding the hydrogel disc, these can exclusively bind to the regions of the hydrogel that present the highest affinity, i.e. the most perfectly created binding sites. This explains the greater loading ability of the imprinted discs (see imprinting factors on Table 2). By contrast, as the NRF concentration increases, once the high affinity binding points saturate, the drug molecules can be progressively uptaken by low affinity regions, and the differences in loading between the imprinted and the non-imprinted hydrogels become harder to see [52]. This is particularly evident in the case of NRF since there is a strong ionic interaction of the amino group of each drug molecule with acrylic acid. This should prompt the drug to bind to as much as AA available in the non-imprinted hydrogel, with a predominantly 1:1 stoichiometry. In the imprinted hydrogels, each binding cavity is formed with more AA groups; one of them interacting ionically and the others contributing with hydrogen-bonds or hydrophobic interactions to stabilize the bound molecule and, therefore, increasing the binding energy. In highly concentrated drug

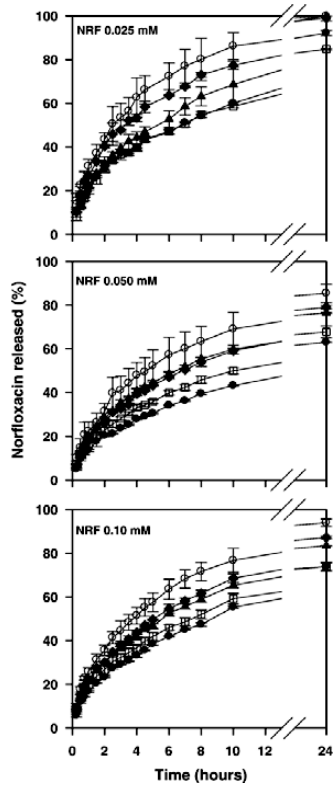

Fig. 9. NRF release profiles in lachrymal fluid from PHEMA hydrogels synthesized with AA 100 mM and EGDMA 160 mM using different NRF:AA molar ratios; zero, i.e. non-imprinted hydrogels (○), 1:16 (♦), 1:8 (▲), 1:4 (□), and 1:2 (●). The hydrogels (thickness 0.9 mm) were previously loaded by immersion in 0.025 mM, 0.050 mM or 0.10 mM NRF solutions ($n=3$).

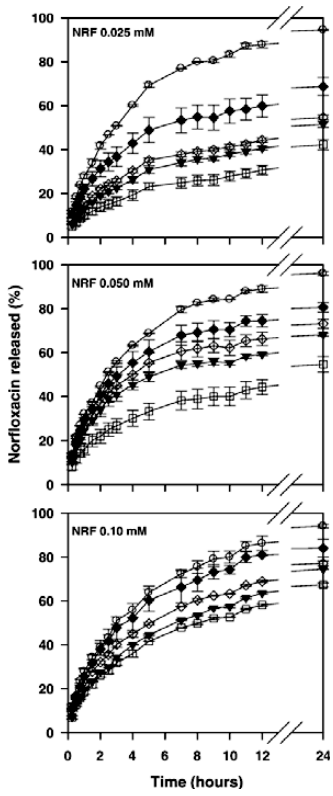

Fig. 10. NRF release profiles in lachrymal fluid from PHEMA hydrogels synthesized with AA 200 mM and EGDMA 160 mM using different NRF:AA molar ratios; zero, i.e. non-imprinted hydrogels (○), 1:16 (♦), 1:10 (◇), 1:6 (▼), and 1:4 (□). The hydrogels (thickness 0.4 mm) were previously loaded by immersion in 0.025 mM, 0.050 mM or 0.10 mM NRF solutions (n=3).

solutions, this may even result in a lower amount of drug for saturating the perfectly constructed imprinted hydrogels, compared to the non-imprinted hydrogels or to hydrogels imprinted using inadequate template:functional monomer stoichiometry. This is clearly shown in Fig. 7 for hydrogels loaded by immersion in 0.10 mM NRF; i.e. imprinted hydrogels containing a fix AA proportion (200 mM) showed a decrease in the loading as the proportion of NRF used during synthesis increased up to reaching the NRF:AA 1:4 molar ratio. This is due to that in all cases the total number of functional groups is the same, but the number of each of them that gather to form the binding site is different. In the non-imprinted hydrogels, the AA groups are randomly distributed and each of them constitutes a potential binding site. In the NRF:AA 1:4 imprinted hydrogels, once the NRF used for synthesis is removed and the hydrogels are immersed in a NRF solution, each binding site is formed by four AA (ideal condition). Therefore, each NRF molecule reloaded by the optimally synthesized hydrogels consumes four functional groups. The hydrogels with compositions in between those of the non-imprinted and the NRF:AA 1:4 imprinted hydrogels (i.e. those ranging from NRF:AA 1:16 to 1:6), present upon synthesis a certain number of cavities with four AA while the remaining AA groups are randomly distributed. As a consequence, when they are immersed in a highly concentrated NRF solution, the drug molecules can be a host by the imprinted cavities (with a 1:4 stoichiometry) and by the randomly distributed AA groups (with 1:1 or 1:2 stoichiometry). On the other hand, the loading is also conditioned by the strength of the binding; the 1:4 cavities providing the highest affinity. This explains the curvature of the plot for 0.10 mM loading: as the NRF proportion used for synthesis increased, the number of total binding sites decreases but the strength of the binding increases. In summary, the balance between both factors determines the saturation levels.

Table 2 summarizes the amounts of NRF loaded by the imprinted hydrogels prepared with NRF:AA 1:3 to 1:6 molar ratios, which were very similar for each type of hydrogel. It is interesting to note the greater loading ability of the thinnest PHEMA-co-AA 200 mM hydrogels. The discs of 0.4 mm thickness took up the same amounts of NRF as the discs of 0.9 mm thickness (i.e. 0.07 mg, 0.14 mg and 0.22 mg/disc, when immersed in NRF solutions of 0.025 mM, 0.050 mM, and 0.10 mM, respectively), despite the thickest discs weighing more than double. Since all these hydrogels are loosely cross-linked, the high density of the polymeric chains should not be enough to hinder the free diffusion of the drug through the inner parts of the network. However, owing to the high affinity of the hydrogels for

Table 3
NRF release rate constants (K_H; $\%min^{-1/2}$) in lachrymal fluid obtained by fitting of the release profiles to the Higuchi equation, for the three types of hydrogels synthesised in the presence of different NRF:AA molar ratios and then loaded by immersion in NRF solutions (0.025 mM, 0.050 mM, and 0.10 mM)

NRF:AA	AA 100 mM (0.9 mm) loaded in NRF			NRF:AA	AA 200 mM (0.9 mm) loaded in NRF			AA 200 mM (0.4 mm) loaded in NRF		
	0.025 (mM)	0.050 (mM)	0.10 (mM)		0.025 (mM)	0.050 (mM)	0.10 (mM)	0.025 (mM)	0.050 (mM)	0.10 (mM)
0	3.73	3.09	3.43	0	3.87	3.16	2.68	3.92	3.86	3.37
1:16	3.37	2.60	2.85	1:16	3.81	3.24	2.50	2.24	2.82	3.05
1:12	2.91	2.67	2.51	1:12	3.59	3.05	2.56	1.84	2.77	2.85
1:8	2.99	2.48	2.66	1:10	3.45	3.15	2.51	1.62	2.65	2.58
1:6	2.97	2.29	2.29	1:8	3.42	3.00	2.47	1.54	2.25	2.57
1:4	2.49	2.09	2.24	1:6	2.76	2.91	2.40	1.47	2.12	2.44
1:3	2.64	2.06	2.31	1:4	2.71	2.26	2.12	1.11	1.57	2.21

Variation coefficients were below 10%.

the drug (isotherms similar to those shown in Fig. 3), the free drug remaining in solution once sorption equilibrium was reached (less than the 25% of the initial one) may be too low to enable further sorption. This ability of the hydrogels to make use of almost all drug in solution, far from being a drawback (drug solubility in water did not allow more concentrated solutions to be prepared), has an interesting practical importance since it avoids any concern over drug waste during loading of these hydrogels if used as therapeutic contact lenses.

The ability of NRF imprinted hydrogels to load timolol was evaluated to test the specificity of the binding receptors (Fig. 8). Timolol has spatial size similar to that of NRF (estimated using CS Chem3D Std® software v. 4.0, Cambridge Soft Corporation), and has previously shown a high affinity for PHEMA-co-AA hydrogels [26]. By contrast, the nature and spatial distribution of the chemical groups is quite different. When immersed in 0.050 mM drug solutions, NRF imprinted hydrogels loaded remarkably lower amounts of timolol than of NRF, and similar to those loaded by the non-imprinted hydrogels. This proves the ability of the imprinted cavities to specifically recognize NRF. This test was carried out using loading drug solutions of concentration (0.050 mM) not enough to saturate the hydrogels and, as a consequence, the binding affinity is the main factor for loading. This explains that hydrogels prepared with the NRF:AA 1:4 loaded more NRF than those synthesized with lower molar ratios.

NRF-loaded hydrogels did not release the drug when immersed in water (only a 4% after 24 h), which confirms the strength of the interactions and opens also the possibility of storing the drug-loaded lenses in aqueous medium. Once immersed in lachrymal fluid, the hydrogels were able to sustain drug release for more than one day, although remarkable differences in release were observed as a function of the NRF:AA molar ratio used to prepare the hydrogels (Figs. 9 and 10). In all cases, the release constants, obtained by fitting of Higuchi equation (Table 3), for imprinted hydrogels with NRF:AA molar ratio above 1:16 were lower than those for the non-imprinted ones ($p<0.001$). Imprinted hydrogels prepared with NRF:AA 1:3 or 1:4 molar ratios showed the greatest ability to control the release of the drug, sustaining the process for 2 to 5 d. The net difference in release rate between imprinted and non-imprinted hydrogels was greater for those loaded in the most diluted drug solution. These findings clearly correlate with the ITC results. The NRF:AA 1:4 molar ratio was the one predicted by calorimetric titration as the minimum needed to saturate the binding points of the drug and, therefore, the one that can provide the most perfectly created imprinted cavities. Once immersed in diluted NRF solutions, the drug is host in these high affinity cavities and such an affinity is responsible for sustaining the release. It is also interesting to note that the PHEMA-co-AA hydrogels showed a release rate independent of their thickness (release profiles were practically superimposed for 0.9 and 0.4 mm thickness). This clearly corroborates that the release is controlled by the affinity of the cavities for the drug and not by the diffusion of the free drug through the network. Otherwise, the thinnest discs would show a significantly greater release rate [23].

The minimum inhibitory concentration, MIC, of norfloxacin for most bacteria is below 2.6 μg/ml [42]. This concentration is attained in the in vitro experiments in 30–60 min when using hydrogels loaded by immersion in NRF 0.1 mM. Taking into account that the volume of lachrymal fluid in the postlens region is much smaller than the one used for the in vitro experiments, it is foreseeable that the MIC can be achieved in few minutes.

4. Conclusions

The use of AA as functional monomer and the application of the molecular imprinting technology enabled the development of hydrogels with a high NRF loading ability (up to 300 times more than that shown by PHEMA conventional hydrogels) and able to sustain the release for several hours or even days. Since the development of a drug-imprinted network is a very specific process, the ITC analysis is an extremely useful tool to elucidate the stoichiometry of the complexes and for a rational design of imprinted lenses. The success of attaining lenses able to control drug release is directly linked to the creation of high affinity binding points. The drug:functional monomer ratio strongly determines the structure of the imprinted cavities and, therefore, is a critical variable in the optimization of the performance of the lenses as drug delivery devices. The synthesis with the NRF:AA 1:4 molar ratio provides hydrogels of reproducible behaviour, disregarding of the total content in AA (100 or 200 mM) or the thickness (0.4 or 0.9 mm), which is an index of the robustness of the imprinting technique developed.

Acknowledgements

This work was supported by the Ministerio de Educación y Ciencia and FEDER, Spain (SAF2005-01930; RYC2001-8). The authors thank V. de Brouwer for the help in the initial steps of this work, P. Taboada for the assistance with the ITC experiments, and H. Hiratani for the valuable comments during the development of the work.

References

[1] I.K. Reddy, M.G. Ganesan, Ocular therapeutics and drug delivery: an overview, in: I.K. Reddy (Ed.), Ocular Therapeutics and Drug Delivery, Technomic, Lancaster, Pennsylvania, USA, 1996, pp. 3–29.
[2] H. Pinto-Alphandary, A. Andremont, P. Couvreur, Targeted delivery of antibiotics using liposomes and nanoparticles: research and applications, Int. J. Pharm. 13 (2000) 155–168.
[3] P.Y. Robert, A. Tassy, Bioavailability of antibiotics, J. Fr. Ophtalmol. 23 (2000) 510–513.
[4] C. Castro, C. Evora, M. Baro, I. Soriano, E. Sanchez, Two-month ciprofloxacin implants for multibacterial bone infections, Eur. J. Pharm. Biopharm. 60 (2005) 401–406.
[5] M. Patrick, A.K. Mitra, Overview of ocular drug delivery and iatrogenic ocular cytopathologies, in: A.K. Mitra (Ed.), Ophthalmic Drug Delivery Systems, Marcel Dekker, New York, 1993, pp. 1–27.
[6] I.P. Kaur, M. Kanwar, Ocular preparations: the formulation approach, Drug Dev. Ind. Pharm. 28 (2002) 473–493.
[7] C.G. Wilson, Topical drug delivery in the eye, Exp. Eye Res. 78 (2004) 737–743.
[8] P.M. Hughes, O. Olejnik, J.E. Chang-Lin, C.G. Wilson, Topical and systemic drug delivery to the posterior segments, Adv. Drug Del. Rev. 57 (2005) 2010–2032.
[9] M.F. Refojo, F.L. Leong, I.M. Chan, F.I. Tolentino, Absorption and release of antibiotics by a hydrophilic implant for scleral buckling, Retina 3 (1983) 45–49.

[10] M.R. Jain, Drug delivery through soft contact lenses, Br. J. Ophthalmol. 72 (1988) 150–154.
[11] T.P. Heyrman, M.L. McDermott, J.L. Ubels, H.F. Edelhauser, Drug uptake and release by a hydrogel intraocular lens and the human crystalline lens, J. Cataract Refract. Surg. 15 (1989) 169–175.
[12] J.M. Chapman, L. Cheeks, K. Green, Drug interaction with intraocular lenses of different materials, J. Cataract Refract. Surg. 18 (1992) 456–459.
[13] C. Alvarez-Lorenzo, H. Hiratani, A. Concheiro, Contact lenses for drug delivery: achieving sustained release with novel systems, Am. J. Drug Del. (submitted for publication).
[14] L. Krejci, I. Brettschneider, R. Praus, Hydrophilic gel contact lenses as a new drug delivery system in ophtalmology and as a therapeutic bandage lenses, Acta Univ. Carol., Med. 21 (1975) 387–396.
[15] J.A. Silbert, A review of therapeutic agents and contact lens wear, J. Am. Optom. Assoc. 67 (1996) 165–172.
[16] J.L. Creech, A. Chauhan, C.J. Radke, Dispersive mixing in the posterior tear film under a sift contact lens, IEC Res. 40 (2001) 3015–3026.
[17] E.M. Hehl, R. Beck, K. Luthard, R. Guthoff, B. Drewelow, Improved penetration of aminoglycosides and fluoroquinolones into the aqueous humour of patients by means of Acuvue contact lenses, Eur. J. Clin. Pharmacol. 55 (1999) 317–323.
[18] G. Wajs, J.C. Meslard, Release of therapeutic agents from contact lenses, Crit. Rev. Ther. Drug Carr. Syst. 2 (1986) 275–289.
[19] T.T. McMahon, K. Zadnik, Twenty-five years of contact lenses: the impact on cornea and ophthalmic practice, Cornea 19 (2000) 730–740.
[20] C.C.S. Karlgard, N.S. Wong, L.W. Jones, C. Moresoli, In vitro uptake and release studies of ocular pharmaceutical agents by silicon-containing and p-HEMA hydrogel contact lens materials, Int. J. Pharm. 257 (2003) 141–151.
[21] J.P. Vairon, L. Yean, J.C. Meslard, F. Subira, C. Bunel, Immobilisation reversible sur polymers et liberation controlee, Application aux lentilles corneennes reservoirs de medicaments, L'actualité Chimique, Septembre–Octobre, 1992, pp. 330–350.
[22] D. Gulsen, A. Chauhan, Ophthalmic drug delivery through contact lenses, Invest. Ophthalmol. Visual Sci. 45 (2004) 2342–2347.
[23] D. Gulsen, C.C. Li, A. Chauhan, Dispersion of DMPC liposomes in contact lenses for ophthalmic drug delivery, Curr. Eye Res. 30 (2005) 1071–1080.
[24] R. Uchida, T. Sato, H. Tanigawa, K. Uno, Azulene incorporation and release by hydrogel containing methacrylamide propyltrimethylammonium chloride, and its application to soft contact lens, J. Control. Release 92 (2003) 259–264.
[25] T. Sato, R. Uchida, H. Tanigawa, K. Uno, A. Murakami, Application of polymer gels containing side-chain phosphate groups to drug-delivery contact lenses, J. Appl. Polym. Sci. 98 (2005) 731–735.
[26] C. Alvarez-Lorenzo, H. Hiratani, J.L. Gomez-Amoza, R. Martinez-Pacheco, C. Souto, A. Concheiro, Soft contact lenses capable of sustained delivery of timolol, J. Pharm. Sci. 91 (2002) 2182–2192.
[27] H. Hiratani, C. Alvarez-Lorenzo, Timolol uptake and release by imprinted soft contact lenses made of *N*,*N*-diethylacrylamide and methacrylic acid, J. Control. Release 83 (2002) 223–230.
[28] H. Hiratani, C. Alvarez-Lorenzo, The nature of backbone monomers determines the performance of imprinted soft contact lenses as timolol drug delivery systems, Biomaterials 25 (2003) 1105–1113.
[29] H. Hiratani, A. Fujiwara, Y. Tamiya, Y. Mizutani, C. Alvarez-Lorenzo, Ocular release of timolol from molecularly imprinted soft contact lenses, Biomaterials 26 (2005) 1293–1298.
[30] H. Hiratani, Y. Mizutani, C. Alvarez-Lorenzo, Controlling drug release from imprinted hydrogels by modifying the characteristics of the imprinted cavities, Macromol. Biosci. 5 (2005) 728–733.
[31] C.J. Allender, C. Richardson, B. Woodhouse, C.M. Heard, K.R. Brain, Pharmaceutical applications for molecularly imprinted polymers, Int. J. Pharm. 195 (2000) 39–43.
[32] M.E. Byrne, K. Park, N.A. Peppas, Molecular imprinting within hydrogels, Adv. Drug Del. Rev. 54 (2002) 149–161.
[33] C. Alvarez-Lorenzo, A. Concheiro, Molecularly imprinted polymers for drug delivery, J. Chromatogr., B 804 (2004) 231–245.
[34] C.F. van Nostrum, Molecular imprinting: a new tool for drug innovation, Drug Discov. Today (2005) 119–124.
[35] K. Sreenivasan, Surface-imprinted polyurethane having affinity sites for ampicillin, Macromol. Biosci. 5 (2005) 187–191.
[36] D. Cunliffe, A. Kirby, C. Alexander, Molecularly imprinted drug delivery systems, Adv. Drug Del. Rev. 57 (2005) 1836–1853.
[37] Martindale, The complete drug reference, in: K. Parfitt (Ed.), 32nd ed., Pjarmaceutical Press, London, 1999, p. 233.
[38] P.C. Donshik, Extended wear contact lenses, Ophthalmol. Clin. North Am. 16 (2003) 79–83.
[39] T. Wong, S. Ormonde, G. Gamble, C.N.J. McGhee, Severe infective keratitis leading to hospital admission in New Zealand, Br. J. Ophthalmol. 87 (2003) 1103–1108.
[40] M.E. Zegans, H.I. Becker, J. Budzik, G. O'Toole, The role of bacterial biofilms in ocular infections, DNA Cell Biol. 21 (2002) 415–420.
[41] R. Mely, Therapeutic and cosmetic indications of lotrafilcon: a silicone hydrogel extended-wear lenses, Ophthalmologica 218 (2004) 33–38.
[42] M.N. Kim, A.H. Lim, J.S. Yoon, Antibacterial activity of polymers with norfloxacin moieties against native and norfloxacin-tolerance-induced bacteria, J. Appl. Polym. Sci. 96 (2005) 936–943.
[43] W.P. Fish, J. Ferreira, R.D. Sheardy, N.H. Snow, T.P. O'Brien, Rational design of an imprinted polymer: maximizing selectivity by optimizing the monomer-template ratio for a chinchonidine MIP, prior to polymerization using microcalorimetry, J. Liq. Chromatogr. Relat. Technol. 28 (2005) 1–15.
[44] W.I. Higuchi, Analysis of data on the medicament release from ointments, J. Pharm. Sci. 51 (1962) 802–804.
[45] S. Siegel, N.J. Castellan, Nonparametric Statistics for the Behavioural Sciences, 2nd ed., McGraw-Hill, New York, 1988, pp. 213–215.
[46] A.M. Mika, R.F. Childs, Acid/base properties of poly(4-vinylpyridine) anchored within microporous membranes, J. Membr. Sci. 152 (1999) 129–140.
[47] G. Di Marco, M. Lanza, M. Pieruccini, Dynamical mechanical measurements in dry PHEMA and its hydrogels, Nuovo Cim., D 16 (1994) 849–854.
[48] M.F. Refojo, F.L. Leong, Poly(methylacrylate-co-hydroxyethylacrylate) hydrogel implant material of strength and softness, J. Biomed. Mater. Res. 15 (1981) 497–509.
[49] B. Sustar, N. Bukovec, P. Bukovec, Polymorphism and stability of norfloxacin, (1-ethyl-6-fluoro-1,4-dihydro-4-oxo-7-(1-piperazinil)-3-quinolinocarboxylic acid, J. Therm. Anal. 40 (1993) 475–481.
[50] K. Ito, J. Chuang, C. Alvarez-Lorenzo, T. Watanabe, N. Ando, A.Yu. Grosberg, Multiple point adsorption in a heteropolymer gel and the Tanaka approach to imprinting: experiment and theory, Prog. Polym. Sci. 28 (2003) 1489–1515.
[51] C. Baggiani, L. Anfossi, C. Giovannoli, C. Tozzi, Binding properties of 2,4,5-trichlorophenoxyacetic acid-imprinted polymers prepared with different molar ratios between template and functional monomer, Talanta 62 (2004) 1029–1034.
[52] R.J. Umpleby, S.C. Baxter, A.M. Rampey, G.T. Rushton, Y.Z. Chen, K.D. Shimizu, Characterization of the heterogeneous binding site affinity distributions in molecularly imprinted polymers, J. Chromatogr., B 804 (2004) 141–149.

3.3. Timolol-imprinted soft contact lenses: influence of the template/ functional monomer ratio and the hydrogel thickness

Enviado

Timolol-imprinted soft contact lenses: influence of the template/functional monomer ratio and the hydrogel thickness

FERNANDO YAÑEZ[1], ANUJ CHAUHAN[2], ANGEL CONCHEIRO[1], CARMEN ALVAREZ-LORENZO[1,*]

[1]Departamento de Farmacia y Tecnologia Farmaceutica, Facultad de Farmacia, Universidad de Santiago de Compostela, 15782-Santiago de Compostela, Spain.

[2] Department of Chemical Engineering, University of Florida, Gainesville, FL 32611-6005, USA.

*Correspondence to: C. Alvarez-Lorenzo (E-mail: carmen.alvarez.lorenzo@usc.es)

Abstract

Isothermal titration calorimetry (ITC) was used to identify the optimal timolol:functional monomer ratio for preparing soft contact lenses (SCLs) able to sustain drug release. The ITC profiles revealed that each timolol molecule requires 6 to 8 acrylic acid (AAc) monomers to saturate the binding interaction, pointing out that these ratios could be the most suitable for creating imprinted cavities. Various sets of poly(hydroxyethyl methacrylate-co-AAc) hydrogels of 0.2 and 0.9 mm thickness were prepared with timolol:AAc molar ratios ranging from 1:6 to 1:32 and also in the absence of timolol. The hydrogels were reloaded with timolol by immersion in 0.04, 0.06, 0.08 and 0.10 mM drug solutions. Both imprinted and non-imprinted hydrogels showed a high affinity for the drug owing to the presence of AAc. Nevertheless, the imprinted hydrogels prepared with the 1:6 or 1:8 timolol:AAc molar ratio loaded less amount of timolol but sustained the release better than the other imprinted and non-imprinted hydrogels. These differences are explained in terms of the different arrangement of the functional monomers along the network. The imprinting effect was more noticeable in the case of the thinnest hydrogels, where the contribution of diffusional path to the release rate is smaller. The results obtained prove the interest of ITC for the rational design of drug-imprinted networks to be used as medicated SCLs.

Keywords: hydrogel thickness; isothermal titration calorimetry (ITC); molecular imprinting; ocular controlled release; soft contact lenses; template: functional monomer ratio.

INTRODUCTION

Soft contact lenses (SCL) have been proposed as drug carriers for sustained delivery to the ocular structure since various decades ago.[1,2] SCLs preferentially release the drug molecules to the post-lens tear film, between the cornea and the lens, resulting in a prolonged contact with the cornea surface.[3] In this way, the drug escapes from the protective ocular mechanisms and the sorption through the conjunctiva is also minimized. Therefore, drug-eluting SCLs may be particularly convenient for clinical conditions requiring a high intraocular concentration of drug, such as anterior segment inflammations, angle closure glaucoma or infections. The immersion of the SCL in a drug solution or the instillation of the eye drops on the surface of the lens after insertion have been shown to improve both ocular bioavailability and pharmacological response of various drug molecules, compared to conventional eye drops administration.[4-7] Thus, the development of a combination device for simultaneous refractive correction and drug release may fill a relevant therapeutic gap.[8,9] Nevertheless, drug eluting-SCLs have still to face up to the fact that, if the drug does not interact with the polymeric network, the drug loading and release is only driven by passive diffusion through the aqueous phase of the network. This limits both the amount loaded and the control of the release, which may be insufficient for a prolonged delivery.[10,11]

Over the last few years, several approaches are being explored to improve the performance of SCLs as drug delivery devices: i) chemically-reversible immobilization of drugs through labile bonds;[12-14] ii) incorporation of drug-loaded colloidal systems into the lens;[15-18] iii) copolymerization with functional monomers able to interact directly with the drug;[19-21] and iv) molecular imprinting.[22-27] The molecular imprinting technology pursues the optimization of the spatial distribution of monomers able to interact with the drug (named functional monomers) in order to achieve the maximum efficiency of the interactions between the drug and the polymeric network. To do that, the drug molecules are used as templates during polymerization with the purpose of creating “tailored-active sites” or “imprinted pockets” with the size and the most suitable chemical groups to interact with the drug.[28-29] Upon washing out the drug molecules that served as templates, the polymer network is expected to recognize the drug when enters in contact with it again, and to accommodate the drug molecules more efficiently than conventional

hydrogels prepared in the absence of the drug. Research on drug-imprinted SCLs has focused so far on three therapeutic groups, namely β-adrenergic antagonists (timolol),[30] antimicrobials (norfloxacin),[24] and antihistamines (ketotifen),[31-34] and on comfort ingredients (hyaluronic acid).[35]

The aim of this work was to gain insight into the development of timolol-imprinted SCL by exploring the influence of timolol: acrylic acid (AAc) ratio during synthesis and of the hydrogel thickness in the micrometer range. Timolol has been already found suitable for preparing imprinted networks using as functional monomers those bearing carboxylic acid groups, probably because the ability of timolol to behave as donor and acceptor of hydrogen bonds.[22,30,36] Differently from conventional highly-cross-linked imprinted networks, the peculiar optical and mechanical features of the SCLs restrict the nature and proportion of the functional monomers and the degree of cross-linking. Thus, the lower physical stability of the cavities in the imprinted lenses has to be compensated maximizing the affinity for the drug. In this sense, the selection of the optimum timolol:functional monomer ratio is a key parameter for the achievement of the imprinting effect and the adequate performance of the SCLs as drug delivery systems. In addition to the trial and error approach, various computacional and analytical techniques may provide information about the stoichiometry, strength and stability of the drug-functional monomers complexes during the lens synthesis.[37-41] We have previously seen that the isothermal titration calorimetry (ITC) is a suitable technique for identifying the optimal norfloxacin:AAc ratio when this antimicrobial agent was used as template of imprinted SCL.[24] In the present work we want to elucidate the interest of ITC as a tool for the rational design of soft contact lenses that can sustain the release of timolol once applied onto the eyes, and to determine to what extent the thickness of the hydrogels may affect the role of the imprinted cavities in the drug release control.

EXPERIMENTAL

Materials

2- Hydroxyethyl methacrylate (HEMA) and acrylic acid (AAc) were supplied by Merck (Germany). Ethyleneglycol dimethacrylate (EGDMA), timolol maleate salt (S-[-]-isomer form), and dichlorodimethylsilane were from Sigma-Aldrich (USA). 2,2´-Azobis(2-methyl-propionitrile) (AIBN) was obtained from Acros (Belgium). All other chemicals were of reagent grade.

Calorimetric titration of timolol with AAc

The interactions between timolol and AAc in HEMA solution were evaluated by ITC (VP-ITC MicroCal Inc., Northampton, MA). The experiments were carried out in duplicate (reproducibility within ± 5%) at 25ºC, titrating the AAc solution (0.50 M, 0.290 ml) onto the timolol solution (0.01M, 1.439 ml). The binding experiment involved sequential additions of 1 µl aliquots of the AAc solution in the reaction cell under continuous stirring at 280 rpm. Control experiments were carried out under identical conditions to obtain the heats of dilution and mixing involved in the injection of AAc solution into the HEMA medium. The net reaction enthalpy was obtained by subtracting the dilution enthalpies from the apparent titration enthalpies.

Synthesis of the hydrogels

AAc (1.87 g) and EGDMA (10.27 g) were mixed with 130 ml of HEMA. To 20 ml aliquots of this solution (0.15 mol HEMA, $4 \cdot 10^{-3}$ mol AAc and $8 \cdot 10^{-3}$ mol EGDMA), different amounts of timolol maleate were added to obtain timolol maleate:AAc molar ratios of 0 (non-imprinted networks) or 1:6, 1:8, 1:12, 1:16, and 1:32 (imprinted networks). AIBN (0.032 g) was added to each solution and the monomers solutions were immediately injected in moulds made of two glass plates separated with silicone frames of 0.2 and 0.9 mm thickness. The glasses were previously treated with dichlorodimethylsilane, dried for 2 hour, and successively washed with distilled water and ethanol four times and dried in an oven.

Polymerization was carried out at 50ºC for 12 hours followed by 24 hours at 70ºC. The gels were removed from the moulds and immersed in boiling water for 15 min to

remove unreacted monomers. Then, 10-mm diameter discs were immediately cut from the gels with a cork borer and washed successively with water, 0.9% NaCl, HCl 0.1N and distilled water at room temperature. The washing solution was replaced 4 times a day, encompassing a complete washing period of 7 days. The removal of unreacted monomers and timolol was confirmed by the absence in the washing solutions of UV absorption bands between 190 and 900 nm. Then, the hydrogels were dried in an oven for 24 h at 40ºC.

Swelling kinetics

Dried hydrogels were weighed (W_0) and placed in 10 ml of water at 25°C. Swelling, Q_t, at various times t was calculated as relative weight gain:

$$Q_t = 100\ (W_t - W_0)/W_0 \qquad \text{(Eq. 1)}$$

The sample being weighed (W_t) on each occasion after careful wiping of its surface with a soft tissue

Timolol loading

Dried hydrogels were weighed and placed in timolol solutions at different concentrations (0.04, 0.06, 0.08 and 0.100 mM). The volume of the drug solution was chosen to be proportional to the volume of the hydrogels; i.e., 2 ml for hydrogels with a thickness of 0.2 mm, and 8 ml for 0.9 mm-thick hydrogels. The experiments were carried out in triplicate for each hydrogel. Timolol concentration in the loading solution was monitored by recording the absorbance at 294 nm (Agilent 8453 spectrophotometer, Germany).

The amount loaded by equilibrium between the aqueous phase of the network and the loading solution, which leads the drug concentration within the hydrogel to be equal to that of the loading solution, can be estimated using the following equation proposed by Kim et al. [42]:

$$Loading\ (aqueous\ phase) = (Vs/Wp)\cdot C_0 \qquad \text{(Eq. 2)}$$

where *Vs* is the volume of water sorbed by hydrogel (mL) and *Wp* is the weight (g) of the dried hydrogel,, and C_0 concentration of drug in the loading solution (mg/mL).

Timolol release

After loading, each hydrogel disk was rinsed with distilled water and placed in 2 ml (0.2 mm thickness) or 8 ml (0.9 mm thickness) of 0.9% NaCl solution. Samples of the release medium (1 ml) were withdrawn at regular time intervals and their timolol concentration measured spectrophotometrically at 294 nm. The samples were returned to the corresponding container immediately after each measure in order to maintain the initial volume of 0.9% NaCl. The experiments were carried out in triplicate. The release profiles up to a fraction released of 0.6 were fitted to the square root kinetics:

$$\frac{M_t}{M_\infty} = K_H \cdot t^{1/2} \qquad \text{(Eq. 3)}$$

where M_t and M_∞ represent the amount of timolol released at time *t* and at the end of the release test, respectively. The release rate constant K_H was estimated by linear regression.

Statistical analysis

Statgraphics Plus 5.1 software (Statistical Graphics Corp., USA) was used to carry out ANOVA of the release rate constants. Multiple range test was used to identify the systems that are statistically different from each other.

RESULTS AND DISCUSSION

Design and synthesis of the hydrogels

The first step of the present work was to identify the optimal timolol:AAc ratio required to form imprinted cavities. Thus, ITC experiments were carried out titrating the drug with AAc in the same medium (HEMA) where the hydrogels were going to be synthesized. The net reaction enthalpy was obtained by subtracting the dilution enthalpies from the apparent titration enthalpies (Figure 1). ITC studies revealed that maximum binding interaction between timolol and AAc occurs at a 1:2 molar ratio, and that the process saturates at around 1:8 molar ratio. Thus, hydrogels comprising timolol:AAc molar ratios inside and above this range were synthesized and tested to evidence the

imprinting effect. Since timolol maleate is not soluble above 33.3 mM in the monomers solution, this concentration was chosen for preparing the hydrogels with the highest timolol proportion; that is, timolol:AAc 1:6.

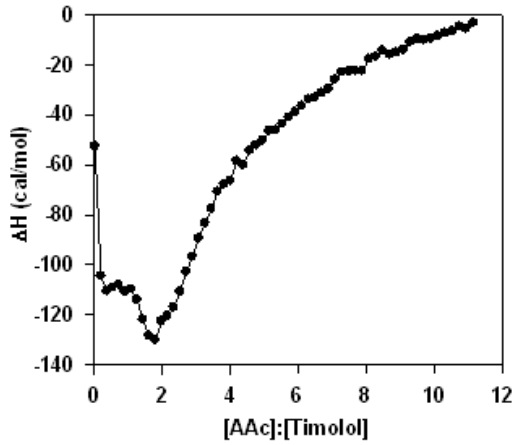

Figure 1. *ITC titration at 298K of timolol 0.01 M with AAc 0.50 M in HEMA solution.*

After polymerization, the hydrogels were boiled in water, which is a common procedure for removal of unreacted species and sterilization of SCLs, cut as 10 mm discs and then intensively washed to remove the drug template molecules. Non-imprinted hydrogels underwent the same process for comparative purposes. All hydrogels were totally transparent (transmittance above 80% at 600 nm) and swelled up to a similar extent in water (Figure 2). However, some differences in the swelling rate were observed as a function of the proportion of timolol added during hydrogel synthesis (Figure 3). These differences, although small, revealed that the imprinted hydrogels prepared with timolol:AAc 1:6 molar ratio require more time to swell, although the degree of swelling at equilibrium was statistically equal for all hydrogels. One can hypothesize that the entrance of water depends on the diffusional path (i.e., the thickness of the hydrogel) and on the conformational changes underwent by the polymer chains as they become hydrated. This last factor may be affected by the spatial distribution of the ionizable monomers in the chain. In the case of the 1:6 imprinted hydrogels, the imprinted cavities may consist in 6 AAc mers quite close in the space and interacting among themselves

through hydrogen bonds. Imprinted cavities with a larger number of AAc mers may lead to a not so tight structure. The lower the timolol:AAc molar ratio, the higher the likehood of a random distribution. The changes in swelling rate caused by a different merging of AAc mers were particularly evident for the thinnest hydrogels.

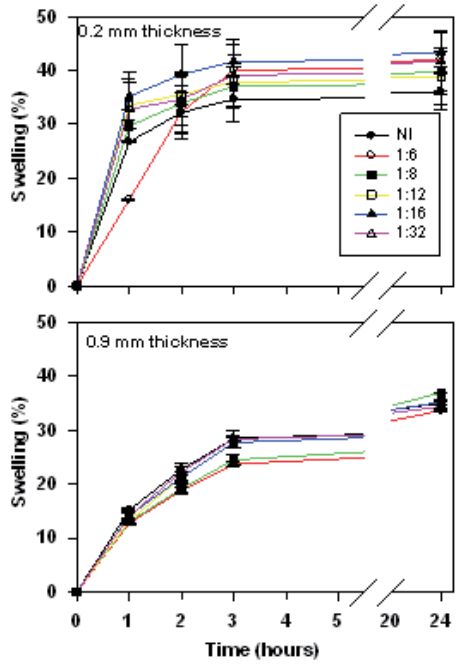

Figure 2. Swelling of the hydrogels in water at 25ºC.

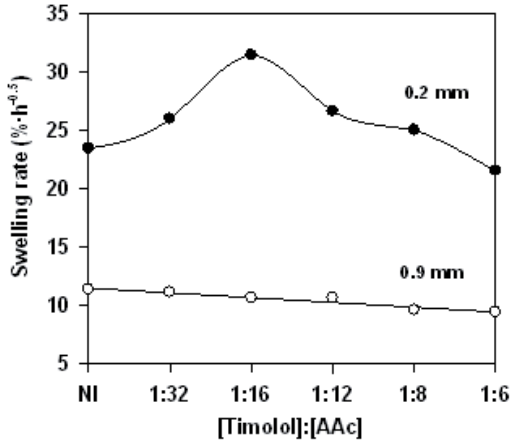

Figure 3. *Dependence of the swelling rate obtained by fitting of the water uptake to the square-root kinetics (r^2 > 0.97) on the proportion of timolol incorporated to the hydrogels during synthesis.*

Timolol loading

The hydrogels were immersed in timolol solutions of various concentrations with the aim of testing their affinity for timolol. Since all hydrogels (including the non-imprinted ones) have a similar degree of swelling at equilibrium, the same monomeric composition and the same content in the functional monomer (AAc), the differences in the loading (Figure 4) can be attributed to the arrangement of the functional monomers due to the presence of timolol during polymerization. The amounts of timolol loaded are two orders of magnitude above those expected if the drug was only hosted in the aqueous phase of the hydrogels; i.e., 0.007, 0.010, 0.014 and 0.017 mg/g for the hydrogels immersed in 0.04, 0.06, 0.08 and 0.10 mM, respectively. This means that the presence of AAc itself notably enhances the affinity of the hydrogels for timolol. We had previously observed that pHEMA hydrogel without functional monomer just takes up the amount of drug that can be hosted in the aqueous phase.[36]

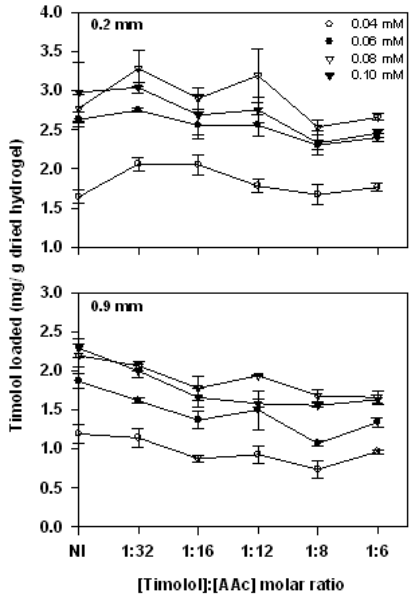

Figure 4. *Timolol loaded by imprinted and non-imprinted hydrogels prepared with AAc 200 mM and different thickness. The concentrations of the timolol solutions used to load the hydrogels are indicated in the plot legend.*

As expected, the higher the concentration of the drug solution, the greater the amount loaded. Nevertheless, the values obtained with the 0.08 and 0.10 mM timolol solutions were quite similar or even smaller for the latter, which may indicate that the hydrogels are close to saturation. For a given concentration of timolol loading solution, it is interesting to note the progressive decrease in the amount loaded as the [timolol]:[AAc] molar ratio increases from 1:32 to 1:6. Norfloxacin-imprinted SCLs also showed a decrease in the loading as the proportion of template increased.[24] This phenomenon can be attributed to that, although the total number of functional groups is the same in all hydrogels, the number of each of them that gather to form the binding site is different. In the non-imprinted hydrogels, the AAc groups are randomly distributed and each of them constitutes a potential binding site although of low affinity. Oppositely, in the timolol:AAc 1:6 and 1:8 imprinted hydrogels, each binding site is formed by six or eight AAc mers, which is the the number identified as optimum by ITC. Therefore, each timolol molecule reloaded by the optimally synthesized hydrogels consumes six to eight functional groups. The hydrogels prepared with timolol contents in between those of the non-imprinted hydrogel and the timolol:AAc 1:6 and 1:8 imprinted hydrogels, i.e., those ranging from timolol:AAc 1:12 to 1:32, may have imprinted cavities with six/eight AAc mers and also others worsely constructed with the remanent AAc groups randomly distributed (probably individually or as dimers). As a consequence, when the hydrogeles are immersed in the timolol solution, the drug molecules can be hosted by the imprinted cavities (with a 1:6 or 1:8 stoichiometry) and by some randomly distributed AAc groups (likely with a lower stoichiometry, e.g. 1:1 or 1:2), resulting in a greater loading and similar to that of the non-imprinted hydrogels. Thus, the lowest the amount of timolol added before polymerization, the less the number of imprinted cavities and the highest the number of non-imprinted binding sites.

On the other hand, the loading rate was mainly conditioned by the thickness of the hydrogels. In the first 48 hours, the amount loaded was nearly 75% of the total amount loaded by 0.2-mm hydrogels and ca. 50% by 0.9-mm hydrogels. The time required to achieve the equilibrium was 6 days for 0.2-mm and 18 days for 0.9-mm hydrogels. This time is remarkably larger than that spent in the swelling, which indicates that the

diffusion of the drug into the hydrogels is slower than the movement of water. Timolol is a relatively large molecule (Mw 432.5 Da). Additionally, the interaction with the AAc mers and the fit into the imprinted cavities may take some time. Nevertheless, all hydrogels tested are loosely cross-linked and thus the polymeric network is not expected to hinder the diffusion of the drug towards the inner parts of the network. It has been reported that drug equilibration throughout the lens can remarkably determine the performance as delivery device, because when the drug diffuses out from the surface layers, they can be replenished from the deeper part which acts as a reservoir making a more sustained and reproducible release possible.[4,43] Consequently, all hydrogels were loaded until equilibrium before carrying out the release experiments.

Timolol release

Isotonic saline solution was used as the release medium with the purpose of mimicking the ionic strength and pH conditions on the ocular surface. One can expect that the ions disturb the binding of timolol to the AAc mers by inducing their ionization. However, no burst effect was observed for any timolol-loaded hydrogel. The 0.2-mm hydrogels were able to sustain timolol release for one day, while the 0.9-mm hydrogels controlled the delivery for 10 days. For the aim of clarity, only the release profiles of the hydrogels that behave more differently are shown, once normalized by the thickness, in Figure 5. The release rate constants for all hydrogels, obtained by fitting of the square-root kinetics, are reported in Table 1.

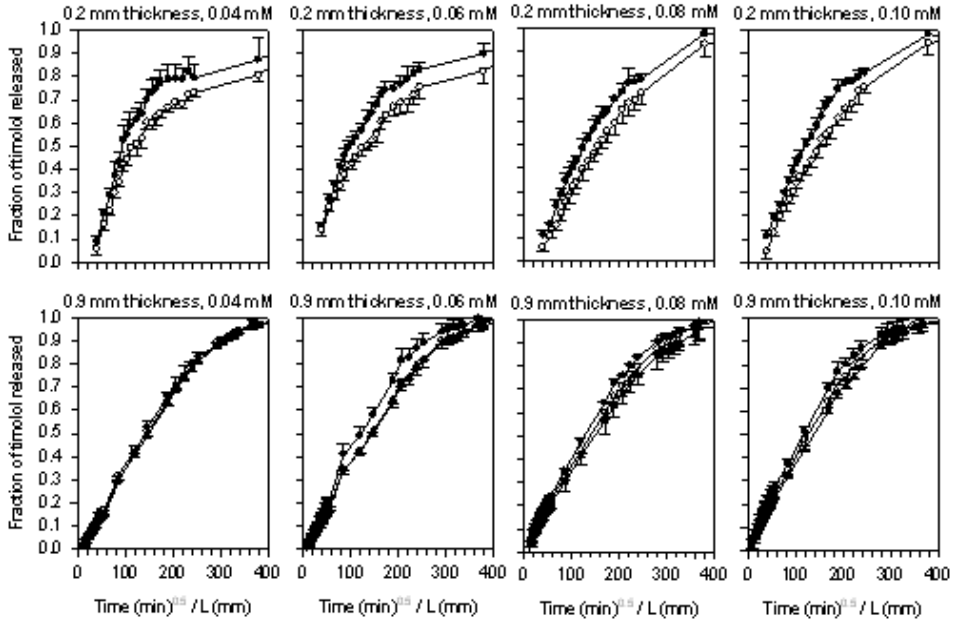

Figure 5. *Timolol release profiles in NaCl 0.9% at 37ºC from hydrogels of different thickness that were loaded by immersion in drug solutions of various concentrations 0.04, 0.06, 0.08 and 0.10 mM. Solid circles represent non-imprinted hydrogels, white circles the imprinted 1:6 hydrogels, and the solid triangles the imprinted 1:16 hydrogels*

Although both non-imprinted and imprinted hydrogels showed similar release patterns, some differences may be highlighted. In the case of the thinnest hydrogels, the faster release rate was recorded for the non-imprinted networks and the slower release was achieved with the timolol:AAc 1:6 and 1:8 imprinted hydrogels (differences with the non-imprinted hydrogels were statistically significant at α <0.01). All other 0.2-mm hydrogels showed an intermediate behaviour. This finding suggest that the better the imprinted cavities were created, the stronger their affinity for timolol and, consequently, the greater their ability to retain the drug.

Hydrogel thickness (mm)	Loading concentration (mM)	Timolol:AAc molar ratio					
		Non-imprinted	1:32	1:16	1:12	1:8	1:6
0.2	0.04	0.067	0.063	0.057	0.049	0.046	0.048
		(0.006)	(0.003)	(0.002)	(0.002)	(0.001)	(0.001)
	0.06	0.050	0.046	0.045	0.042	0.035	0.034
		(0.004)	(0.005)	(0.004)	(0.003)	(0.002)	(0.001)
	0.08	0.043	0.044	0.041	0.038	0.031	0.036
		(0.001)	(0.004)	(0.003)	(0.002)	(0.004)	(0.002)
	0.10	0.044	0.046	0.041	0.041	0.039	0.037
		(0.002)	(0.005)	(0.004)	(0.002)	(0.001)	(0.001)
0.9	0.04	0.0087	0.0081	0.0079	0.0079	0.0080	0.0080
		(0.0002)	(0.0003)	(0.0001)	(0.0003)	(0.0001)	(0.0001)
	0.06	0.0096	0.0088	0.0083	0.0081	0.0082	0.0080
		(0.0005)	(0.0004)	(0.0001)	(0.0002)	(0.0001)	(0.0001)
	0.08	0.0093	0.0077	0.0075	0.0081	0.0079	0.0080
		(0.0003)	(0.0004)	(0.0007)	(0.0001)	(0.0001)	(0.0003)
	0.10	0.0118	0.0109	0.0099	0.0099	0.0098	0.0107
		(0.0009)	(0.0006)	(0.0001)	(0.0004)	(0.0011)	(0.0004)

Table 1. *Timolol release rate constant values (K_H, hours$^{-1/2}$) obtained by fitting of the release profiles to the square-root model. Mean values and, in parenthesis, standard desviations.*

The imprinting effect was somehow attenuated in the thicker hydrogels probably due to that the release is determined by two factors: the affinity of the drug for the imprinted cavities and the length of the diffusional path through the hydrogel network. The contribution of this latter factor is greater as the thickness of the hydrogel increases. Furthermore, in the case of the 0.9-mm hydrogels we observed that any imprinted hydrogel release timolol at a slightly slower rate than the non-imprinted ones (release rates from 1:8, 1:12 and 1:16 hydrogels were statistically different from that of the non-imprinted hydrogels at $\alpha < 0.01$). The release of timolol from the thick hydrogels implies that the drug molecules may have more chances to find imprinted cavities (or at least

AAc mers more or less gathered together) during the movement towards the surface. The drug may fall down into the cavity and then escape from it to probably enters into another high affinity region and so on. The interaction with those cavities should make the movement slower. The higher the number the cavities, the higher the likelihood of fallen into one. The imprinted hydrogels prepared with timolol:AAc 1:16 seems to be particularly efficient from that point of view. As explained above, these hydrogels may combine optimally constructed imprinted cavities (i.e., timolol:AAc 1:6 or 1:8) and also a certain number of cavities with less AAc mers. We have previously observed that imprinted networks prepared with N,N-dimethylacrylamide, tris(trimethylsiloxy)silylpropyl methacrylate and timolol:methacrylic acid 1:16 molar ratio provided a better control of timolol release than those synthesized in the presence of greater content in timolol and than those non-imprinted ones.[30]

CONCLUSIONS

The ITC analysis has been shown as an adequate tool to elucidate the stoichiometry of the timolol:AAc complexes and to design imprinted lenses using a rational basis. Those imprinted hydrogels prepared with the timolol:AAc molar ratio identified as optimum by ITC (1:6 and 1:8) consists of a lower number of imprinted cavities, but with higher affinity for the drug. This results in hydrogels that load lower amounts of timolol but that release it at lower rate than the non-imprinted hydrogels. The improvement in the performance as drug delivery systems of the imprinted hydrogels prepared with the timolol:AAc molar ratio 1:6 was more evident in the case of the thin 0.2 mm hydrogels. The greater the thickness of the hydrogels, the slower the water uptake, the drug uptake and the release rate. However, in the case of the thick 0.9 mm hydrogels, the influence of the timolol:AAc molar ratio used during hydrogel synthesis was quantitatively less relevant; the hydrogels with more cavities although with lower affinity sustained the drug as well as (or even better than) those hydrogels possessing the best formed imprinted cavities. This effect is explained by the greater likelihood of the drug to fall down and to escape from the imprinted cavities as the drug molecules move through the thicker network towards the hydrogel surface.

Acknowledgments

The authors thank the support of MICINN and FEDER (SAF2008-01679), and Xunta de Galicia (PGIDT07CSA002203PR), Spain. F. Yañez is grateful to MICINN for a FPI grant. P. Taboada is acknowledged for the assistance with the ITC experiments.

REFERENCES

1 Sedlacek, J. Cs Oftal 1965, 21, 509-512.

2 Gasset, A.; Kaufman, H.E. Am J Ophtalmol 1970, 69, 252-259.

3 Li, C.C.; Chauhan, A. Ind Eng Chem Res 2006, 45, 3718-3734.

4 Jain, M.R. Brit J Ophthalmol 1988, 72, 150-154.

5 Rubinstein, M.P.; Evans, J.E. Cont Lens Anterior Eye 1997, 20, 9-11.

6 Vandorselaer, T.; Youssfi, H.; Caspers-Valu, L.E.; Dumont, P.; Vauthier, L. J Fr Ophtalmol 2001, 24, 1025-1033.

7 Hehl, E.M.; Beck, R.; Luthard, K.; Guthoff, R.; Drewelow, B. Eur J Clin Pharmacol 1999, 55, 317-323.

8 Xinming, L.; Yingde, C.; Lloyd, A.W.; Mikhalovsky, S.V.; Sandeman, S.R.; Howel, C.A.; Liewen, L. Cont Lens Anterior Eye 2008, 31, 57-64.

9 Novack, G.D. Clin Pharmacol Ther 2009, 85, 539-543.

10 Karlgard, C.C.S.; Wong, N.S.; Jones, L.W.; Moresoli, C. Int J Pharm 2003, 257, 141-151.

11 Tian, X.; Iwatsu, M.; Sado, K.; Kanai, A. CLAO J 2001, 27, 216-220.

12 Wajs, G.; Meslard, J.C. Crit Rev Ther Drug 1986, 2, 275-289.

13 Vairon, J.P.; Yean, L.; Meslard, J.C.; Subira, F.; Bunel, C. L´actualité Chimique 1992, Septembre-Octobre, 330-335.

14 Anne, D.; Heidi, B.; Yves, M.; Patrick, V. J Biomed Mater Res A, 2007, 80A, 41–51.

15 Gulsen, D.; Chauhan, A. Int J Pharm 2005, 292, 95-117.

16 Gulsen, D.; Li, C.C.; Chauhan, A. Current Eye Res 2005, 30, 1071-1080.

17 Gulsen, D.; Chauhan, A. J Membr Sci 2006, 269, 35-48.

18 Kapoor, Y.; Chauhan, A. Int J Pharm 2008, 361, 222-229.

19 Miranda, M.N.; Garcia-Castineiras, S. CLAO J 1983, 9, 43-48.

20 Uchida, R.; Sato, T.; Tanigawa, H.; Uno, K. J Control Rel 2003, 92, 259-264.

21 Sato, T.; Uchida, R.; Tanigawa, H.; Uno, K.; Murakami, A. J Appl Polym Sci 2005, 98, 731-735.

22 Hiratani, H.; Alvarez-Lorenzo, C. J Control Release 2002, 83, 223-230.

23 Alvarez-Lorenzo, C.; Hiratani, H.; Concheiro, A. Am J Drug Deliv 2006, 4, 131-151.

24 Alvarez-Lorenzo, C.; Yañez, F.; Barreiro-Iglesias, R.; Concheiro, A. J Control Release 2006, 113, 236-244.

25 Byrne, M.E.; Salian, V. Int J Pharm 2008, 364, 188-212.

26 White, C.J.; Byrne, M.E. Expert Opin Drug Deliv 2010, 7, 765-780.

27 Alvarez-Lorenzo, C.; Yañez, F.; Concheiro, A. J Drug Deliv Sci Tec 2010, in press.

28 Ramström, O.; Ansell, R.J. Chirality 1998, 10, 195-209.

29 Wulff, G.; Biffis, A. In Molecularly Imprinted Polymers; Sellergren, B., Ed.; Elsevier:Amsterdam, 2001; pp 71-111.

30 Hiratani, H.; Mizutani, Y.; Alvarez-Lorenzo, C. Macromol Biosci 2005, 5, 728–733.

31 Venkatesh, S.; Sizemore, S.P.; Byrne, M.E. Biomaterials 2007, 28, 717-724.

32 Venkatesh, S.; Sizemore, S.P.; Byrne, M.E. Mater Res Soc Symp Proc 2006, 897E.

33 Venkatesh, S.; Saha, J.; Pass, S.; Byrne, M.E. Eur J Pharm Biopharm 2008, 69, 852-860.

34 Ali, M.; Horikawa, S.; Venkatesh, S.; Saha, J.; Pass, S.; Hong, J.W.; Byrne, M.E. J Control Release 2007, 124, 154-162.

35 Ali, M.; Byrne, M.E. Pharm Res 2009, 26, 714-726.

36 Alvarez-Lorenzo, C.; Hiratani, H.; Gómez-Amoza, J.L.; Martinez-Pacheco, R.; Souto, C.; Concheiro, A. J Pharm Sci 2002, 91, 2182-2192.

37 Molinelli, A.; O'Mahony, J.; Nolan, K.; Smyth, M.R.; Jakusch, M.; Mizaikoff, B. Anal Chem 2005, 77, 5196-5204.

38 McStay, D.; Al-Obaidi, A.H.; Hoskins, R.; Quinn, P.J. J Opt A Pure Appl Opt 2005, 7, S340-S345.

39 Fish, W.P.; Ferreira, J.; Sheardy, R.D.; Snow, N.H.; O'Brien, T.P. J Liquid Chromatogr Related Techn 2005, 28, 1-15.

40 Nicholls, I.A.; Andersson, H.S.; Charlton, C.; Henschel, H.; Karlsson, B.C.G.; Karlsson, J.G.; O'Mahony, J.; Rosengren, A.M.; Rosengren, K.J.; Wikman, S. Biosens Bioelectron 2009, 25, 543-552.

41 Yañez, F.; Chianella, I.; Piletsky, S.A.; Concheiro, A.; Alvarez-Lorenzo, C. Anal Chim Acta 2010, 659, 178-185.

42 Kim, S.W.; Bae, Y.H.; Okano, T. Pharm Res 1992, 9, 283-290.

43 Lesher, G.A.; Gunderson, G.G. Optometry Vision Sci 1993, 70, 1012-1018.

3.4. Macromolecule release and smoothness of semi-interpenetrating PVP–pHEMA networks for comfortable soft contact lenses

European Journal of Pharmaceutics and Biopharmaceutics **69**, 1094–1103 (2008).

Available online at www.sciencedirect.com
ScienceDirect
European Journal of Pharmaceutics and Biopharmaceutics 69 (2008) 1094–1103
European Journal of Pharmaceutics and Biopharmaceutics
www.elsevier.com/locate/ejpb

Research paper

Macromolecule release and smoothness of semi-interpenetrating PVP–pHEMA networks for comfortable soft contact lenses

Fernando Yañez, Angel Concheiro, Carmen Alvarez-Lorenzo *

Departamento de Farmacia y Tecnología Farmacéutica, Universidad de Santiago de Compostela, Santiago de Compostela, Spain

Received 2 November 2007; accepted in revised form 23 January 2008
Available online 1 February 2008

Abstract

Knowledge about the microstructure and the release rate of hydrophilic macromolecules is required for a rational development of comfortable and safe contact lenses. Semi-interpenetrating networks of poly(hydroxyethyl methacrylate) (pHEMA) with poly(vinyl pyrrolidone) (PVP) were prepared by free radical polymerization of HEMA in the presence of PVP K30 or K90F, under anhydrous conditions or after addition of water, and evaluated in terms of swelling, porosity, PVP release rate, air–water surface tension, and friction coefficient. The greater water content was during polymerization, the higher was the swelling degree and porosity. Microphase separation above a certain volume of water resulted in hydrogels with bumpy surface and interconnected pores. All hydrogels showed a high optical clarity and slowly released PVP (20% after 9 days). In general, the greater the content of PVP or the higher its molecular weight was, the lower the friction coefficients were. In the case of hydrogels prepared with water, the friction was influenced by the balance between the ability to hold water in the network (which contributes to the sliding and PVP release) and the deleterious effect of an irregular surface. Controlled delivery of PVP revealed as a critical factor for improving the frictional behavior of pHEMA contact lenses.

Keywords: Semi-IPNs; Sustained release of poly(vinyl pyrrolidone); Comfortable lenses; Rheological evaluation of surface friction; Porosity

1. Introduction

Dry eye syndrome (DES) encompasses a heterogeneous group of ocular surface disorders that leads to an abnormal tear film and causes inadequate ocular lubrication [1]. When the homeostasis of the tear film is lost due to insufficient supply, excessive loss or anomalous composition of tears, the ability to protect the ocular surface epithelium decreases. As a consequence, DES also involves ocular surface epitheliopathy, tear hyperosmolality, unstable preocular tear film, and more or less intense inflammation and ocular irritation [2]. DES affects to 10–20% in adult population and up to the 70% of contact lenses wearers [1,3]. Except silicone lenses which do not absorb water [4], most contact lens alters the tear film increasing the evaporation and the discomfort at the end of the day, which causes 35% of wearers give up the use of contact lenses [5,6].

Although the prevention and management of DES requires a global approach [1], ophthalmic drops of hydrophilic polymers have been shown useful as tear film stabilizers, reducing the friction with the ocular tissues and washing out foreign bodies [7,8]. This prompted the incorporation of hydrophilic polymers to lens structure to be slowly released, wrapping the lens with a cushion-like layer able to soften the contact with the eye and the lid [9]. Polyvinyl alcohol (PVA) and poly(vinyl pyrrolidone) (PVP), which constitute two of the six categories of ophthalmic demulcents recognized by FDA [10], can be already found

* Corresponding author. Departamento de Farmacia y Tecnología Farmacéutica, Facultad de Farmacia, Universidad de Santiago de Compostela, 15782 Santiago de Compostela, Spain. Tel.: +34 981563100; fax: +34 981547148.
E-mail address: ffrusdog@usc.es (C. Alvarez-Lorenzo).

0939-6411/$ - see front matter © 2008 Elsevier B.V. All rights reserved.
doi:10.1016/j.ejpb.2008.01.023

in some commercialized soft contact lenses [11,12]. Nelfilcon A lenses (i.e. functionalized PVA macromer) to which PVA was added during polymerization can sustain PVA release for several hours [13], showing an improvement in comfort related to enhancing wettability of the contact lenses [9]. PVP can be locked into etafilcon A (hydroxyethyl methacrylate-co-methacrylic acid) matrix and is claimed not to be released from the lens over one day of wearing; the increase in comfort being attributed to an enhancement in moisture retention and a reduction of the coefficient of friction [12], although no published data have been found.

For a rational understanding and design of lubricating lenses, a deeper knowledge of the effect of the hydrophilic polymer on their features is required. Despite the fact that contact lenses have been used for many years, their surface physical properties have received a little attention [14]. Linear polymers incorporated into cross-linked networks can act as dangling chains, resulting in a substantial reduction in the coefficient of friction [15], which could notably contribute to the comfort feeling. The time that the lens retains/controls the release of the hydrophilic polymer should be another key factor. The achievement of prolonged delivery not only for one day but also for one week, which is the time most disposable lenses are used, would have great practical interest. Compared to artificial tears that are intermittently applied, a sustained delivery from the soft contact lens could resemble better the lubrication role of natural tears.

The aim of this work was to design contact lenses based on poly(hydroxyethyl methacrylate), pHEMA, containing free chains of PVP forming semi-interpenetrating networks (semi-IPNs), and to elucidate the incidence of composition variables, such as molecular weight and proportion of PVP or volume of water added to the monomeric solution, on the PVP release rate and the frictional properties of the lenses. Addition of water to the monomers solution before polymerization may be motivated for different needs: (i) dissolution of high proportion of hydrophylic polymers; (ii) loading of colloidal particles to obtain drug sustained delivery [16]; and (iii) formation of a porous structure [17–19]. Since water is not a solvent for pHEMA, when its concentration is above the equilibrium water uptake of pHEMA, phase separation occurs during polymerization and the hydrogels become translucent or opaque. Therefore, an adequate control of water proportion in the monomer mixture is required to attain a wide range of porosities without altering the transparency of hydrogels [16]. In the particular case of soft contact lenses, porosity determines the degree of swelling and the mesh size of the network and, consequently, the diffusion of oxygen, nutrients and macromolecules through the hydrogel [19,20]. Since the porosity and hence a heterogeneous microstructure of the hydrogels can also affect PVP release rate and their sliding friction, these aspects were given special attention.

2. Materials and methods

2.1. Materials

Ophthalmic grade 2-hydroxyethyl methacrylate (HEMA) was from Merck (Darmstadt, Germany), and 2,2′-azobis(isobutyronitrile) (AIBN) and ethyleneglycol dimethacrylate (EGDMA) from Sigma–Aldrich (Madrid, Spain). Poly(vinyl pyrrolidone) (PVP) Kollidon® 30 of 44000–54000 Da and Kollidon® 90F of $1\,10^6$–$1.5\,10^6$ Da were from BASF (Barcelona, Spain). Purified water was obtained by reverse osmosis (MilliQ®, Millipore Iberica SA, Madrid, Spain). All other reagents were of analytical grade.

2.2. Hydrogels synthesis

The synthesis of the hydrogels was carried out in two different ways: at anhydrous conditions and in presence of different proportions of water. To prepare the anhydrous gels, EGDMA cross-linker (80 mM) and AIBN initiator (10 mM) were dissolved in HEMA (36 ml). The monomers solution was divided in 6 ml portions into which 0.3, 0.6 or 0.9 g of PVP K30 or 0.3 g of PVP K90F was added. Once dissolved, the monomers solutions were injected into a mould constituted by two glass plates covered internally with a polypropylene sheet and separated by a silicone frame 0.9 mm wide [21]. The moulds were then placed in an oven at 50 °C for 12 h and then heated at 70 °C for 24 h. Each gel sheet was boiled for 15 min to remove unreacted monomers and to facilitate the cutting of discs of 10 mm in diameter. Finally, they were dried in an oven at 50 °C. To check the reproducibility of the synthesis and the features of the hydrogels, the hydrogel with 0.9 g of K30 was synthesized and evaluated twice. Another set of hydrogels was prepared as follows: EGDMA (80 mM), AA (100 mM) and AIBN (10 mM) were dissolved in HEMA (30 ml). Mixtures of these monomers and water at volume ratios of 5.4:0.6, 4.8:1.2, 4.2:1.8, 3.6:2.4, 3:3, and 2.4:3.6 were prepared. To 6 ml portions of these solutions 0.9 g of PVP K30 was added. Once dissolved, they were injected into the moulds, polymerized and washed as described above.

2.3. Hydrogels characterization

2.3.1. Elemental analysis

The content in nitrogen of each hydrogel was determined using a Carlo-Erba 1108 Elemental Analyzer (Fisons Instruments, Ipswich, UK).

2.3.2. FTIR analysis

IR spectra of the hydrogels were recorded over the range 400–4000 cm^{-1}, in a Bruker IFS 66V FT-IR (Ettlingen, Germany) spectrometer using the KBr pellet technique.

2.3.3. Swelling kinetics

Dried hydrogels were weighed (W_0) and placed in 15 ml of water at 25 °C. Swelling, Q_t at various times t was calculated as relative weight gain; the sample being weighed (W_t) on each occasion after careful wiping of its surface with a soft tissue:

$$Q_t = 100(W_t - W_0)/W_0 \quad (1)$$

2.3.4. Porosity

Porosity, ε, of the hydrogels was determined from the equilibrium water content according to the model of Yanagawa et al. [19], which takes into account the water molecules present in the non-porous phase:

$$\varepsilon = (W_W - W_0 - W_{\mathrm{wnp}})/W_{\mathrm{w}} \quad (2)$$

where W_{w} is the weight of the swollen porous hydrogel, W_0 is the weight of the dry porous hydrogel, and W_{wnp} is the amount of water in the non-porous phase. The value of W_{wnp} of each hydrogel was estimated as:

$$W_{\mathrm{wnp}} = (W_{\mathrm{wnh}} - W_{\mathrm{dnh}}) \cdot W_0/W_{\mathrm{dnh}} \quad (3)$$

where W_{wnh} and W_{dnh} are the weights of swollen and dry non-porous hydrogel, respectively.

2.3.5. Transmittance

The transmittance of swollen discs immersed in water was recorded between 190 and 800 nm using an Agilent 8453 (Böblingen, Germany) spectrophotometer.

2.3.6. Scanning electron microscopy (SEM)

Water-swollen discs were immersed in liquid nitrogen, cut and stored at −80 °C for one day before freeze-drying. The samples were mounted on double-sided tape on aluminum stubs and sputter-coated with gold/palladium. Micrographs of the surface and the transversal cut were taken using a LEO-435VP (Leo Electron Microscopy, Cambridge, UK) apparatus.

2.3.7. PVP release test

Hydrogel dried discs were immersed in 20 ml water, 10 ml samples were taken every 24 h and this volume was replaced with fresh water. Each sample was mixed with 5 ml of 0.2 M citric acid solution and 2 ml of I_2/KI (0.81 g of freshly sublimed iodine and 1.44 g of KI in 1000 ml of water). After exactly 10 min, the absorbance of the solution was measured at 420 nm (Agilent 8453, Böblingen, Germany) against a blank prepared with water instead of the PVP solution [22]. The experiments were carried out in quadruplicate.

2.3.8. Friction force

The friction force of water-swollen discs was measured, in duplicate, at 25 °C using a Rheolyst AR1000N rheometer (TA Instruments, Crawley, UK) equipped with an AR2500 data analyzer and a Peltier plate. The discs were immersed in 11 ml of water and analyzed, in duplicate, after 1, 2, 3 and 4 days. The surface of the discs (11.9 mm diameter) was blotted with filter paper and immediately glued (Loctite® Super Glue-3, Henkel, Barcelona, Spain) to a 4 cm steel plate geometry. One milliliter of the aqueous medium was put on the surface of the Peltier plate and the geometry was moved towards the plate to an initial gap of 1 mm. The experiment consisted of a conditioning step applying 5 ± 0.1 N normal force (W) for 15 min and a peak hold step with an angular velocity of 0.05 rad/s for other 15 min. Since the velocity changes with the distance from the center of the axis, the obtained torque, T, is a total value over the velocity range from 0 to ωR, where R is the radius of the gel disc. The total friction, F, and the coefficient of friction, μ, were determined as follows [23]:

$$F = \frac{4T}{3R} \quad (4)$$

$$\mu = \frac{F}{W} \quad (5)$$

At each sampling time, the amount of PVP released was determined (as described above) in the medium from which the analyzed discs were taken.

2.4. Characterization of PVP solutions

2.4.1. Surface tension

The surface tension of PVP solutions in water (10–60 mg/l) was measured, in triplicate, by the platinum ring method using a Lauda Tensiometer TD1 (Königshofen, Germany) applying the needed density corrections.

2.4.2. Bound water

PVP solutions (5–30%) were stored at room temperature for 72 h and then sealed in aluminum pans and placed in a differential scanning calorimeter DSC Q100 (TA Instruments, New Castle DE, USA) with a refrigerated cooling accessory. The samples were cooled to –30 °C and heated to 60 °C, at 5 °C/min, to determine the amounts of free water and freezing (interfacial) water. The experiments were carried out, in triplicate, using nitrogen as purge gas at a flow rate of 50 mL/min. The calorimeter was calibrated for baseline using no pans, for cell constant and for temperature using indium (melting point 156.61 °C, enthalpy of fusion 28.71 J/g), and for heat capacity using sapphire standards. The enthalpy of the melting/freezing peaks was referred to the amount of water in each sample. The melting enthalpy of pure water (0% PVP) was 340 J/g. A plot of the melting enthalpy vs. PVP concentration (% w/w) gave a straight line. The PVP concentration that corresponded to the zero enthalpy indicated the composition of the PVP solution in which all water is bounded to the polymer.

3. Results and discussion

3.1. Swelling and microstructure of the hydrogels

PVP K30 was easily dispersed in HEMA up to 0.15 g/ml. By contrast, the greater molecular weight and

thickening ability of PVP K90F prevented a homogeneous mixing in proportions above 0.05 g/ml, and thus only this concentration of K90F was assayed. Once all components were added to the monomers solutions, the polymerization was carried out immediately to prevent crystallization or precipitation of any component, particularly AIBN, when water was added to the reaction mixture [18]. Hydrogels synthesized in the absence of water were completely transparent and showed a continuous and homogeneous surface. By contrast, those hydrogels made with monomer:water proportions of 4.2:1.8 visually evidenced some points of microphase separation, which rose in number and dimensions as the proportion in water increased. It was previously observed that pHEMA hydrogels do not phase separate when the content in water is below the saturation value of the gel (swelling equilibrium). By contrast, above this value, the exceeded amount of water phase separates and disperses in micron-sized regions of the network creating pores after polymerization [24]. Once synthesized, the hydrogels were boiled, which is a common method of cleaning and sterilizing contact lenses.

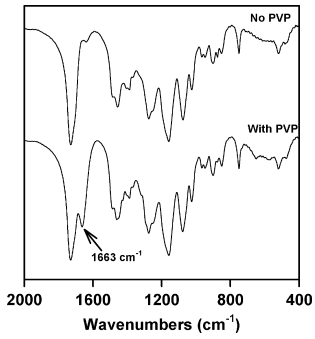

Fig. 1. FTIR spectra of pHEMA hydrogels prepared without PVP or with 128.6 mg PVP per gram of dried hydrogel.

All hydrogels featured the bands characteristic of pHEMA; mainly the C=O ester groups at 1727 cm^{-1}. The absorbance at 1663 cm^{-1} due to the C=O and N–C stretching vibrations of PVP increased as its content in the hydrogels raised [25]. The peak of unreacted C=C bonds at 1637 cm^{-1} was not observed (Fig. 1). To determine the amount of PVP remaining in the hydrogels after

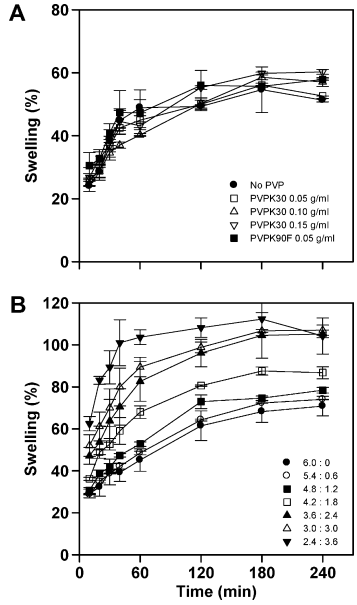

Fig. 2. Swelling profiles of (A) pHEMA hydrogels synthesized incorporating different proportions of PVP K30 or K90F, in the absence of water; and (B) pHEMA hydrogels prepared with 0.15 g of PVP K30 per ml and different monomer:water v/v ratios.

Table 1
Proportions of the main components used to synthesize the hydrogels, expected contents in PVP K30 and nitrogen, observed nitrogen content, porosity and PVP K30 release rate (fitting to square-root kinetics provided in all cases $R^2 > 0.95$)

Composition of the synthesis mixture HEMA:water:PVP	Expected PVP content (mg/g monomers plus PVP)	Expected *N* (%)	Observed *N* (%)	Porosity	Release rate ($day^{-0.5}$)
6.0:0:0	0	0	0	–	–
6.0:0:0.3	46.9	0.56–0.59	0.41	–	0.038
6.0:0:0.3[a]	46.9	0.56–0.59	0.59	–	0.039
6.0:0:0.6	89.5	1.07–1.15	1.12	–	0.030
6.0:0:0.9	128.6	1.54–1.64	1.49	–	0.027
5.4:0.6:0.9	142.8	1.71–1.83	1.39	0.020 (0.006)	0.033
4.8:1.2:0.9	157.9	1.89–2.02	1.69	0.018 (0.004)	0.026
4.2:1.8:0.9	176.5	2.12–2.26	1.67	0.077 (0.012)	0.048
3.6: 2.4: 0.9	200.0	2.40–2.56	2.03	0.132 (0.029)	0.066
3.0:3.0:0.9	230.7	2.77–2.95	2.29	0.145 (0.019)	0.059
2.4:3.6:0.9	272.7	3.27–3.49	2.72	0.150 (0.025)	0.079

[a] PVP K90F was used instead of K30.

boiling, the proportion of N (which is only present in PVP at 12–12.8%) was quantified by elemental analysis and compared with the predicted contents assuming that no PVP was lost during boiling (Table 1). In the set of hydrogels prepared in absence of water, only the one containing the lowest proportion of K30 showed a small lost of PVP. On the other hand, as the proportion of water in the polymerization medium increased, the more significant the amount of PVP washed out during boiling. Nevertheless, most PVP still remained in the hydrogels.

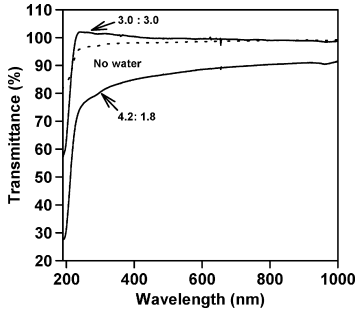

Fig. 3. UV–vis transmittance of some PVP–pHEMA hydrogels prepared with different monomer:water v/v ratios.

The different losses of PVP during boiling can be related to the important differences observed in the degree of swelling and porosity of the hydrogels. Those prepared at anhydrous conditions did not show influence by PVP, either on the swelling rate or the equilibrium swelling degree (Fig. 2A). By contrast, the porous hydrogels prepared in the presence of water remarkably increased their swelling as the proportion of water used in the synthesis rose (Fig. 2B). Porosity values obtained from the comparison of the aqueous swelling of each hydrogel synthesized in presence of water with that of the hydrogel of the same composition prepared in absence of water are shown in Table 1. This approach has been developed to estimate the increase in porosity caused by the synthesis in the presence of water, assuming that the ability to bind water by the polymeric chains after hydrogel synthesis is the same disregarding the content in water during polymerization [19]. This hypothesis is plausible since the composition of the hydrogels is the same and their cross-linking degree is quite low and, consequently, the mobility of the chains should not be impeded by entropic constrains. Replacement with water of 0.6 or 1.2 ml of monomer solution (from a total volume of 6 ml) only led to a minor increase in swelling and porosity. Volumes of 1.8 to 3.6 ml of water

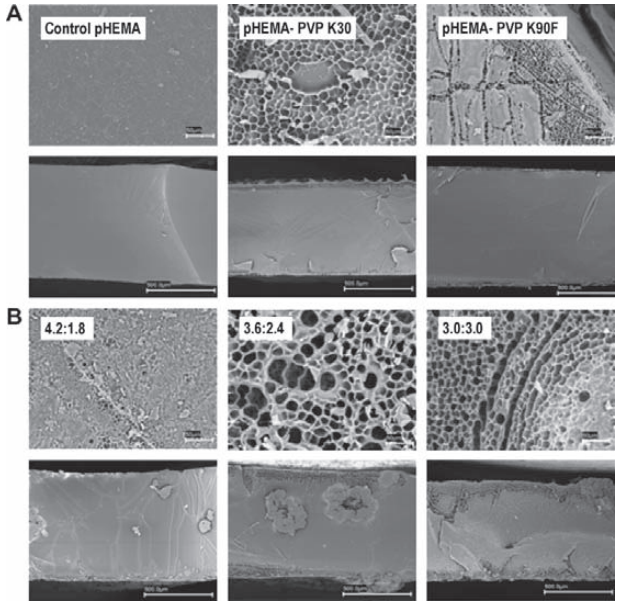

Fig. 4. SEM photographs of the surface (top) and the transversal section (bottom) of (A) pHEMA hydrogels synthesized without or with PVP K30 or K90F, in the absence of water; and (B) pHEMA hydrogels prepared with 0.15 g of PVP K30 per ml and different monomer:water v/v ratios.

progressively increased the porosity of the hydrogels up to a 15%.

The transmittance at 600 nm is commonly used as an index of the transparency of the contact lenses. All hydrogels at the swollen state gave values above 85% transmittance; most of them being above 95%. The maximum transparency in the whole visible range corresponded to non-porous pHEMA-hydrogels and to the porous hydrogels with high swelling degree (Fig. 3). pHEMA hydrogel used as control (i.e. prepared without PVP or water) just showed a minor decrease in transmittance below 200 nm. The transmittance of the hydrogels is conditioned by the light absorption (PVP absorbs below 200 nm) and on the light scattering. The light scattering of porous hydrogels not only depends on the size and distribution of pores, but also on their content in water; these factors contributing in an opposite way [20,24]. In the case of hydrogels synthesized in presence of water, the minimum in transmittance was observed for those prepared with 4.2:1.8 monomer:water proportion; hydrogels made with lower content in water (low porosity) or greater content in water (more swollen) being more transparent. Nevertheless, all PVP–pHEMA hydrogels can be considered to have an excellent optical clarity.

SEM images of freeze-dried hydrogels provided additional information on porosity and evidenced differences in surface morphology among the swollen hydrogels (Fig. 4). Freeze-drying of the specimens usually yield good images of the polymer matrix as it is in the swollen state, if no melting of the solvent occurs during the drying [26]. This was the case in our experiments. The control pHEMA hydrogels prepared without PVP had the smoothest surface and no pores were observed. The only minor irregularities found may be due to some swollen non-crosslinked pHEMA chains anchored to the pHEMA network, which could contribute to the low adhesive force of contact lenses as reported by Kim et al. [27]. The greater the content in PVP, the more uneven the surface of the freeze-dried hydrogels was. This could be due to the PVP which was being released from the lens. The transversal cuts indicated that the lenses have a homogeneous inner structure without apparent pores and that the chains of PVP which are still partially attached to the network may form polymer brushes at the lens surface. On the other hand, we observed that hydrogels synthesized in aqueous medium showed a spongy-like structure with a quite bumpy surface in the case of those prepared with 1.8 ml or more water (in a total of 6 ml). These latter hydrogels presented protuberances of polymer network and craters that came from inner parts of the hydrogel, which showed interconnected pores. These observations are mainly related to the microphase separation during synthesis, which leads to domains of different densities in the polymer.

3.2. PVP release

Fig. 5 shows the amounts of PVP released from the hydrogels prepared without water. These hydrogels showed a fast delivery of PVP in the first 24 h and then the release became more sustained. Similar behavior was observed for hydrogels prepared with water. Despite the important amount of PVP released, the relatively high initial load of the lenses and their sustained delivery made it possible for the content of the discs in the PVP to be still high on the 9th day of the assay (ca. 80% of the initial PVP amount). The release profiles were well fitted to square-root kinetics (Table 1), which means that diffusion is the main mechanism involved in the release, as expected for

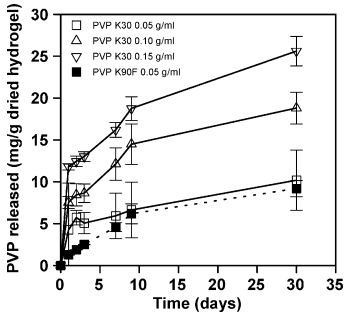

Fig. 5. PVP release profiles from PVP–pHEMA hydrogels prepared with different proportions of PVP (mg/ml) in the absence of water.

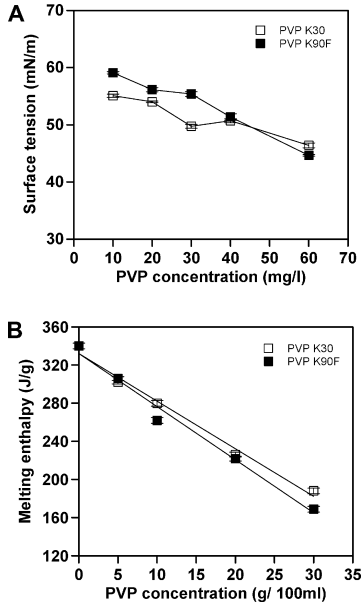

Fig. 6. Surface tension (A) and melting enthalpy (B) of PVP solutions.

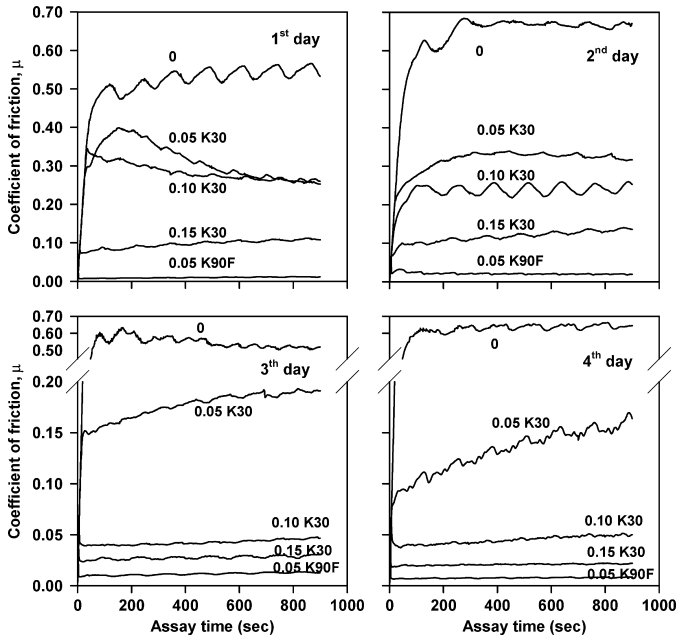

Fig. 7. Coefficients of friction of PVP–pHEMA hydrogels prepared with different proportions of PVP (mg/ml) in the absence of water, after 1-to-4 days of swelling in water.

a non-erodible device. It is known that the release rate of small size molecules (as common drugs) from a conventional soft contact lens occurs quite rapidly and obeys the diffusion laws; the thickness of the lens, its degree of hydration, and the drug concentration in the lens being critical factors [28,29]. The high molecular weight of PVP makes the entanglement of its long chains in the pHEMA mesh possible and hinders the movement of PVP through the network. This explains that its release can be sustained for much longer (beyond 30 days). As it could be expected, the diffusion rate increased as the water content of the lens raised owing to the increase in mesh size of the network.

When PVP is used as demulcent in ophthalmic solutions, its concentration ranges from 0.1% to 2% (i.e. 0.05–1.0 mg per drop) and several applications per day are commonly required [7,8]. The amounts of PVP released by the discs every 24 h were also in the 0.05–1.0 mg range (each disc weighs 60–70 mg). One difference in the role of PVP as demulcent if solutions or lenses were applied *in vivo* would be related to that most volume of the drop is lost due to defense mechanisms of the eye. The sustained delivery from the lens and the prolonged time of permanence in the post-lens lachrymal fluid could greatly enhance both the amount and the residence time of PVP on the ocular surface, as observed for drugs delivered from contact lenses [30]. On the other hand, concentrations of PVP in the range of those released from the hydrogels significantly decreased the surface tension of the release medium (Fig. 6A), which could contribute to the enhancement of the wettability of the contact lenses. This is directly related to the ability to maintain a stable tear layer in the eye and thus is a critical factor for their comfort and *in vivo* performance [31].

3.3. Friction coefficient

The friction test was carried out using a rheometer, which has two main advantages over the commonly used tribometer: (a) the temperature of the sample and of the liquid trapped between the geometry and the solid surface (Peltier plate) can be precisely controlled; and (b) its high sensitivity enables the measuring of the torque of low friction gels [15]. The friction experiments were carried out from dried hydrogels that were rehydrated in water for 1–4 days. The set up consisted of attaching the discs to the upper movable geometry of the rheometer, while 1 ml of the medium in which the disc swelled (and thus released

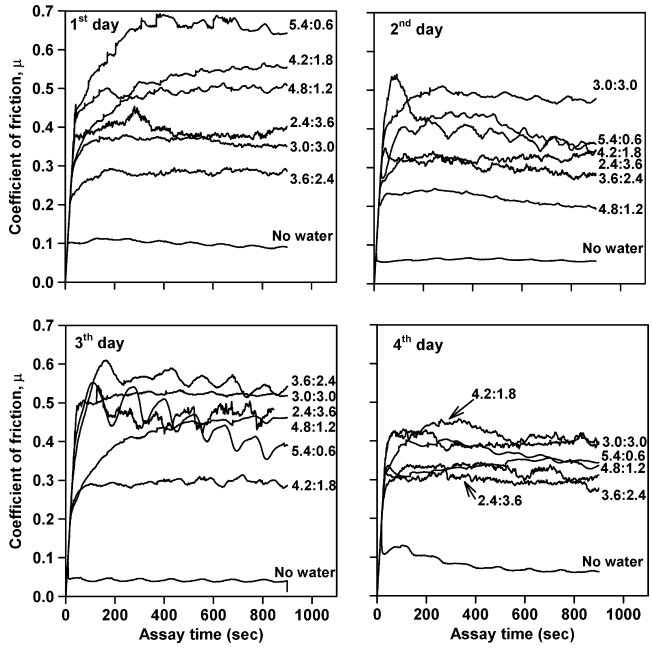

Fig. 8. Coefficients of friction of PVP–pHEMA hydrogels prepared with 0.15 mg of PVP per ml, using different monomer:water ratios, after 1-to-4 days of swelling in water.

PVP) was deposited on the Peltier plate to avoid dehydration of the hydrogel. The use of this medium, instead of pure water, should mimic the *in vivo* situation better. Not only the PVP interpenetrated into the lens and protruded out from the surface, but also the PVP already released from the disc should contribute to the lubricant effect. A minimum of 15 min for conditioning step was necessary to avoid influence of relaxation on the measurement of the friction. The values of the coefficients of friction are shown in Figs. 7 and 8; variability between replicates being below 5%. The results obtained are in the range of 0.02–1.7 previously found for pHEMA hydrogels of various cross-linking densities and hydration degrees intended to be used as synthetic articular cartilage [32].

Regarding hydrogels prepared in absence of water, control pHEMA hydrogel exhibited μ values of around 0.5, which remained constant after 24 h of hydration. By contrast, hydrogels containing PVP K30 showed time-dependent μ values; i.e. they progressively decreased from the 1st to the 4th day. Additionally, the greater the amount of PVP added to the monomer soup, the lower the μ value. As can be observed in Fig. 7, after 3 days of hydration pHEMA hydrogels prepared with 0.10 or 0.15 g PVP (per gram of hydrogel) showed a decrease in μ values greater than 10-fold with respect to control hydrogels. Such a low friction, which is comparable to that found for PVA hydrogels intended for joint lubrication [33], may be due to the contribution of both: (a) the lubrication of the hydrogel–Peltier plate interface by the PVP released from the lens (estimated by simultaneous monitoring of PVP concentration in the swelling medium at the time of the friction experiment; Fig. 9); and (b) the increase in the hydrodynamic solvent layer thickness and the decrease in shear resistance due to that the PVP brushes at the hydrogel surface deform more easily than the cross-linked pHEMA network [15].

The greater lubricious efficiency of PVP K90F was clearly evidenced from the 1st day. This means that an increase in the molecular weight of PVP (in the range evaluated) favorably contributes to making the surface of the lenses more slippery. The greater thickening ability and a slightly greater affinity for water of PVP K90F explain this finding [34]. It was previously reported that highly hydrophylic polymer gels have a low coefficient of friction due to the greatest amount of water that can be sorbed to their structure [35]. DSC analysis of PVP solutions (Fig. 6B) indicated that those prepared with 60% PVP K90F and 40% water have all water as bound water whilst in the case

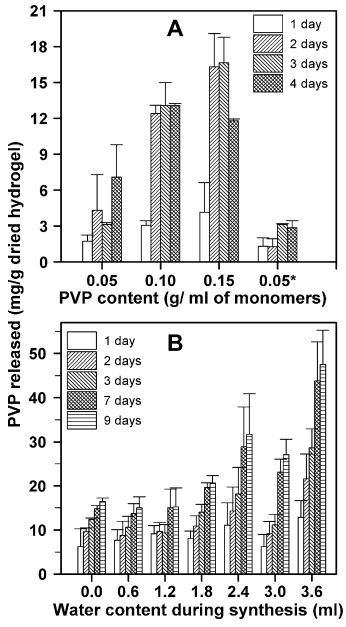

Fig. 9. PVP released from the PVP–pHEMA hydrogels subjected to the friction assay at the time at which the friction coefficient was recorded. (A) hydrogels prepared in the absence of water with different proportions of PVP K30 or 0.05 g/ml of PVP K90F(*); (B) hydrogels prepared with 0.15 g of PVP K30 per ml and different monomer:water v/v ratios (total volume 6 ml).

of PVP K30 solutions, the maximum content in water for being all as bound water is 33%. Thus, when the disc is pressed during the assay, less water molecules are squeezed out of the hydrogel and more remain attracted to the hydrophilic polymer forming a more efficient lubrication film on the hydrogel–Peltier plate interface.

Hydrogels prepared with PVP K30 (0.15 g/g) in the presence of water also showed a decrease in μ values as a function of hydration time (Fig. 8). After the first 24 h, hydrogels prepared from 5.4:0.6, 4.8:1.2 and 4.2:1.8 had μ values similar to the control pHEMA without PVP. Any hydrogel prepared in aqueous medium with PVP K30 (0.15 g/g) showed greater friction coefficient than the hydrogel prepared with PVP K30 (0.15 g/g) without water. Amongst hydrogels prepared in aqueous medium, increased proportions of water during synthesis slightly decreased the friction, but their μ values were still much higher than those observed for hydrogels prepared with PVP in the absence of water. On the 4th day all porous hydrogels reached similar μ values, despite those synthesized in presence of greater proportions of water released more PVP (Fig. 9). It should be noted that these latter hydrogels also have a more irregular and bumpy surface, which clearly counteracts the lubricant effect of PVP. To sum up, an adequate equilibrium between interpenetrating lubricant agent and surface topology of the lenses is required to achieve a minimum in friction.

4. Conclusions

The results obtained clearly prove that high proportions of PVP can be incorporated to pHEMA-based hydrogels, without compromising their optical clarity, for providing a slow delivery of PVP by diffusion. The adequate choice of PVP molecular weight and of the contents in water and PVP during synthesis may enable to achieve a significant decrease in the surface tension of the aqueous medium surrounding the hydrogels and a marked reduction of their friction coefficients, which are critical factors for the comfort of extended-wear soft contact lenses.

Acknowledgements

Work financed by Ministerio de Educación y Ciencia (SAF2005-01930), FEDER and Xunta de Galicia (PGIDT06PXIC20303PN, infrastructure Grants DOG 04/06/97 and PGIDT 00PX120303PR). F. Yañez thanks MEC for a FPI fellowship. BASF is acknowledged for PVP samples.

References

[1] M.E. Johnson, P.J. Murphy, Changes in the tear film and ocular surface from dry eye syndrome, Prog. Retin. Eye Res. 23 (2004) 449–474.
[2] M.A. Lemp, Report of the National Eye Institute/Industry workshop on clinical trials in dry eyes, CLAO J. 21 (1995) 221–232.
[3] K. Maruyama, N. Yokoi, Y. Takehisa, S. Kinoshita, Effect of environmental conditions on tear dynamics in soft contact lens wearers, Invest. Ophthalmol. Vis. Sci. 45 (2004) 2563–2568.
[4] A.S. Bacon, C. Astin, J.K. Dart, Silicone rubber contact lenses for the compromised cornea, Cornea 13 (1994) 422–428.
[5] F. Fornaseiro, J.M. Prausnitz, C.J. Radke, Post-lens tear-film depletion due to evaporative dehydration of a soft contact lens, J. Membrane Sci. 275 (2006) 229–243.
[6] N. Pritchard, D. Fonn, D. Brazeau, Discontinuation of contact lens wear: a survey, Int. Contact Lens Clin. 26 (1999) 157–162.
[7] M. Calonge, The treatment of dry eye, Surv. Ophthalmol. 45 (2001) S227–S239.
[8] M.B. Abelson, R. Anderson, Demystifying demulcents, Rev. Ophtalmol. 13 (2006) Available from: <http://www.revophth.com/index.asp?page=1_13162.htm>.
[9] R.C. Peterson, J.S. Wolffsohn, J. Nick, L. Winterton, J. Lally, Clinical performance of daily disposable soft contact lenses using sustained release technology, Contact Lens Anterior Eye 29 (2006) 127–134.
[10] FDA, Ophthalmic demulcents, Part 349.12. Subheading of ophthalmic drug products for over-the-counter human use, 21CFR349 (2006) Available from: <http://www.fda.gov/cder/otcmonographs/Ophthalmic/optthalmic(349).pdf>.
[11] S. Schwarz, J. Nick, Effectiveness of lubricating daily disposable lenses with different additives, 36th ECLSO Congress, Dubrovnik (2006) Available from: <http://www.kbsm.hr/hod/eclso2006/eclso_posters.html>.

[12] J. Veys, J. Meyler, Do new daily disposable lenses improve patient comfort?, Optician online 07 April (2006) Available from: <http://www.opticianonline.net/Articles>.
[13] L.C. Winterton, J.M. Lally, K.B. Sentell, L.L. Chapoy, The elution of poly(vinyl alcohol) from a contact lens: the realization of a time release moisturizing agent/artificial tear, J. Biomed. Mater. Res. B 80 (2007) 424–432.
[14] S.H. Kim, A. Opdahl, C. Marmo, G.A. Somorjai, AFM and SFG studies of pHEMA-based hydrogel contact lens surfaces in saline solution: adhesion, friction, and the presence of non-cross-linked chains at the surface, Biomaterials 23 (2002) 1657–1666.
[15] J.P. Gong, Y. Osada, Surface friction of polymer gels, Prog. Polym. Sci. 27 (2002) 3–38.
[16] D. Gulsen, A. Chauhan, Ophthalmic drug delivery through contact lenses, Invest. Ophthalmol. Vis. Sci. 45 (2004) 2342–2347.
[17] T.V. Chirila, An overview of the development of artificial corneas with porous skirts and the use of PHEMA for such an application, Biomaterials 22 (2001) 3311–3317.
[18] T.D. Dziubla, M.C. Torjman, J.I. Joseph, M. Murphy-Tatum, A.M. Lowman, Evaluation of porous networks of poly(2-hydroxyethyl methacrylate) as interfacial drug delivery devices, Biomaterials 22 (2001) 2893–2899.
[19] F. Yanagawa, Y. Onuki, M. Morishita, K. Takayama, Involvement of fractal geometry on solute permeation through porous poly(2-hydroxyethyl methacrylate) membranes, J. Control. Release 110 (2006) 395–399.
[20] B.J. Tighe, Contact lens materials, in: J. Stone, A.J. Phillips (Eds.), Contact Lenses. A Textbook for Practitioner and Student , second ed., Butterworths, London, 1981, pp. 377–399.
[21] C. Alvarez-Lorenzo, H. Hiratani, J.L. Gomez-Amoza, R. Martinez-Pacheco, C. Souto, A. Concheiro, Soft contact lenses capable of sustained delivery of timolol, J. Pharm. Sci. 91 (2002) 2182–2192.
[22] K. Müller, Identification and determination of polyvinylpyrrolidone (PVP) as well as determination of active substances in PVP-containing drug preparations, Pharm. Acta Helv. 43 (1968) 107–122.
[23] J.P. Gong, G. Kagata, Y. Osada, Friction of gels. 4. Friction on charged gels, J. Phys. Chem. B 130 (1999) 6007–6014.
[24] D. Gulsen, A. Chauhan, Effect of water content on transparency, swelling, lidocaine diffusion in p-HEMA gels, J. Membrane Sci. 269 (2006) 35–48.
[25] BASF, Kollidon: Polyvinylpyrrolidone for the Pharmaceutical Industry, eighth ed., Ludwigshafen 2003, pp. 51–52.
[26] I.E. Pacios, A. Pastoriza, I.F. Pierola, Effect of the crosslinking density and the method of sample preparation on the observed microstructure of macroporous and conventional poly(*N*,*N*-dimethylacrylamide) hydrogels, Colloid Polym. Sci. 285 (2006) 263–272.
[27] D.H. Kim, C. Marmo, G.A. Somorjai, Friction studies of hydrogel contact lenses using AFM: non-crosslinked polymers of low friction at the surface, Biomaterials 22 (2001) 3285–3294.
[28] G. Wajs, J.C. Meslard, Release of therapeutic agents from contact lenses, Crit. Rev. Ther. Drug 2 (1986) 275–289.
[29] C. Alvarez-Lorenzo, H. Hiratani, A. Concheiro, Contact lenses for drug delivery: achieving sustained release with novel systems, Am. J. Drug Del. 4 (2006) 131–151.
[30] H. Hiratani, A. Fujiwara, Y. Tamiya, Y. Mizutani, C. Alvarez-Lorenzo, Ocular release of timolol from molecularly imprinted soft contact lenses, Biomaterials 26 (2005) 1293–1298.
[31] C. Maldonado-Codina, P.B. Morgan, In vitro water wettability of silicone hydrogel contact lenses determined using the sessile drop and captive bubble techniques, J. Biomed. Mater. Res. 83A (2007) 496–502.
[32] M.E. Freeman, M.J. Furey, B.J. Love, J.M. Hampton, Friction, wear, and lubrication of hydrogels as synthetic articular cartilage, Wear 241 (2000) 129–135.
[33] Y.S. Pan, D.S. Xiong, R.Y. Ma, A study on the friction properties of poly(vinyl alcohol) hydrogel as articular cartilage against titanium alloy, Wear 262 (2007) 1021–1025.
[34] M. Mayo-Pedrosa, C. Alvarez-Lorenzo, I. Lacik, R. Martinez-Pacheco, A. Concheiro, Sustained release pellets based on poly(*N*-isopropyl acrylamide): matrix and in situ photopolymerization-coated systems, J. Pharm. Sci. 96 (2007) 93–105.
[35] Y. Ishikawa, K. Hiratsuka, T. Sasada, Role of water in the lubrication of hydrogel, Wear 261 (2006) 500–504.

3.5. Hydrogels porosity and bacteria penetration: where is the pore size threshold?

Enviado

Hydrogels porosity and bacteria penetration: where is the pore size threshold?

Fernando Yañez[1], Jose L. Gomez-Amoza[1], Beatriz Magariños[2], Angel Concheiro[1], Carmen Alvarez-Lorenzo[1,*]

[1]Departamento de Farmacia y Tecnologia Farmaceutica, Facultad de Farmacia, Universidad de Santiago de Compostela, 15782-Santiago de Compostela, Spain.

[2]Departamento de Microbiologia y Parasitologia, Facultad de Biologia, Universidad de Santiago de Compostela, 15782-Santiago de Compostela, Spain

*Correspondence to: C. Alvarez-Lorenzo (E-mail: carmen.alvarez.lorenzo@usc.es)

Abstract

The relationship between the microstructure of poly(2-hydroxyethyl methacrylate) (polyHEMA) hydrogels and the growth of microorganisms on their surface and their penetration through the network was evaluated. The hydrogels were prepared using solutions of HEMA and ethyleneglycol dimethacrylate (EGDMA) with water ranging from 0 to 60% wt. As the content in water upon synthesis increased the glass transition temperature and the degree of swelling of the hydrogels increased. Image analysis of SEM micrographs of the hydrogel surface and BET analysis of nitrogen adsorption isotherms were respectively used to characterize the size distributions of macropores and mesopores. The higher the water proportion, the greater the size of meso (linear dependence) and macropores (segmental mode dependence), the area occupied by the macropores at the surface of the hydrogels, and the specific surface of the hydrogels. Hydrogels synthesized with 30% or less water showed a quite close distribution of pores with a mean size below 1 μm and effectively hindered the penetration of Gram+ *Staphylococcus aureus* (0.5-1 μm cocci) and Gram- *Pseudomonas aeruginosa (*0.5-0.8 μm x 1.5-3 μm bacilli). Logistic regression analysis points out that the probability of penetration of *Staphylococcus aureus* or *Pseudomonas aeruginosa* is above 50% when the mean pore size is greater than 3.67 μm or 5.56 μm, respectively.

Keywords: polyHEMA, porosity, water in monomer solution, BET, bacterial penetration, grain analysis of SEM micrographs.

1. Introduction

The concern about contamination of hydrogels with microorganisms is particularly relevant when hydrogels are intended to be exposed to the environment, such as in the case of the wound dressings and the contact lenses [1,2]. Hydrogels used as dressings are intended to treat wounds being permeable to water vapour, gases and small protein molecules, but impermeable to microorganisms [3]. Corneal infections are associated with ocular trauma, allergic hypersensitivity reactions or contact with contaminated water [4,5]. Contact lens wearers have a greater prevalence of infections due to contamination during management, maintenance in homemade saline solutions, or practicing of sports like swimming [6-8]. Microbial keratitis may be caused by several Gram+ and Gram- bacteria [9, 10]. Gram+ bacteria are also commonly associated to contact lens induced peripheral ulcers, while Gram- are involved in the contact lens induced acute red eye syndrome [9,11]. *Pseudomonas aeruginosa* and *Staphylococcus aureus* easily adhere to soft contact lenses made of poly(hydroxyethyl methacrylate) (polyHEMA) [12-14] and lead to progressive destruction of the corneal epithelium and stroma [15-17].

The effects of the content in water and the copolymerization with ionic monomers on bacterial adhesion to and penetration through polyHEMA hydrogels have been evaluated in detail [18-20]. In general, the higher the content in water, the lower the adhesion of bacteria [21]. However, the influence of hydrogel porosity on the penetration of microorganisms has received much less attention. It is well known that the polymerization of HEMA in aqueous solution renders hydrogels of increasing porosity as the content in water in the monomeric solution increases. The proportion of water has to be below 40-60% to obtain transparent hydrogels. If the content in water is above 80% a markedly phase separation occurs and macroporous networks are obtained [22]. It has been shown that the synthesis in the presence of water may alter the degree of swelling of poly(HEMA) hydrogels and the release rate of solutes, including antimicrobial drugs [23, 24]. Yanagawa et al. [25] have recently used image analysis of SEM micrographs of polyHEMA hydrogels synthesized with different degree of cross-linking in the absence of water and in the presence of 80% v/v to characterize the fractal geometry of the internal structure of the macroporous networks. Nevertheless, there is still a paucity of

information about the influence of water on the pore size and porous microstructure of polyHEMA hydrogels.

The aim of this work was to investigate the influence of the porous microstructure of polyHEMA hydrogels, keeping constant their composition, on the growth of microorganisms on their surface and their penetration through the network. The hydrogels were prepared by photopolymerization of mixtures of HEMA with a fixed molar ratio of cross-linking agent EGDMA and various proportions of water, without exceeding 60 %wt in order to obtain transparent hydrogels still useful for preparing soft contact lenses or transparent wound dressings.

2. Experimental

2.1. Materials

Ophthalmic grade 2-hydroxyethyl methacrylate (HEMA) was supplied by Merck (Germany); ethyleneglycol dimethacrylate (EGDMA) by Sigma-Aldrich (Spain) and Irgacure® 2959 was from CIBA (Spain). Dichloromethylsilane was purchased from Sigma-Aldrich (Germany). All other reagents were of analytical grade. Ultrapure water obtained by reverse osmosis (resistivity > 18.2 MΩ cm; MilliQ®, Millipore Spain) was used.

2.2. Synthesis of hydrogels

EGDMA cross-linker (80 mM, equivalent to 1 mol%) was dissolved in HEMA (6 ml). Aliquots of the monomeric solution were mixed with volumes of water ranging from 0 to 60% v/v. After addition of Irgacure 2959 (0.1% mol of monomers), the monomers solutions were immediately injected into moulds constituted by two glass plates separated by a silicone frame 0.4 mm wide [26]. Previously, the glass plates were covered with dichloromethylsilane to avoid polymer adhesion on the glass after polimerization. The moulds were irradiated with a UV-lamp at 366 nm (1100 $\mu W/cm^2$; Camag, Switzerland) for 50 to 90 min. After polymerization, each hydrogel was immersed in boiling water for 15 min to remove unreacted monomers and to facilitate the cut of 10 mm discs. The discs were washed in water for 2 weeks, replacing the medium every 12 h.

2.3. Differential scanning calorimetry

Pieces of dried discs (4-6 mg) were weight in aluminium crucibles and then heated from 30 to 100 °C, cooled to 0 °C and heated again up to 200 °C, at a rate of 10 °C/min, in a DSC Q-100 apparatus (TA Instruments, UK) equipped with a refrigerated cooling accessory. Nitrogen was used as purge gas at a flow rate of 50 ml/min. The calorimeter was calibrated for cell constant and temperature using indium (melting point 156.61 °C, enthalpy of fusion 28.71 J/g), and for heat capacity using sapphire standards. Tg is reported as the midpoint of the glass transition.

2.4. SEM images analysis

Freeze-dried hydrogels were cut in small pieces, mounted on double-sided tape on aluminum stubs and sputter-coated with gold/palladium, and micrographs were taken at x500, x1000 and x2000 (scale factors of 0.676, 0.336 and 0.169 μm/pixel, respectively) using a scanning electron microscope (LEO-435VP SEM, Leo Electron Microscopy, UK). The images were then analyzed using grain analysis modulus (SPIP 4.6.0, Image Metrology A/S, Denmark). The images were 600x600 pixels coded in 256 gray levels (black=0, white=255). The 2D images were considered as a flat x-y map of pixels that can be transformed in 3D images, the gray tone function being the z dimension [27]. Size distribution of pores and holes on the surface of the hydrogels was estimated using the grain analysis modulus of SPIP 4.6.0 software (Image Metrology A/S, Denmark). The segmentation of the image was carried out applying an automatic threshold that uses the mean profile of the surface as the base line. The frequency distributions of pores at the surface were fitted by non-linear regression (GraphPad Prism v.4.02, GraphPad Software Inc., San Diego, CA) to a normal distribution, and the mean sizes and the standard deviations were estimated. The fraction of the hydrogel surface occupied by the pores was also calculated.

2.5. Nitrogen adsorption

Nitrogen adsorption experiments were carried out in a Micromeritics ASAP 2000 (Norcross GA, USA) apparatus using freeze-dried hydrogel discs that had been degasified by being kept for 8 h at 70°C and 10^{-3} mm Hg. Nitrogen adsorption at 77 K was measured

over the relative pressure range 0.01–0.98. Each hydrogel was run in duplicate. Specific surface area (S_{BET}) was estimated from the volume of a nitrogen monolayer (Vm, calculated from the BET equation) using the equation [28]:

S_{BET} (m^2g^{-1}) = 4.37 V_m (cm^3g^{-1}),

where V_m is the volume of nitrogen necessary to form the monolayer.

Mean pore size and micropore volume were estimated from the nitrogen desorption isotherms on the assumption that equilibrium between the gas phase and the adsorbed phase during desorption is determined by (1) physical adsorption on the pore walls and (2) capillary condensation in the inner capillary volume; a numerical method was used to solve the Barret et al. [29] equation,

$$\Delta Vp = Rn\cdot\left(\Delta Vc - C\cdot\Delta t\cdot\sum Sp\right)$$

where ΔVp is the actual pore volume emptied in the desorption step, C the correction factor to allow for the change in curvature of the pore wall as pore size changes, ΣSp the sum of the surface areas over all the desorption steps, and Rn is calculated using the expression,

$$Rn = \frac{r_p^2}{\left(r_k + t\right)^2}$$

where r_p is the actual pore radius, r_k the mean capillary condensate radius, and t the decrease in multilayer thickness during the desorption step.

2.6. Swelling in water and optical transparency

Dry hydrogels were immersed in water at 25ºC and the increase in weight was measured in triplicate, at different times. The degree of swelling at each time was calculated as follows [30]:

$$Q = (Wt - Wd)x100 / Wd$$

where W_t is the weight of the swollen hydrogel at a time t and W_d is the weight in the dry state. The equilibrium water content (EWC) was taken as the degree of swelling after 24 hours in water. The swollen hydrogels were fixed to the inner side of a quartz cell containing water and the transmittance was recorded at 600 nm (Agilent 8453, Germany).

2.7. Microbial growth and penetration tests

Suspensions (20 μL) of *Pseudomonas aeruginosa* (CCT 110, 7.8 10^8 CFU/ml) or *Staphylococcus epidermidis* (ATCC 25923, 3.2 10^9 CFU/ml) were dropped on the centre of the upper surface of hydrogel discs previously placed on Petri plates with sterile TSA (tryptose soy agar). The suspension was carefully deposited to avoid contamination of the TSA plate. The plates were then incubated for 24 h at 30 ºC and the growth of bacteria on the surface of the hydrogels was visually inspected [31]. The penetration of bacteria that pass through the hydrogel was evidenced by colonies that grew on the agar surrounding the discs.

2.8. Mathematical fitting and statistical analysis

The following models were used to evaluate the influence of the proportion of water during hydrogel synthesis on the glass transition temperature, the microstructure and the degree of swelling of the hydrogels, applying GraphPad Prism 5.00 (GraphPad Software Inc., 2007) software.

a) Linear: $y=a+b\cdot x$, where x is the proportion of water in the monomer solution.

b) Segmental:

$$y_1 = a_1 + b_1 x \qquad \text{if } x < x_0$$

$$y_2 = (a_1 + b_1 x_0) + b_2 (x-x_0) \qquad \text{if } x \geq x_0$$

being x is the proportion of water in the monomer solution, x_0 the proportion of water from which a change in the variable under study is observed, a_1 and $(a_1 + b_1 x_0)$ are the intercepts and b_1 and b_2 the slopes of the two linear segments.

An extra-sum of squares F test based on statistical hypothesis tests was carried out to choose the most adequate model for each variable under study. The null hypothesis is that the simplest model (the one with fewer parameters) is correct. The improvement attained with the most complicated model was quantified as the difference in sum-of-squares. Some improvements that may be just expected to occur by chance are determined by the number of data points and the number of parameters in each model. An F test was used to compare the difference in sum-of-squares with the difference one would expect by chance. The result was expressed as the F ratio, from which an α value is calculated. If the α value is small, the simplest model (the null hypothesis) is wrong and the most

complicated model should be accepted. Usually the threshold α value is set at its traditional value of 0.05. If the α value is less than 0.05, the most complicated model fits significantly better than the simpler model does.

Logistic regression (Statgraphics Plus 5.1, Statistical Graphics Corp., Warreton VA, USA) was used to determine the influence of the proportion of water in the monomeric solution on the growth of bacteria on the surface and the penetration of bacteria into the hydrogel. To do that, the value of 1 (with a probability to occur = ø) was assigned when bacteria grew on the hydrogel or pass through it. Otherwise, the value of 0 (with a probability to occur= 1-ø) was assigned. The logistic regression model applied was as follows:

$$\phi = \{ exp(a+b \cdot x)\} / \{(1+exp(a+b \cdot x)\}$$

where *a* is a constant and *b* the coefficient of the dependent variable.

The likely-hood ratio test that provides a χ^2 value (Statgraphics Plus 5.1, Statistical Graphics Corp., Warreton VA, USA) was applied to contrast the statistical significance of the model.

3. Results and discussion

3.1. Microstructure

All hydrogels showed a clear and transparent appearance (>90% transmittance at 600 nm) disregarding the content in water of the monomeric solutions. It has been previously reported that the addition of water slows down the polymerization rate of HEMA by UV irradiation, although at the low light intensity we used to carry out the polymerization no relevant differences in the degree of conversion are expected [32]. Nevertheless, UV radiation time was increased from 50 to 90 min as the proportion of water raised in the monomeric solution in order to ensure a complete polymerization.

DSC experiments were carried out to elucidate the influence of water on the glass transition temperature (Tg) of the polymers. Hydrogels obtained in the absence of water (0% mol) showed a glass-to-rubber transition at 109 ºC, which is in agreement with the value previously reported for polyHEMA networks [33,34]. Increasing the proportion of water in the monomeric solution, the Tg of the hydrogels raised from up to 124 ºC

(Figure 1). A close positive relationship was found between the Tg and the proportion of water (R^2=0.963; $F_{1,5\ d.f.}$=129.7; a<0.01). This finding suggests that microphase separation makes the hydrogels to be stiffer.

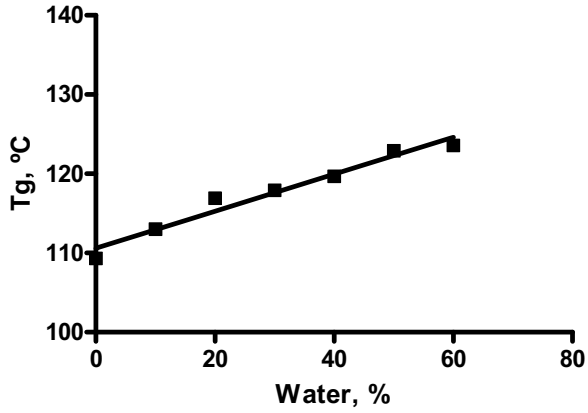

Figure 1. *Linear correlation between the proportion of water in the monomer solutions and the Tg.*

The microstructure of the hydrogels was characterized in terms of macropores (those with size above 0.050 μm) and mesopores (size between 0.002 and 0.050 μm; [35]) applying image analysis of SEM micrographs and nitrogen adsorption, respectively. Some SEM micrographs of the hydrogels taken at a scale factor of 0.169 μm·pixel^{-1} are shown in Figure 2. Remarkable differences in the size and number of macropores were observed for hydrogels prepared with different proportions of water.

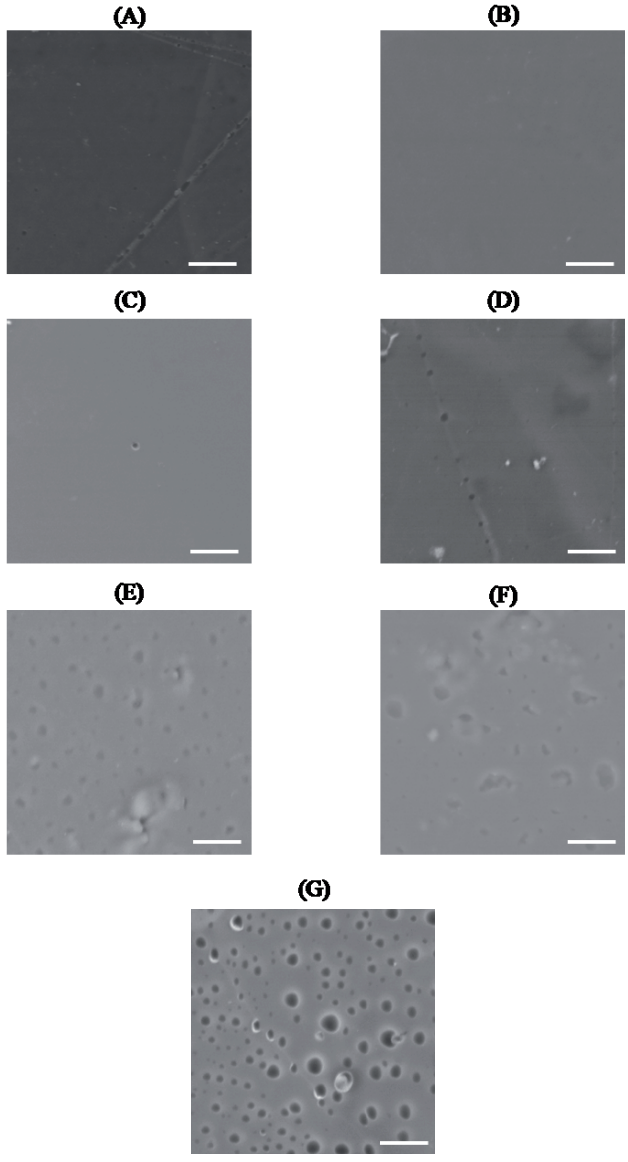

Figure 2. *SEM micrographs (x2000, scale bar length corresponds to 20 μm) of the surfaces of HEMA hydrogels synthesized in the presence of different proportions of water: (A) 0%; (B) 10%; (C) 20%; (D) 30%; (E) 40%; (F) 50% and (G) 60% water.*

The pore size distribution of the macropores was obtained from the SEM images using the grain analysis modulus (SPIP 4.6.0, Image Metrology A/S, Denmark). Images were segmented according to threshold level automatically chosen by the software as a function of the grey level of the mean profile of the image (Figure 3).

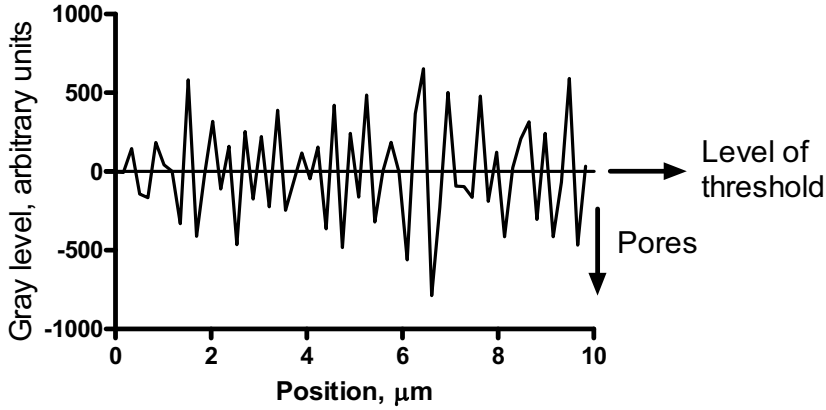

Figure 3. *Threshold level as a function of the mean gray level of the SEM image.*

Hydrogels synthesized from monomer solutions with 30% or less water showed at their surface pores with a size below 1.5 μm, which cover less than 2% of the total surface of the hydrogel (Figure 4). Hydrogels prepared with 50% or more water exhibited a large number of macropores greater than 10 μm; the surface covered by the pores was up to 10%. An intermediate behavior was observed when the monomer solution contained 40% water, since although small pores predominated, some large pores (>10 μm) were also visualized.

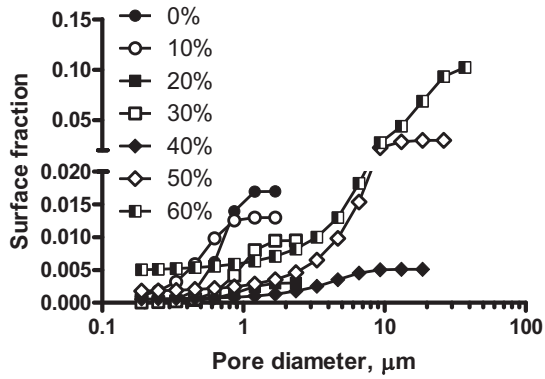

Figure 4. *Cumulative pore size distributions of macropores at the surface of the hydrogels.*

Pore size distributions were fitted to normal distributions and the mean pore size and the standard deviation were calculated (Table 1). Hydrogels synthesized with 30% or less water showed a quite close distribution of pores with a mean size below 1 μm. By contrast, greater contents in water of the monomer solution resulted in greater mean pore sizes and wider distributions.

Hydrogel	**Water:HEMA** (volume ratio)	**Mean diameter of macropores** (μm)	**S.D.** (μm)	R^2
A	0:100	0.69	0.19	0.976
B	10:90	0.48	0.21	0.970
C	20:80	0.89	0.34	0.975
D	30:70	0.91	0.29	0.963
E	40:60	3.38	2.63	0.983
F	50:50	6.47	4.02	0.993
G	60:40	14.74	8.79	0.973

Table 1. Proportion of water in the monomer solutions and mean diameter and standard deviation of pore sizes at the surface of the hydrogels after fitting to a normal distribution the pores measured using SEM image analysis.

The influence of water on the mean pore size ($F_{2,3\ d.f.}$=14.99, α<0.05) and on the surface occupied by pores ($F_{2,3\ d.f.}$=117.6, α<0.01) was well fitted by the segmental model (Figure

5). A marked change in the behavior was observed at around 40% water in the monomer solution. The slope values obtained for the first linear section, 0.01 and -0.03, and the second linear segment, 0.57 and 0.74, indicated that proportions of water below 40% do not have a relevant effect on the mean size of the pores at the surface neither on the area that they occupy. Oppositely, greater proportions of water cause remarkable increases in both pore size and area occupied by the pores at the surface of the hydrogel.

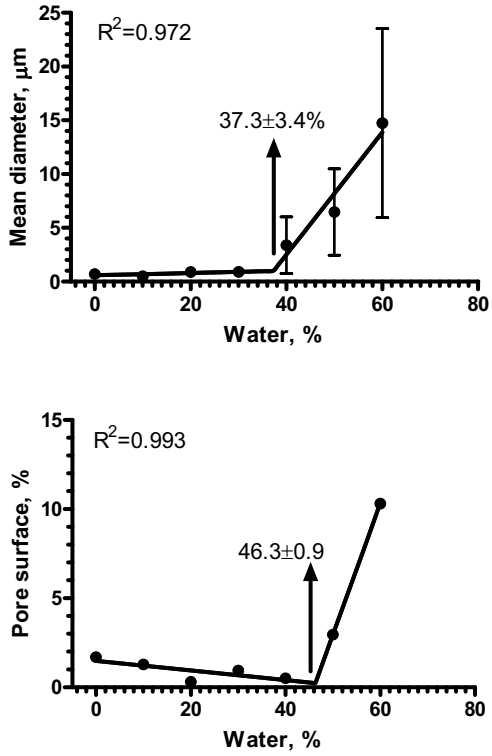

Figure 5. *Dependence of the mean pore size and the area occupied by the pores at the surface of the hydrogels on the proportion of water in the monomer solutions.*

Nitrogen adsorption enabled to characterize the microstructure of the hydrogel matrix through the estimation of the size distribution of the mesopores (Figure 6). The size distributions were well fitted to a log-normal distribution and the pore volume and the specific surface of the network obtained are shown in Table 2.

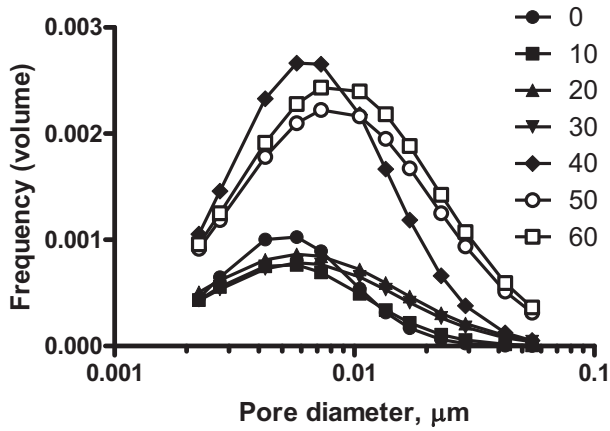

Figure 6. *Mesopore size distributions obtained by nitrogen adsorption.*

Hydrogel	Water:HEMA (volume ratio)	Mean diameter of mesopores (μm)	Geometric S.D.	R^2	Pore volume (cm^3g^{-1})	Specific surface (m^2g^{-1})
A	0:100	0.0051	1.88	0.984	0.000718	1.831
B	10:90	0.0051	2.13	0.987	0.000639	2.246
C	20:80	0.0060	2.57	0.969	0.000887	2.189
D	30:70	0.0061	2.47	0.987	0.000772	1.558
E	40:60	0.0064	2.15	0.989	0.002235	2.901
F	50:50	0.0081	2.62	0.994	0.002347	3.797
G	60:40	0.0084	2.61	0.995	0.002576	3.750

Table 2. *Mean diameter and geometric standard deviation of mesopores after fitting to a log normal distribution the porosity data obtained by N_2 adsorption, pore volume of the mesopores and specific surface of the hydrogels.*

The mean mesopore size, the volume of the mesopores and the specific surface of the hydrogels raised as the proportion of water in the monomer solutions increased. However, differently from that observed for macropores, the effect of water was additive and a linear regression fitted the dependence of the pore size, pore volume and specific surface on the water proportion: $F_{2,3\ d.f.}$= 1.69, 0.99 and 2.13, respectively. In all cases, α was

greater than 0.05 and thus the null hypothesis, which determines the choice of the simplest model, was accepted (Figure 7).

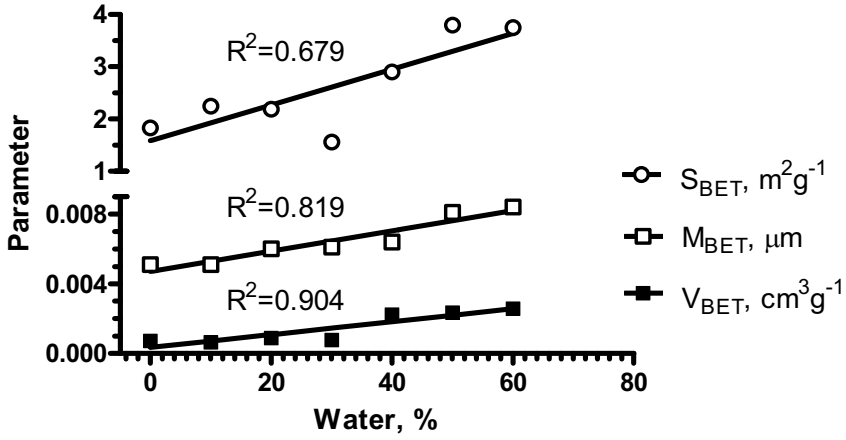

Figure 7. *Dependence of the mean diameter and volume of mesopores and the specific surface of the hydrogels on the proportion of water in the monomer solutions.*

3.2. Degree of swelling

The equilibrium water content (EWC) of the hydrogels increased with the proportion of water in the monomer solution (Figure 8) in agreement with the fact that the hydrogel macro and mesoporosity also became greater. An increase in the degree of swelling has been also previously reported for hydrogels as porosity augments [36,37]. The dependence of the EWC on the proportion of water upon synthesis was fitted by the segmental model ($F_{2,3\ d.f.}$=207.0; α<0.01); the slope up to 40% water was ten times lower than that found for proportions of water above 40% (Figure 8). This profile clearly resembles the patterns observed for the parameters used to characterize the macroporosity from SEM micrographs (see Figure 5). Therefore, the size and the surface occupied by the pores at the surface of the hydrogels seem to play a relevant role in the capability of the hydrogels to uptake water. In fact, close positive relationships between EWC values and the macropores surface (R^2=0.884) and their mean size (R^2=0.972) were observed.

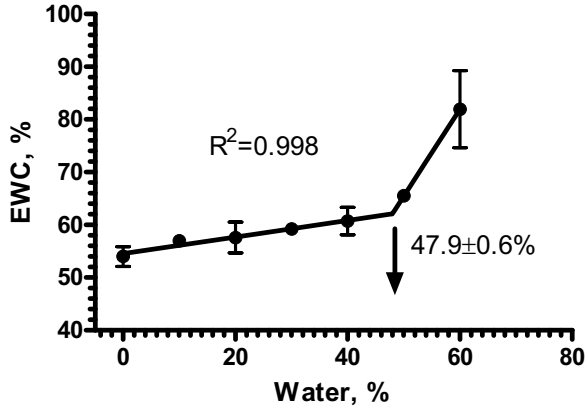

Figure 8. *Dependence of the swelling degree of the hydrogels on the proportion of water in the monomer solutions.*

3.3. Microbial growth and penetration tests

Ideally hydrogels intended to be used as components of medical devices should not allow the pass of microorganisms through their matrix. However, the likelihood of contamination of soft contact lenses by Gram+ bacteria such as *Staphylococcus aureus* (cocci measuring 0.5 to 1 μm [38]) or Gram- like *Pseudomonas aeruginosa (*bacilli measuring 0.5 to 0.8 μm by 1.5 to 3 μm [39]) is quite high. Therefore, the influence of hydrogel microstructure on bacterial growth and penetration was tested by placing the hydrogels on a culture medium (TSA) followed by dropping the microorganism suspension (20 μl) on the hydrogel upper surface. After 24 hours, both bacterial were not able to grow on hydrogels prepared under anhydrous conditions (Table 3). *S. aureus* proliferated on hydrogels prepared with a proportion of water ≥ 10% and was able to penetrate into the hydrogels prepared with a proportion of water ≥ 40%. *P. aeruginosa* required greater proportions of water during synthesis to grow (≥ 30%) and to pass through the hydrogels (≥ 50%). Thus, both bacteria were able to penetrate and cross hydrogels synthesized in the presence of 50% or 60% water, evidencing a clear discoloration of the culture medium.

Hydrogel	Water:HEMA (volume ratio)	Bacterial penetration test	
		Pseudomonas aeruginosa	*Staphylococcus aureus*
A	0:100	------	------
B	10:90	------	Growth on the hydrogel
C	20:80	------	Growth on the hydrogel
D	30:70	Growth on the hydrogel	Growth on the hydrogel
E	40:60	Growth on the hydrogel	Bacterial penetration
F	50:50	Bacterial penetration	Bacterial penetration
G	60:40	Bacterial penetration	Bacterial penetration

Table 3. *Results of the microbiological tests carried out to evaluate the influence of the proportion of water in the monomer solution on the growth and penetration of microorganisms.*

Logistic regression was applied to statistically characterize the influence of water on the growth and penetration of microorganisms. A value of 1 was assigned to hydrogels where bacteria grow on the surface or pass through the network. Otherwise, a value of 0 was assigned. The results obtained (Figure 9) evidence the relevant role of water on the growth and penetration of *Staphylococcus aureus* and *Pseudomonas aeruginosa*.

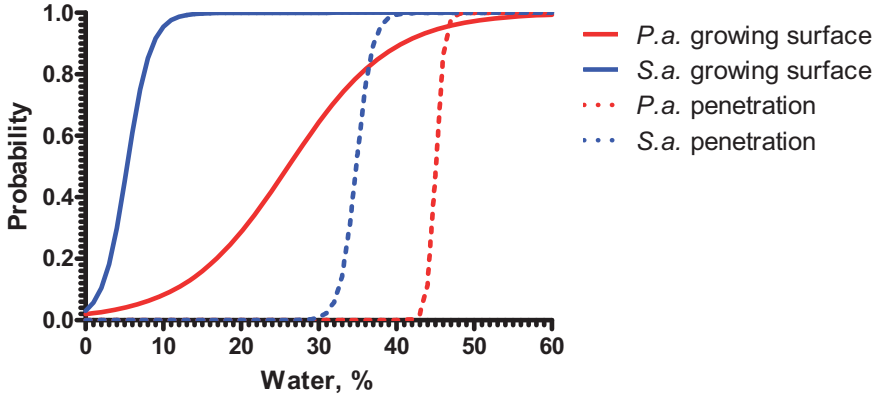

Figure 9. *Logistic regression fitting of the dependence on the proportion of water in the monomer solutions of the growth at the hydrogel surface of Pseudomonas aeruginosa (χ^2=7.51; 1 d.f.; α<0.01; explained variation=78.6%) or Staphylococcus aureus (χ^2=5.58; 1 d.f.; α<0.05; explained variation=97.3%) or the penetration of Pseudomonas aeruginosa (χ^2=8.38; 1 d.f.; α<0.01; explained variation=99.9%) or Staphylococcus aureus (χ^2=9.53; 1 d.f.; α<0.01; explained variation =99.7%).*

The relevant differences observed for both bacteria (possessing different shapes and sizes) clearly indicate that the pore structure at the hydrogel surface mainly determines the ability of the microorganisms to penetrate into the hydrogels. Furthermore, the results of the logistic regression of the bacteria penetration versus the mean pore size of the macropores (as determined by SEM image analysis) point out that the probability of bacteria penetration is above 50% when the mean pore size is greater 5.56 μm for *Pseudomonas aeruginosa*, or 3.67 μm for *Staphylococcus aureus* (Figure 10). As expected, no logistic regression could be obtained between the bacteria penetration and the parameter derived from the nitrogen adsorption, which means that mesopores do not have a relevant role in the penetration of bacteria with one dimension close to 0.5 μm.

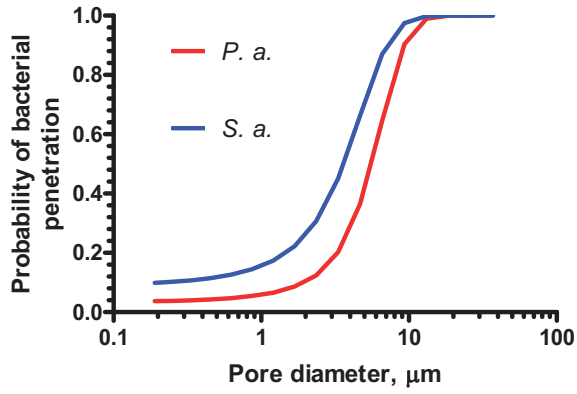

***Figure 10**. Results of the logistic regression between the mean macropore size at the surface of the hydrogels and the penetration of Pseudomonas aeruginosa (χ^2=6.54; 1 d.f.; α<0.05; explained variation=68.4%) or Staphylococcus aureus (χ^2=6.56; 1 d.f.; α<0.05; explained variation=78.3%) inside the hydrogels.*

4. Conclusions

Microstructure of polyHEMA hydrogels is highly dependent on the proportion of water present in the monomer solutions. Mesoporosity linearly raised with the water content upon synthesis, while macroporosity showed a marked increase when water was above 40%. The growth and the penetration of bacteria commonly contaminating medical

devices, such as *Pseudomonas aeruginosa* and *Staphylococcus aureus*, are highly dependent on the macroporosity of the hydrogels. Logistic regression analysis points out that the likelihood of bacteria penetration is above 50% when the mean pore size is greater 5.56 μm for *Pseudomonas aeruginosa*, or 3.67 μm for *Staphylococcus aureus.* Therefore the design of hydrogels that prevent the growth of bacteria requires a rigorous control of the microstructure and the effect of water in the monomer solution on the pore size.

Acknowledgements

The authors thank the support of MICINN and FEDER (SAF2008-01679), and Xunta de Galicia (PGIDT07CSA002203PR), Spain. F. Yañez is grateful to MICINN for a FPI grant. P. Diaz is acknowledged for the assistance with the BET experiments.

References

[1] U. Gopinathan, F. Stapleton, S. Sharma, M.D.P. Willcox, D.F. Sweeney, G.N. Rao, B.A. Holden, Microbial contamination of hydrogel contact lenses, J. Appl. Microbiol. 82 (1997) 653-658.

[2] B.S. Atiyeh, S.N. Hayek, An update on management of acute and chronic open wounds: the importance of moist environment in optimal wound healing, Curr. Pharm. Biotechnol. 3 (2002) 179-195.

[3] C. Weller, G. Sussman, Wound Dressings Update, J Pharm. Pract. Res. 36 (2006) 318-324.

[4] P. Garg, A.K. Bansal, S. Sharma, G.K. Vemuganti, Bilateral infectious keratitis after laser in situ keratomileusis: A case report and review of the literature, Ophthalmology 108 (2001) 121–125.

[5] T.J. Liesegang, Bacterial and fungal keratitis, en: H.E. Kaufman, B.A., Barron, M.B., McDonald, S.R.,Waltman (Eds.), The cornea, Churchill Livingstone, New York, 1988, pp 217–270.

[6] T.T. McMahon, K. Zadnik, Twenty-five years of contact lenses: The impact on cornea and ophthalmic practice, Cornea 19 (2000) 730-740.

[7] T. Wong, S. Ormonde, G. Gamble, C.N.J. McGhee, Severe infective keratitis leading to hospital admission in New Zealand, Brit. J. Ophthalmol. 87 (2003) 1103-1108.

[8] M.E. Zegans, H.I. Becker, J. Budzik, G. O'Toole, The role of bacterial biofilms in ocular infections, DNA Cell. Biol. 21 (2002) 415-420.

[9] M.D.P. Willcox, N. Harmis, B.A. Cowell, T. Williams, B.A. Holden, Bacterial interactions with contact lenses; effects of lens material, lens wear and microbial physiology, Biomaterials 22 (2001) 3235-3447.

[10] K.F. Tabbara, H.F. El-Sheikh, B. Aabed, Extended wear contact lens related bacterial keratitis, Br. J. Ophtalmol. 84 (2000) 327-328.

[11] B.A. Holden, D. La Hood, T. Grant, J. Newton-Howes, C. Baleriola-Lucas, M.D. Willcox, D.F. Sweeney, Gram-negative bacteria can induce contact lens related acute red eye (CLARE) responses, CLAO J. 22 (1996) 47-52.

[12] S.M. Fleiszig, D.J. Evans, M.F. Mowrey-McKee, R. Payor, T.S. Zaidi, V. Vallas, E. Muller, G.B. Pier, Factors affecting *Staphylococcus epidermidis* adhesion to contact lenses, Opto. Vision Sci. 73 (1996) 590–594.

[13] B.A. Cowell, M.D. Willcox, R.P. Schneider, A relatively small change in sodium chloride concentration has a strong effect on adhesion of ocular bacteria to contact lenses, J Appl. Microbiol. 84 (1998) 950–958.

[14] R.L. Taylor, M.D. Willcox, T.J. Williams, J. Verran, Modulation of bacterial adhesion to hydrogel contact lenses by albumin, Opto. Vision Sci. 75 (1998) 23–29.

[15] R.P. Kowalski, A.N. Pandya, L.M. Karenchak, An in vitro resistance study of levofloxacin, ciprofloxacin and ofloxacin using keratitis isolates of Staphylococcus aureus and Pseudomonas aeruginosa, Ophthalmology,108 (2001) 1826–1829.

[16] M.C. Callegan, M. Engelberg, D.W. Parke, B.D. Jett, M.S. Gilmore, Bacterial endophthalmitis: Epidemiology, therapeutics, and bacterium-host interactions. Clin Microbiol Rev. 15 (2002) 111–124.

[17] T. Bourcier, F. Thomas, V. Borderie, C. Chaumeil, L. Laroche, Bacterial keratitis: Predisposing factors, clinical and microbiological review of 300 cases, Br J Ophthalmol. 87 (2003) 834–838.

[18] S.M. Fleiszig, D.J. Evans, M.F. Mowrey-McKee, R. Payor, T.S. Zaidi, V. Vallas, E. Muller and G.B. Pier, Factors affecting *Staphylococcus epidermidis* adhesion to contact lenses, Opto Vision Sci. 73 (1996) 590–594.

[19] B.A. Cowell, M.D. Willcox, R.P. Schneider, A relatively small change in sodium chloride concentration has a strong effect on adhesion of ocular bacteria to contact lenses, J Appl Microbiol. 84 (1998) 950–958.

[20] R.L. Taylor, M.D. Willcox, T.J. Williams, J. Verran, Modulation of bacterial adhesion to hydrogel contact lenses by albumin, Opto Vision Sci. 75 (1998) 23–29.

[21] A.D. Cook, R.D. Sagers, W.G. Pitt, Bacterial adhesion to poly(HEMA)-based hydrogels, J. Biomed. Mater. Res. 27 (1993) 119–126.

[22] T.V. Chirila, Y. Chen, B.J. Griffin, I.J. Constable, Hydrophilic sponges based on 2-hydroxyethyl methacrylate. I. Effect of monomer mixture composition on the pore size, Polym. Int. 32 (1993) 221-232.

[23] S. Lu, K.S. Anseth, Photopolymerization of multilaminated poly(HEMA) hydrogels for controlled release, J. Controlled Release 57 (1999) 291–300.

[24] T.L. Tsou, S.T. Tang, Y.C. Huang, J.R. Wu, J.J. Young, H.J. Wang, Poly(2-hydroxyethyl methacrylate) wound dressing containing ciprofloxacin and its drug release studies. J Mater. Sci. Mater. Med. 16 (2005) 95-100.

[25] F. Yanagawa, Y. Onuki, M. Morishita, K. Takayama, Involvement of fractal geometry on solute permeation through porous poly (2-hydroxyethyl methacrylate) membranes, J. Control. Release 110 (2006) 395–399.

[26] C. Alvarez-Lorenzo, H. Hiratani, J.L. Gomez-Amoza, R. Martinez-Pacheco, C. Souto, A. Concheiro, Soft contact lenses capable of sustained delivery of timolol, J. Pharm. Sci. 91 (2002) 2182-2192.

[27] D. Chappard, I. Degasne, G. Hure, E. Legrand, M. Audran, M.F. Basle, Image analysis measurements of roughness by texture and fractal analysis correlate with contact profilometry, Biomaterials 24 (2003) 1399-1407.

[28] N.G. Stanley- Wood, Enlargement and compaction of particle solids, Butterworths, London, 1983.

[29] E.P. Barrett, L.G. Joyner, P.P. Halenda, The determination of pore volume and area distributions in porous substances. I.Computations from Nitrogen Isotherms, J. Am. Chem. Soc. 73 (1951) 373–380.

[30] G. Mabilleau, I.C. Stancu, T. Honore, G. Legeay, C. Cincu, M.F. Basle, D. Chappard, Effects of the length of crosslink chain on poly(2-hydroxyethyl methacrylate) (pHEMA) swelling and biomechanical properties, J Biomed. Mater. Res. A 77 (2006) 35–42.

[31] S. Lj. Tomic, M.M. Mic, S.N. Dobic, J.M. Filipovic, E.H. Suljovrujic, Smart poly(2-hydroxyethyl methacrylate/itaconic acid) hydrogels for biomedical application, Radiat. Phys. Chem. 79 (2010) 643–649.

[32] L. Li, L.J. Lee, Photopolymerization of HEMA/EGDMA hydrogels in solution, Polymer 46 (2005)11540–11547.

[33] G. Di Marco, M. Lanza, M. Pieruccini, Dynamical mechanical measurements in dry PHEMA and its hydrogels, Nuovo Cim. D 16 (1994) 849–854.

[34] P. Andrade-Vivero, E. Fernandez-Gabriel, C. Alvarez-Lorenzo, A. Concheiro, Improving the loading and release of NSAIDs from pHEMA hydrogels by copolymerization with functionalized monomers, J. Pharm. Sci. 96 (2007) 802-813.

[35] J. Rouquérol, D. Avnir, C. W. Fairbridge, D. H. Everett, J. H. Haynes, N. Pericone, J. D. F.Ramsay, K. S. W. Sing, K. K. Unger, Recommendations for the characterization of porous solids, Pure Appl. Chem. 66 (1994) 1739–1758.

[36] Q. Liu, E.L. Hedberg, Z. Liu, R. Bahulekar, R.K. Meszlenyi, A.G. Mikos, Preparation of macroporous poly(2-hydroxyethyl methacrylate) hydrogels by enhanced phase separation. Biomaterials 21 (2001) 2163-2169.

[37] Y.H. Wu, H.B. Park, T. Kai, B.D. Freeman, D.S. Kalika, Water uptake, transport and structure characterization in poly(ethylene glycol) diacrylate hydrogels, J. Membr. Sci. 347 (2010) 197–208.

[38] U. Vijaranakul, M.J. Nadakavukaren, B.L.M. Jonge, B.J. Wilkinson, R.K. Jayaswal, Increased cell size and shortened peptidoglycan interpeptide bridge of NaCl-stressed *Staphylococcus aureus* and their reversal by glycine betaine, J. Bacteriol. 177 (1995) 5116–5121.

[39] K.A. Whitehead, J. Colligon, J. Verran, Retention of microbial cells in substratum surface features of micrometer and sub-micrometer dimensions. Colloids Surf. B 41 (2005) 129-138.

3.6. Computational modeling and molecular imprinting for the development of acrylic polymers with high affinity for bile salts

Analytica Chimica Acta **659**, 178–185 (2010).

Analytica Chimica Acta 659 (2010) 178–185

Contents lists available at ScienceDirect

Analytica Chimica Acta

journal homepage: www.elsevier.com/locate/aca

Computational modeling and molecular imprinting for the development of acrylic polymers with high affinity for bile salts

Fernando Yañez[a], Iva Chianella[b], Sergey A. Piletsky[b], Angel Concheiro[a], Carmen Alvarez-Lorenzo[a,*]

[a] Departamento de Farmacia y Tecnología Farmacéutica, Facultad de Farmacia, Universidad de Santiago de Compostela, 15782 Santiago de Compostela, Spain
[b] Cranfield University, Bedford MK45 4DT, England, United Kingdom

ARTICLE INFO

Article history:
Received 1 September 2009
Received in revised form
20 November 2009
Accepted 24 November 2009
Available online 1 December 2009

Keywords:
Computational modeling
Cholic acid
Freundlich isotherm
Molecularly imprinted polymer (MIP)
Trap systems

ABSTRACT

This work has focused on the rational development of polymers capable of acting as traps of bile salts. Computational modeling was combined with molecular imprinting technology to obtain networks with high affinity for cholate salts in aqueous medium. The screening of a virtual library of 18 monomers, which are commonly used for imprinted networks, identified N-(3-aminopropyl)-methacrylate hydrochloride (APMA·HCl), N,N-diethylamino ethyl methacrylate (DEAEM) and ethyleneglycol methacrylate phosphate (EGMP) as suitable functional monomers with medium-to-high affinity for cholic acid. The polymers were prepared with a fix cholic acid:functional monomer mole ratio of 1:4, but with various cross-linking densities. Compared to polymers prepared without functional monomer, both imprinted and non-imprinted microparticles showed a high capability to remove sodium cholate from aqueous medium. High affinity APMA-based particles even resembled the performance of commercially available cholesterol-lowering granules. The imprinting effect was evident in most of the networks prepared, showing that computational modeling and molecular imprinting can act synergistically to improve the performance of certain polymers. Nevertheless, both the imprinted and non-imprinted networks prepared with the best monomer (APMA·HCl) identified by the modeling demonstrated such high affinity for the template that the imprinting effect was less important. The fitting of adsorption isotherms to the Freundlich model indicated that, in general, imprinting increases the population of high affinity binding sites, except when the affinity of the functional monomer for the target molecule is already very high. The cross-linking density was confirmed as a key parameter that determines the accessibility of the binding points to sodium cholate. Materials prepared with 9% mol APMA and 91% mol cross-linker showed enough affinity to achieve binding levels of up to 0.4 mmol g^{-1} (i.e., 170 mg g^{-1}) under flow (1 mL min^{-1}) of 0.2 mM sodium cholate solution.

1. Introduction

Hypercholesterolemia represents a serious health problem in wealthy economies and its incidence is rising in developing countries and poor communities owing to shifts in the alimentary habits [1]. Such a global concern on hypercholesterolemia makes cheap and patient-friendly therapeutic approaches particularly attractive. Diet control and prescription of 3-hydroxy-3-methyl-glutaryl-CoA (HMG-CoA) reductase inhibitors are common efficient strategies, but the first one does require willpower and the second one is not exempt of collateral effects [2,3]. The use of traps that can capture bile acids involved in the emulsification of fatty acids at the intestine is a particularly useful alternative or coadjutant in a broad range of therapies for patients [4,5]. Bile acids consist of a curved steroidal skeleton with a hydrophilic α face, which includes a carboxylic acid group, and a hydrophobic β face, which provides amphiphilic character and self-associative behavior [6]. The commercially available anionic resins (colestipol and cholestyramine, among others) exchange their chloride anions with anionic bile acids in the gastrointestinal tract, resulting in insoluble complexes that are eliminated in the feces [7]. This leads to lower adsorption of fats and to the conversion of plasma cholesterol to bile acid in order to normalize bile acid levels, which results in a decrease of cholesterol levels [3].

The search on novel polymeric materials capable of acting as selective and efficient traps is mostly based on the optimization of hydrophobic and ionic interactions [8–11]. The results obtained with natural and synthetic polymers indicate that a bile acid sequestrant should meet the following features [12–15]: (i) to possess cationic groups that enable a fast interaction with bile salts; (ii) to contain hydrophobic groups to enhance the stability of the complexes; and (iii) to swell to a certain extent to make the net-

* Corresponding author. Tel.: +34 981563100; fax: +34 981547148.
E-mail address: carmen.alvarez.lorenzo@usc.es (C. Alvarez-Lorenzo).

0003-2670/$ – see front matter © 2009 Elsevier B.V. All rights reserved.
doi:10.1016/j.aca.2009.11.054

Table 1
Composition (mg) of the polymer networks synthesized with or without (control) functional monomer, in the presence (MIP) or absence (NIP) of the template cholic acid.

Polymer network	DEAEM		EGMP		APMA·HCl		Control	
	MIP	NIP	MIP	NIP	MIP	NIP	MIP	NIP
Functional monomer (mg)	272	272	262	262	262	262	0	0
Cholic acid (mg)	150	0	150	0	150	0	150	0
EGDMA (mg)	2578	2578	2539	2539	2737	2737	3000	3000
DMSO (mL)	3	3	3	3	3	3	3	3
AIBN (mg)	30	30	30	30	30	30	30	30

work accessible to the bile salt. Molecular imprinting technology has been tested as tool to optimize performances of selective traps [16–18]. This technology consists in adding the target molecule to a monomers solution for enabling the arrangement of the monomers around the target analyte according to their interaction capability. Such an arrangement is fixed during polymerization. After extraction of the template molecules, the resultant polymeric networks exhibit pockets with size and shape specific for the template and with the most favorable chemical groups for the reuptake once in contact again with the template molecules [19–21]. Both non-covalent and covalent imprinting have been applied for creating bile acids traps using vinyl or acrylic monomers [16–18]. Although the imprinting effect in aqueous environment is harder to achieve than in organic media, imprinted networks have shown a greater uptake of sodium cholate, both *in vitro* and *in vivo*, than the non-imprinted networks [16–18].

Typically, the selection of the nature and the relative proportion of the monomers used for creating polymeric traps is based on literature data, previous experience of researchers, and the results of trial and error assays. Such a procedure involves hard and time consuming experimental work and remarkable costs for materials. Recent approaches to the rational design of functional polymeric networks have shown that *in silico* screening of suitable monomers for each specific target molecules can significantly shorten the process and improve the success rate [22]. Despite molecular imprinting technology has been routinely used for more than 20 years, implementation with computational modeling is still relatively novel [23]. The aim of this work was to apply computational modeling for the screening of monomers with affinity for cholic acid and use some of the selected monomers for synthesizing cholate-imprinted and non-imprinted networks. Adsorption isotherms were analyzed to test the predictive value of the computational modeling results. For the networks with better performance, the cross-linking density was tuned in order to elucidate the incidence of the mesh size in the capture of sodium cholate from an aqueous environment. The experiments were carried out both at equilibrium state to obtain relevant parameters of the adsorption process and in dynamic mode (i.e., under a certain flow of cholate solution) to simulate physiological conditions. The results were compared with those obtained using commercially available colestipol and conclusions about the incidence of computational design and molecular imprinting on the structure of the binding sites were extracted.

2. Experimental

2.1. Materials

Cholic acid, sodium cholate, ethyleneglycol dimethacrylate (EGDMA), 1,1′-azobis(isobutyronitrile) (AIBN), ethyleneglycol methacrylate phosphate (EGMP), and 2-(diethylamino)ethyl methacrylate (DEAEM) were from Sigma–Aldrich (Spain). N-(3-aminopropyl)-methacrylamide hydrochloride (APMA·HCl) was from Polysciences (Germany). 2-Hydroxyethyl methacrylate (HEMA) was from Merck (Germany). Dimethylsulfoxide (DMSO) was puriss. grade (≥99.5%) from Fluka (Spain) and used as received in bottles containing molecular sieves ($H_2O \leq 0.01\%$). All other chemicals were analytical or HPLC grade and used without further purification.

2.2. Molecular modeling

The computational design used for preparing the networks has been described elsewhere [23–26]. Briefly, the workstation used to simulate monomer–template interactions was a Silicon Graphics Octane running IRIX 6.5 operating system, configured with two 195 MHz reduced instruction set processors, 1 GB memory and a 20 GB fixed drive. The system was used to execute the software package SYBYL 7.0™ (Tripos Inc., St. Louis, MO, USA). The structure of cholic acid was drawn and its energy minimized using the dielectric constant value of DMSO to get stable conformations. A virtual library containing 18 of the most commonly used monomers in molecular imprinting was used and the energy of these monomers minimized as the template 'in DMSO'. The LEAPFROG™ algorithm (30,000 iterations) was applied to screen the library of functional monomers for their possible interactions with the template.

2.3. Synthesis of the networks

Each functional monomer EGMP, DEAEM or APMA·HCl (9% mol) was mixed with the cross-linker EGDMA (91% mol). The monomers solutions (3 mL) were diluted with the same volume of DMSO (Table 1) and 30 mg (1.2% mol) AIBN were added. In the case of the imprinted networks, 150 mg of cholic acid (2.5% mol) were incorporated too. The reaction mixtures were purged with nitrogen and then left to polymerize at 70 °C for 24 h. The bulk polymers were ground in methanol using a manual mortar and then wet-sieved through 125 and 38 μm meshes (Endecotts, UK). The particles

Table 2
Composition (% mol) of the polymer networks synthesized with APMA·HCl and various degrees of cross-linking.

Polymer network	Cholic acid	HEMA	APMA·HCl	EGDMA
APMA·HCl	0 (NIP)–2.5 (MIP)	0	9.0	91.0
A	0	6.2	9.9	83.9
B	0	12.1	9.7	78.2
C	0	23.3	9.3	67.4
D	0	33.5	8.9	57.5
E	0	43.1	8.6	48.3
F	0 (NIP)–2.5 (MIP)	60.0	8.3	31.7
G	0 (NIP)–2.5 (MIP)	92.3	9.2	21.5

retained on the 38 μm mesh underwent Soxhlet extraction with methanol (500 mL, 24 h) and then were dried under vacuum. Networks containing APMA·HCl were also prepared with lower degrees of cross-linking, replacing a certain volume of EGDMA by HEMA, as indicated in Table 2.

2.4. SEM images

Particles of each polymer network were analyzed by scanning electron microscopy (LEO-435VP SEM, Leo Electron Microscopy, UK). Samples were mounted on double-sided tape on aluminum stubs and sputter-coated with gold/palladium, and micrographs were taken at various magnifications.

2.5. Degree of swelling

50 mg dried particles were immersed in 1 mL water and mechanically shaken for 2 h. Then, the wet particles were gently filtered, weighed and placed in an oven at 50 °C for 2 days. The degree of swelling was calculated using the equation:

$$Q = \frac{Ww - Wd}{Wd} \times 100 \quad (1)$$

where *Ww* and *Wd* are the weights of the particles after swelling and once dried, respectively. The experiments were carried out in duplicate.

2.6. Adsorption isotherms

Equilibrium batch binding experiments were performed, in triplicate, with 1.5 mg of polymers that were loaded in ultracentrifuge columns (Pierce Centrifuge Columns 0.8 mL, ThermoScientific, Rockford, IL, USA) and mixed with 500 μL of sodium cholate solution (0.1–0.5 mM in water, pH values ranging from 6.40 to 6.73). The columns were placed into Eppendorf tubes and mechanically shaken at room temperature for 12 h and then centrifuged for 2 min at 600 rpm. The concentration of sodium cholate remaining in the medium was spectrophotometrically quantified as previously reported [27]. Briefly, 3 mL of sulfuric acid 96% (w/w) were poured into test tubes containing 1 mL of sodium cholate solution inside a water/ice bath. After mixing, the test tubes were heated to 70 °C for 30 min and then the absorbance was measured at 389 nm (Agilent 8354, Germany).

The adsorption isotherms were characterized using the Freundlich model:

$$\log B = m \cdot \log F + \log a \quad (2)$$

where B (μmol per gram of polymer) and F (mol L^{-1}) are the concentrations of bound and free sodium cholate, respectively, and a and m are the fitting constants that yield a measure of physical binding parameters [28]. The pre-exponential factor a is a measure of the capacity (number of binding sites) and average affinity of the network. The constant m is a heterogeneity index; m values close to 1 indicate that all binding sites are identical from an energetic point of view, while m values near 0 indicate heterogeneous binding points [29].

The affinity distribution of the binding sites (i.e., the plot of the number of sites, N, that have association constant, K) was estimated using the following equation [28]:

$$N(K) = 2.303 \cdot a \cdot m \cdot (1 - m^2) e^{-2.303 \cdot m \cdot \log K} \quad (3)$$

within the limits $K_{min} = 1/F_{max}$ and $K_{max} = 1/F_{min}$.

2.7. Binding of sodium cholate from aqueous medium

20 mg of each polymer were packed in 1 mL filtration tubes (Supelco, Bellefonte, PA, USA), which were placed in a VisiPrep 12-vial vacuum manifold (Supelco, Bellefonte, PA, USA) connected to a vacuum pump. The cartridges containing the polymers were washed with 2 mL of water, 2 mL of 0.1% NaOH in 50:50 ethanol:water solution, 2 mL of 0.1 M formic acid, and 2 mL of methanol. Then, 1 mL aliquots of 0.2 mM sodium cholate solutions in phosphate buffer pH 7.4 were successively passed through the polymers up to a total volume of 30 or 50 mL. The flow rate of the solution through the cartridge, with the vacuum pump connected since the beginning of the experiment, was 1 mL min^{-1}. Each extracted portion was collected and the concentration of unbound sodium cholate was spectrophotometrically determined as explained in Section 2.6. The experiments were carried out in triplicate.

3. Results and discussion

3.1. Design of the polymer networks

In silico screening of the most suitable monomers for preparing a certain functional polymer is gaining attention owing to the considerable number of monomers that can be tested in short time and without consumption of materials [25,26]. Our strategy comprised the development of a library of monomers, the selection of monomers with affinity for the target molecule, the synthesis of polymers using these monomers, and their testing in re-binding experiments. A virtual library of 18 commonly used functional monomers that are capable of interacting with cholic acid through electrostatic, hydrophobic, van der Waals forces or dipole–dipole interactions was screened against the template. The interaction energies obtained by docking template and monomer structures, minimized using the dielectric constant value of DMSO, are reported in Table 3. DMSO was selected for the modeling as it was the porogen chosen for the preparation of MIPs by radical polymerization. In fact it has been previously shown that MIPs prepared in polar organic solvents (DMF and DMSO) also possess good affinity for the template in aqueous solutions [30–32]. Strong interactions such as electrostatic, present between monomers and template at the polymerization stage in a polar solvent, have high chances to take place also in aqueous solution during the re-binding. Normally, when MIPs need to work in aqueous solutions, the modeling is also repeated minimizing molecular structures

Table 3
Binding energies, estimated using the LEAPFROG algorithm, of cholic acid with the monomers contained in the virtual library.

Monomer	Binding energy (kcal mol^{-1})
Allylamine protonated	−50.14
N-(3-aminopropyl) methacrylamide hydrochloride (APMA·HCl)	−48.43
Aminoethyl methacrylate·HCl	−47.87
Ethyleneglycol methacrylate phosphate (EGMP)	−41.75
N,N′-Methylenebis(acrylamide)	−39.73
Ethyleneglycol methacrylate phosphate deprotonated	−37.99
Acrylamido-2-methyl-1-propanesulfonic acid	−33.67
Aminoethyl methacrylate	−32.20
Itaconic acid	−31.42
Itaconic acid deprotonated	−30.01
1,3,5-Trihydroxylstyrene	−29.97
N,N-Diethylamino ethylmethacrylate protonated (DEAEM·HCl)	−29.82
Acrylamide	−27.39
N,N-Diethylamino ethylmethacrylate (DEAEM)	−27.14
Ethyleneglycol dimethacrylate (EGDMA)	−25.52
Methacrylic acid deprotonated	−25.16
N-(3-aminopropyl) methacrylamide (APMA)	−24.39
Allylamide	−23.69

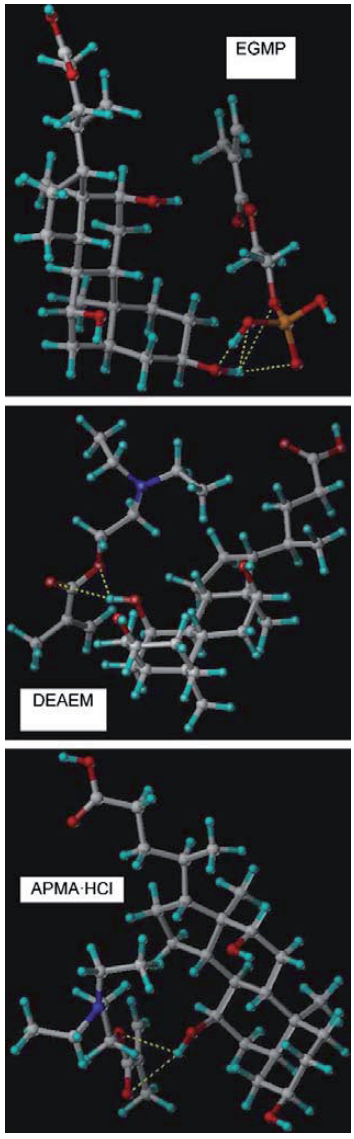

Fig. 1. Computational modeling of the interaction of cholic acid with EGMP, DEAEM, and APMA·HCl.

using the dielectric constant of water. Nevertheless, since the molecules of solvents are not physically included during the screening process, the energy values for monomers–template complexes, when structures are minimized either in water or in polar organic solvents, are usually very similar.

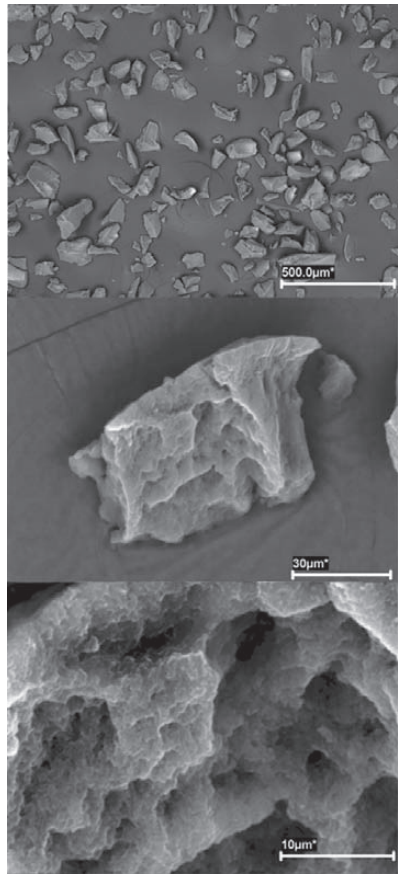

Fig. 2. SEM micrographs of APMA·HCl-based networks.

The results in Table 3 show that allylamine, in its charged (protonated) form, demonstrated the strongest energy of interaction with sodium cholate. However this monomer was not considered for the MIP preparation, since, as shown previously [33], allylamine is prevalently neutral in a wide range of pH values and practically never protonated. APMA·HCl and EGMP were also among the monomers with the highest affinity for cholic acid (Table 3). Aminoethyl methacrylate both in HCl salt and free base showed strong interactions with the template and was initially considered for the preparation of MIPs. However it was subsequently discarded because of its limited solubility in DMSO and other polar solvents. DEAEM, which is the most basic monomer among those tested [33], showed a binding energy lower than APMA and EGMP but slightly greater than the cross-linker agent EGDMA. Most of the monomers that appear in Table 3 between EGMP and DEAEM are either very weak bases, which are known to be neutral, or possess anionic acid groups, which interacted with cholic acid through the same positions as EGMP and were not therefore considered for further experiments. According to the modeling, EGMP and DEAEM can

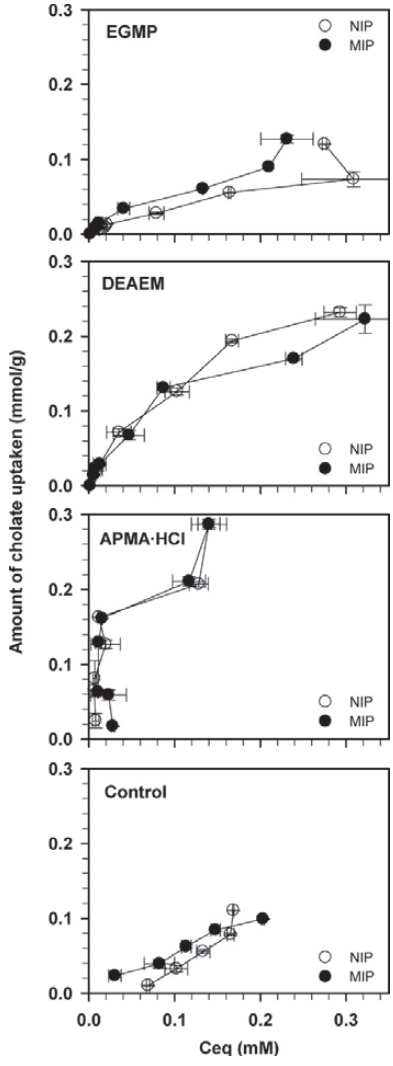

Fig. 3. Binding isotherms of sodium cholate in water by imprinted (MIP) and non-imprinted (NIP) networks prepared with EGMP, DEAEM, APMA·HCl or without functional monomers (control). The functional monomer and cross-linker proportions upon synthesis were 9% mol and 91% mol, respectively. For preparation of imprinted networks, 2.5% mol of template was added to the polymerization mixture.

interact with cholic acid through hydrogen bonds, while APMA·HCl can also electrostatically interact with the carboxylic groups (Fig. 1). Since hydrogen bonds cannot be established in aqueous solutions, among the three monomers APMA·HCl was from the beginning the most promising for production of polymeric networks with high affinity for cholic acid. Nevertheless also EGMP and DEAEM were selected as functional monomers and used for the production of MIPs specific for the target molecule.

Table 4
Fitting of the sodium cholate isotherms to the Freundlich model ($\alpha < 0.01$). Parameter a is related with the binding affinity and parameter m is the heterogeneity index. The standard errors are shown in parenthesis.

Polymer network	m	Log a	r^2	$F_{1,5\ d.f.}$
EGMP-NIP	0.811 (0.065)	4.824 (0.276)	0.969	153.50
EGMP-MIP	0.717 (0.042)	4.638 (0.186)	0.983	291.67
DEAEM-NIP	0.735 (0.038)	5.031 (0.169)	0.987	374.37
DEAEM-MIP	0.641 (0.042)	4.606 (0.189)	0.978	225.70
APMA·HCl-NIP*	0.306 (0.093)	3.577 (0.424)	0.781	10.70
APMA·HCl-MIP*	0.367 (0.104)	3.833 (0.555)	0.688	9.43
Control-NIP	1.617 (0.138)	7.990 (0.530)	0.986	136.97
Control-MIP	1.396 (0.084)	7.296 (0.329)	0.993	275.82

* The first two points of these isotherms were discarded for the fitting; $\alpha < 0.05$.

Both imprinted (MIP) and non-imprinted (NIP) networks were prepared in order to test also the effect of the molecular imprinting on the affinity of the networks for sodium cholate. Cholic acid was used as template molecule since the sodium salt is not soluble in the monomers solution. The functional monomer:template molar ratio was set at 4:1, which is a common molar ratio in non-covalent imprinting for ensuring the saturation of the binding points of template [34,35]. Non-imprinted networks were prepared in the absence of template. After polymerization, the polymers were mechanically crashed and wet-sieved in methanol, and the portion of particles retained between 38 and 125 μm meshes was used for the following experiments. The particles were subjected to Soxhlet extraction with methanol to ensure the complete removal of both fines and unreacted monomers and template molecules. SEM micrographs of APMA·HCl-based networks are shown in Fig. 2. The high DMSO proportion used during synthesis led to porous networks. Similar morphologies were observed for the other polymer networks.

3.2. Sodium cholate binding isotherms

Binding isotherms clearly showed the incidence of the functional monomer on the affinity of the polymers for sodium cholate (Fig. 3). Despite the high binding energies identified for EGMP by the computer modeling, the networks prepared with this monomer showed a binding isotherm similar to that of networks prepared without functional monomer. This finding was not, however, surprising since it can be easily explained by the inability of the monomer to form hydrogen bonds in aqueous medium and also by the electrostatic repulsion between the anionic groups of the functional monomer and cholate molecules. Such electrostatic repulsion was not highlighted by the modeling because cholic acid was screened against the monomers in its neutral form. Oppositely, DEAEM and APMA·HCl significantly enhanced the binding capability of the polymer networks. The isotherm obtained for APMA·HCl-based networks showed a high binding affinity with remarkably low concentrations at equilibrium, which means that most sodium cholate was absorbed by the network. This isotherm, which resembles that described for colestipol, suggests that the APMA·HCl-based networks might efficiently retain bile salts in the gastrointestinal tract [7]. As predicted by the modeling, the protonated amine group of APMA enables ionic interactions with the carboxylic acid group of cholate, while hydrophobic interactions between the apolar face of cholate and the cross-linking points can help to stabilize the adsorption.

The binding isotherms were fitted to the Freundlich model (Statgraphics Plus 5.1, Statistical Graphics Corp.) in order to gain insight into the heterogeneity of the binding sites (which is a common phenomenon in imprinted networks) from an energy point of view

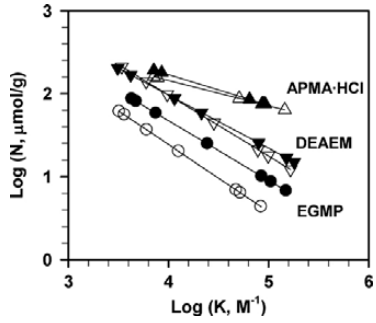

Fig. 4. Affinity distributions based on the fitting to the Freundlich model of the sodium cholate isotherms, obtained for imprinted (full symbols) and non-imprinted (open symbols) networks prepared with different functional monomers.

[36]. Freundlich isotherm measures the heterogeneity of binding site as affinity distributions (AD) and heterogeneity index (m) [29]. The values in Table 4 show that control networks have m values above 1, which indicates that the networks are homogeneous; i.e., there are not specific binding points (Table 4). The other polymers have m values between 0 and 1, confirming the existence of binding sites of varying affinity and selectivity, probably due to differences in chemical groups distribution and in depth and shape of the binding pockets. APMA·HCl-based networks show the lowest m values. This means that in these polymers there are both high and low affinity domains; the first ones may correspond to the sites in which

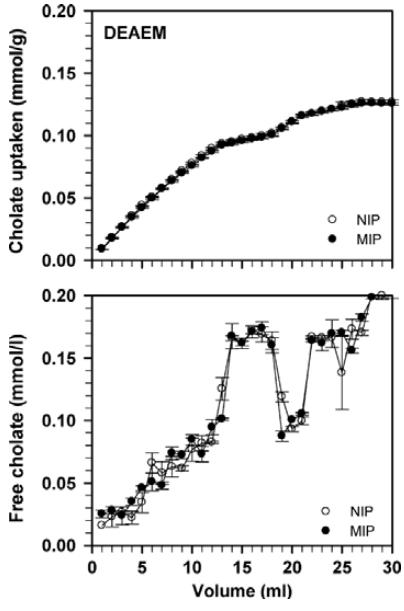

Fig. 5. Sodium cholate retained by polymer particles (top graph) and remaining free in the medium (bottom graph) after flowing the solution through the polymer prepared with DEAEM.

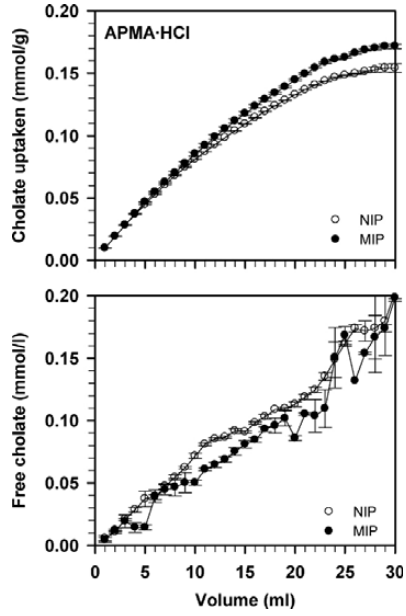

Fig. 6. Sodium cholate retained by polymer particles (top graph) and remaining free in the medium (bottom graph) after flowing the solution through the polymer prepared with APMA·HCl.

APMA·HCl is located. No incidence of the cross-linking degree on the binding isotherms was observed in the range evaluated (data not shown). EGMP and DEAEM MIPs showed m values lower than the corresponding non-imprinted networks. This suggests that the presence of template during the polymerization contributes to the heterogeneity of the material, increasing the affinity of the binding sites by causing an adequate spatial arrangement of the monomers. The networks with APMA·HCl showed such a high affinity for the template that the imprinting did not seem to improve the binding sites. Such a high affinity is also responsible for the relatively worse fitting to the Freundlich model compared to the other networks.

Affinity distributions of the binding sites of each polymer are shown in Fig. 4. The exponential decay (linear log–log plot) is characteristic of the isotherm region far from saturation [29]. The subsaturation region, in which the high affinity binding sites are preferentially filled, is the most interesting for a wide range of applications of non-covalently imprinted networks. This is because the difference between imprinted and non-imprinted networks is particularly evident at low loadings. In addition it is very difficult to reach saturation in most non-covalently imprinted polymers because of the heterogeneity of the material. As expected from the m values, the affinity distributions shown in Fig. 4 indicate that the networks have association constants ranging from 3100 to 160,000 L mol^{-1}, with predominance, in all polymers, of sites with low affinity. When compared with the networks prepared with the other functional monomers, EGMP polymers showed the least amount of binding points with also the lowest affinity. The imprinting notably enhanced both the number of binding sites and their affinity. On the other hand, the APMA·HCl networks possessed many more binding sites of high association constant, but the con-

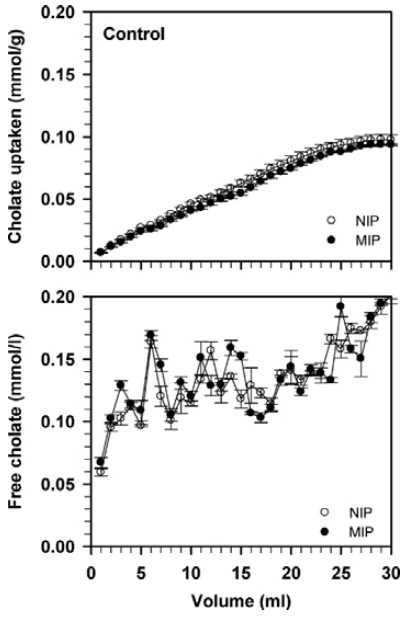

Fig. 7. Sodium cholate retained by polymer particles (top graph) and remaining free in the medium (bottom graph) after flowing the solution through the polymer prepared without functional monomer.

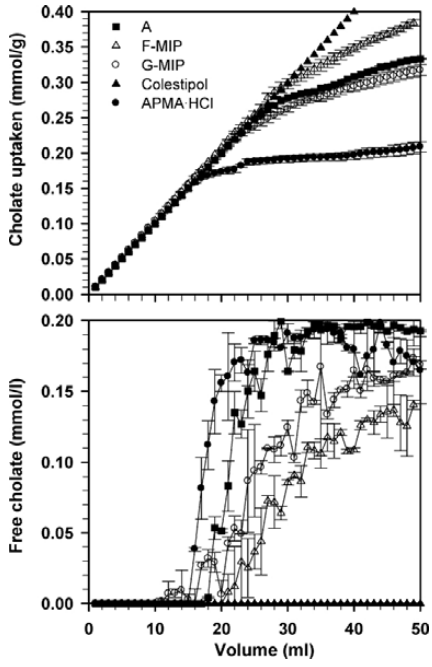

Fig. 8. Sodium cholate retained by polymer particles (top graph) and remaining free in the medium (bottom graph) after flowing the solution through the polymers prepared with APMA·HCl and different degrees of cross-linking and through commercially available colestipol granules. Profiles of MIP and NIP were superimposable for F and G networks.

tribution of the imprinting was not evident. These results confirm that APMA·HCl itself was able to create high affinity binding sites and that the arrangement during synthesis did not lead to a relevant improvement in the association constant. Networks prepared with DEAEM showed an intermediate behavior and the imprinting contributed to increase the number of high affinity binding sites. On the bases of these results EGMP polymers were abandoned and further testing was continued using only APMA·HCl and DEAEM networks.

3.3. Removal of sodium cholate from aqueous medium

The capability of the polymers to act as traps of sodium cholate in phosphate buffer pH 7.4 was tested in a dynamic mode, i.e., under a relatively rapid flow of cholate solution through the polymer bed. This was done in the attempt to simulate the conditions in the gut. Under these experimental conditions, only the networks with a high affinity and capable of rapidly capturing the target molecules would be able to effectively retain sodium cholate. The amounts of sodium cholate retained and non-retained by the networks made with and without (controls) functional monomers are depicted in Figs. 5–7. Both DEAEM and APMA·HCl polymers showed higher binding capacity than the control polymers. Between the two monomers, APMA·HCl provided the networks with the highest binding capacity, significantly diminishing the concentration of sodium cholate in the aqueous medium.

3.4. Effect of the degree of cross-linking

In the attempt to optimize the performance of the APMA·HCl networks, we evaluated the feasibility of decreasing the degree of cross-linking of the polymer network, by replacing part of EGDMA with a structurally related monofunctional monomer such as HEMA. Cholate molecule is relatively large, about 17 Å length and 5.3 Å width estimated using CS Chem3D Std® (CambridgeSoft Corp., MA). The mesh size of the network prepared with 91% mol EGDMA (8.7 Å distance between two adjacent cross-linking points) [37] is too low to enable sodium cholate to reach all the binding points even after swelling in water. Therefore, a set of polymers were prepared with decreasing content of EGDMA and fix proportion of functional monomer APMA·HCl (Table 2). The capability of the resulting MIPs and NIPs to trap sodium cholate in the dynamic mode was evaluated. As can be seen in Fig. 8, the loading significantly improved (twofold) when the EGDMA was reduced up to 31.7 mol% (F networks in Table 2); below this proportion the amount loaded leveled off or even decreased. The initial improvement can be clearly attributed to the easiness of the cholate molecules to diffuse through the polymer network as the mesh size increases. The APMA·HCl particles, in the range of cross-linking evaluated, had similar degrees of swelling in water (250–300%), but are significantly different in mesh size. Upon synthesis, the distance between adjacent cross-linking points was estimated from the number of molecules of cross-linker EGDMA per unit of volume (cm^3) of network [37]:

$$R_X = \frac{10}{\sqrt[3]{[\mathrm{EGDMA}]\,N_A}} \quad (4)$$

with N_A being the Avogadro's number. For example, the distance between adjacent cross-linking points is expected to be 12 and 14.3 Å for F and G networks, respectively. These values are 37% and 64% larger than the distance of the APMA·HCl networks prepared with the highest degree of cross-linking.

The non-imprinted polymers prepared with APMA·HCl behaved as well as the imprinted ones due to the ability of the functional monomer itself to bind strongly sodium cholate creating high affinity binding sites (F MIP and NIP profiles were superimposable, Fig. 8). This is quite advantageous from the point of view of potential pharmaceutical applications of the materials as traps of bile acids *in vivo*. In fact MIPs usually require prolonged washing steps to achieve total removal of template and in most cases the risk of template leaching, once in contact with physiological fluids, is not completely eliminated. This would be a major issue and could compromise MIPs approval for clinical use. It would be much easier to get approval for a sorbent like APMA·HCl NIP, which has got affinity and binding capacity for sodium cholate high enough to be used in clinical applications and at the same time would not be affected by issues as template leaching.

The results of this work revealed that computational modeling is adequate for a fast identification of the most suitable monomers to create efficient traps for a certain substance. Once the functional monomer is chosen, a conventional polymer synthesis enables the synthesis of high affinity networks avoiding waste of time and resources. This rational approach can therefore be of general application for creating traps for a wide range of substances with foreseeable high performances.

4. Conclusions

Computational modeling is a useful tool for the screening monomers with affinity for a given target molecule, enabling a rational design of functional networks. Nevertheless, since the modeling is performed using some approximations such as a 'virtual' inclusion of solvent through the use of its dielectric constant during minimization, differences can occur between modeling and experimental results especially when polymerization and rebinding steps are done in different liquids. In this specific case the use of functional monomers containing amine groups notably enhanced the capability of the acrylic networks to uptake sodium cholate. Combination of the screened functional monomers with molecular imprinting technology remarkably improved the performance of networks made of monomers with affinity for the target, through an adequate arrangement of the monomers into pockets suitable to host the target molecules. However, molecular imprinting technology is of less relevance when the functional monomer itself, as predicted by the computer modeling, has a strong affinity for the template/analyte. In addition, in this work we showed that by tuning the degree of cross-linking of networks with high affinity functional monomers it is possible to enable optimization of the loading capability, making the materials useful as traps of undesirable biological molecules.

Acknowledgments

This work was financed by MICINN (SAF2008-01679), FEDER and Xunta de Galicia (PGIDT07CSA002203PR). F. Yañez is grateful to MICINN for a FPI grant and a travel fellowship to finance the stay in Prof. S.A. Piletsky's lab at Cranfield University.

References

[1] D. Pella, R.B. Singh, B. Tomlinson, C.W. Kong, in: N.S. Dhalla, A. Chockalingam, H.I. Berkowitz, P.K. Singal (Eds.), Frontiers in Cardiovascular Health, vol. 9, Kluwer Academic Publishers, Norwell, MA, 2003, pp. 473–487.
[2] T.D. Filippatos, D.P. Mikhailidis, Curr. Pharm. Des. 15 (2009) 490–516.
[3] R. Hou, A.C. Goldberg, Endocr. Metab. Clin. 38 (2009) 79–97.
[4] D.W. Russell, J. Lipid Res. 50 (2009) S120–S125.
[5] A. Corsini, E. Windler, M. Farnier, Eur. J. Cardiovasc. Prev. Rehabil. 16 (2009) 1–9.
[6] X.X. Zhu, A. Benrebouh, Y.H. Zhang, S. Gouin, Polym. Preprints 41 (2000) 1030–1031.
[7] W.H. Mandeville, W. Braunlin, P. Dhal, A. Guo, C. Huval, K. Miller, J. Petersen, S. Polomoscanik, D. Rosenbaum, R. Sacchiero, J. Ward, S.R. Holmes-Farley, Mater. Res. Soc. Symp. Proc. 550 (1999) 3–15.
[8] P.K. Dhal, C.C. Huval, S.R. Holmes-Farley, Ind. Eng. Chem. Res. 44 (2005) 8593–8604.
[9] L.-S. Wu, T.J. McCormick, R.-K. Chang, J. Pang, T. McCummings, M. Ramos, M.A. Hussain, Pharm. Res. 16 (1999) 1136–1139.
[10] M.A. Schreiber, K.L. Moyer, B.J. Mueller, M.A. Ramos, J.S. Green, et al., J. Pharm. Biomed. Anal. 25 (2001) 343–351.
[11] M.A. Hussain, R.K. Chang, E. Sandefer, R.C. Page, G.A. Digenis, Pharm. Res. 20 (2003) 460–464.
[12] W.E. Baille, W.Q. Huang, M. Nichifor, X.X. Zhu, J. Macro. Sci. A 37 (2000) 677–690.
[13] P. Zarras, J. Polym. Sci. A 42 (2004) 701–713.
[14] M. Nichifor, X.X. Zhu, W. Baille, D. Cristea, A. Carpov, J. Pharm. Sci. 90 (2001) 681–689.
[15] N.S. Cameron, F.G. Morin, A. Eisenberg, R. Brown, Biomacromolecules 5 (2004) 24–31.
[16] C.C. Huval, X. Chen, S.R. Colmes-Farley, H. Mandeville, C. Steven, et al., Mater. Res. Soc. Symp. Proc. 787 (2004) 85–90.
[17] Y. Wang, J. Zhang, X.X. Zhu, A. Yu, Polymer 48 (2007) 5565–5571.
[18] T. Kobayashi, T. Kusunoki, Q. Zhang, K. Takeda, J. Chem. Eng. Jpn. 40 (2007) 516–522.
[19] C. Alvarez-Lorenzo, A. Concheiro, J. Chromatogr. B 804 (2004) 231–245.
[20] C. Alvarez-Lorenzo, A. Concheiro, in: M.R. El-Gewely (Ed.), Biotechnology Annual Review, vol. 12, Elsevier, Amsterdam, 2006, pp. 225–268.
[21] F. Puoci, F. Iemma, G. Cirillo, M. Curcio, O.I. Parisi, U.G. Spizzirri, N. Picci, Eur. Polym. J. 45 (2009) 1634–1640.
[22] I.A. Nicholls, S.A. Piletsky, B. Chen, I. Chianella, A.P.F. Turner, in: M. Yan, O. Ramstrom (Eds.), Molecularly Imprinted Materials: Science and Technology, Part IV, Marcel Dekker, New York, 2005, pp. 363–394.
[23] A. Guerreiro, A. Soares, E. Piletska, B. Mattiasson, S. Piletsky, Anal. Chim. Acta 612 (2008) 99–104.
[24] S.A. Piletsky. R.M. Day, B. Chen, S. Subrahmanyam, O. Piletska, A.P.F. Turner, Patent PCT/GB01/00324, 2000.
[25] S.A. Piletsky, K. Karim, E.V. Piletska, C.J. Day, K.W. Freebairn, C.H. Legge, A.P.F. Turner, Analyst 126 (2001) 1826–1830.
[26] S. Subrahmanyam, S.A. Piletsky, E.V. Piletska, B. Chen, K. Karim, A.P.F. Turner, Biosens. Bioelectron. 16 (2001) 631–637.
[27] A. Fini, P. Zuman, Collect. Czech Chem. Commun. 58 (1993) 53–61.
[28] A.M. Rampey, R.J. Umpleby, G.T. Rushton, J.C. Iseman, R.N. Shah, K.D. Shimidzu, Anal. Chem. 76 (2004) 1123–1133.
[29] R.J. Umpleby, S.C. Baxter, A.M. Rampey, G.T. Rushton, Y. Chen, K.D. Shimizu, J. Chromatogr. B 804 (2004) 141–149.
[30] I. Chianella, M. Lotierzo, S.A. Piletsky, I.E. Tothill, B. Chen, K. Karim, A.P.F. Turner, Anal. Chem. 74 (2002) 1288–1293.
[31] I. Chianella, S.A. Piletsky, I.E. Tothill, B. Chen, A.P.F. Turner, Biosens. Bioelectron. 18 (2003) 119–127.
[32] M. Romero-Guerra, I. Chianella, E.V. Piletska, K. Karim, A.P.F. Turner, S.A. Piletsky, Analyst 134 (2009) 1565–1570.
[33] E.V. Piletska, A.R. Guerreiro, M. Romero-Guerra, I. Chianella, A.P.F. Turner, S.A. Piletsky, Anal. Chem. 607 (2008) 54–60.
[34] H. Hiratani, Y. Mizutani, C. Alvarez-Lorenzo, Macromol. Biosci. 5 (2005) 728–733.
[35] C. Alvarez-Lorenzo, F. Yañez, R. Barreiro-Iglesias, A. Concheiro, J. Control. Release 113 (2006) 236–244.
[36] J.A. Garcia-Calzon, M.E. Diaz-Garcia, Sensors Actuat. B 123 (2007) 1180–1194.
[37] C. Alvarez-Lorenzo, O. Guney, T. Oya, Y. Sakai, M. Kobayashi, T. Enoki, Y. Takeoka, T. Ishibashi, K. Kuroda, K. Tanaka, G. Wang, A.Yu. Grosberg, S. Masamune, T. Tanaka, Macromolecules 33 (2000) 8693–8697.

3.7. Supercritical fluid-assited preparation of imprinted contact lenses for drug delivery

Enviado

SUPERCRITICAL FLUID-ASSISTED PREPARATION OF IMPRINTED CONTACT LENSES FOR DRUG DELIVERY

Fernando Yañez[1], Lahja Martikainen[3], Mara E. M. Braga[3], Carmen Alvarez-Lorenzo[1*], Angel Concheiro[1], Catarina M. M. Duarte[2], Maria H. Gil[3], Hermínio C. de Sousa[31]

[1]Departamento de Farmacia y Tecnología Farmacéutica, Facultad de Farmacia, Universidad de Santiago de Compostela, 15782-Santiago de Compostela, Spain.

[2]Nutraceuticals and Delivery Laboratory, Instituto de Biologia Experimental e Tecnológica (IBET), Apartado 12, 2781-901 Oeiras, Portugal, and Instituto de Tecnologia Química e Biológica (ITQB), Universidade Nova de Lisboa, Avenida da Republica, 2780-157 Oeiras, Portugal.

[3]CIEPQPF, Chemical Engineering Department, FCTUC, University of Coimbra, Rua Sílvio Lima, Pólo II – Pinhal de Marrocos, 3030-790 Coimbra, Portugal.

Abstract

The aim of this work was to develop an innovative supercritical fluid (SCF)-assisted molecular imprinting method for endowing commercial soft contact lenses (SCLs) with the ability to load specific drugs and to control their release. This approach seeks to overcome the limitation of the common loading of preformed SCLs by immersion in concentrated drug solutions (only valid for highly water-soluble drugs) and of the molecular imprinting methods that require to choose the drug before polymerization and thus to create drug-tailored networks. In particular, we focused on the improvement of the flurbiprofen load/release capacity of daily-wear Hilafilcon B commercial SCLs by the use of sequential SCF flurbiprofen impregnation and extraction steps. Supercritical carbon dioxide ($scCO_2$) impregnation assays were performed at 12.0 MPa and at 40 ºC, while $scCO_2$ extractions were performed at 20.0 MPa and at 40 ºC. Conventional flurbiprofen sorption and drug removal experiments in aqueous solutions were carried out for comparison purposes. SCF-processed SCLs presented recognition ability and a higher affinity for flurbiprofen in aqueous solution than for the structurally-related ibuprofen and dexamethasone, which suggests the creation of molecularly imprinted cavities driven by both physical (swelling/plasticization) and chemical (carbonyl groups in the network with

[1] Corresponding authors: Tel + 351 239 798 749. E-mail: hsousa@eq.uc.pt, carmen.alvarez.lorenzo@usc.es

C-F group in the drug) interactions. Processing with $scCO_2$ did not alter the critical functional properties of SCLs (glass transition temperature, transmittance, oxygen permeability, contact angle,…), enabled the control of drug loaded/released amounts (by the application of several consecutive processing cycles) and permitted the preparation of hydrophobic drug-based therapeutic SCLs in much shorter process times than those using conventional aqueous-based molecular imprinting methods.

Keywords: Therapeutic contact lenses, molecular imprinting, supercritical fluid technology, flurbiprofen, controlled drug release.

1. Introduction

Conventional ophthalmic drug delivery systems (DDS) such as topical eye drops, although can be easily administered, usually lead to poor ocular drug bioavailability due to their short residence time on cornea surface and the efficient defense mechanisms of the eye [1]. Drug formulation in nanoparticle/nanocapsule suspensions, liposomes, collagen shields or ocular inserts may enable the achievement of greater drug concentrations in the ocular tissues [2,3]. The potential of soft contact lenses (SCLs) as ophthalmic DDS was firstly tested by Sedlacek [4] and later by Waltman and Kaufman [5] and by Jain [6]. SCLs loaded by immersion in a drug solution (or suspension/emulsion) provide more sustained release drug levels in tears and also in the post-lens tear film fluid, compared to topical drop instillation, thus enhancing drug cornea permeation and minimizing the occurrence of untoward systemic absorption [7-10]. Moreover, and if compared to other polymeric matrices, SCLs can be worn more frequently and during more time because of their excellent biocompatibility, comfort and patient compliance/acceptance. Medicated SCLs may combine the role as DDS with the correction of refractive deficiencies, performing as a combination product according to FDA regulations [11]. Nevertheless, few drugs can be effectively loaded in commercial SCLs, which also lack of control of the drug delivery once placed onto the cornea [12-15]. To overcome these problems and also to attain more sustained drug release profiles, several approaches have been proposed [9,15-17], among which the use of molecularly imprinted SCLs has been suggested as an improved biomimetic method for the preparation of therapeutic SCLs [8,15,18-20].

The traditional molecular imprinting method consists in adding a template molecule (e.g., a drug) to a monomeric solution in order to induce the spatial arrangement of the monomers according to their interaction capabilities with the template [21-25]. The subsequent polymerization and cross-linking fix such spatial assembly and, after the removal of the template drug, the resultant polymeric network exhibit "cavities" with size and shape specific for that template. Once in contact again with the template, the polymer networks can easily reuptake it into the previously formed specific cavities. In addition, the release of the template is performed in a more sustained manner owing to the strength of the polymer-drug interactions [15,18,20,22,24]. Two important concerns on the preparation of molecularly imprinted polymers (MIPs) for DDS are that the template (i.e., the drug of interest) has to be stable under the polymerization conditions, and that no toxic solvents should remain on the device. In the particular case of SCLs, the cross-linking density has to be compatible with the required flexibility of the material and thus the imprinted cavities should possess high affinity for the drug in order to compensate their lower physical stability [24,26,27].

Despite traditional molecular imprinting methods involve the formation of the polymer network in the presence of the template, if we consider just the involved phenomena (polymer/template interaction) as well as the obtained final result ("cavities" of adequate shape/volume, chemical affinity and recognition ability), the term "imprinting" may also be used anytime a specific "imprint" is produced in a certain structure by an specific template molecule and at the molecular (nano)scale [25,28,29]. Commercial SCLs comprise in their structure several co-monomers and cross-linkers, each one of them having specific chemical and physical functionalities but usually of the acrylate- and/or of the silicone-type. Due to the low cross-linking density of SCLs, there is still enough chain mobility and plenty of available free volume between polymeric chains (otherwise, SCLs would not swell upon water sorption). Therefore, these loose chains together with any other side-chain branches can still be "reorganized" and even "fixed" when a template molecule is incorporated in the network and can establish specific interactions with certain regions of the polymer. These physical rearrangements, organization and imprinting phenomena, also known as post-imprinting, have been demonstrated in other low density cross-linked hydrogels [22,29-32].

It is well known that some drugs may be deposited into (or extracted from) polymeric matrices by i) dissolving them in compressed high volatile fluids (like carbon dioxide) at temperatures and pressures near or above their critical values, and ii) contacting the resulting mixtures with those polymeric matrices. Under these conditions, the compressed fluid mixture can act also as a plasticizer agent, causing the swelling of the polymeric network and helping drug diffusion into (or out of) them. Supercritical fluids (SCFs) have already demonstrated their applicability in several polymer processing areas, namely as solvents for additive extractions and for polymerization reactions, as porogenic, foaming, viscosity reducers or plasticizer agents, as solvents (or anti-solvents) to micronize drugs and polymeric materials and as solvents (or anti-solvents) to incorporate additives into solid polymeric (or composite) systems [33-40]. Supercritical carbon dioxide ($scCO_2$) is the most commonly used SCF because it is an abundant and cheap, non-flammable, relatively inert and GRAS ("generally recognized as safe") solvent, soluble in aqueous media and it can plasticize and decrease the glass transition temperature of most polymeric materials. Furthermore, it has a low critical temperature (31.05 ºC) that allows working at relatively low temperatures, suitable for thermal-labile substances [33-35]. Compared to common liquid plasticizers, $scCO_2$ penetrates deeper in dense polymeric networks and can be easily removed after processing [36,41].

Supercritical solvent impregnation (SSI) and supercritical fluid extraction (SFE) using $scCO_2$ already proved their advantages for the development of drug impregnated polymeric materials which can be used as DDSs for many biomedical applications including therapeutic SCLs [42,43]. SSI allows the drug impregnation/dispersion of most polymeric articles (films, particles, fibers, finished devices, etc.) and, when properly employed, it does not alter and/or damage their physical, chemical, and mechanical properties. Drug loading and even depth of penetration can be easily controlled by the regulation of several operational conditions, and in the end drugs can be homogeneously impregnated/dispersed in relatively short times and without leaving any harmful solvent residues [44-48]. SSI also permits to have previously prepared polymeric articles (like commercial SCLs) and later, impregnate them with the desired drugs, according to the specific needs of an envisaged therapeutic application, and without interfering with the polymeric ophthalmic article synthesis/manufacture method. This particular feature can

also lead to the development of other very interesting and useful medical and commercial applications [42,43]. On the other hand, and taking advantage of most of the above referred SCFs properties, SFE permits the efficient extraction of additives from several solid matrices including polymeric ones. In fact, polymeric materials are one of the few materials in which the most important advantages of SCFs can be fully exploited. This is mainly due to the relatively high densities and diffusivities and to the low surface tensions of SCFs which, when combined with polymer swelling and plasticization effects, considerably enhances additives extraction yields and rates. Moreover, they can be also employed to extract undesired residual solvents, oligomers or monomers, or any other additives present in polymeric materials [34-39,45,49].

In the present work, we explore the suitability of applying SCF-based technologies, namely SSI and SFE, in an innovative method to induce specific nano-range structural changes in pre-formed commercially available SCLs with the aim of creating specific and high-affinity "cavities" for a certain template drug. By doing this, we expect to enhance drug loading and to achieve more sustained/extended delivery. SCFs have been already tried in the preparation of MIPs but just as the solvent for the emulsion polymerization of the comonomer mixture [50]. To the best of our knowledge, this is the first time the technique is used to induce a post-imprinting modification. Commercial SCLs are swollen cross-linked hydrogels and thus, when in contact with a $scCO_2$ phase, they should not be considered as dry polymeric materials but instead as a kind of "gas-expanded liquids", in which the $scCO_2$ mobile phase may dissolve. It is expected that $scCO_2$ plasticizes and swells wet SCLs and facilitates the template impregnation/extraction processes as well as the potential rearrangement of the polymeric chains. In addition, the dissolution of $scCO_2$ inside the water-swollen SCLs may decrease the inner pH (due to the formation of carbonic acid) and the total polarity of water inside SCLs [47,48]. Depending on the involved polymeric materials, this may also affect the polymer ionization state and the polymer chain conformation, as well as the solubility of the drugs to be impregnated/extracted, especially if they are hydrophobic or have low polarities, or if their solubilities strongly depend on pH. After, under slow depressurization, CO_2 is vented leaving the drug molecularly dispersed inside the SCLs polymeric matrix. pH is also expected to return to its initial value. Drug removal, applying SCF extraction or

immersion in aqueous media, and subsequent re-uptake experiments, may evidence the previous formation of cavities with size and shape complementary to those of the template drug molecules. If the conformation of the created cavities is stable enough, the ability of the lens to load the template drug should be greater than before processing and such improvement should be maintained or even further increased after successive reloading and release sequential steps. On the other hand, and also due to the created specific cavities, drug release should be more sustained. In such a way, we may consider that the pre-formed polymeric networks were "drug-imprinted" at the molecular scale by the use of this innovative SCF-assisted molecular imprinting method. The experiments were carried out with daily-wear Hilafilcon B commercial contact lenses (Bausch & Lomb®) using the poorly-water soluble non-steroidal anti-inflammatory (NSAID) flurbiprofen as template (Figure 1). A driven force for the post-imprinting may be the interaction between the carbonyl groups of these SCLs and the C-F of the drug, since this type of interactions are well-known to play a key role in many biorecognition processes *in vivo* [51,52]. In addition to flurbiprofen loading and release experiments, the competitive binding of structurally-similar drugs, ibuprofen and dexamethasone, was analyzed in order to verify if the employed SCF processes were able to render SCLs with improved and specific affinity for flurbiprofen.

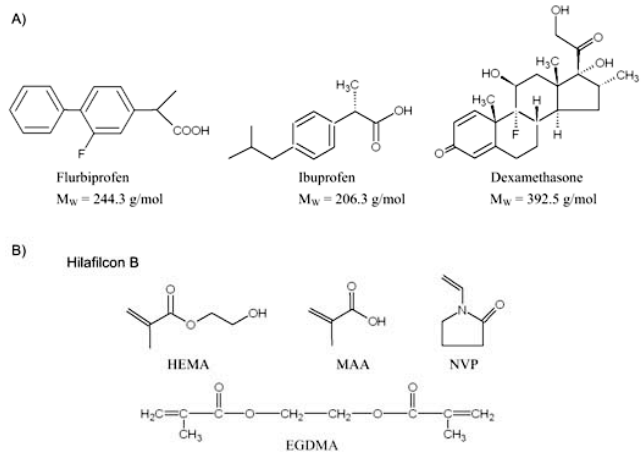

Figure 1. *Chemical structures of (A) employed drugs and (B) constituting monomers, co-monomers and cross-linkers for Hilafilcon B contact lenses. HEMA: 2-hydroxyethyl methacrylate; MAA: methacrylic acid; EGDMA: ethyleneglycol dimethacrylate; NVP: N-vinylpyrrolidone.*

2. Materials and Methods

Hilafilcon B SCLs (Pure Vision™, 59% (w/w) water content, 8.6 mm base curve, -8.00, 14 mm Ø) were kindly supplied by Bausch & Lomb® (Lisbon, Portugal) and by Mart-Optic (Coimbra, Portugal). Flurbiprofen (≥99%, TLC), ibuprofen (≥98%, HPLC) and dexamethasone (≥98%, HPLC) were from Sigma-Aldrich (Barcelona, Spain). Carbon dioxide (99.998%) was from Praxair (Spain) and ethanol (≥99.0%) from Panreac Química, (Barcelona, Spain). Purified water (MilliQ®, Millipore, resistivity > 18 MΩ.cm) was obtained by reverse osmosis. Before their use, Hilafilcon B SCLs were abundantly washed with Milli-Q water (under stirring, for 12 hours) in order to remove absorbed substances from the SCLs liquid storage solutions. Washed SCLs were then stored at room temperature and at a controlled ~83% relative humidity environment (saturated potassium chloride atmosphere).

2.1 Flurbiprofen loading/extraction procedures

Commercial SCLs were loaded with flurbiprofen by applying two approaches: *i*) supercritical solvent impregnation (SSI) or *ii*) immersion in drug aqueous solutions. Drug removal was performed using supercritical fluid extraction (SFE) or leaching/extraction in water. Combined sequential loading/removal procedures (3 consecutive cycles) were employed: SSI followed by SFE, or water immersion followed by water leaching (conventional method). The loading/removal processing cycles are shown in the flowchart depicted in Figure 2.

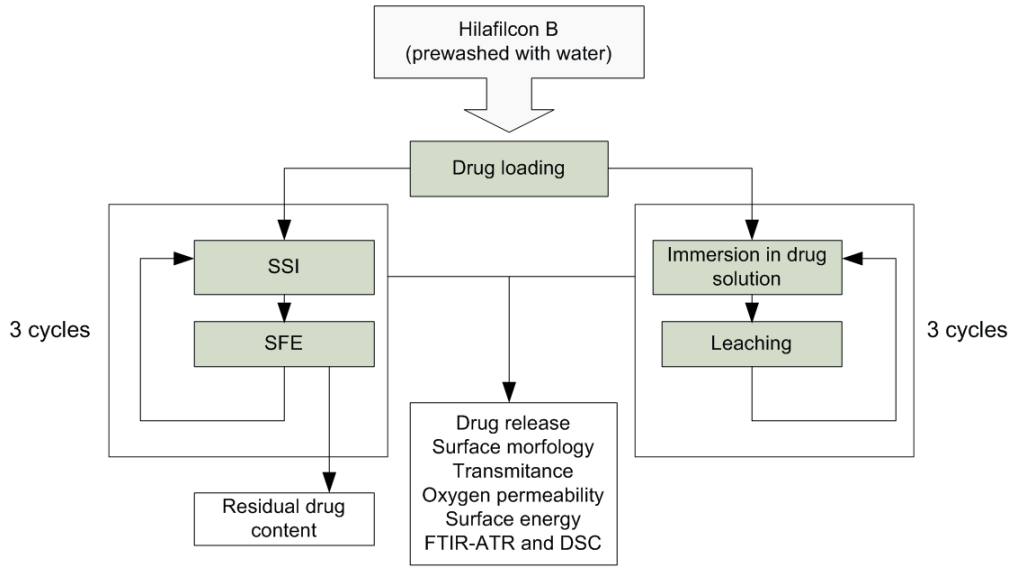

***Figure 2**. Schematic representation of employed SCLs drug loading/removal methods.*

2.1.1. Conventional drug-loading by immersion in drug aqueous solution

SCLs were placed in falcon tubes containing 40 ml of a flurbiprofen aqueous solution (8 mg/l) and kept, under stirring (100 rpm and 37 ºC), for 2.5 hours. Drug-loading kinetics experiments were also carried out under similar conditions monitoring the decrease in the concentration of flurbiprofen in the solution at various time points up to 13 hours. All experiments were performed in triplicate.

2.1.2. Drug leaching/extraction method

SCLs loaded by conventional immersion in a drug aqueous solution were transferred to 80 ml of water (at 37 ºC and 100 rpm) and the drug concentration was monitored spectrophotometrically at 247.5 nm (model V-650, Jasco, Japan) for 8 consecutive hours. Then the medium was replaced by fresh water at pre-determined time intervals (every 24 hours). Leaching was carried out until no detectable amounts of flurbiprofen were measured in water (after 4 days). The experiments were carried out in triplicate.

2.1.3. Supercritical Solvent Impregnation (SSI) drug loading method

SSI experiments were performed at 40 ºC and 12 MPa using a discontinuous supercritical impregnation apparatus (Figure 3A) previously described [42-48]. CO_2 was introduced and pressurized into a temperature-controlled high-pressure impregnation cell loaded with 3.5 mg of flurbiprofen. Six commercial Hilafilcon B SCLs were impregnated per experiment. Contact lenses were placed inside the high-pressure stainless steel cell (internal volume 10×10^{-6} m^3) and fitted in a stainless steel support in order to maintain two SCLs at three different height levels inside the cell. The flurbiprofen amount was ~5.5 times above the amount needed to saturate $scCO_2$ at the operational process conditions [53]. Magnetic stirring (700 rpm) enabled and helped the drug solubilization and the high-pressure mixture homogenization. After a 2.5-h impregnation period, the compressed fluid was removed by slow expansion in order to prevent drug-loaded SCLs from any damage. Average depressurization rates were 0.06 MPa/min. Drug-loaded SCLs were then recovered in a semi-dry state and stored until further processing/analysis.

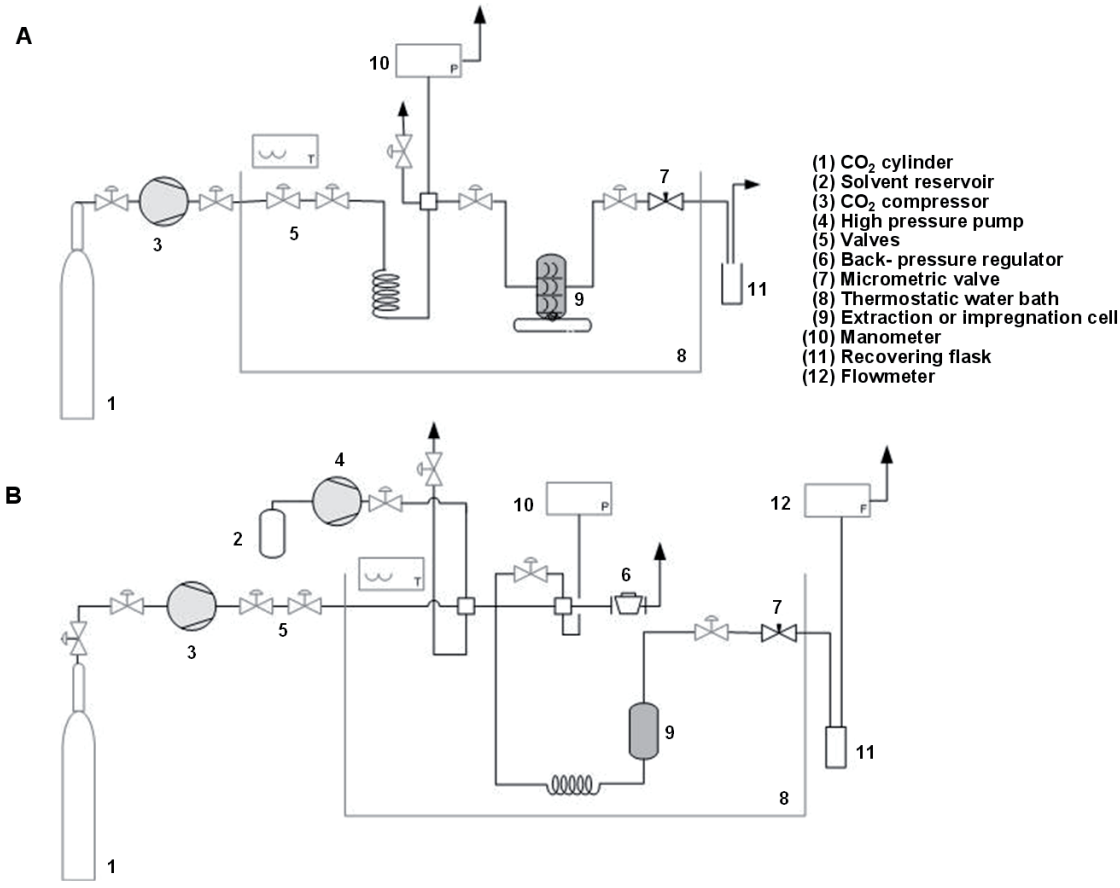

***Figure 3**. Schematic diagram of the employed SSI (**A**) and SFE (**B**) apparatuses.*

SSI flurbiprofen-loaded SCLs underwent two different drug removal procedures: (a) extraction with $scCO_2$ (by SFE) and then washing in water (to quantify the residual amount of flurbiprofen still remaining in lenses); and (b) direct immersion in water in order to record the drug release profiles. SCLs subjected to drug removal according to option (a) were re-impregnated with flurbiprofen using the same SSI procedure described above, and then subjected again to the SFE extraction and release in water tests (see Figure 2). In total, three successive SSI loading and SFE/water removal cycles were carried out. All experiments were carried out in triplicate.

2.1.4. Supercritical Fluid Extraction (SFE) drug removal method

Flurbiprofen extraction/removal experiments from drug-loaded SCLs (by SSI) were carried out using the SFE apparatus (Figure 3B) previously described [45]. Drug-loaded SCLs were fitted in a stainless steel support and placed inside a high-pressure stainless steel extraction cell (internal volume was 30×10^{-6} m^3), which was immersed into a temperature-controlled water bath at 40 ºC. $scCO_2$ was introduced and pressure was maintained for 14h at 12 MPa, in a static swelling- and extraction-period. Then, pressure was increased up to 20.0 MPa and a continuous $scCO_2$ extraction was carried for 5h, at a constant $scCO_2$ flow rate (~0.1 l/min). For the continuous extraction period, and considering the extraction duration, the $scCO_2$ flow rate and the flurbiprofen drug solubility in $scCO_2$ at the operational conditions, the total amount of $scCO_2$ that passed through the cell was calculated to be almost 200 times the CO_2 amount that would be necessary to solubilize the introduced flurbiprofen amount (at the employed operational conditions). The system was then slowly depressurized (~0.1 l/min) and the outlet CO_2 effluent was passed/bubbled through 10 ml of ethanol retained in a cold trap. Extracted SCLs were then recovered and, at the end of experiment, the equipment tubing lines were washed with 200 ml of ethanol. All flurbiprofen dissolved in ethanol was later concentrated in a Multivapor™ under vacuum control (Büchi, Flawil, Switzerland) and quantified spectrophotometrically at 247.5 nm (model V-650, Jasco, Japan). Experiments were carried out for three contact lenses per experiment.

Any remaining amounts of flurbiprofen (named as residual drug) still present in the SFE-extracted SCLs were later removed by immersion in 80 ml of water (at 37 ºC and 100 rpm), replacing the medium every 24 hours and monitoring drug concentration spectrophotometrically at 247.5 nm (model V-650, Jasco, Japan). The experiments were carried out in triplicate until no detectable amounts of flurbiprofen were measured in water (after 4 days).

2.2. Contact lenses storage

All processed SCLs were stored at room temperature and at a ~83% relative humidity environment (saturated potassium chloride atmosphere) in order to maintain the commercial SCLs hydration/water content.

2.3. Drug release in water

SCLs previously loaded with flurbiprofen, either by applying SSI or by immersion in aqueous drug solutions, were immersed in 80 ml of water, at 37 ºC, and kept under stirring at 100 rpm for 8 h. 2.5 ml aliquots were collected at pre-determined time periods and the released drug was quantified using an UV-spectrophotometer at 247.5 nm (model V-650, Jasco, Japan). The assays were carried out (in triplicate) without renovation of the medium.

2.4. Molecular imprinting proof-of-concept

SCLs processed by three SSI/SFE process cycles and unprocessed SCLs (used as control) were immersed in 20 ml of $3.3 \cdot 10^{-5}$M flurbiprofen, ibuprofen or dexamethasone aqueous solutions during 14 h. Drug concentration in the medium was spectrophotometrically monitored during the loading process and in the subsequent release experiments in water. All assays were done in duplicate.

2.5. SCLs general characterization

2.5.1. Surface morphology – Dried non-processed and processed SCLs were coated with gold (approximately 300 Á), in an argon atmosphere, and then observed using scanning electron microscopy, SEM (Jeol, model JSM-5310, Japan) at 20 kV, under various magnifications.

2.5.2. FTIR-ATR spectroscopy - Non-processed and $scCO_2$-processed SCLs (3 cycles SSI/SFE) were analysed in the 400-4000 cm^{-1} range using a GladiATR single reflection equipment (Pike Technologies, Madison USA) 32 scans and 2 cm^{-1} of resolution.

2.5.3. Differential scanning calorimetry (DSC) - Experiments were carried out, in duplicate, using a DSC Q100 (TA Instruments, New Castle DE, USA) with a refrigerated cooling accessory. Nitrogen was used as the purge gas and at a flow rate of 50 ml/min. The calorimeter was calibrated for baseline using no pans, for cell constant and

temperature using indium (melting point 156.61 ºC, enthalpy of fusion 28.71 J g^{-1}), and for heat capacity using sapphire standards. To determine the glass transition temperature, T_g, experiments were performed using non-hermetic aluminium pans, in which 5-10 mg dried disks pieces were accurately weighed, then covered with the lid and program-heated from 30 to 100 ºC, cooled to 0 ºC and finally heated again up to 300 ºC, always at 10 ºC min^{-1}.

2.5.4. Water content and swelling capacity **-** Non-processed and $scCO_2$-processed SCLs were dried in a forced air convection oven for 72 h at 40 ºC. Then, SCLs were immersed in water and their weights were measured every 24 h until constant weight was achieved (generally after 5 consecutive days). Experiments were carried out in triplicate.

2.5.5. Oxygen permeability - Non-processed and $scCO_2$-processed SCLs were swollen in a 0.9% NaCl solution and their oxygen permeabilities were measured in triplicate using a Createch permeometer (model 210T, Rehder Development Company, Castro Valley, USA) at room temperature and at 100 % of relative humidity.

2.5.6. Contact angle/surface free energy measurements **-** The contact angles of Milli-Q water, ethylene glycol and formamide on non-processed and on $scCO_2$-processed SCLs were evaluated at four regions/quadrants of each lens (previously cut into four pieces). Measurements were performed using the sessile drop (6-7 µl) method and using a contact angle determination apparatus (OCA20, Dataphysics Instruments GmbH, Germany). The surface energy of was estimated using the extended Fowkes (xF) method which is generally recommended to modified polymer surfaces [54,55].

2.6. Model fitting and statistical analysis

2.6.1. Relative amounts of released to loaded flurbiprofen – The percentage of drug released was calculated according to equation:

$$Relative\ released\ /\ loaded\ drug\ (\%) = \frac{Released\ drug}{\left(Loaded\ drug\ +\ Residual\ drug\right)} \times 100$$

Eq. (1)

where “released drug” is the amount of flurbiprofen (per mg of wet lens) that was released in water during a 8-hours release period, “loaded drug” is the amount of flurbiprofen (per mg of wet lens) extracted by water leaching or by SCF extraction, and “residual drug” is the amount of flurbiprofen (per mg of wet lens) still present in the SFE-extracted SCLs and that was removed by leaching in water.

2.6.2. Diffusion coefficients – Drug release profiles below 60% amount released were fitted to Equation 2 [56-58]:

$$\frac{M_t}{M_\infty} = kt^n \qquad \text{Eq. (2)}$$

where M_t and M_∞ represent the cumulative (absolute) amount of drug released at time, t, and at infinite time, respectively, k is a kinetic constant that incorporates structural and geometric characteristics of the delivery device (polymer + drug), and, n, is the release exponent, which can inform about the drug release mechanism. The following equations were also used [58]:

$$\frac{M_t}{M_\infty} = 4\left(\frac{D\,t}{\pi\,l^2}\right)^{1/2} \qquad \text{Eq. (3)}$$

$$\frac{M_t}{M_\infty} = 1 - \left(\frac{8}{\pi^2}\right)\exp\left(-\frac{\pi^2 D\,t}{l^2}\right) \qquad \text{Eq. (4)}$$

where l is the thickness of the sample and D the diffusion coefficient, which is assumed to be constant. Equation 3 is valid just for the first 60% of the total release ($M_t/M_\infty \leq 0.6$) while equation 4 is valid for the last 60% of the total release ($M_t/M_\infty \geq 0.4$) and has been widely used to obtain diffusion coefficients from drug release experimental data. After linearization and regression analysis of these equations, the drug diffusion coefficients, D, can be determined from the resulting slopes.

2.6.3. Statistical analysis **-** Statistical analysis were carried out using the analysis of variance (ANOVA) and the Tukey HSD test from Statistica 5.0 (StatSoft, Inc., Tulsa OK, USA).

3. Results and Discussion

In the present work sequential steps comprising $scCO_2$ impregnation (to load the drug template) and $scCO_2$ extraction (to remove the drug template) were applied, and the effects of these successive steps on some physical and mechanical properties of commercially available SCLs, as well as, on their performance as drug delivery devices were evaluated. Flurbiprofen was chosen as the drug template because this non-steroidal anti-inflammatory (NSAID) is widely used to treat common ocular inflammatory processes and after eye surgery. Its poor aqueous solubility ($5 \cdot 10^{-5}$ M or 12 mg/l) [59-60] notably hinders its uptake by SCLs from aqueous solutions. On the other hand, $scCO_2$ has been shown to be a useful solvent for several hydrophobic drugs [61] including flurbiprofen [53]. Thus, the first aim of the work was to elucidate how much flurbiprofen could be impregnated in daily-wear Hilafilcon B commercial SCLs (Bausch & Lomb®) using $scCO_2$ at 12.0 MPa and 40 ºC, compared to the conventional loading by immersion in a saturated drug aqueous solution. The flurbiprofen-impregnated SCLs were divided into two groups (as shown in Figure 2): one was used to check the drug release kinetics in water, while the other group underwent extraction with $scCO_2$ followed by washing in water in order to quantify the total amount of drug that had been loaded. Some lenses underwent successive impregnation/extraction with $scCO_2$.

3.1. Flurbiprofen loading/impregnation and release/extraction

The total amount of flurbiprofen impregnated using $scCO_2$ was estimated as the sum of the amount extracted by $scCO_2$ plus a minor amount that was still remaining and could be removed with water (Figure 4A, grey columns). It is evident that consecutive SSI/SFE processing cycles led to greater amounts of flurbiprofen impregnated; i.e., the amount of drug in the lenses enhanced almost 2-fold from a single processing cycle (just one SSI and SFE step) to a 2-cycles processing (SSI step followed by 1st SFE step and then by 2nd SSI and 2nd SFE step) and then increased 2-fold more after the 3-cycles processing (1st SSI and 1st SFE step, followed by 2nd SSI and 2nd SFE step and, finally, followed by 3rd SSI and 3rd SFE step). From the 1-cycle to the 3-cycles procedure, the loading capacity of Hilafilcon B SCLs increased around 450%; i.e., up to 55 mg/g. By contrast, similar loading/extraction cycles carried out in aqueous medium (i.e., immersion in a drug

solution followed by release in water) lead to a significantly lower amount loaded (< 1 mg/g) and consecutive loading/extraction steps did not improve the yield but decreased it, probably due to some irreversible binding of the hydrophobic drug to the network, which prevents more molecules to be adsorbed. If one compares the time required for the processing of the lenses (drug loading/removal) with $scCO_2$ (less than 1 day) and with water-based solutions (4-5 days), the advantage of the former procedure is even more evident.

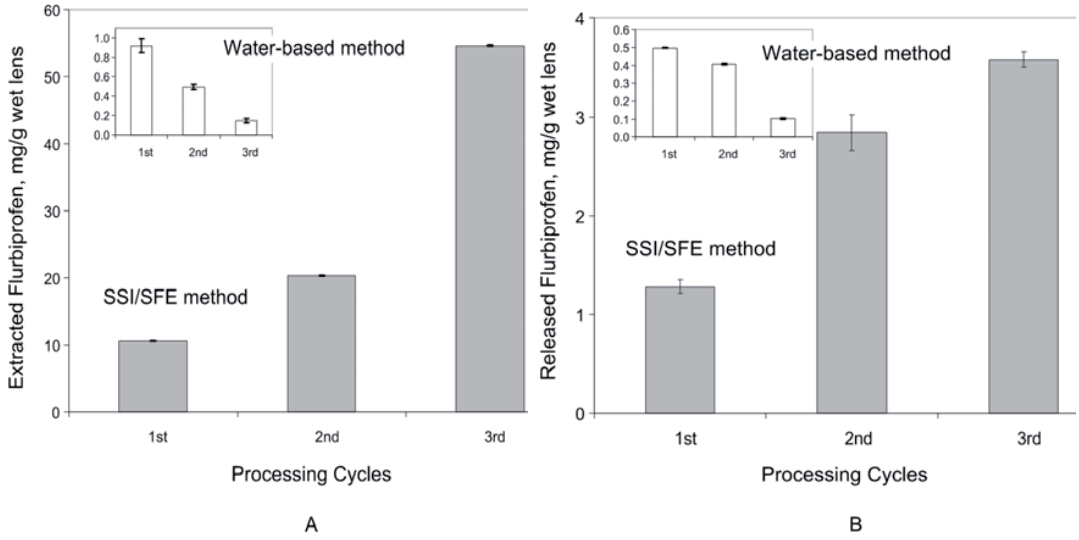

Figure 4. *Flurbiprofen loaded/removed in Hilafilcon B SCLs after consecutive drug loading/removal cycles.* ***A)*** *Extracted flurbiprofen amounts (per mg of wet SCLs) obtained for SCLs loaded by immersion and leaching in water (□) (small graph) and by $scCO_2$ SSI followed by $scCO_2$ SFE (■). After $scCO_2$ SFE experiments, SCLs were further extracted in water to remove any residual drug still present inside SCLs and these values are also represented (■) although they are not completely visible.* ***B)*** *Flurbiprofen released (per mg of wet SCLs) for 8 hours in water from SCLs loaded by immersion in water (□) (small graph) or that underwent successive SSI/SFE cycles (■).*

Commercial ophthalmic drops contain 0.03% flurbiprofen, i.e., each drop contains around 15 µg of flurbiprofen. Therefore, each $scCO_2$-processed SCL (43-44 mg weight) contain the same amount of drug as 29 or 160 drops of the ophthalmic solution, after 1 or 3 processing cycles. SCLs loaded by immersion in water just took up as 2.5 drops of flurbiprofen solution.

The global efficiency of SCF-based processes is governed by the employed operational conditions (pressure, temperature, processing time, co-solvent addition and composition, flow rates, depressurization rate, etc.) and by the physicochemical interactions that may be established between the involved substances (the lens, $scCO_2$, water, and the drug) in the process [36,38,41,45-48]. In the present case, the most relevant interactions to be considered are the $scCO_2$/flurbiprofen interactions (which determine flurbiprofen solubility in $scCO_2$), the water-swollen SCLs/$scCO_2$ interactions (which lead to lens swelling and plasticization) and the flurbiprofen/water-swollen SCLs interactions (which control flurbiprofen solubility and partitioning in the lens) [36,38,41,47,48]. $scCO_2$ is a non-polar solvent (despite the fact that, under certain circumstances, it can form quadrupoles) which has a higher affinity for low-polarity small hydrophobic drugs (such as flurbiprofen) than water. Therefore the $scCO_2$/flurbiprofen interactions are favorable and, at the employed operational conditions, $scCO_2$ dissolves more flurbiprofen molecules per volume unit than water; drug solubility was estimated as ~160 mg/l and ~510 mg/l at 40 ºC in $scCO_2$ during SSI (12 MPa) and SFE (20 MPa), respectively, and ~12 mg/l at 25 ºC in water (0.1 MPa). This means that flurbiprofen can rapidly be dissolved and loaded into a $scCO_2$ phase which is a quite helpful feature for the employed SCF-based impregnation and extraction methods.

Hilafilcon B SCLs are cross-linked polymeric materials that comprise the co-monomers represented in Figure 1, which can easily establish hydrogen bonding with flurbiprofen and water as well as establish favorable phenyl/methyl/carbonyl/fluorine-$scCO_2$ interactions [36,38,39,41,45-48,62-64]. The intense H-bonding between ibuprofen and polyvinylpyrrolidone (PVP) after $scCO_2$ impregnation as well as the ability of the $scCO_2$ molecules to interact with the Lewis basic-type carbonyl group of PVP have been previously reported [65]. These interactions are also plausible in the case of flurbiprofen. The relative magnitude of $scCO_2$/flurbiprofen and flurbiprofen/water-swollen SCLs interactions should control the flurbiprofen “solubility” in the swollen SCL as well as its partition coefficient between the SCL and the $scCO_2$ phase. If the $scCO_2$/flurbiprofen interactions are less favorable than the flurbiprofen/water-swollen SCL interactions, then flurbiprofen will have a higher partition coefficient into the SCL, which is a very positive aspect for the SSI process. Otherwise, the drug may be easily removed from the SCLs

during a SFE process or during depressurization. Regarding $scCO_2$/water-swollen SCLs interactions, $scCO_2$ easily dissolves in the SCLs and promotes an additional swelling, which may be helpful for both drug impregnation and extraction processes. Nevertheless, the $scCO_2$-water and the flurbiprofen-water interactions may also play important roles in these processes [46-48].

One of the great advantages of the SCF-based processes is that the relative magnitudes of the $scCO_2$/flurbiprofen and the $scCO_2$/water-swollen SCL interactions can be easily tuned, simply by regulating operational pressure, temperature and processing time. For example, by using $scCO_2$ at the conditions employed in this work (40 ºC at 12 and 20 MPa) the density of the $scCO_2$ phase (and consequently its solvent power) is lower at 12 MPa than at 20 MPa. This means that the $scCO_2$/flurbiprofen interactions are favored at higher pressures. However, the transport properties are also affected: at 20 MPa the $scCO_2$ viscosity is greater while its diffusivity is lower than at 12 MPa. This means that the transport properties and the plasticization/swelling effects are favored at lower pressures (because of the enhanced $scCO_2$/water-swollen SCL interactions). Therefore, if we intend a process in which the partition of a drug between a SCL and a $scCO_2$ phase is fairly high and in which the plasticization/swelling effects and the potential chain rearrangements caused by these effects are quite significant (such as the SSI process employed in this work), then we should choose to work at relatively low pressures. Oppositely, if we intend a process in which the solubility of a drug in a $scCO_2$ phase should be improved and in which the plasticization/swelling effects are decreased (such as the SFE process) then we should work at relatively high pressures. Under these conditions, the transport properties are not favored and thus the processing time has to be increased in order to compensate this drawback.

In sum, the advantages of loading SCLs with flurbiprofen using impregnation with $scCO_2$ compared to immersion in an aqueous solution can be summarized as follows. Firstly, it is possible to dissolve more flurbiprofen in $scCO_2$ than in water (this is also true for other low polarity hydrophobic drugs). Secondly, SCF-based processes can be easily "tuned" in order to improve drug loading, drug partition coefficients and the polymer swelling/plasticization effects that regulate the impregnation and extraction yields. Furthermore, the physical rearrangement of the polymeric chains to enable a better

hosting of the drug molecules may be possible. Thirdly, SCF-based methods are remarkably faster.

The progressive enhancement in the amount of drug-impregnated (Figure 4A) suggests that the consecutive flurbiprofen SSI incorporation and SFE extraction steps cause conformational changes in polymeric network that create cavities where the drug can fit into. If the conformation of these formed cavities is stable enough to be memorized in the polymeric network when the drug is extracted, the ability of SCLs to reload flurbiprofen should be greater than before processing. In fact, such improvement may be further increased after successive reload/release cycles since more cavities could be generated.

On the other hand, if the affinity of the drug for the polymer increases as these tailored cavities increase in number, flurbiprofen release should be more sustained. The amounts of flurbiprofen released for 8 hours in water (Figure 4B) were remarkably lower (roughly one tenth) than those loaded by SSI (Figure 4A). Although there is an increase in the amount released as more SSI/SFE processing cycles are applied, the ratio between the amount released and that loaded was not kept constant but decreased from the 1 to the 3-cycles processed SCLs (Table 1). The whole drug release profiles in water are shown in Figure 5. SCLs loaded by the SSI/SFE method sustained the release for ~3-4 hours, while those SCLs loaded by immersion in the flurbiprofen aqueous solution released significantly lower amounts and controlled the release just for ~1-2 hours. Interestingly, increasing the time of immersion in the flurbiprofen solution, from 2.5 h up to 13 h, did not lead to either greater amounts of loaded or released drug (Figure 6). Release experiments were carried out under near *sink* conditions, since the intrinsic solubility of flurbiprofen in water is 12 mg/l at 25 ºC [59] and the maximum concentration achieved in the release medium was ~1.9 mg/l.

As expected, the $scCO_2$-processed SCLs released greater amount of drug than those loaded in the flurbiprofen solution, although the percentage released was lower for the former lenses (Table 1). It should be noticed that SCLs released less flurbiprofen in 8 hours (~54-80%, Table 1) than the amount they can uptake in 2.5 hours in water. This finding indicates that Hilafilcon B SCLs have per se some affinity for flurbiprofen. However, the lower percentages released by the SCF-processed SCLs (~6-14%, Table 1)

suggest that the possible rearrangement of the polymer network during the successive SSI/SFE steps enables a higher affinity drug hosting. Performed ANOVA analysis showed that there are significant differences between the results obtained after a different number of processing cycles. For example, and for the released flurbiprofen amounts from SCLs after 3 cycles processing, the Tukey test (95% significance) indicated statistical p-values ≤ 0.004 and ≤ 0.0002 for SCF-based and for water-based methods, respectively.

Cycles	SCF-based methods				Water-based methods		
	Released	Loaded (µg/mg of wet lens)	Residual	Relative released/loaded drug (%)	Released	Loaded (µg/mg of wet lens)	Relative released/loaded drug (%)
1st cycle	1.28 ±0.07	10.53	0.013 ±0.003	11.98	0.498 ±0.002	0.92 ±0.07	54.27
2nd cycle	2.84 ±0.18	20.29	0.020 ±0.002	13.86	0.406 ±0.004	0.49 ±0.03	82.39
3rd cycle	3.58 ±0.08	54.54	0.063 ±0.023	6.48	0.102 ±0.003	0.147 ±0.002	69.58

Mean values ± standard deviation.

Table 1. *Flurbiprofen loaded by SCLs that underwent SSI or conventional loading by immersion in a drug aqueous solution, and flurbiprofen released in water referred as total amount or as relative percentage of the amount loaded.*

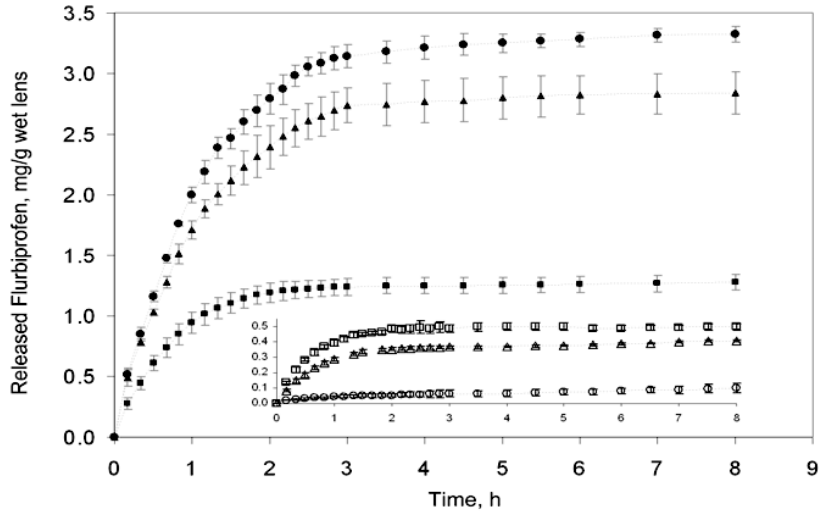

Figure 5. *Kinetics of flurbiprofen release in water for Hilafilcon B SCLs loaded by immersion and leaching in water (small graph, empty symbols: (□) 1-cycle; (Δ) 2-cycles; and (○) 3-cycles) and by $scCO_2$ SSI followed by $scCO_2$ SFE (filled symbols: (■) 1-cycle; (▲) 2-cycles; and (●) 3-cycles).*

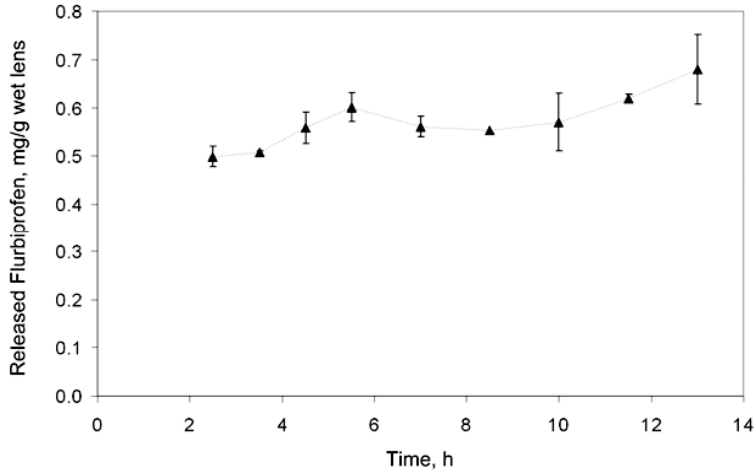

Figure 6*. Total amount of released flurbiprofen from SCLs loaded by immersion in aqueous flurbiprofen solutions for several pre-determined periods of time (from 2.5 up 13 hours).*

Release profiles fitted to equation 2 (Table 2) rendered release exponents quite similar for SCF- and for water-processed lenses ($0.6 < n < 0.7$), with the exception of the 3-cycles water-processed SCLs. The exponent values suggest that drug release occurred

by an anomalous transport type (i.e., the superposition of Fickian-controlled and swelling-controlled release [57]) disregarding the loading/removal method. This means that neither the process nor the number of cycles apparently alter drug release mechanism. On the other hand, the release rate constant (k) decreased as the number of cycles increased, which may indicate that the affinity between SCL and flurbiprofen is raised as the lens undergoes processing. Similarly, flurbiprofen diffusion coefficients, D_1 and D_2, obtained by the short-time (equation 3) and by the late-time release approaches (equation 4), respectively, become smaller as the number of consecutive processing cycles (for SCF-based and for water-based processing) increases. The decrease is particularly evident in the case of the SCF-processed lenses (Table 2), which confirm the enhancement of the affinity for the drug probably due to a molecular imprinting effect.

3.2. Molecular imprinting effect

To gain insight into the conformational changes underwent by the SCLs that could render flurbiprofen-imprinted cavities, a proof-of-concept comparing the sorption of flurbiprofen with that of ibuprofen and dexamethasone from aqueous solutions was performed. Flurbiprofen, ibuprofen and dexamethasone present some similarities in terms of chemical structure (Figure 1) and have comparable (low) solubilities in water (12 mg/l, 11 mg/l and 115 mg/l, respectively) [59,66]. SCF-processed SCLs (after 3 SSI and SFE cycles) and non-processed SCLs (non-imprinted control polymers) were immersed into solutions of each drug and after loading, the release profiles in water were recorded. SCF-processed SCLs could uptake more flurbiprofen from an aqueous drug solution and in shorter periods of time than control SCLs (Figure 7A). Furthermore, flurbiprofen uptake is much more efficient than the ibuprofen and dexamethasone ones (Figure 7B). This is also valid for control SCLs which somehow confirms that Hilafilcon B SCLs have per se a higher structural affinity for flurbiprofen than for ibuprofen and dexamethasone. The loading of dexamethasone by SCF-processed SCLs and control SCLs was the lowest, being quite similar for both lenses. The relatively high standard deviations were mostly due to the difficulties of the employed analytical method for such highly diluted drug aqueous solutions. Drug release profiles in water showed the opposite behaviour: the

most sustained and slowest drug release was attained for the flurbiprofen-loaded SCLs (Table 3).

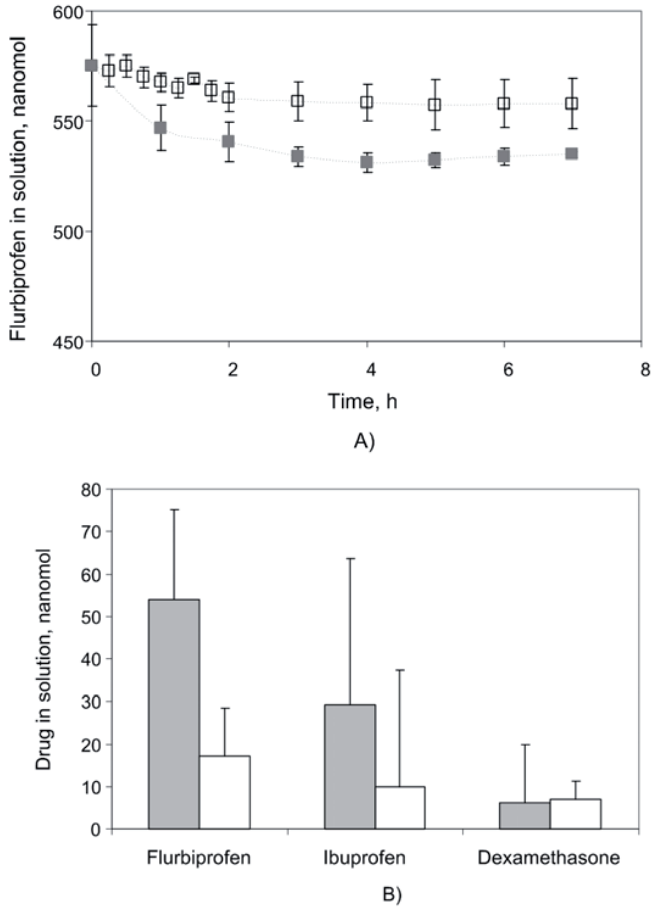

***Figure** 7. Molecular imprinting proof-of-concept for SCF-processed SCLs. **A)** Sorption kinetics from flurbiprofen aqueous solutions. **B)** Total sorption from aqueous drug solutions (after 14h of immersion). SCF-processed SCLs (MIP) (■); Non-processed/control SCLs (NIP) (□).*

The fitting of the drug loading and release profiles to equations 2 and 3 are shown in Table 3.

A) Obtained by the Korsmeyer-Peppas equation: kinetic constant, *k*, and release exponent, *n*.

Drugs	Samples	Sorption			Release		
		n	***k***	***R²***	***n***	***k***	***R²***
Flurbiprofen	MIP-CO_2	0.904	0.741	0.999	0.663	0.764	0.990
	NIP	0.729	0.412	0.944	0.523	0.879	0.930
Ibuprofen	MIP-CO_2	0.923	0.582	0.998	0.557	0.846	0.952
	NIP	0.905	0.594	0.999	0.490	0.820	0.933
Dexamethasone	MIP-CO_2	0.819	0.727	0.987	0.638	0.780	0.964
	NIP	0.872	0.649	0.994	0.529	0.911	0.922

Results were obtained considering just the first 60% of the total release curve.

B) Obtained by Equation 3: diffusion coefficient, *D*.

Drugs	Samples	Sorption		Release	
		$D_1 \times 10^3$ (mm^2/h)	R^2	$D_1 \times 10^3$ (mm^2/h)	R^2
Flurbiprofen	MIP-CO_2	1.34	0.999	1.22	0.993
	NIP	0.47	0.926	3.32	0.986
Ibuprofen	MIP-CO_2	0.36	0.983	2.11	0.999
	NIP	0.79	0.998	2.17	0.990
Dexamethasone	MIP-CO_2	0,84	0.998	1.73	0.999
	NIP	0.56	0.999	2.80	0.999

D_1: Correlated by Eq. (3) and just considering the first 60% of the total release curve.

Table 3*. Kinetic parameters of the loading and release of flurbiprofen, ibuprofen and dexamethasone by non-processed SCLs (NIP) and 3-cycles processed SCLs (MIP-CO_2).*

The loading exponents were quite similar for the three drugs ($0.7 < n < 0.9$) in the SCF-processed and the control SCLs. The same occurred for the corresponding release profiles

in water, although the exponent values were lower ($0.5 < n < 0.6$). Slightly lower n values were observed for SCF-processed SCLs compared to the control SCLs. Regarding the rate constant (k), the sorption was faster for flurbiprofen (and dexamethasone) than for ibuprofen. The release rate and the diffusion coefficients (D_1) followed the opposite trend. SCF-processed SCLs presented higher sorption and lower release flurbiprofen diffusion coefficients than those obtained for dexamethasone and ibuprofen (in this order). Additionally, SCF-processed SCLs presented also higher sorption and lower release flurbiprofen diffusion coefficients than those achieved with control SCLs.

Because the three drugs were at the same molar concentration in the loading solutions, the differences in loading and release could be related to their affinity for the SCLs, their relative sizes/volumes in solution (hydrodynamic Stokes radius or, as an approximation, their solid molar volumes), and the network average mesh sizes. Since all employed SCF-processed SCLs passed through the same processing steps, all of them should possess the same network average mesh sizes. The same is expected to occur with the non-processed (control) SCLs which did not pass through any processing step. However, dexamethasone has a higher solid molar volume (268.8 cm^3/mol), as estimated by the Fedors and by the Immirzi-Pirini methods [67-69], than flurbiprofen or ibuprofen (183.8 cm^3/mol or 182.1 cm^3/mol, respectively). Such a greater size may lead to some constraints on its diffusion and uptake by SCLs, which explains the low dexamethasone loading.

Flurbiprofen and ibuprofen have quite similar molecular weights and molar volumes. Therefore, their different loading may come from a different interaction with the polymeric structure of SCF-processed Hilafilcon B SCLs. Flurbiprofen possesses a fluorine atom in one of the aromatic phenyl groups (a C-F bond) and an additional phenyl group compared to ibuprofen, which has an $–CH_2$-$CH(CH_3)$-CH_3 end-group. The comonomers present in Hilafilcon B SCLs have a carbonyl group, which is well-known to interact strongly and favourably with the C-F groups in many chemical/biochemical systems and it is often involved in several protein/enzyme molecular biorecognition events [51,52]. This type of non-covalent multipolar interaction usually presents a very characteristic geometry: the electronegative organofluorine atom tends to interact orthogonally with the electrophilic carbonyl group, and the C-F bond approaches the plane of the carbonyl group from an angle between 100º and 140º [51,52,70,71]. The

flurbiprofen-imprinted SCLs may exert such biomimetic recognition distinguishing between flurbiprofen and ibuprofen. Dexamethasone also has a C-F bond, but its high molecular size should hinder the penetration into the cavities arranged to host flurbiprofen.

It is feasible that during the SSI process the swelling/plasticization effect and the interaction of $scCO_2$ with the carbonyl groups of the SCL, and the flurbiprofen-SCLs interactions and templating (through the C-F/carbonyl interactions) promote the polymeric arrangement and the creation of specific "cavities" with chemical and structural recognition abilities for flurbiprofen, i.e., a molecular imprinting effect. Such post-imprinted "cavities" may be then responsible for the higher sorption of flurbiprofen from aqueous drug solutions as well as for the observed more sustained drug release profiles.

3.3. Effect of SCF-processing on the SCL features

SEM micrographs of the surfaces and cross-sections of non-processed (control), of SCF-processed (3 cycles SSI/SFE) and of water-processed (3-cycles water soaking/water leaching) are shown in Figure 8. No apparent morphological changes are visible on processed and on non-processed SCLs. Higher magnifications were not possible because the electron beam energy degraded the SCLs.

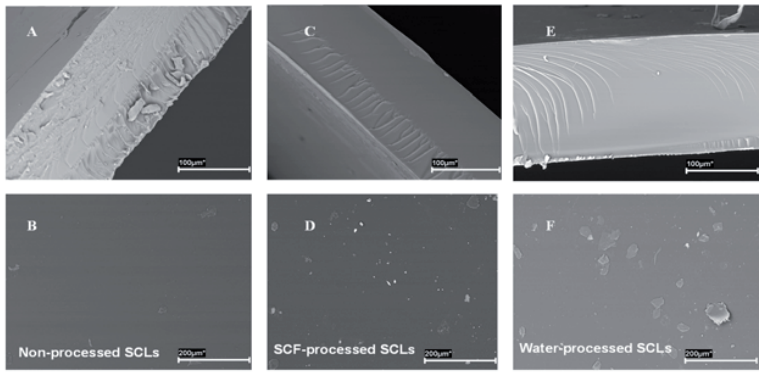

Figure 8. *SEM micrographs of non-processed (control), of SCF-processed and of water-processed SCLs. Top: cross-section images (A, C and E); Bottom: surface images (B, D and F).*

The FTIR-ATR spectra (Figure 9A) of non-processed SCLs (control) and of SCF-processed SCLs (2 cycles SSI/SFE) did not evidence the presence of remaining flurbiprofen. It also seems that no relevant changes occurred in any of the characteristic structural peak of SCLs. However, a careful analysis of the typical IR bands of SCLs comonomers (Figure 9B and 9C) revealed that the strong peak corresponding to the C=O stretching vibration (~1720 cm^{-1}) was slightly shifted from 1716 cm^{-1} (for non-processed SCLs) to 1718 cm^{-1} (for SCF-processed SCLs). The same also happened for the –OH stretching vibration (~3300-3500 cm^{-1}): the corresponding peak was shifted from 3373 cm^{-1} (for non-processed SCLs) up to 3383 cm^{-1} (for SCF-processed SCLs). Despite the FTIR resolution is 2 cm^{-1}, these findings are in agreement with the hypothesis of that using consecutive flurbiprofen SSI/SFE steps, the combined effects of SCLs plasticization/swelling and of flurbiprofen-SCL specific interactions (especially through the C-F/carbonyl groups) may have caused some SCLs structural rearrangements for creating imprinted cavities.

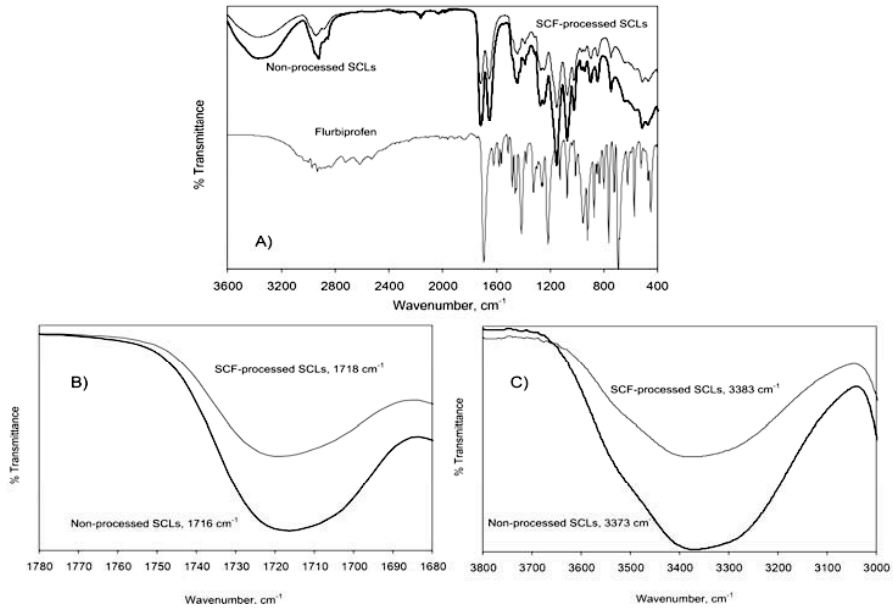

***Figure 9**. A) FTIR-ATR spectra of non-processed SCLs (thick black line), of SCF-processed SCLs (thin black line) and of flurbiprofen (thin grey line). B) FTIR spectra for the stretching vibration of carbonyl (C=O) group: non-processed SCLs (thick black line); SCF-processed SCLs (thin grey line). C) FTIR spectra for the stretching vibration of hydroxyl (-OH) group: non-processed SCLs (thick black line); SCF-processed SCLs (thin grey line).*

The glass transition temperature of the dried SCLs (91-92 ºC) was not altered by the successive SCF-processing steps. Non-processed and SCF-processed SCLs showed similar degree of swelling in water at equilibrium: 57.01% (s.d. 0.92) and 57.88% (s.d. 1.56), respectively, and close to that indicated by the supplier (59% w/w). The mean transmittance values in the 400-900 nm range of control, SSI-processed, and flurbiprofen-loaded in water SCLs were 97.4% (s.d. 0.3), 94.7% (s.d. 0.8) and 93.7% (s.d. 1.5), respectively. The oxygen permeability (Dk/L) of non-processed SCLs (14.82 barrer/cm) and of 3-cycles SCF-processed SCLs (14.79 barrer/cm, s.d. 0.66) was also not affected by the processing with $scCO_2$.

The water contact angles and surface free energies (calculated by the extended Fowkes (xF) method) are presented in Table 4. The SCF-based and the water-based methods did not affect greatly the water contact angles for Hilafilcon B SCLs (63-74 º) and the surface free energies (26-31 mN/m). The variability in these results can be explained by the drying (water loss) of the SCLs during the measurements since the sessile drop method is highly sensitive to surface dehydration [48,72]. It is clear that the most important contributions for the obtained surface energies are those derived from the dispersive and from the hydrogen bonding components. Therefore, all SCLs keep their wettability properties and their surface characteristics after the employed processing methods.

Process	Contact Angle,º (H_2O)	Surface free energy			
		σ_S	σ_S^D	σ_S^P	H-H
		mN/m, average value ± standard deviation			
Control	69.6±1.9	33.7±2.8	10.0±4.2	0.15± 0.21	23.6±6.7
1st cycle SCF processing	68.1±3.2	31.0±6.0	15.7±11.8	0.10± 0.19	15.2±15.5
2nd cycle SCF processing	70.8±5.0	26.4±1.2	11.3±4.4	0.11±0.22	15.0±5.5
3rd cycle SCF processing	64.6±0.6	30.1±0.7	17.7±3.3	2.94±4.15	9.5±6.7
1st cycle water processing	63.7±6.1	30.6±6.5	7.4±4.2	0.00±0.00	23.9±10.0
2nd cycle water processing	70.8±2.5	32.9±6.5	6.5±4.5	0.77±1.20	25.6±10.3
3rd cycle water processing	73.5±0.7	35.4±3.8	5.8±1.0	1.55±2.18	28.0±7.0

σ_S : surface free energy of the solid; σ_S^D : dispersive component; σ_S^P : polar component; **H-H**: hydrogen bond component

Table 4*. SCLs water contact angles and surface free energies (calculated by the extended Fowkes (xF) method).*

4. Conclusions

The supercritical fluid-processing of SCLs developed in the present work enables the loading of preformed SCLs with a specific drug for its sustained release. Using $scCO_2$ as the loading/extraction solvent, it was possible to impregnate daily-wear Hilafilcon B commercial SCLs with flurbiprofen to a greater extent and in a faster way than using water-based processes. The application of sequential flurbiprofen impregnation and extraction steps results in the rearrangement of some polymeric regions of the SCLs driven by the combined effect of $scCO_2$ on polymer swelling/plasticization and of the specific flurbiprofen-SCLs interactions (mainly through the C-F/carbonyl interactions). This leads to the creation of effective and specific "cavities" with chemical and structural recognition abilities for flurbiprofen, i.e., to a true molecular imprinting effect. Such post-imprinted "cavities" may be then responsible for the observed higher flurbiprofen sorption from aqueous solutions as well as for the obtained more sustained release profiles, compared to structurally-related drugs. In addition, the employed SCF-based processes did not alter some critical functional properties of commercial SCLs. Therefore, SCF-assisted methods may be useful for the preparation of combination products for the

treatment of ocular diseases using SCLs as the delivery device, while maintaining their functionality as corrective of refractive deficiencies.

Acknowledgments

This work was financially supported by FCT-MCTES under contract PTDC/SAU-FCF/71399/2006 and by MICINN and FEDER (SAF2008-01679, PT2009-0038). Authors also acknowledge Bausch & Lomb (Portugal) and Mart-Optic (Coimbra, Portugal) for supplying the contact lenses for this study. F. Yañez acknowledges Ministerio de Ciencia e Innovación of Spain for FPI fellowship (SAF2005-01930). M.E.M. Braga acknowledges FCT-MCTES for the postdoctoral fellowship (SFRH/BPD/21076/2004).

References

[1] Kearns VR, Williams RL. Drug delivery systems for the eye. Exp Rev Med Dev 2009;6:277-290.

[2] Calvo P, Vila-Jato JL, Alonso MJ. Comparative in vitro evaluation of several colloidal systems, nanoparticles, nanocapsules, and nanoemulsions, as ocular drug carriers. J Pharmacol Sci 1996;85:530-536.

[3] Le Bourlais C, Acar L, Zia H, Sado PA, Needham T, Leverge R. Ophthalmic drug delivery systems; recent advances. Prog Retin Eye Res 1998;17:33-58.

[4] Sedlacek J. Possibility of application of eye drugs with the aid of gel-contact lenses. Ceskoslovenská Oftalmologie 1965;21:509–512.

[5] Waltman SR, Kaufman HE. Use of hydrophilic contact lenses to increase ocular penetration of topical drugs. Invest Ophth Visual Sci 1970;9:250–259.

[6] Jain MR. Drug delivery through contact lenses. Brit J Ophthalmol 1988;72:150–154.

[7] Lesher GA, Gunderson GG. Continuous drug delivery through the use of

disposable contact lenses. Optom Vis Sci 1993;70:1012–1018.

[8] Hiratani H, Fujiwara A, Tamiya Y, Mizutani Y, Alvarez-Lorenzo C. Ocular release of timolol from molecularly imprinted soft contact lenses. Biomaterials 2005;26:1293–1298.

[9] Gulsen D, Chauhan A. Ophthalmic drug delivery through contact lenses. Invest Ophthalmol Vis Sci 2004;45:2342-2347.

[10] Gulsen D, Li CC, Chauhan A. Dispersion of DMPC liposomes in contact lenses for ophthalmic drug delivery. Curr Eye Res 2005;30:1071–1080.

[11] Novack GD. Ophthalmic drug delivery: development and regulatory considerations. Clin Pharmacol Ther 2009;85:539-543.

[12] Wajs G, Meslard JC. Release of therapeutic agents from contact lenses. Crit Rev Ther Drug 1986;2:275-289.

[13] McMahon TT, Zadnik K. Twenty-five years of contact lenses - The impact on the cornea and ophthalmic practice. Cornea 2000;19:730–740.

[14] Karlgard CCS, Wong NS, Jones LW, Moresoli C. In vitro uptake and release studies of ocular pharmaceutical agents by silicon-containing and p-HEMA hydrogel contact lens materials. Int J Pharm 2003;257:141–151.

[15] Alvarez-Lorenzo C, Hiratani H, Concheiro A. Contact lenses for drug delivery. Achieving sustained release with novel systems. Am J Drug Del 2006;4:131–151.

[16] Xinming L, Yingde C, Lloyd AW, Mikhalovsky SV, Sandeman SR, Howel CA, Liewen L. Polymeric hydrogels for novel contact lens-based ophthalmic drug delivery systems: A review. Cont Lens Anterior Eye 2008;31:57-64.

[17] Peng CC, Kim J, Chauhan A. Extended delivery of hydrophilic drugs from silicone-hydrogel contact lenses containing Vitamin E diffusion barriers. Biomaterials 2010;31:4032-4047.

[18] Alvarez-Lorenzo C, Yañez F, Barreiro-Iglesias R, Concheiro A. Imprinted soft contact lenses as norfloxacin delivery systems. J Control Release 2006;113:236-244.

[19] Alvarez-Lorenzo C, Yañez F, Concheiro A. Ocular drug delivery from molecularly-imprinted contact lenses. J Drug Deliv Sci Tech 2010; in press.

[20] White CJ, Byrne ME. Molecularly imprinted therapeutic contact lenses. Expert Opin. Drug Deliv 2010;7.765-780.

[21] Komiyama M, Takeuchi T, Mukawa T, Asanuma H. Molecular Imprinting, From Fundamentals to Applications. Wiley-VCH, Weinheim, 2003.

[22] Alvarez-Lorenzo C, Concheiro A. Molecularly imprinted polymers for drug delivery. J Chromatogr B 2004;804:231–245.

[23] Sellergren B, Allender CJ. Molecularly imprinted polymers: A bridge to advanced drug delivery. Adv Drug Deliv Rev 2005;57,1733-1741.

[24] Cunliffe D, Kirby A, Alexander C. Molecularly imprinted drug delivery systems. Adv Drug Del Rev 2005;57:1836-1853.

[25] Piletsky S, Turner A. Molecular Imprinting of Polymers, Landes Bioscience, Georgetown, TX, USA, 2006.

[26] Byrne ME, Park K, Peppas NA. Molecular imprinting within hydrogels. Adv Drug Deliv Rev 2002;54:149-161.

[27] Peppas NA, Huang Y. Polymers and gels as molecular recognition agents. Pharm Res 2002;19:578-577.

[28] Bruggemann O, Haupt K, Ye L, Yilmaz E, Mosbach K. New configurations and applications of molecularly imprinted polymers. J Chromatogr A 2000;889:15–24.

[29] Ye L, Mosbach K. The technique of molecular imprinting – principle, state of the art, and future aspects. J Incl Phenom Macro 2001;41:107–113.

[30] Enoki T, Tanaka K, Watanabe T, Oya T, Sakiyama T, Takeoka Y, et al. Frustrations in polymer conformation in gels and their minimization through molecular imprinting. Phys Rev Lett 2000;85:5000-5003.

[31] Hiratani H, Alvarez-Lorenzo C, Chuang J, Guney O, Grosberg AY, Tanaka T. Effect of reversible cross-linker, n,n'-bis(acryloyl)cystamine, on calcium ion adsorption by imprinted gels. Langmuir 2001;17:4431-4436.

[32] Alvarez-Lorenzo C, Guney O, Oya T, Sakai Y, Kobayashi M, Enoki T, et al. Polymer gels that memorize elements of molecular conformation. Macromolecules 2000;33:8693-8697.

[33] Elvassore N, Kikic I. Pharmaceutical Processing with Supercritical Fluids. In: Bertucco A, Vetter G, editors. High pressure process technology: fundamentals and applications. Amsterdam:Elsevier Science, 2001. pp. 612-625.

[34] McHugh MA, Krukonis VJ. Supercritical Fluid Extraction. 2nd Ed.,

Boston:Butterworth-Heinemann, 1994.

[35] Beckman E. Supercritical and near-critical CO_2 in green chemical synthesis and processing. J Supercritic Fluids 2004;28:121–191.

[36] Kazarian SG. Supercritical fluid impregnation of polymers for drug delivery. In: York P, Kompella UB, Shekunov BY, editors. Supercritical fluid technology for drug product development. New York:Marcel Dekker, 2004.

[37] Davies OR, Lewis AL, Whitaker MJ, Tai H, Shakesheff KM, Howdle SM. Applications of supercritical CO_2 in the fabrication of polymer systems for drug delivery and tissue engineering. Adv Drug Del Rev 2008;60:373–387.

[38] Kikic I, Vecchione F. Supercritical impregnation of polymers. Curr Opin Solid State Mater Sci 2003;7:399-405.

[39] Kikic I. Polymer-supercritical fluid interactions. J Supercrit Fluids 2009; 47:458–465.

[40] Kemmere MF, Meyer T. Supercritical carbon dioxide in polymer reaction engineering. Weinheim:Wiley-VCH, 2005.

[41] Kazarian SG. Polymer processing with supercritical fluids. Polymer Sci Ser C+ 2000;42:78–101.

[42] de Sousa HC, Gil MHM, Leite EOB, Duarte CMM, Duarte ARC. Method for preparing sustained-release therapeutic ophthalmic articles using compressed fluids for impregnation of drugs. EP Patent 2006, EP1611877A1.

[43] de Sousa HC, Gil MHM, Leite EOB, Duarte CMM, Duarte ARC. Method for preparing therapeutic ophthalmic articles using compressed fluids. US Patent 2006, US20060008506A1.

[44] Duarte ARC, Simplício AL, Vega-Gonzalez A, Subra-Paternault P, Coimbra P, Gil MH, de Sousa HC, Duarte CMM. Impregnation of an intraocular lens for ophthalmic drug delivery. Current Drug Deliv 2008;5:102–107.

[45] Braga MEM, Vaz MT, Costa HSR, Ferreira EI, Gil MH, Duarte CMM, de Sousa HC. Supercritical solvent impregnation of ophthalmic drugs on chitosan derivatives. J Supercrit Fluids 2008;44:245-257.

[46] Natu MV, Gil MH, de Sousa HC. Supercritical solvent impregnation of poly(ε-caprolactone)/poly(oxyethylene-b-oxypropylene-b-oxyethylene) and poly(ε-

caprolactone)/ poly(ethylene-vinyl acetate) blends for controlled release applications. J. Supercrit Fluids 2008;47:93–1027.

[47] Costa VP, Braga MEM, Guerra JP, Duarte ARC, Duarte CMM, Leite EOB, Gil MH, de Sousa HC. Development of therapeutic contact lenses using a supercritical solvent impregnation method. J Supercrit Fluids 2010;52:306–316.

[48] Costa VP, Braga MEM, Duarte CMM, Alvarez-Lorenzo C, Concheiro A, Gil MH, de Sousa HC. Anti-glaucoma drug-loaded contact lenses prepared using supercritical solvent impregnation. J Supercrit Fluids 2010;53:165–173.

[49] Sellergren B. Polymer- and template-related factors influencing the efficiency in molecularly imprinted solid-phase extractions. Trends Anal Chem 1999;18:164-174.

[50] Duarte ARC, Casimiro T, Aguiar-Ricardo A, Simplício AL, Duarte CMM. Supercritical fluid polymerisation and impregnation of molecularly imprinted polymers for drug delivery. J Supercrit Fluids 2006;39:102-106.

[51] Paulini R, Muller K, Diederich F. Orthogonal multipolar interactions in structural chemistry and biology. Angew Chem Int Ed 2005;44:1788-1805.

[52] Hagmann WK. The many roles for fluorine in medicinal chemistry. J Med Chem 2008;51;4359-4369.

[53] Duarte ARC, Coimbra P, de Sousa HC, Duarte CMM. Solubility of flurbiprofen in supercritical carbon dioxide. J Chem Eng Data 2004;49:449-452.

[54] Owens DK, Wendt RC. Estimation of the surface free energy of polymers. J Appl Polym Sci 1969;13:1741–1747.

[55] Rudawska A, Jacniacka E. Analysis for determining surface free energy uncertainly by the Owens-Wendt method. Int J Adhes Adhes 2009;29:451-457.

[56] Korsmeyer RW, Gurny R, Doelker E, Buri P, Peppas NA. Mechanisms of solute release from porous hydrophilic polymers. Int J Pharm 1983;15:25-35.

[57] Ritger PL, Peppas NA. A simple equation for description of solute release II. Fickian and anomalous release from swellable devices. J Control Release 1987;5:37-42.

[58] Lin CC, Metters AT. Hydrogels in controlled release formulations: Network design and mathematical modelling. Adv Drug Del Rev 2006;58:1379-1408.

[59] Anderson BD, Conradi RA. Predictive relationships in the water solubility of salts of a nonsteroidal anti-inflammatory drug. J Pharmacol Sci 1985;74:815-820.

[60] Perlovich GL, Kurkov SV, Bauer-Brandl A. The difference between partitioning and distribution from a thermodynamic point of view: NSAIDs as an example. Eur J Pharm Sci 2006;27:150-157.

[61] Gupta RB, Shim JJ. Solubility in Supercritical Carbon Dioxide. Boca Raton:CRC Press, 2006.

[62] Condo PD, Sumpter SR, Lee ML, Johnston KP. Partition coefficients and polymer-solute interaction parameters by inverse supercritical fluid chromatography. Ind Engin Chem Res 1996;35:1115–1123.

[63] Xu Q, Chang Y. Complex interactions among additive/supercritical CO_2/polymer ternary systems and factors governing the impregnation efficiency. J Appl Polym Sci 2004;93:742–748.

[64] Raveendran P, Ikushima Y, Wallen SL. Polar attributes of supercritical carbon dioxide. Accounts Chem. Res. 2005;38:478–485.

[65] Kazarian SG, Martirosyan GG. Spectroscopy of polymer/drug formulations processed with supercritical fluids: in situ ATR-IR Raman study of impregnation of ibuprofen into PVP. Int J Pharm 2002;232:81–90.

[66] Yalkowsky SH, Yan H. Handbook of aqueous solubility data: an extensive compilation of aqueous solubility data for organic compounds extracted from the AQUASOL Database. Boca Raton:CRC Press, 2003.

[67] Fedors RF. A method for estimating both the solubility parameters and molar volumes of liquids. Pol Eng Sci 1974;14:147-154.

[68] Lyman WJ, Reehl WF, Rosenblatt DH. Handbook of Chemical Property Estimation Methods. New York:McGraw-Hill, 1982.

[69] Poling BE, Prausnitz JM, O'Connell JP. The Properties of Gases and Liquids, 5th Ed. New York:McGraw-Hill, 2001.

[70] Olsen JA, Banner DW, Seiler P, Obst-Sander U, D'Arcy A, Stihle M, et al. A fluorine scan of thrombin inhibitors to map the fluorophilicity/fluorophobicity of an enzyme active site: evidence for C-F/C=O interactions. Angew Chem Int Ed 2003;42:2507-2511.

[71] Pagliaro M, Ciriminna R. New fluorinated functional materials. J Mater Chem 2005; 15:4981-4991.

[72] Read ML, Morgan PB, Maldonado-Codina C. Measurement errors related to contact angle analyses of hydrogel and silicone hydrogel contact lenses. J Biomed Mater Res Part B 2009; 91:662-668.

Discusión General

4. RESULTADOS Y DISCUSIÓN

4.1. Desarrollo de lentes de contacto *imprinted* con norfloxacino. Selección de monómeros funcionales y establecimiento por ITC de la relación óptima monómero funcional/fármaco.

El éxito de la terapia antimicrobiana requiere que se mantengan concentraciones eficaces de fármaco en el área infectada, durante periodos de tiempo prolongados. Cuando la infección afecta a ciertas zonas del organismo, como las estructuras oculares y óseas, la administración por vía sistémica no siempre permite alcanzar este objetivo (Pinto-Alphandary y col., 2000). En el caso particular del ojo, las barreras hemato-ocular y hemato-retiniana dificultan el

acceso del fármaco a las estructuras del ojo de manera que se requieren concentraciones plasmáticas muy altas para que se alcancen concentraciones eficaces en el área de infección, lo que implica riesgos de aparición de efectos secundarios graves. Por consiguiente, para tratar infecciones agudas se suele acudir a la aplicación directa del agente antimicrobiano haciendo uso de un dispositivo adecuado. La administración de fármacos por vía periocular o intraocular, utilizando disoluciones inyectables o implantes, resulta incomoda y dolorosa e implica riesgos importantes que la relegan al tratamiento de infecciones graves en el ámbito hospitalario (Reddy y Ganesan, 1996). Para tratar las infecciones más comunes se suele acudir a las formas de aplicación tópica, a pesar de que el intenso efecto de drenaje asociado a la secreción lacrimal y al pestañeo hace que la penetración en las estructuras oculares se limite al 1-5% de la dosis aplicada (Patrick y Mitra, 1993). Ello obliga a efectuar instilaciones frecuentes de dosis elevadas, que dan lugar a perfiles oculares pulsátiles con el consiguiente riesgo de absorción sistémica. Para incrementar la biodisponibilidad ocular, se puede acudir a colirios de elevada viscosidad, a sistemas de gelificación *in situ* y bioadhesivos o a insertos (Deshpande y col., 1998; Kaur y Kanwar, 2002; Davis y col., 2004). Estos últimos son especialmente eficaces, pero producen sensación de cuerpo extraño y pueden causar problemas de visión borrosa.

La eficacia de los tratamientos con agentes antimicrobianos también se puede ver afectada por la capacidad de los microorganismos para desarrollar *in vivo* resistencias a antibióticos a los que son susceptibles *in vitro*. Esta pérdida de sensibilidad se debe, en la mayor parte de los casos, a la capacidad de las bacterias para formar películas o *biofilms* sobre la superficie de las estructuras biológicas. La dificultad para penetrar a través del biofilm, la posible inactivación del fármaco por exoenzimas y exopolisacáridos, y la concurrencia de fenómenos de eflujo determinan que la concentración en el foco de infección pueda llegar a ser

muy baja (Smith, 2006). Este problema se plantea también cuando los microorganismos entran en contacto con ciertos productos sanitarios, como catéteres, implantes o lentes de contacto, sobre los que se adsorben desarrollando biofilms difíciles de erradicar (Schierholz y Beuth, 2001). De hecho, el uso de lentes de contacto constituye un factor de riesgo para la incidencia de infecciones oculares. Por lo tanto, las lentes de contacto cargadas con fármacos antimicrobianos encierran un indudable potencial para el tratamiento de infecciones o para su prevención en pacientes con daño corneal.

En la primera etapa de la Tesis se abordó la puesta a punto de un nuevo procedimiento de moldeado molecular dirigido a preparar lentes de contacto blandas de HEMA para liberación modificada de norfloxacino, haciendo uso de la microcalorimetría isotérmica para establecer *a priori* la relación molar fármaco:monómero funcional más adecuada para crear cavidades imprinted. El norfloxacino es una fluoroquinolona de amplio espectro que se utiliza en el tratamiento de infecciones por gérmenes Gram+ y Gram-, como *P. aeruginosa*, *S. aureus* y *E. coli* (Kim y col., 2005). Por vía ocular, se administra en colirios al 0.3%, que se instilan cada 30-120 min durante los primeros días del tratamiento (Consejo General COF, 2009), lo que constituye una pauta terapéutica de difícil cumplimiento y representa una evidente molestia para el paciente. Por lo tanto, el desarrollo de dispositivos capaces de cargar una dosis suficiente de fármaco y liberarlo de manera sostenida, encierra un considerable interés. El trabajo se ha planteado en las siguientes etapas: i) preselección del monómero funcional, teniendo en cuenta la capacidad para interaccionar con el fármaco y la biocompatibilidad (Monti y col., 2006); ii) estudio de las interacciones fármaco/monómero por microcalorimetría isotérmica (ITC); iii) aplicación del moldeado molecular a la síntesis de hidrogeles, desarrollando el proceso en diferentes condiciones experimentales; y iv) identificación de las condiciones de

carga y cesión más adecuadas desde el punto de vista de las aplicaciones de los hidrogeles como lentillas o como implantes.

En lo que se refiere a la viabilidad del moldeado molecular, el norfloxacino presenta *a priori* unas características muy adecuadas, ya que cuenta con dos grupos ionizables en su estructura, un grupo ácido carboxílico (pKa_1= 6.34±0.06) y un grupo amina (pKa_2= 8.75±0.07) (Mazuel, 1991), que pueden interaccionar electrostáticamente con los grupos cargados de otras moléculas. Además, presenta grupos -OH, -NH, =O, $-NR_3$ capaces de establecer puentes de hidrógeno, asi como un anillo aromático que puede interaccionar hidrofóbicamente (Figura 4.1). Todo ello sirvió de base para seleccionar inicialmente dos monómeros funcionales con capacidad potencial para interaccionar con el norfloxacino: el ácido acrílico (AAc), un ácido débil de pKa= 4.5, susceptible de formar puentes de hidrógeno, y la 4-vinil piridina (VP), una base débil de pKb= 8.5 (Mika y Childs, 1999) con afinidad por grupos ácido carboxílico y que también podría interaccionar con el anillo aromático del fármaco formando enlaces π-π. En la Figura 4.1 se muestran las estructuras del norfloxacino y de los monómeros utilizados en el estudio.

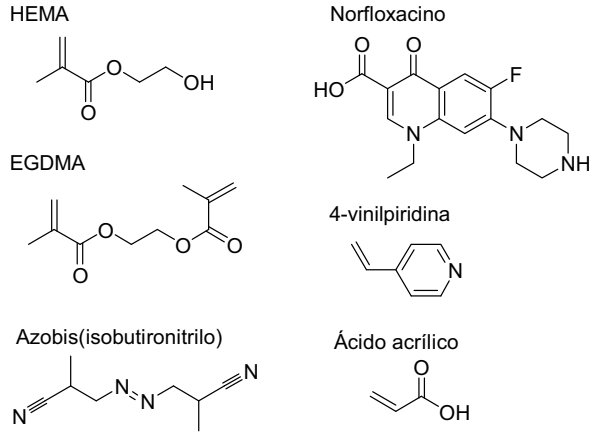

Figura 4.1. *Estructura del fármaco y de los monómeros.*

4.1.1. Hidrogeles no *imprinted*

Con el fin de delimitar la utilidad del AAc y la VP como monómeros funcionales, se prepararon en primer lugar hidrogeles no *imprinted* de 0.9 mm de espesor con distintas proporciones de cada uno de estos monómeros (0, 50, 100 y 200 mM). Los hidrogeles se lavaron con agua a ebullición, que es un procedimiento de esterilización habitual para las lentillas, y se cortaron en discos de 10 mm (peso medio 70±10 mg).

En los espectros IR de los hidrogeles secos, no se detectaron bandas de absorción a 1638 cm^{-1} y a 950 cm^{-1}, lo que puso de manifiesto la ausencia de centros reactivos y de monómeros residuales (Figura 4.2). Las bandas más intensas correspondieron a los grupos éster (1729 cm^{-1}) y éter (1275, 1159, 1075 cm^{-1}) de HEMA (Sellergren y Hall, 2001). Todos los hidrogeles mostraron, además, una elevada transparencia a la luz visible.

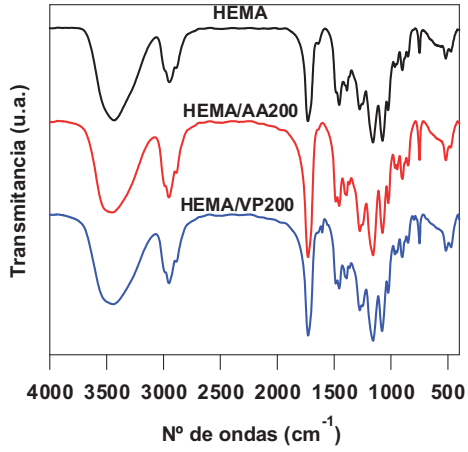

Figura 4.2. *Espectros IR de muestras de hidrogeles secos de HEMA sin comonómero o con AAc o VP.*

Los reogramas de cizalla oscilatoria mostraron que, a temperatura ambiente, los hidrogeles secos presentan la elevada rigidez que es característica del polihidroxietilmetacrilato (pHEMA), con valores de G´ más altos que de G´´ (Figura 4.3). A medida que se incrementa la temperatura, los dos módulos descienden, observándose un punto de corte a 120-130ºC, que se manifiesta como un máximo en el valor de tan δ y es indicativo de que a esta temperatura tiene lugar una transición vítrea (Figura 4.3).

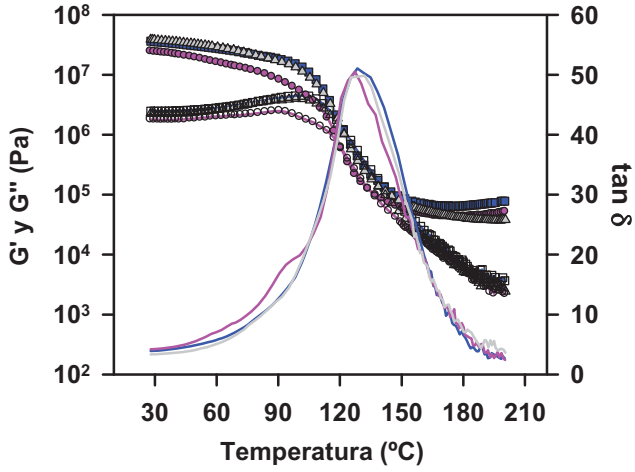

Figura 4.3. *Influencia de la temperatura en los módulos elástico (G', símbolos llenos) y viscoso (G´´, símbolos huecos) de hidrogeles de HEMA sin comonómero (gris), con AAc 100 mM (rosa) o con VP 100 mM (azul).*

Los hidrogeles mostraron una temperatura de transición vítrea, Tg confirmada por DSC, con un valor próximo al recogido en la bibliografía para el pHEMA (Di Marco y col., 1994) y que resultó ser independiente del contenido en AAc o VP. Una vez hidratados, mostraron una marcada flexibilidad como consecuencia del efecto plastificante del agua. Los valores de G´ y G´´ se situaron en el intervalo comprendido entre 10^4 y 10^6 Pa (Figura 4.4), que es característico de los entramados poliméricos uniformemente reticulados y con notable resistencia

mecánica, lo que los hace aptos para su manejo y los dota de una elevada capacidad para adaptarse a la forma de los tejidos biológicos sin causar fricción mecánica (Refojo y Leong, 1981).

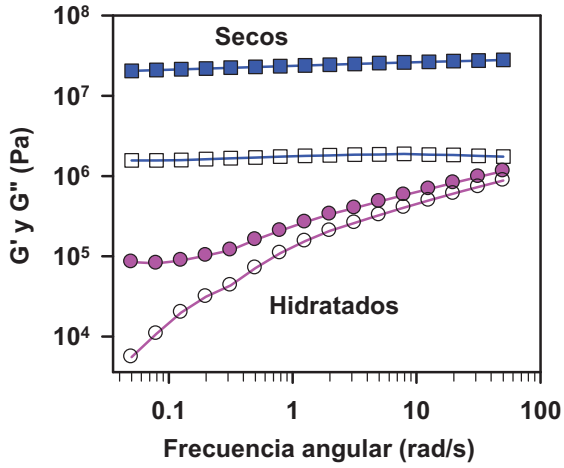

Figura 4.4. *Dependencia de los módulos elástico (G', símbolos llenos) y viscoso (G'', símbolos huecos) respecto de la frecuencia angular de hidrogeles de HEMA con AAc 100 mM, secos y una vez hidratados.*

La capacidad de incorporación de agua y la velocidad de hidratación fueron ligeramente más altos en los hidrogeles preparados con AAc (Q= 60 ±5 %), que en los preparados con el monómero menos hidrofílico VP (Q= 55 ±5 %). Los hidrogeles son capaces de incorporar cantidades de agua ligeramente superiores a su peso seco, ajustándose el proceso a una cinética tipo raíz cuadrada (r^2>0.97), lo que indica que la penetración del agua se produce principalmente por difusión Fickiana. Los valores de las constantes de velocidad indican que las moléculas de agua penetran con gran facilidad en la estructura de los hidrogeles con AAc (4.7 ±0.2 % $s^{-0.5}$) o con VP (4.0 ±0.1 % $s^{-0.5}$). Por lo tanto, desde el punto de vista de su posible utilización como componente de lentes de contacto, estos hidrogeles presentan unas características estructurales y mecánicas muy adecuadas.

La capacidad de los hidrogeles para incorporar norfloxacino se evaluó por inmersión en disoluciones de fármaco 0.025, 0.05 y 0.10 mM. Los hidrogeles elaborados con AAc mostraron una intensa afinidad por el fármaco (Figura 4.5), absorbiéndolo en su práctica totalidad (aprox. 90% en el caso de pHEMA-AAc 200 mM) de la disolución de carga. Los hidrogeles preparados con VP incorporaron cantidades mucho más bajas de norfloxacino, aunque muy superiores que los hidrogeles de HEMA sintetizados sin comonómero funcional (Tabla 4.1). Sólo los hidrogeles preparados con AAc 100 ó 200mM fueron capaces de incorporar en cada disco cantidades superiores a 0.18 mg, que es la dosis habitual cuando el fármaco se administra en forma de colirio, instilando 2 gotas de 25 µl cada hora durante 24 h, y que el 5% de la dosis instilada penetra a través de la cornea.

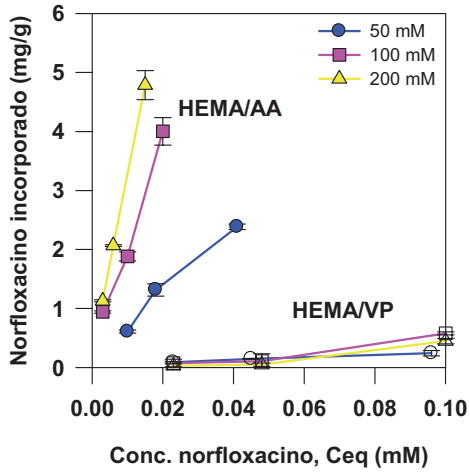

Figura 4.5. *Isotermas de absorción de norfloxacino en hidrogeles de HEMA con AAc (símbolos llenos) o VP (símbolos vacíos).*

Hidrogeles de PHEMA	NORFLOXACINO		
	0.025 mM	0.05 mM	0.100 mM
EGDMA80-control	0.005 (0.001)	0.009 (0.002)	0.018 (0.002)
EGDMA80-VP50	0.088 (0.014)	0.146 (0.007)	0.241 (0.045)
EGDMA80-VP100	0.074 (0.065)	0.106 (0.062)	0.579 (0.025)
EGDMA80-VP200	0.029 (0.030)	0.048 (0.029)	0.447 (0.045)
EGDMA80-AAc50	0.668 (0.118)	1.315 (0.104)	2.384 (0.045)
EGDMA80-AAc100	0.942 (0.020)	1.883 (0.077)	4.003 (0.232)
EGDMA80-AAc200	1.129 (0.018)	2.067 (0.013)	4.786 (0.247)

Tabla 4.1. *Cantidad de norfloxacino incorporado (mg/g gel seco) a los hidrogeles tras su inmersión en disoluciones de fármaco de distinta concentración.*

Los resultados comentados ponen de manifiesto que el AAc desempeña un papel muy importante en el proceso de incorporación de norfloxacino, participando en el establecimiento de interacciones electrostáticas con el grupo amino y de asociaciones por puentes de hidrógeno con otros grupos funcionales del fármaco. En cambio, las asociaciones hidrofóbicas que puede establecer la VP con el norfloxacino no son suficientemente fuertes como para que se promueva eficazmente la carga. La intensidad de las interacciones de norfloxacino con el AAc explica que los hidrogeles elaborados con este monómero cedan lentamente el fármaco en fluido lacrimal, sosteniéndose el proceso durante 12 h (Figura 4.6).

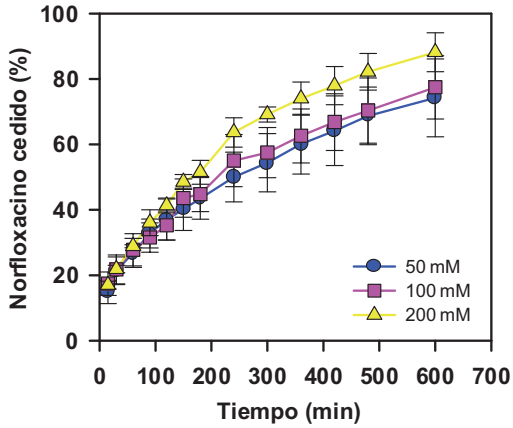

Figura 4.6. *Perfiles de cesión en fluido lacrimal de hidrogeles no imprinted sintetizados con las proporciones de AAc que se indican y cargados por inmersión en una disolución de norfloxacino 0.10 mM.*

4.1.2. Hidrogeles *imprinted*

La optimización mediante técnicas de moldeado molecular se centró en los hidrogeles que incorporan AAc como comonómero funcional. El logro de los objetivos que se persiguen con el moldeado molecular sólo es posible si se cumplen las condiciones siguientes:

i) el fármaco es estable en las condiciones de polimerización. El norfloxacino se disuelve con facilidad en HEMA y presenta una notable estabilidad química, que permite descartar cualquier posibilidad de que se produzcan procesos degradativos a la temperatura a la que transcurre el proceso (Sustar y col., 1993).

ii) el fármaco y los monómeros funcionales dan lugar a la formación de complejos y se han de incorporar a la mezcla de polimerización en proporciones adecuadas a su estequiometría. Para elucidar la proporción óptima norfloxacino:AAc se aplicó la microcalorimetría isotérmica, que aporta información sobre la energía asociada a los procesos de interacción fármaco:monómero (O´Brien y col., 2002; Fish y col., 2005).

iii) la proporción de agente reticulante es mayor que la de monómero funcional. Por lo tanto, para la preparación de los hidrogeles con AAc 100mM y 200mM, se incorporó EGDMA en concentración 160 mM y 320 mM, respectivamente.

En primer lugar, se llevó a cabo una valoración calorimétrica de norfloxacino con AAc para establecer la energía asociada a la interacción y la estequiometría de los complejos (VP-ITC, MicroCal Inc.; Northampton, MA). El ensayo se llevó a cabo con 0.290 ml de una disolución AA 0.50 M en HEMA en el inyector y 1.439 ml de disolución de norfloxacino 0.01M en HEMA en la cubeta receptora. Una vez estabilizado el sistema a 25ºC, se inició el vertido de la disolución de AAc en pulsos de 1 μL a intervalos de 5 min. La entalpía asociada al proceso de interacción se estimó, utilizando el programa Microcal Origin, a partir del perfil de valoración, una vez corregido el efecto que produce la simple dilución de la disolución de AAc en el medio disolvente (HEMA). En la figura 4.7 se muestra el perfil calorimétrico obtenido. Entre norfloxacino y AAc se produce una interacción exotérmica. Para la relación molar 1:1 se observa un punto de inflexión y la incorporación de cantidades adicionales de AAc da lugar a intercambios energéticos cada vez menores. El proceso se satura cuando se alcanza una relación molar norfloxacino:AAc 1:4. A la vista de estos resultados, se concluye que esta relación es *a priori* la más adecuada para conseguir la formación de cavidades con elevada afinidad por norfloxacino. Con un contenido más bajo en AAc, la capacidad de interacción de norfloxacino no estará totalmente cubierta; mientras que si la proporción de AAc es más alta, una parte de los monómeros funcionales no podrá llegar a establecer interacciones con moléculas de fármaco durante la síntesis, con lo que se distribuirán aleatoriamente en el hidrogel.

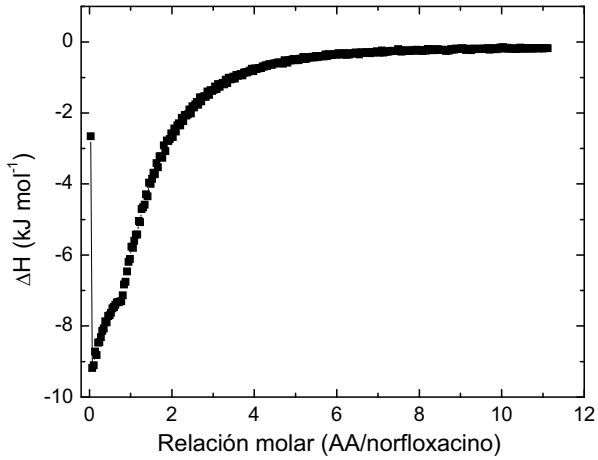

Figura 4.7. *Perfil obtenido en la valoración calorimétrica del proceso de interacción de norfloxacino con AAc en medio HEMA, a 25ºC.*

Tomando como base la información comentada y con el fin de confirmar experimentalmente la relación óptima para formar cavidades con afinidad por el norfloxacino elevada, se sintetizaron hidrogeles *imprinted* de HEMA con la composición que se indica a continuación:

i) 100 mM AAc, 160 mM EGDMA y relación molar norfloxacino:AAc 1:2, 1:3, 1:4, 1:6, 1:8, 1:10 y 1:12.

ii) 200 mM AAc, 320 mM EGDMA y relación molar norfloxacino:AAc 1:4, 1:6, 1:8, 1:10, 1:12 y 1:16.

En todos los casos se obtuvieron materiales transparentes, con aspecto y propiedades mecánicas idénticas a las de los hidrogeles no *imprinted*. La capacidad de incorporación de agua tampoco se vio modificada por el moldeado molecular (Figura 4.8). Los espectros IR confirmaron la ausencia de monómeros residuales.

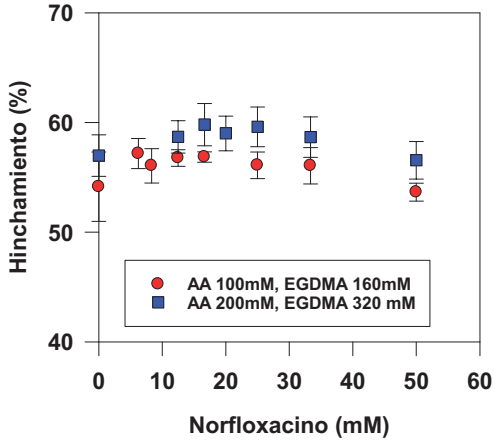

Figura 4.8. *Influencia de la concentración de norfloxacino en la mezcla de polimerización sobre la capacidad de hinchamiento de los hidrogeles de HEMA con AAc.*

En la figura 4.9 se muestra la influencia de la concentración de norfloxacino en la mezcla de polimerización sobre la capacidad de los hidrogeles de HEMA preparados con AAc 200 mM para captar el fármaco. El moldeado molecular incrementó notablemente la capacidad de incorporación de fármaco de los hidrogeles, sobre todo cuando la síntesis se llevó a cabo con bajas proporciones de norfloxacino.

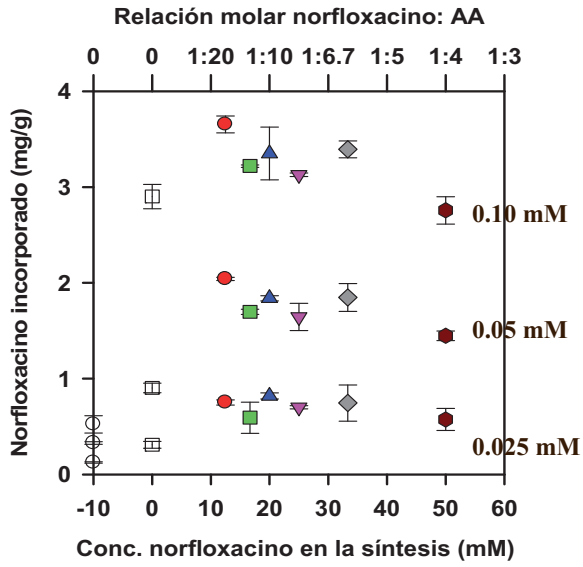

Figura 4.9. *Capacidad de incorporación de norfloxacino de hidrogeles HEMA con AAc 200 mM y EGDMA 320 mM sintetizados en presencia de fármaco y cargados por inmersión en disoluciones de norfloxacino 0,025, 0,050 y 0,10 mM. También se muestran los resultados obtenidos con hidrogeles sintetizados sin AAc (círculos abiertos sobre el eje de coordenadas).*

Los hidrogeles preparados con la relación estequiométrica 1:4, que de acuerdo con los resultados de la valoración calorimétrica deben contar en sus cavidades con un número de grupos AAc óptimo desde el punto de vista de la interacción con el fármaco, mostraron una capacidad de carga ligeramente inferior a la de los restantes hidrogeles *imprinted.* Si la relación norfloxacino:AAc es más baja, una parte de los grupos AAc del entramado polimérico se distribuyen aleatoriamente y pueden formar de complejos de estequiometría 1:2 ó 1:3. Por lo tanto, en estos hidrogeles el número de puntos de unión accesibles será mayor, lo que facilitará la incorporación de más moléculas de fármaco.

Para evaluar la capacidad de reconocimiento selectivo de norfloxacino por los hidrogeles, se llevó a cabo un estudio de absorción de timolol, una molécula de dimensiones similares, que también puede interaccionar con AAc (Figura 4.10).

Los hidrogeles *imprinted* para norfloxacino mostraron una capacidad de incorporación de timolol similar a la de los hidrogeles no *imprinted*, y muy inferior en todos los casos a la capacidad de carga de norfloxacino (Figura 4.11), lo que confirma la selectividad de los hidrogeles obtenidos.

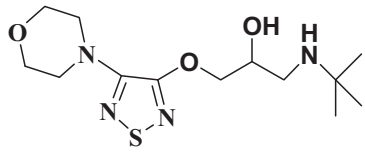

Figura 4.10. *Estructura del timolol.*

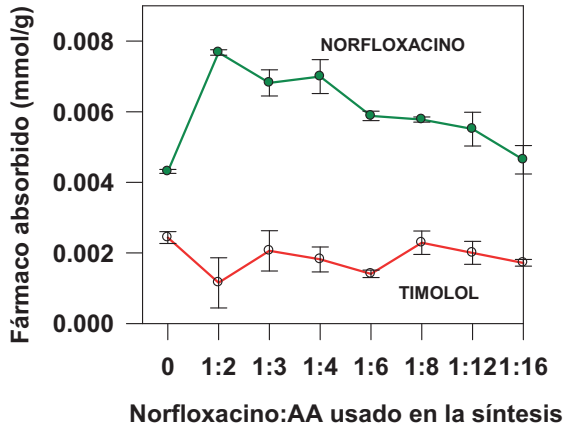

Figura 4.11. *Adsorción de timolol maleato y norfloxacino por hidrogeles de HEMA con AAc 100 mM y EGDMA 160 mM, sumergidos en disoluciones de uno u otro fármaco de concentración 0.05 mM.*

En la figura 4.12, se muestran, a modo de ejemplo, los perfiles de cesión de los hidrogeles cargados por inmersión en disolución 0.10 mM de norfloxacino.

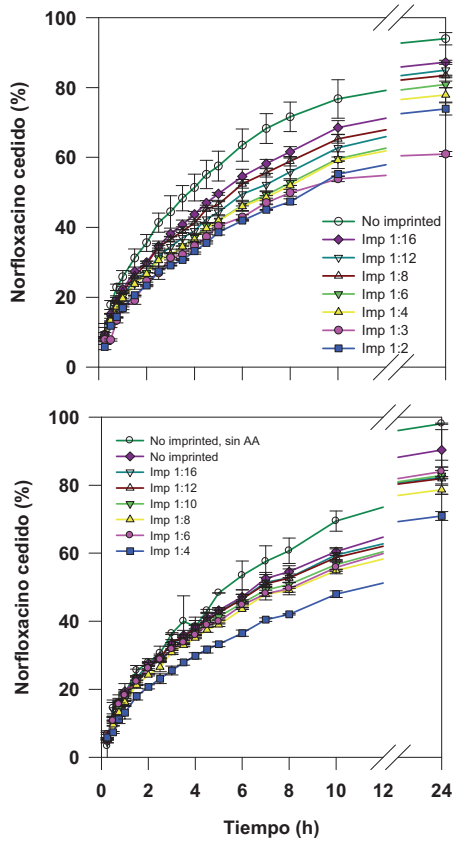

Figura 4.12. *Cesión de norfloxacino en fluido lacrimal artificial a partir de hidrogeles de HEMA con AAc 100mM y EGDMA 160 mM (gráfico superior) o de HEMA con AAc 200 mM y EGDMA 320 mM (gráfico inferior).*

La proporción de norfloxacino en la mezcla de polimerización ejerció una marcada influencia sobre la cesión. En todos los casos, los hidrogeles *imprinted* cedieron más lentamente el fármaco que los hidrogeles convencionales de HEMA sin o con AAc, llegando a prolongarse el proceso durante 72 h en el caso de los hidrogeles imprinted preparados con relaciones molares norfloxacino:AAc 1:3 y 1:4 y cargados en disolución de norfloxacino 0.1 mM. Los perfiles observados para los hidrogeles cargados en disoluciones 0.025 mM y 0.05 mM mostraron una tendencia similar.

En resumen, la incorporación de AAc a entramados de pHEMA y la aplicación de técnicas de moldeado molecular permite desarrollar hidrogeles con una elevada capacidad de carga de norfloxacino (hasta 300 veces mayor que la de los hidrogeles de pHEMA convencionales) y que son capaces de prolongar la cesión de fármaco durante 48-72 h. La relación fármaco:monómero funcional condiciona la estructura de las cavidades y es una variable crítica en la optimización de estos sistemas.

4.2. Desarrollo de lentes de contacto *imprinted* con timolol. Establecimiento por ITC de la relación óptima monómero funcional/fármaco.

La primera aplicación del moldeado molecular en el desarrollo de lentes de contacto medicadas se centró en el timolol (Alvarez-Lorenzo y col., 2002). Esta aproximación permitió obtener hidrogeles de HEMA o de N,N-dietilacrilamida (DEAA), con una baja proporción de ácido metacrílico (MAA; 1.28-5.12 %-mol) y de agente reticulante (0.32-8.34 %-mol), que se mostraron adecuados para cargar timolol y cederlo de forma controlada (Alvarez-Lorenzo y col., 2002; Hiratani y Alvarez-Lorenzo, 2002). Las lentes de contacto basadas en estos hidrogeles proporcionaron *in vivo* niveles de fármaco en fluido lacrimal más elevados y sostenidos que los que se consiguen con colirios comerciales de timolol (Hiratani y col., 2005a). El objetivo de la segunda etapa de la Tesis fue profundizar en el diseño de lentes de contacto imprinted con timolol explorando la influencia de la relación timolol:AAc en la mezcla de polimerización y el efecto del espesor de la lámina de hidrogel sobre la carga y la cesión del fármaco.

Para ello, en primer lugar se llevó a cabo una valoración microcalorimétrica de timolol con AAc en HEMA, siguiendo un procedimiento similar al descrito en

el apartado anterior. El timolol se puede comportar como dador y como aceptor en la formación de enlaces por puentes de hidrógeno, por lo que el AAc se presenta a priori un buen monómero funcional para este fármaco. El perfil de ITC (Figura 4.13) puso de manifiesto que la interacción entre el fármaco y el AAc es fuertemente exotérmica, con un máximo de entalpía para la relación molar timolol:AAc 1:2. La interacción no se satura hasta la relación 1:8. Tomando como base estos resultados se prepararon hidrogeles con AAc 200 mM y relaciones molares timolol:AAc dentro del intervalo 1:6 a 1:32. Dado que la solubilidad del maleato de timolol en HEMA es 33.3 mM, se seleccionó esta concentración, que corresponde a una relación molar timolol:AAc 1:6, como la más alta para la preparación de los hidrogeles.

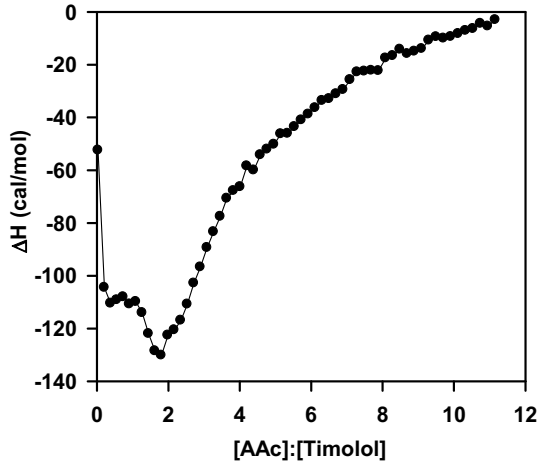

Figura 4.13. *Valoración calorimétrica de timolol con AAc en medio HEMA, a 25ºC.*

Después de eliminar el fármaco molde y los monómeros residuales con agua a ebullición, los hidrogeles se lavaron con disoluciones acuosas de distinta concentración salina. A continuación se llevaron a cabo ensayos de hinchamiento. Todos los hidrogeles resultaron ser completamente transparentes y captaron cantidades similares de agua (Figura 4.14), aunque se observaron algunas

diferencias en la velocidad de hinchamiento dependiendo de la proporción de timolol en la mezcla de polimerización (Figura 4.15).

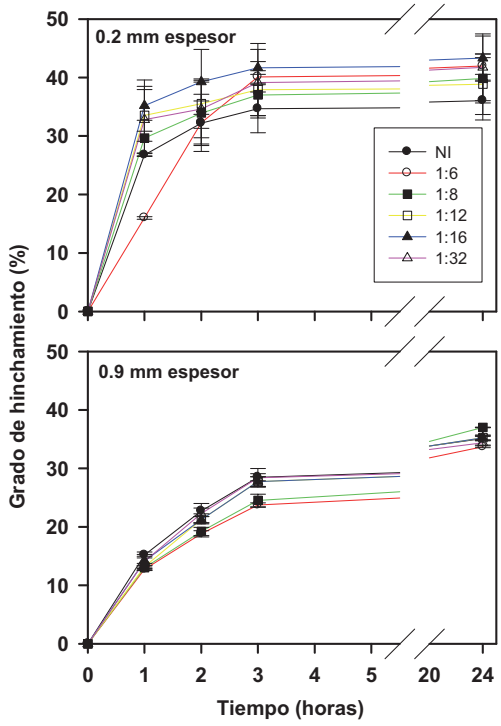

Figura 4.14. *Perfiles de hinchamiento en agua a 25ºC de hidrogeles de pHEMA con AAc 200 mM y diferente grosor, sintetizados a partir de mezclas de polimerización con distintos contenidos en timolol.*

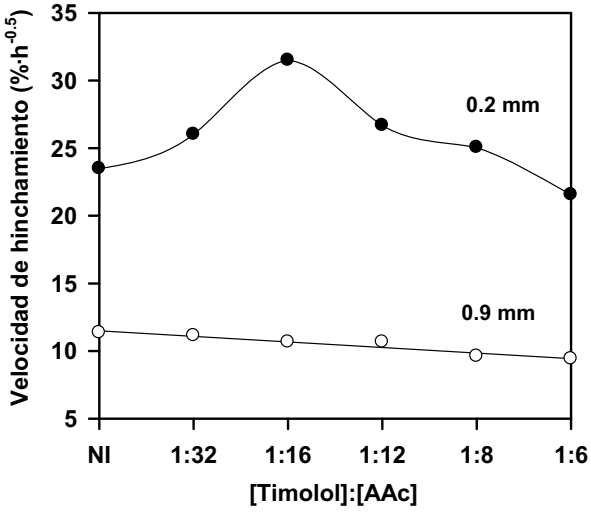

Figura 4.15. *Dependencia de la velocidad de hinchamiento de hidrogeles de pHEMA con AAc 200 mM y diferente grosor, caracterizada ajustando la incorporación de agua a la cinética de la raíz cuadrada (r^2 > 0.97), respecto de la proporción de timolol incorporada al hidrogel durante la síntesis.*

Las diferencias en la velocidad de hinchamiento, aunque de escasa magnitud revelaron que los hidrogeles imprinted preparados con la relación molar timolol:AAc 1:6 necesitan más tiempo para hinchar. La entrada de agua depende del camino difusional condicionado, sobre todo, por el espesor del hidrogel y de los cambios conformacionales que experimentan las cadenas de polímero al hidratarse, que se pueden ver afectados por la distribución espacial de los monómeros ionizables. En el caso de los hidrogeles imprinted 1:6, las cavidades pueden contar con 6 unidades de AAc bastante próximas entre sí e interaccionando entre ellas mediante puentes de hidrógeno. Las cavidades imprinted con un mayor número de unidades AAc presentarán, por efecto de las fuerzas de repulsión, una disposición más abierta. Por otra parte, y como ya se ha comentado en el apartado anterior, cuanto más baja es la relación molar

timolol:AAc, mayor es la tendencia de las unidades de AAc a distribuirse de manera aleatoria.

Para evaluar la afinidad por el timolol, los hidrogeles se sumergieron en disoluciones con distinta concentración de fármaco. Dado que la composición monomérica de todos los hidrogeles, incluidos los no imprinted, es la misma y que en el equilibrio su grado de hinchamiento fue similar, las diferencias que se observaron en la cantidad de timolol incorporado (Figura 4.16) deben tener su origen en cambios en la disposición espacial de los monómeros funcionales promovidos por el timolol durante la polimerización. La carga de fármaco fue superior en dos órdenes de magnitud a la estimada asumiendo que el fármaco se aloja exclusivamente en la fase acuosa de los hidrogeles (0.007, 0.010, 0.014, y 0.017 mg/g para los hidrogeles sumergidos en disoluciones de timolol 0.04, 0.06, 0.08 y 0.10 mM, respectivamente). En un estudio previo se comprobó que los valores calculados por este procedimiento coinciden con los que se alcanzan cuando se cargan hidrogeles de pHEMA que no cuentan en su estructura con monómero funcional. Por lo tanto, se puede concluir que la presencia de AAc en el entramado polimérico incrementa notablemente la afinidad de los hidrogeles por el timolol.

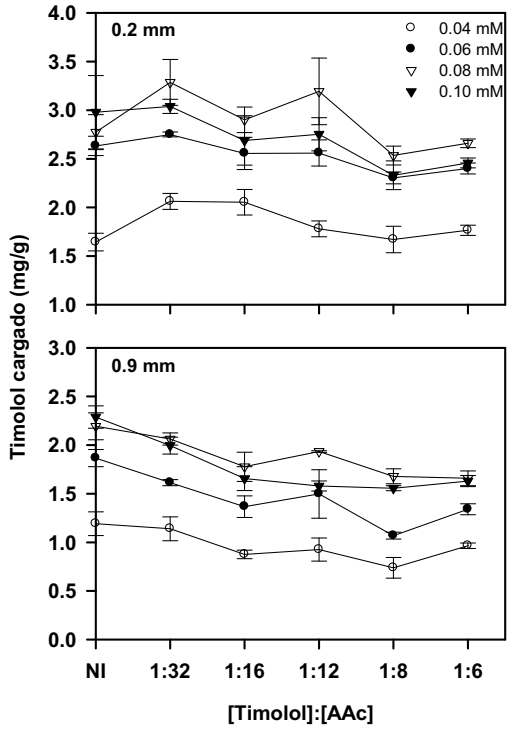

Figura 4.16. *Timolol incorporado a hidrogeles imprinted y no imprinted de pHEMA con AAc 200 mM y de distintos espesor. La carga se llevó a cabo utilizando disoluciones con la concentración que se indica.*

Aunque en general la cantidad de timolol cargada aumenta con la concentración de la disolución de fármaco, la similitud de los resultados obtenidos con las disoluciones de timolol 0.08 y 0.10 mM indica que los hidrogeles están próximos a saturarse. Por otra parte, para cada concentración de la disolución de timolol, se observó un descenso progresivo de la cantidad cargada a medida que se fue incrementando desde 1:32 a 1:6 la relación molar timolol:AAc. Este efecto es similar al que se encontró con el norfloxacino y se explica porque los grupos funcionales (presentes en el mismo número en todos los hidrogeles) se agrupan de distinta manera para formar el lugar de unión dependiendo de la relación molar fármaco:monómero funcional. En los hidrogeles no imprinted, los grupos AAc están distribuidos aleatoriamente y cada uno de ellos constituye de manera

individual un posible lugar de unión. En cambio, en los hidrogeles imprinted 1:6 y 1:8, cada lugar de unión está formado por seis u ocho unidades de AAc, que es la relación identificada por ITC como óptima para que se establezcan interacciones con timolol. Los hidrogeles preparados con proporciones comprendidas entre las de los no imprinted y los imprinted 1:6 y 1:8, es decir los hidrogeles imprinted 1:12 a 1:32, pueden tener cavidades con seis u ocho AAc junto con otras más imperfectas, construidas con los grupos AAc remanentes, algunos de los cuales se encontrarán individualizados o formando dímeros. Por lo tanto, cuando los hidrogeles se sumergen en la disolución de timolol, las moléculas de fármaco se pueden alojar en las cavidades imprinted (preferentemente en las de estequiometria 1:6 ó 1:8) y pueden interaccionar con los grupos AAc distribuidos de manera aleatoria, previsiblemente con una estequiometria 1:1 ó 1:2. Esto conduce a que se cargue una mayor cantidad de fármaco, que se aproxima a la que incorporan los hidrogeles no imprinted. Por lo tanto, cuanto menos fármaco seadiciona antes de la polimerización, más reducido es el número de cavidades imprinted y más alto el de puntos de unión no imprinted.

La velocidad de incorporación de fármaco a los hidrogeles resultó ser muy dependiente de su grosor. En las primeras 48 horas, la cantidad cargada se aproximó al 75% del valor alcanzado en el equilibrio con los hidrogeles de 0.2 mm, y al 50% en el caso de los hidrogeles de 0.9 mm. Para alcanzar el equilibrio se requirieron, respectivamente, 6 y 18 días, un tiempo considerablemente superior al necesario para completar el hinchamiento. Esto indica que el fármaco difunde a través del hidrogel más lentamente que el agua, debido a su mayor tamaño molecular (432.5 Da). Además, la interacción con los grupos AAc y el alojamiento del timolol en las cavidades imprinted puede requerir algún tiempo. En cualquier caso, el bajo grado de reticulación de los hidrogeles implica que la malla polimérica no suponga un obstáculo relevante frente a la difusión del

fármaco hacia el interior del entramado. En estudios previos se ha puesto de manifiesto la importancia de mantener la lente sumergida en la disolución de carga durante un tiempo suficiente para que el fármaco alcance sus capas más profundas (Jain, 1988; Lesher y Gunderson, 1993). De esta manera, a medida que el fármaco se va cediendo hacia el medio desde los estratos más superficiales de la lente, se puede ir reponiendo por nuevas moléculas procedentes de estratos más profundos, que actúan como reservorio, haciendo posible una cesión sostenida y reproducible. Teniendo en cuenta estos hechos, antes de llevar a cabo los estudios de cesión los hidrogeles se cargaron durante el tiempo necesario para alcanzar el equilibrio.

Los ensayos de cesión se llevaron a cabo utilizando disoluciones salinas isotónicas de fuerza iónica y pH similares a los del fluido lacrimal. Aunque es previsible que los iones induzcan la ionización del AAc perturbando su unión al timolol, en ningún caso se observó efecto burst, sosteniéndose la cesión durante un día con los de 0.2 mm y durante diez días con los de 0.9 mm de espesor. Para facilitar el análisis visual de los resultados, en la Figura 4.17 se muestran los perfiles normalizados por el espesor sólo para los hidrogeles que mostraron un comportamiento extremo.

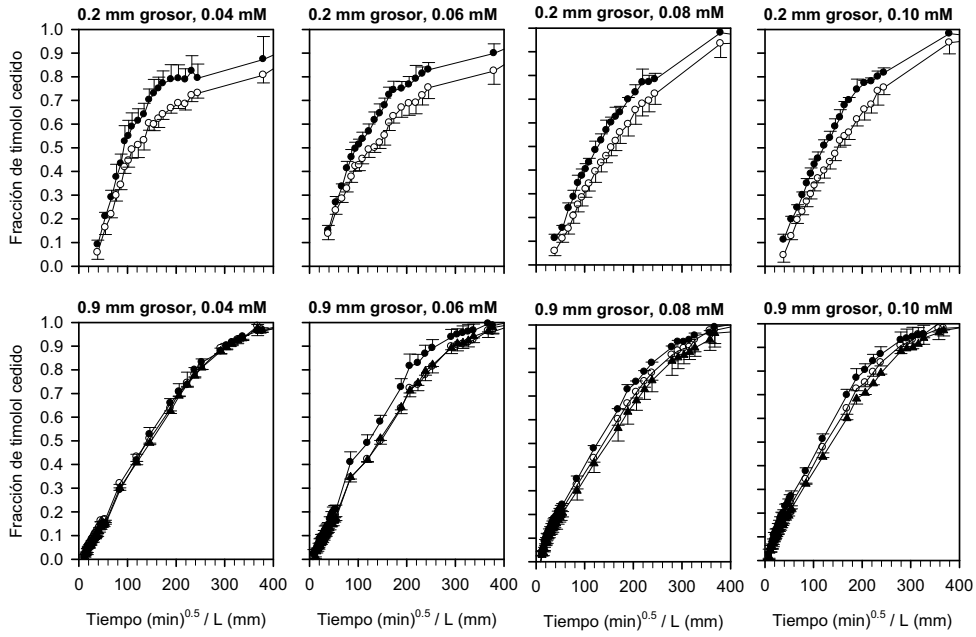

Figura 4.17. *Perfiles de cesión de timolol a 37ºC a partir de hidrogeles no imprinted (círculos negros), imprinted 1:6 (círculos blancos) e imprinted 1:16 (triángulos) de diferente espesor en NaCl al 0.9%. El fármaco se cargó por inmersión en disoluciones de concentración 0.04, 0.06, 0.08 y 0.10 mM.*

Las constantes de velocidad de cesión de timolol obtenidas por ajuste a la cinética de la raíz cuadrada se muestran en la Tabla 4.2. En el caso de los hidrogeles más finos, el timolol se cedió de manera significativamente más rápida a partir de los no imprinted que desde los imprinted 1:6 y 1:8. Los restantes hidrogeles de 0.2 mm mostraron un comportamiento intermedio. Estos resultados prueban que cuanto más perfectas son las cavidades imprinted, mayor es su afinidad por el timolol y, consecuentemente, mayor su capacidad para retener el fármaco. El efecto imprinting se atenuó en los hidrogeles más gruesos. Hay que tener en cuenta que la velocidad de cesión está condicionada por dos factores: i) la afinidad del fármaco por las cavidades imprinted, y ii) la longitud del camino

difusional a través del entramado del hidrogel. La contribución de este último factor se va haciendo más importante a medida que el grosor del hidrogel se incrementa. De hecho, con los hidrogeles de 0.9 mm, se observó que cualquier hidrogel imprinted cede el timolol a una velocidad sólo ligeramente más lenta que el correspondiente hidrogel no imprinted. La cesión de timolol a partir de los hidrogeles más gruesos se produce de manera que las moléculas de fármaco tienen más posibilidades de encontrar cavidades imprinted o, en el peor de los casos, unidades de AAc más o menos agrupadas, durante su desplazamiento hacia la superficie. El fármaco se puede alojar en una cavidad y, una vez que sale de ella, es probable que llegue a otra región de alta afinidad y así sucesivamente. Las interacciones sucesivas con las cavidades imprinted o con los grupos AAc contribuirán a hacer este movimiento más lento. Cuanto mayor es el número de cavidades disponibles, más alta es la probabilidad de que una molécula de fármaco quede retenida en una de ellas. Entre los hidrogeles de 0.9 mm de espesor, los imprinted 1:16 parecen ser los más eficientes desde este punto de vista. Como ya se ha resaltado, en la microestructura de estos hidrogeles se combinan cavidades imprinted 1:6 ó 1:8 (óptimamente construidas) con cavidades con menos unidades de AAc. Estos resultados están en consonancia con los encontrados previamente con hidrogeles preparados con N-dimetil acrilamida y tris(trimetiloxi)sililpropil metacrilato e imprinted también con timolol (Hiratani y col., 2005a). Los hidrogeles imprinted con una relación molar timolol:ácido metacrílico 1:16 proporcionaron un mejor control de la cesión de fármaco que los obtenidos utilizando una proporción de timolol más alta y que los no imprinted.

Concentración de carga (mM)	No imprinted	1:32 Imprinted	1:16 Imprinted	1:12 Imprinted	1:8 Imprinted	1:6 Imprinted
0.2 mm de grosor						
0.04	0.067	0.063	0.061	0.052	0.051	0.051
0.06	0.048	0.044	0.044	0.040	0.036	0.034
0.08	0.043	0.045	0.041	0.040	0.034	0.036
0.10	0.044	0.046	0.041	0.041	0.039	0.037
0.9 mm de grosor						
0.04	0.0084	0.0081	0.0079	0.0079	0.0080	0.0080
0.06	0.0096	0.0084	0.0081	0.0079	0.0080	0.0078
0.08	0.0087	0.0077	0.0075	0.0081	0.0079	0.0080
0.10	0.0091	0.0086	0.0079	0.0079	0.0078	0.0085

Tabla 4.2. *Constantes de velocidad de cesión de timolol (horas$^{-1/2}$) obtenidas mediante ajuste de los perfiles a la cinética de la raíz cuadrada.*

En su conjunto, los resultados obtenidos en los estudios llevados a cabo en las dos primeras etapas de la Tesis con norfloxacino y timolol, ponen de manifiesto que la relación fármaco:monómero funcional es una variable crítica para la optimización de las propiedades de carga y cesión a partir de hidrogeles *imprinted*. El éxito en la consecución de hidrogeles con capacidad para controlar la cesión está directamente ligado a la formación de cavidades con elevada afinidad. Por lo tanto, la utilización de relaciones fármaco:monómero funcional adecuadas, durante el proceso de síntesis, resulta crucial. La microcalorimetría isotérmica, que permite establecer la estequiometría de los complejos fármaco:monómero funcional, se ha mostrado como una técnica muy útil para diseñar la preparación de hidrogeles por moldeado molecular sobre una base racional y conseguir la formación de cavidades "a medida" para fármacos concretos.

4.3. Desarrollo de lentes de contacto confortables de pHEMA semi-interpenetrado con polivinil pirrolidona (PVP).

De unos años a esta parte, las lentes de contacto cargadas con demulcentes están recibiendo una atención creciente dado que, además de ser más cómodas, abren nuevas posibilidades en el tratamiento del síndrome de ojo seco. Bajo este término se agrupan diversas enfermedades de la superficie ocular que tienen como rasgo común la formación de una película de fluido lacrimal de características anormales sobre la superficie del ojo, lo que causa una inadecuada lubrificación (Johnson y Murphy, 2004). Cuando, como ocurre en los pacientes que sufren el síndrome de ojo seco, se pierde la homeostasis por un aporte insuficiente, una pérdida excesiva o una composición anómala del fluido lacrimal, la capacidad de éste para proteger el epitelio de la córnea disminuye. Como consecuencia de ello, se producen epiteliopatías, hiperosmolaridad de la lágrima, inestabilidad del film pre-ocular, e irritación e inflamación ocular relativamente intensas (Lemp, 1995). El síndrome de ojo seco afecta al 10-20% de la población adulta (Johnson y Murphy, 2004) con una prevalencia que alcanza al 70% en los usuarios de lentes de contacto (Maruyama y col., 2004). La prevención y el tratamiento del síndrome de ojo seco encierran una notable complejidad y requieren actuaciones a distintos niveles (Lemp, 1995). La aplicación de gotas de disoluciones de polímeros hidrofílicos o “lágrimas artificiales” permite estabilizar la película de fluido lacrimal, lubrificar la lente y reducir la fricción con los fluidos oculares, facilitando la expulsión de cuerpos extraños. En comparación con la aplicación intermitente de lágrimas artificiales, una cesión sostenida del demulcente a partir de la lente de contacto puede producir un efecto lubrificante más eficaz mimetizando la función fisiológica del fluido lacrimal. Tomando como punto de partida estos hechos, el objetivo de la tercera etapa de la Tesis fue desarrollar lentes de contacto interpenetradas con el polímero demulcente polivinil

pirrolidona (PVP), y delimitar el efecto de la proporción y el peso molecular de la PVP y de la porosidad de los entramados sobre la velocidad de cesión del demulcente y el coeficiente de fricción de las lentes.Una práctica habitual en la síntesis de lentes de contacto consiste en incorporar agua en pequeña proporción a las mezclas de monómeros con el fin de ajustar su porosidad para que resulten más permeables al oxígeno y a los nutrientes. Por esta razón, se incluyó en el estudio la síntesis de hidrogeles con distintas proporciones de agua y se caracterizó el efecto de esta variable sobre la porosidad y el coeficiente.

El trabajo se inició con la preparación de hidrogeles de pHEMA semi-interpenetrados con PVP en condiciones anhidras y en presencia de agua en distintas proporciones (Tabla 4.3). Los hidrogeles anhidros se obtuvieron disolviendo 0.3, 0.6 ó 0.9 g de PVP K30 (44000-54000 Da) ó 0.3 g de PVP K90F ($1\cdot10^6$-$1.5\cdot10^6$ Da) en 6 mL de HEMA al que previamente se incorporó EGDMA (80 mM) como agente reticulante. Las mezclas se inyectaron en moldes de vidrio ortoédricos con el fin de obtener láminas de hidrogel de 0.9 mm de grosor. Para llevar a cabo la polimerización, las mezclas monoméricas se mantuvieron a 50ºC durante 12 h y a 70ºC durante otras 24 h. Una vez extraídas de los moldes, las láminas se mantuvieron en agua a ebullición durante 15 min con el fin de eliminar monómeros residuales y facilitar el corte en discos de 10 mm de diámetro, que se secaron finalmente a 50ºC.

También se prepararon hidrogeles porosos a partir de HEMA, incorporando como monómero funcional AAc (100 mM) y como agente reticulante EGDMA (80 mM). La disolución monomérica se mezcló con agua en relaciones volumétricas 5.4:0.6, 4.8:1.2, 4.2:1.8, 3.6:2.4, 3:3, y 2.4:3.6. A continuación, se adicionaron 0.9 g de PVP K30 a porciones de 6 ml de estas disoluciones. Una vez homogeneizadas, las mezclas monoméricas se inyectaron en moldes y se procedió

a la polimerización en las condiciones indicadas para los hidrogeles anhidros. El AAc debe contribuir a retener la PVP en el entramado mediante el establecimiento de puentes de hidrógeno entre el anillo pirrolidona y el grupo ácido carboxílico del monómero.

HEMA: agua: PVP	Contenido en PVP esperado (mg/g monomeros más PVP)	Contenido en nitrógeno esperado (%)	Contenido en nitrógeno observado (%)	Porosidad	Constante de velocidad de cesión ($días^{-0.5}$)
6.0: 0: 0	0	0	0	-	---
6.0: 0: 0.3	46.9	0.56-0.59	0.41	-	0.038
6.0: 0: 0.3*	46.9	0.56-0.59	0.59	-	0.039
6.0: 0: 0.6	89.5	1.07-1.15	1.12	-	0.030
6.0: 0: 0.9	128.6	1.54-1.64	1.49	-	0.027
5.4: 0.6: 0.9	142.8	1.71-1.83	1.39	0.020 (0.006)	0.033
4.8: 1.2: 0.9	157.9	1.89-2.02	1.69	0.018 (0.004)	0.026
4.2: 1.8: 0.9	176.5	2.12-2.26	1.67	0.077 (0.012)	0.048
3.6: 2.4: 0.9	200.0	2.40-2.56	2.03	0.132 (0.029)	0.066
3.0: 3.0: 0.9	230.7	2.77-2.95	2.29	0.145 (0.019)	0.059
2.4: 3.6: 0.9	272.7	3.27-3.49	2.72	0.150 (0.025)	0.079

** Se usó PVP K90F en lugar de PVP K30.*

Tabla 4.3. *Composición, contenidos en PVP K30 y nitrógeno, porosidad y constante de velocidad estimada por ajuste de los perfiles de cesión de PVP a la cinética de la raíz cuadrada ($r^2 > 0.95$) de los hidrogeles de pHEMA semi-interpenetrados con PVP.*

La PVP K30 se dispersó fácilmente en HEMA hasta una concentración de 0.15 g/ml; en cambio con PVP K90F (de mayor peso molecular y capacidad viscosizante) no se obtuvieron mezclas homogéneas por encima de los 0.05 g/ml y, por lo tanto, este polímero no se pudo ensayar a concentraciones más altas. Los hidrogeles sintetizados en ausencia de agua resultaron ser completamente

transparentes y mostraron una superficie continua y homogénea. En cambio, los hidrogeles que se prepararon a partir de mezclas monómeros:agua 4.2:1.8 mostraron a simple vista puntos indicativos de separación de fases, que aumentaron en número y dimensiones a medida que se fue incrementando la proporción de agua. Se ha observado previamente que, cuando el volumen de agua es inferior al de saturación del sistema (equilibrio de hinchamiento), no se produce separación de fases en los hidrogeles de pHEMA (Refojo y Yasuda, 1965; Gulsen y Chauhan, 2006). En cambio, por encima de este valor, el agua en exceso se separa del entramado en crecimiento, concentrándose en regiones de tamaño micrométrico que dan lugar a la formación de poros después de la polimerización.

La PVP es el único componente de los hidrogeles que cuenta con nitrógeno en su estructura (12-12.8%). Por lo tanto, para calcular la cantidad de PVP remanente en cada hidrogel tras el lavado en agua a ebullición, se determinó su contenido en nitrógeno por análisis elemental. De los hidrogeles preparados en ausencia de agua, sólo el que incorporó la proporción más baja de PVP K30 mostró una pequeña pérdida de PVP (Tabla 4.3). A medida que la proporción de agua en el medio de polimerización se fue incrementando, se hizo más relevante la cantidad de PVP extraída durante el lavado como consecuencia del efecto del agua sobre el grado de hinchamiento y la porosidad. Aún así, los hidrogeles retuvieron la mayor parte de la PVP. Por otra parte, la PVP no afectó ni a la velocidad de hinchamiento ni al grado de hinchamiento en el equilibrio de los hidrogeles preparados en condiciones anhidras. En cambio, el grado de hinchamiento de los hidrogeles porosos aumentó sensiblemente (del 60% al 100%) a medida que se fue incrementando la proporción de agua incorporada a la mezcla monomérica.

Para calcular la porosidad de los hidrogeles tomando como base el contenido en agua, se acudió a la ecuación de Yanagawa y col. (2006):

$$\varepsilon = (W_w - W_0 - W_{wnp})/W_w \quad \text{(Ec. 4.1)}$$

en la que W_w es el peso del hidrogel poroso hinchado, W_0 el peso del hidrogel poroso seco y W_{wnp} la cantidad de agua en la fase no porosa, que se estimó para cada hidrogel aplicando la expresión:

$$W_{wnp} = (W_{wnh} - W_{dnh}) \cdot W_0 / W_{dnh} \quad \text{(Ec. 4.2)}$$

siendo W_{wnh} y W_{dnh} los pesos del hidrogel no poroso hinchado y seco, respectivamente. En la Tabla 4.3 se resumen los valores de porosidad estimados por medio de este modelo. La incorporación de volúmenes de agua comprendidos entre 1.8 y 3.6 ml de agua causó un incremento progresivo de la porosidad de los hidrogeles hasta alcanzar un 15%.

La transmitancia a 600 nm de los hidrogeles en estado hinchado fue en todos los casos superior al 85%, lo que prueba que la PVP no deteriora la claridad óptica de las lentes. Además, los hidrogeles anhidros preparados sin PVP mostraron una superficie homogénea y sin poros cuando se observaron con SEM (Figura 4.18). La presencia de PVP dio lugar a irregularidades en la superficie de los hidrogeles, debido a que algunas de sus cadenas se incorporan parcialmente al entramado. De hecho, los cortes transversales revelaron una estructura interna homogénea, sin poros y con cadenas de PVP sobresaliendo y formando estructuras en forma de pequeños cepillos en la superficie de la lente. Los hidrogeles preparados con cantidades de agua iguales o superiores a 1.8 ml mostraron una estructura esponjosa con poros interconectados y una superficie con pequeñas

protuberancias de aspecto abombado y con cráteres iniciados en los estratos internos del hidrogel. La formación de estas estructuras está relacionada con la separación, durante la síntesis, de microfases que una vez que se forma el polímero dan lugar a zonas de diferente densidad.

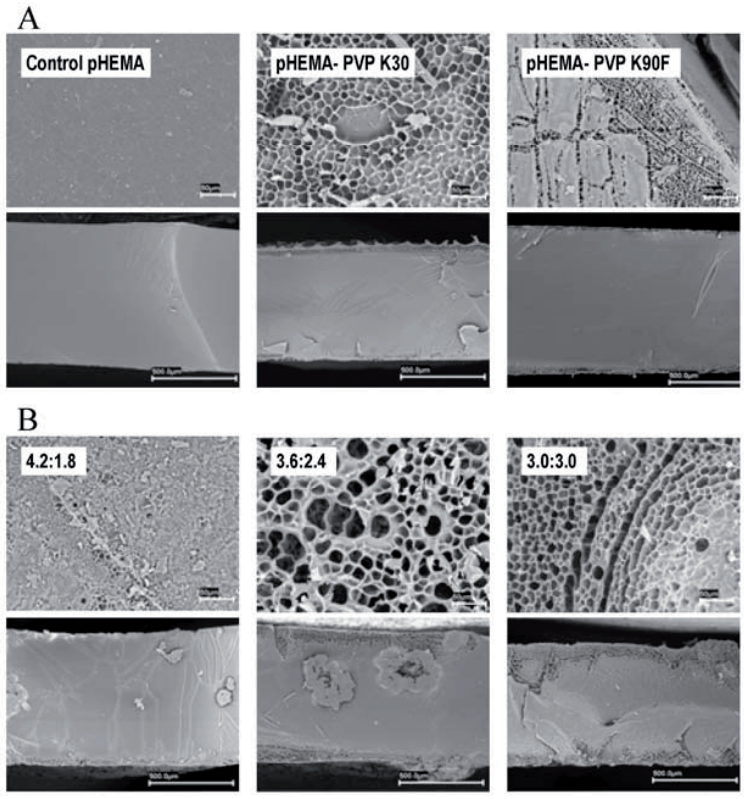

Figura 4.18. *Fotografías SEM de la superficie (fila superior) y de la sección transversal (fila inferior) de (A) hidrogeles de pHEMA sintetizados sin o con PVP K30 o K90F, en ausencia de agua, y de (B) hidrogeles de pHEMA con 0.15 g de PVP K30 por ml y distintas proporciones de agua.*

Tanto los hidrogeles no porosos (preparados a partir de mezclas monoméricas anhidras) como los porosos cedieron una porción significativa de la PVP en las primeras 24 horas. Transcurrido este tiempo, la cesión se hizo más lenta (Figura 4.19) y al cabo de 9 días las lentes aún contenían el 80% de la PVP inicial. El

buen ajuste de los perfiles de cesión a la cinética de la raíz cuadrada sugiere que la difusión es el mecanismo que controla el proceso. El elevado peso molecular de la PVP hace posible que las cadenas se entrecrucen con el entramado de pHEMA y que se ralentice su movimiento. Esto explica que la cesión se pueda sostener durante mucho más tiempo, incluso más de 30 días, que el habitual para los fármacos convencionales. La incorporación de agua a la mezcla monomérica provoca un incremento del tamaño de malla de los hidrogeles y consiguientemente facilita la difusión.

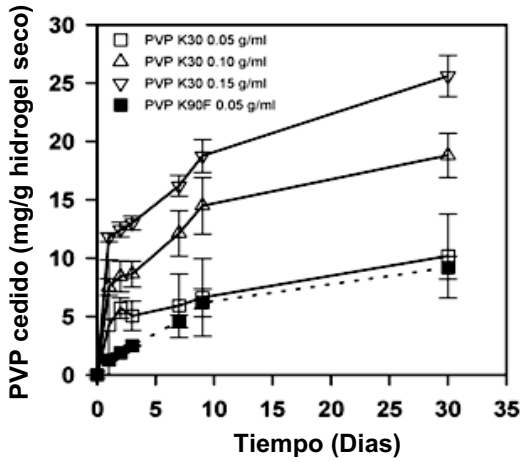

Figura 4.19. *Pefiles de cesión de PVP a partir de hidrogeles de pHEMA preparados en condiciones anhidras con diferentes proporciones de PVP.*

La cantidad de PVP cedida por las lentes al cabo de 24 horas se sitúa dentro del intervalo habitual de dosis diarias de demulcente (0.05-1.0 mg) cuando se administra en forma de gotas. La ventaja de incorporar PVP a las lentes de contacto radica en que es previsible que de esta manera se atenúen sensiblemente las pérdidas por efecto de los mecanismos normales de defensa del ojo.

A continuación, se determinó el coeficiente de fricción de los hidrogeles hinchados. Para ello se les aplicó una fuerza normal de 5 N durante 15 minutos en modo estático y a continuación, bajo esta misma fuerza normal, se sometieron a rotación (0.05 rad/s) durante otros 15 minutos. El ensayo reométrico tiene dos importantes ventajas sobre el procedimiento tribométrico que se utiliza de manera habitual: i) la temperatura de la muestra y la del líquido atrapado entre la geometría y la superficie del plato Peltier se pueden controlar de manera precisa; y ii) la alta sensibilidad del reómetro permite registrar fuerzas de torsión tan bajas como las que se obtienen con geles de bajo coeficiente de fricción. Para cada tiempo de muestreo, las determinaciones se llevaron a cabo humectando la superficie del plato Peltier con una porción del medio acuoso en el que se encontraban sumergidos los discos de hidrogel en el momento del ensayo, con el fin de mimetizar las condiciones en las que se va a encontrar la lente *in vivo*. De hecho, no sólo la PVP interpenetrada en la lente y la que sobresale de su superficie, sino también la PVP ya cedida, pueden contribuir de manera significativa al efecto lubrificante. En la Figura 4.20 se muestran los resultados obtenidos.

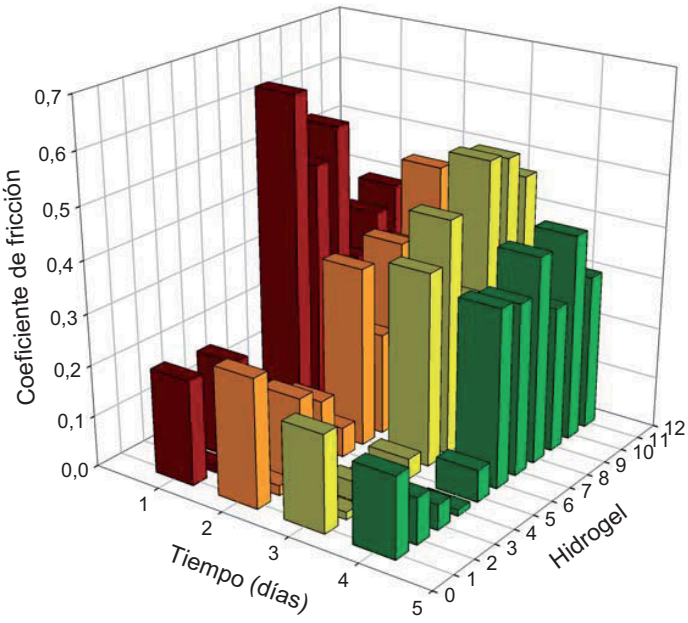

Figura 4.20. *Valores del coeficiente de fricción de los hidrogeles de pHEMA semi-interpenetrados con PVP una vez hidratadas. La composición de los hidrogeles se indica en la Tabla 4.2. (1) 6.0: 0: 0, (2) 6.0: 0: 0.3, (3) 6.0: 0: 0.3*, (4) 6.0: 0: 0.6, (5) 6.0: 0: 0.9, (6) 5.4: 0.6: 0.9, (7) 4.8: 1.2: 0.9, (8) 4.2: 1.8: 0.9, (9) 3.6: 2.4: 0.9, (10) 3.0: 3.0: 0.9, (11) 2.4: 3.6: 0.9. * Se usó PVP K90F en lugar de PVP K30.*

El coeficiente de fricción de los hidrogeles de pHEMA sin PVP se mantuvo en el valor μ 0.5 durante los cuatro días del ensayo. Los coeficientes de fricción de los hidrogeles preparados con PVP K30 en ausencia de agua fueron diez veces más pequeños. Estos valores son del orden de los encontrados por otros autores para hidrogeles de PVP destinados a la construcción de implantes para articulaciones. La mayor efectividad lubrificante de la PVP K90F se puso de manifiesto a todos los tiempos de muestreo, lo que puede estar relacionado con su peso molecular, su capacidad viscosizante y su afinidad por el agua que son sensiblemente mayores que los de la PVP K30.

Los coeficientes de fricción de los hidrogeles sintetizados en presencia de agua resultaron ser más elevados, a pesar de que cedieron más PVP al medio que los hidrogeles anhidros. Este hecho puede estar relacionado con que su superficie más irregular contrarresta el efecto lubrificante de la PVP. Por lo tanto, para minimizar la fricción hay que llegar a un compromiso entre el efecto deslizante del agente demulcente y la topografía de la superficie de las lentes.

La recarga de las lentes de PVP (y, por lo tanto, el posible efecto imprinting no se pudo evaluar debido a la imposibilidad de extraer toda la PVP de las lentes en una escala de tiempo razonable.

4.4. Efecto de la incorporación de agua a la mezcla polimérica sobre la porosidad y la permeabilidad de hidrogeles de pHEMA a microorganismos.

Los cambios en la porosidad que se derivan de la presencia de distintas proporciones de agua en las mezclas monoméricas de las que se parte para sintetizar lentes de contacto, pueden tener importantes repercusiones sobre su permeabilidad al oxígeno y otras moléculas, que son potencialmente relevantes desde el punto de vista de su biocompatibilidad (Sprincl y Kopecek, 1973, Wang y col. 2004, Kopecek, 2009). Un aspecto que ha sido poco estudiado hasta el momento, a pesar de su indudable relevancia, es la posible dependencia de la penetración y la colonización por microorganismos respecto del tamaño de los poros y del porcentaje de volumen poroso de las lentes.

En la cuarta etapa de la Tesis se procedió a preparar por fotopolimerización hidrogeles de pHEMA incorporando agua a la mezcla polimérica en proporciones similares a las ensayadas en el apartado anterior. Con la fotopolimerización el

proceso de síntesis del hidrogel se produce de manera mucho más rápida y la separación de fases ocurre en dominios de pequeño tamaño (microscópicos), con lo que se evita la macroseparación de fases que se observó en la polimerización inducida por calor descrita en el apartado anterior. A continuación, se caracterizó en profundidad la estructura microporosa de las lentes y se analizó su dependencia respecto de la proporción de agua utilizada en la síntesis. Por último, se llevaron a cabo estudios microbiológicos *in vitro* y se evaluó la penetración de distintos microorganismos a través de las lentes, con el fin de identificar el contenido máximo en agua que conduce a la formación de hidrogeles capaces de impedir el paso de microorganismos hacia la córnea.

Los hidrogeles liofilizados presentaron valores de temperatura de transición vítrea muy próximos al valor de Tg característico de pHEMA, si bien se observó un incremento progresivo de la Tg a medida que fue aumentando la proporción de agua durante la síntesis (Tabla 4.4). Este hecho sugiere que la separación de fases conduce a que el entramado sea más rígido.

Agua:HEMA	Tg (ºC)	Grado de hinchamiento (%)
0:100	109,3	54,0
10:90	113,0	56,9
20:80	117,0	57,6
30:70	117,9	59,2
40:60	119,7	60,7
50:50	122,9	65,5
60:40	123,6	81,9

Tabla 4.4. *Temperatura de transición vítrea (Tg) y grado de hinchamiento (%) en agua de hidrogeles de pHEMA preparados con distintas proporciones de agua.*

La estructura microporosa de la matriz de los hidrogeles se caracterizó en términos de mesoporos (tamaño comprendido entre 0.002 y 0.050 μm) y macroporos (tamaño > 0.050 μm) aplicando técnicas de adsorción de nitrógeno y de análisis de imagen de microfotografía de SEM. Los ensayos de adsorción de nitrógeno se llevaron a cabo utilizando un equipo Micromeritics ASAP 2000 (USA). Para determinar la cantidad de N_2 necesario para recubrir los poros accesibles tanto externos como internos con una monocapa de gas, las muestras se sometieron a 70ºC y 10^{-3} mmHg y, a continuación, se expusieron a N_2 gas a 70ºC y una presión relativa de 0.01-0.98 mmHg. El area de superficie BET (S_{BET}) se calculó a partir de las isotermas de adsorción utilizando la ecuación:

$$S_{BET}\ (m^2g^{-1}) = 4.37\ V_m\ (cm^3g^{-1}) \qquad \text{(Ec. 4.3)}$$

donde V_m es el volumen de nitrógeno necesario para formar la monocapa sobre toda la superficie polimérica. Los tamaños de poro se ajustaron a una distribución log-normal y se estimó, por regresión no lineal (GraphPad Prism 5.00, GraphPad Software Inc., 2007), la correspondiente media y desviación estándar geométricas. Los resultados obtenidos (Tabla 4.5 y Figuras 4.21) ponen de manifiesto un cambio brusco en la estructura microporosa a partir del 30-40% de agua.

% Agua	Media (μm)	D.E. geométrica	Volumen poroso, cm^3g^{-1}	Superficie, m^2g^{-1}	R^2
0	0.0051	1.88	0.000718	1.831	0.976
10	0.0051	2.13	0.000639	2.246	0.970
20	0.0060	2.57	0.000887	2.189	0.975
30	0.0061	2.47	0.000772	1.558	0.963
40	0.0064	2.15	0.002235	2.901	0.983
50	0.0081	2.62	0.002347	3.797	0.993
60	0.0084	2.61	0.002576	3.750	0.973

Tabla 4.5. Ajuste a la distribución logarítmico normal de los resultados obtenidos en los análisis de adsorción de nitrógeno aplicando el modelo de BET.

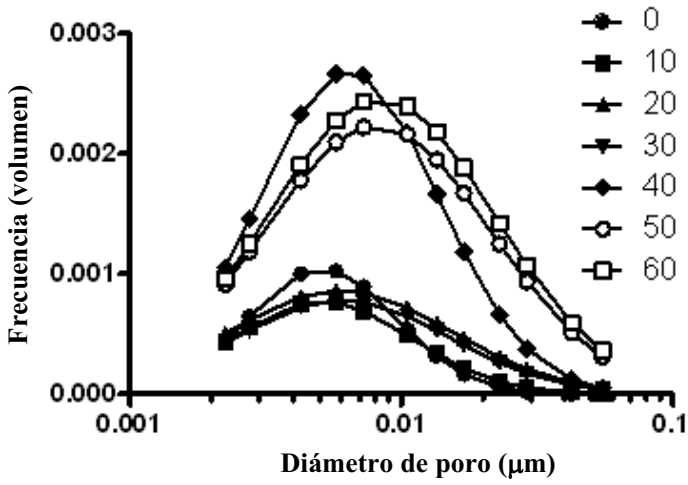

Figura 4.21. *Distribuciones de tamaños de mesoporos obtenidas a partir de datos de adsorción de nitrógeno.*

Para evaluar la influencia de la proporción de agua sobre el tamaño medio de los poros, el volumen microporoso y la superficie específica de los geles secos, los gráficos correspondientes a estos parámetros se ajustaron, por regresión no lineal, al siguiente modelo lineal segmental (GraphPad Prism 5.00, GraphPad Software Inc., 2007):

$Y_1 = A_1 + B_1 X$ si $X<X_0$

$Y_2 = (A_1 + B_1 X_0) + B_2 (X-X_0)$ si $X \geq X_0$

donde X es la proporción de agua, Y es el tamaño medio de los poros, el volumen microporoso o la superficie específica y X_0 representa la proporción de agua a partir de la cual se observa un cambio de comportamiento. A_1, $(A_1 + B_1 X_0)$ y B_1, B_2 son las ordenadas en el origen y las pendientes correspondientes a los dos segmentos lineales, respectivamente.

El tamaño medio y el volumen de los mesoporos y la superficie específica de los hidrogeles se incrememtó linealmente a medida que aumentó la proporción de agua en las disoluciones monoméricas (Figura 4.22).

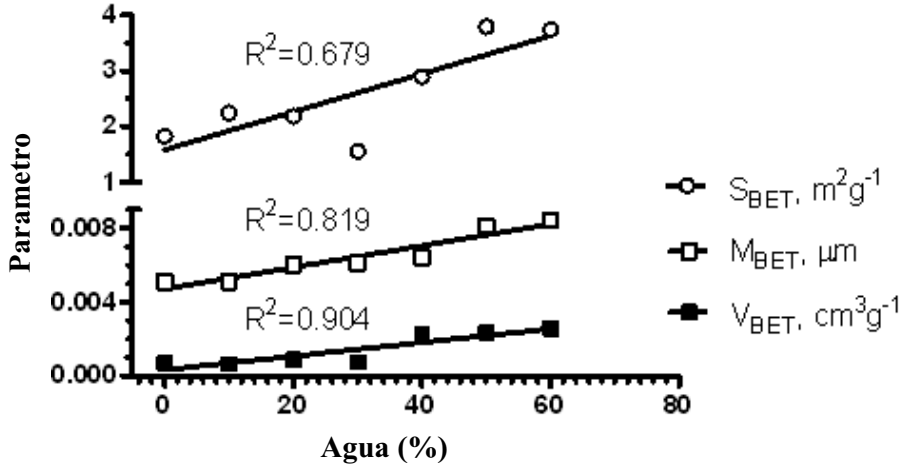

Figura 4.22. *Dependencia del diámetro medio y el volumen de los mesoporos y la superficie específica de los hidrogeles respecto de la proporción de agua en las disoluciones monoméricas.*

Para caracterizar la porosidad superficial de los hidrogeles, se analizaron microfotografías de SEM (Figura 4.23) utilizando el programa SPIP 4.6.0 (Image Metrology A/S, Denmark). Los tamaños de los poros en la superficie de los hidrogeles se ajustaron a una distribución logarítmico-normal, y se calculó la media geométrica y la desviación estándar geométrica (Tabla 4.6).

Hidrogel	Agua:HEMA	Diámetro medio de macroporos (μm)	D.E. (μm)	R^2
A	0:100	0.69	0.19	0.976
B	10:90	0.48	0.21	0.970
C	20:80	0.89	0.34	0.975
D	30:70	0.91	0.29	0.963
E	40:60	3.38	2.63	0.983
F	50:50	6.47	4.02	0.993
G	60:40	14.74	8.79	0.973

Table 4.6. *Proporciones de agua en las soluciones monoméricas, diámetro medio y desviación estándar de los tamaños de poro en la superficie de los hidrogeles tras el ajuste a distribución normal de los poros medidos mediante analisis de imagen SEM.*

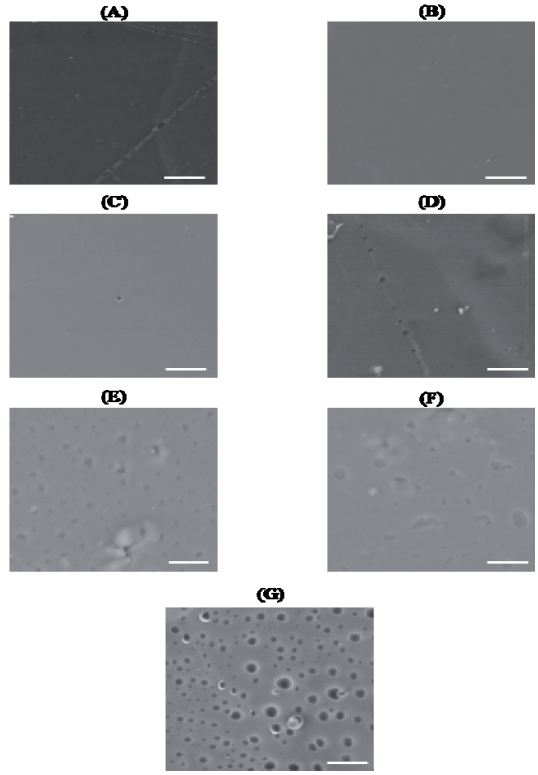

Figura 4.23 *Imágenes de SEM (10,000 X // 10 μm) de la superficie de los hidrogeles de HEMA preparados con* ***(A)*** *un 0% de agua en su composición;* ***(B)*** *10%;* ***(C)*** *20%;* ***(D)*** *30%;* ***(E)*** *40%;* ***(F)*** *50% y* ***(G)*** *60%.*

Los hidrogeles sintetizados a partir de disoluciones monoméricas con una proporción de agua igual o inferior al 30% mostraron en su superficie poros de tamaño inferior a 1.5 μm, que cubren menos del 2% de la superficie total del hidrogel (Figura 4.24). Los hidrogeles preparados con 50% ó 60% de agua presentaron numerosos macroporos de más de 10 μm, que cubren hasta el 10% de la superficie.

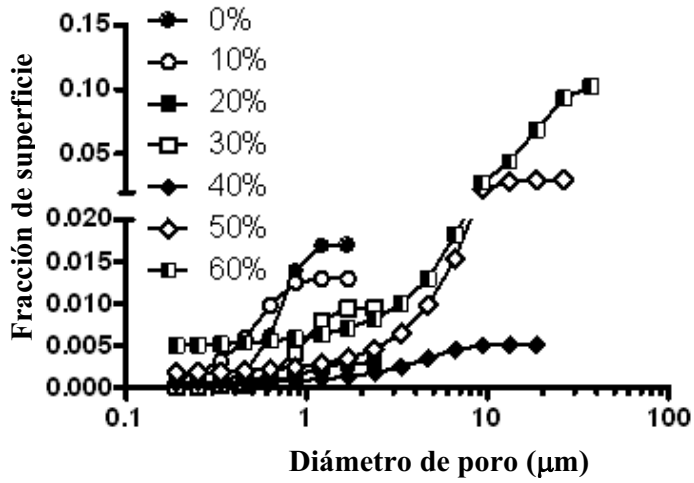

Figura 4.24. *Distribución acumulada de tamaños de poro en la superficie del hidrogel.*

Para evaluar la influencia del agua sobre el tamaño medio y la superficie ocupada por los poros se utilizó un modelo segmental, observándose un cambio de pendiente muy marcado en torno al 40% de agua (Figura 4.25).

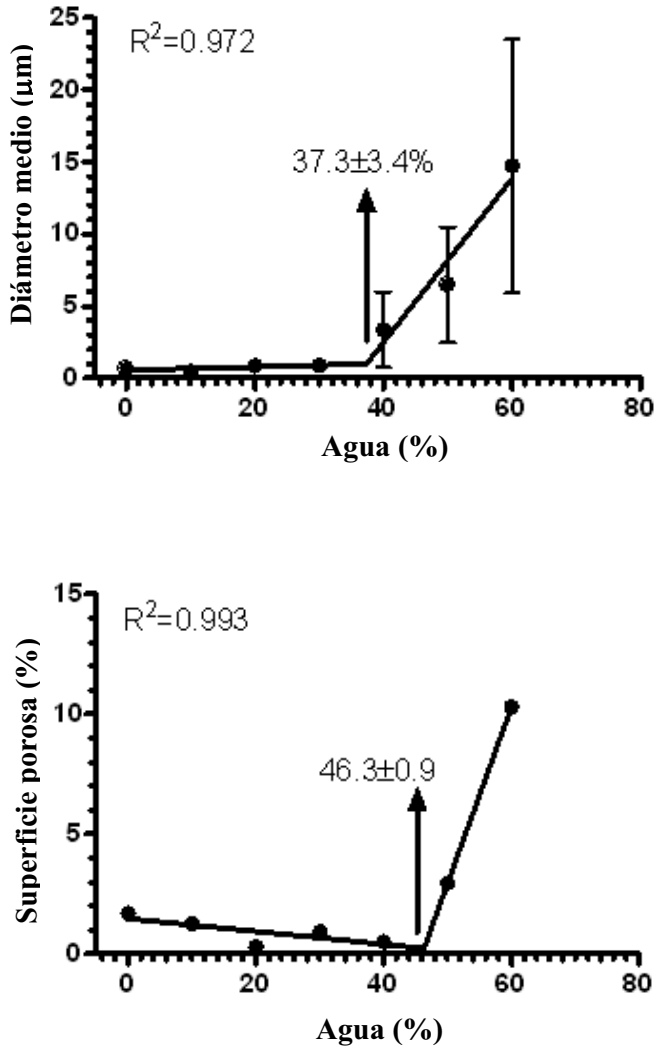

Figure 4.25. *Dependencia del tamaño medio y del area ocupada por los poros en la superficie del hidrogel respecto de la proporción de agua en la disolución monomérica.*

A continuación, se evaluó el grado de hinchamiento de los hidrogeles en agua y se observó que los que se prepararon con un porcentaje de agua igual o superior al 40% alcanzaban un grado de hinchamiento mayor que el de los restantes hidrogeles (tabla 4.4).

Por último, se evaluó la penetración a través de los hidrogeles de dos microorganismos: *Pseudomonas aeruginosa*, un bacilo Gram- de 0.5-0.8 μm de largo por 1.5-3 μm de ancho, y *Staphylococcus aureus*, un coco Gram+ de 0.5-1 μm de diámetro. Los discos hidratados con agua se colocaron sobre placas de agar con medio TSA y, a continuación, se vertieron 20 μl de cultivo microbiano en el centro de cada disco, evitando salpicaduras o contacto con el medio TSA próximo a las lentes. Tras incubar durante 24 horas, se comprobó que sobre la superficie de los hidrogeles preparados en ausencia de agua (de más baja porosidad superficial) no se había producido crecimiento bacteriano. *Ps. aeruginosa* tampoco creció sobre los hidrogeles preparados con las proporciones agua:HEMA 10:90 y 20:80, aunque sí los hizo en los restantes hidrogeles. Además en los hidrogeles preparados con las proporciones agua:HEMA 50:50 y 60:40 se observó la penetración del microorganismo a través de las lentes y su crecimiento en el medio de TSA. En el caso de *S. aureus* se observó crecimiento en la superficie de los hidrogeles a partir de la proporción agua:HEMA 10:90 y penetración en los hidrogeles preparados con agua:HEMA 40:60, 50:50 y 60:40.

Para profundizar en el análisis de la influencia del tamaño de poro sobre la penetración de las bacterias en los hidrogeles se acudió a la regresión logística (Figura 4.26)

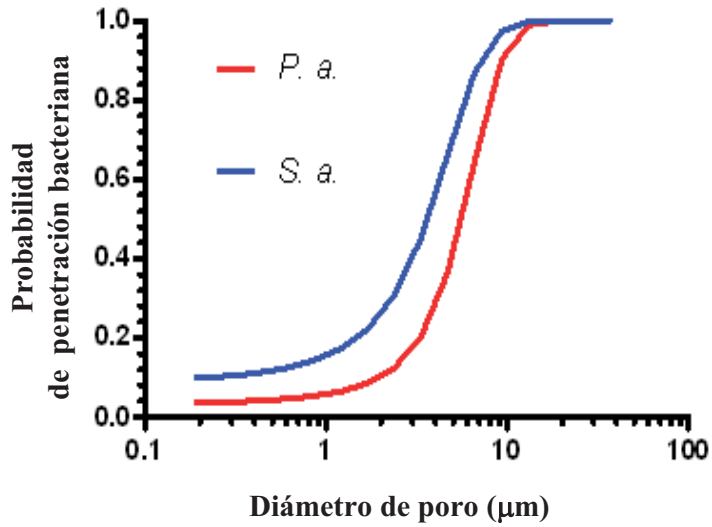

Figura 4.26. *Resultados de la regression logística entre el tamaño medio de los macroporos y la penetración en los hidrogeles de Pseudomonas aeruginosa (χ^2=6.54; 1 g.l.; α<0.05; variación explicada= 68.4%) o de Staphylococcus aureus (χ^2=6.56; 1 g.l.; α<0.05; variación explicada= 78.3%).*

Los resultados obtenidos pusieron de manifiesto que, en los entramados con tamaño medio de poro mayor que 3.67 µm ó 5.56 µm, la probabilidad de que penetren *S. aureus* o *Ps. aeruginosa*, respectivamente, es superior al 50%. Por lo tanto, para prevenir el desarrollo de bacterias en los hidrogeles es necesario controlar rigurosamente su microestructura, tomando en consideración el efecto de la proporción de agua en la disolución monomérica sobre el tamaño de los poros.

4.5. Desarrollo de entramados *imprinted* para sales biliares utilizando la modelización computacional como herramienta de cribado de monómeros y evaluación de su eficacia como sistemas trampa.

Este apartado responde al objetivo de avanzar en el diseño racional de sistemas imprinted aplicando la modelización *in sílico,* un procedimiento que encierra un gran interés como complemento de la ITC, puesto que permite hacer un cribado rápido de monómeros funcionales sin necesidad de trabajo experimental (Piletsky y col., 2000, 2001; Subrahmanyam y col., 2001; Guerreiro y col. 2008). En este caso, el estudio se centró en el desarrollo de sistemas imprinted para ácidos biliares y se ha utilizado la modelización *in silico* para identificar los monómeros funcionales más adecuados. Desde un punto de vista terapéutico, los sistemas imprinted para ácidos biliares pueden tener utilidad en dos áreas diferentes: i) la construcción de implantes o lentes de contacto para la administración ocular de ácidos biliares, como alternativa a la administración por vía subcutánea que está actualmente en fase de evaluación para ralentizar la degeneración de la retina y la formación de cataratas (Boatright y col., 2009); y ii) para el tratamiento de la hipercolesterolemia de manera que actúen como sistemas trampa de ácidos biliares en el aparato digestivo (Corsini y col., 2009; Russell, 2009). Aunque el trabajo se ha centrado exclusivamente en el segundo de estos dos aspectos, la información generada puede servir para abordar la puesta a punto de lentes medicadas, en el futuro.

Los ácidos biliares se sintetizan a nivel hepático a partir del colesterol y, tras su conjugación química con glicina o taurina, se excretan en la bilis a la luz intestinal. En los individuos sanos, los ácidos biliares actúan como agentes emulsificantes de los ácidos grasos ingeridos con la dieta, se reabsorben en un 90% en el intestino principalmente a nivel del ileón, y retornan al hígado a través

de la vena porta (circulación enterohepática; Hou y Goldberg, 2009) (Figura 4.27). Un desajuste en el equilibrio de la síntesis endógena de colesterol o una intensa absorción de lípidos a nivel intestinal, puede derivar en la aparición de hipercolesterolemia (Pella y col., 2003). En la actualidad, la hipercolesterolemia se puede corregir con la instauración de dietas correctas y de tratamientos con inhibidores de la hidroximetilglutaril coenzima A (estatinas). Estos fármacos tienen el inconveniente de que pueden producir efectos secundarios que desaconsejan su uso en niños, en mujeres embarazadas y en pacientes con insuficiencia hepática (Filippatos y Mikhailidis, 2009; Hou y Goldberg, 2009). Una alternativa al tratamiento farmacológico consiste en utilizar sistemas secuestrantes o "trampa" capaces de retener las sales biliares, para que se eliminen a nivel intestinal sin llegar a participar en la absorción de los lípidos. En la actualidad se encuentran en el mercado resinas de intercambio iónico derivadas de polímeros, como el colestipol y la colestiramina. Aunque estas dos resinas cuentan con una alta capacidad secuestrante de ácidos biliares, para que los tratamientos resulten efectivos hay que administrar cantidades diarias elevadas (30 g/día), lo que dificulta el cumplimiento de las pautas posológicas por el paciente (Mandeville y col. 1999).

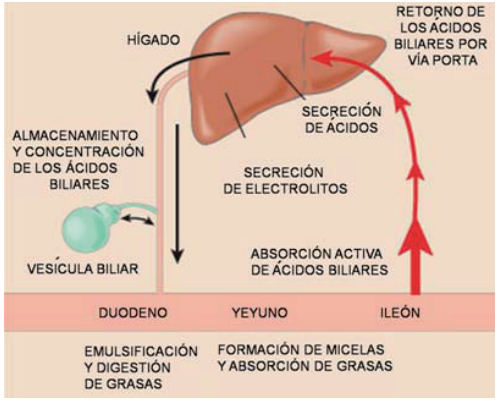

Figura 4.27*. Circulación enterohepática.*

Los ácidos biliares están constituidos por un esqueleto esteroídico curvado con una cara alfa (hidrofílica) hacia la que están orientados los grupos hidroxilo y la cadena carboxílica, y una cara beta (hidrofóbica) con los tres grupos metilo (Figura 4.28). Esta estructura confiere a la molécula un marcado carácter anfifílico (Zhu y col., 2000). El desarrollo de los entramados imprinted comprendió las siguientes etapas: i) selección de los monómeros aplicando un procedimiento de modelización computacional; ii) síntesis de los polímeros; iii) construcción de las isotermas de adsorción; y iv) evaluación de la capacidad de extracción de colato sódico disuelto en un medio acuoso.

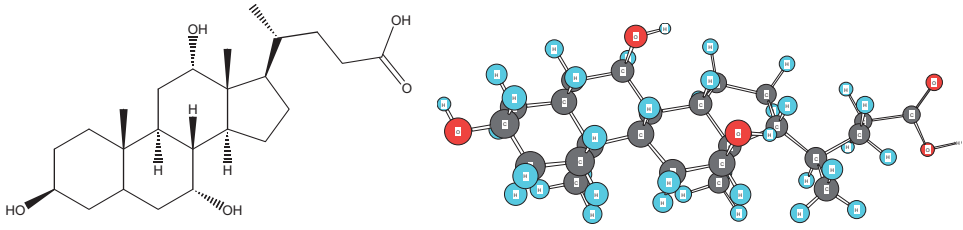

Figura 4.28. *Estructura del ácido cólico y conformación en el estado de mínima energía (CSChem3D Std®, CambridgeSoft Co. 1997).*

En primer lugar se evaluó la energía de interacción del ácido cólico con una serie de monómeros recogidos en la biblioteca virtual del Silicon Graphics Octane y se identificaron los grupos químicos responsables de las interacciones. Para definir la conformación más estable del ácido cólico en dimetilsulfóxido (DMSO), se minimizó su energía conformacional (Chianella y col. 2002, 2003; Romero-Guerra y col., 2009). A continuación, se seleccionaron 18 monómeros entre los que se utilizan habitualmente en la síntesis de hidrogeles y se minimizó su energía aplicando el mismo procedimiento. Por último, se llevó a cabo un barrido de las energías de interacción del ácido cólico con cada uno de estos monómeros utilizando el algoritmo de LEAPFROG. En la tabla 4.7 se muestran las energías de interacción estimadas aplicando el algoritmo. A la vista de los resultados obtenidos se seleccionaron el fosfato de etilenglicol metacrilato (EGMP), el 2-

(dietilamino)etil metacrilato (DEAEM) y el hidrocloruro de N-(3-aminopropil) metacrilamida (APMA·HCl), que dan lugar a energías de interacción medias-altas, superiores a las del agente reticulante EGDMA.

Monómero	Energía de enlace (kcal mol^{-1})
Alilamina protonada	-50.14
Hidrocloruro de N-(3-aminopropil) metacrilamida (APMA·HCl)	-48.43
Hidrocloruro de aminoetil metacrilato	-47.87
Fosfato de etileneglicol metacrilato (EGMP)	-41.75
N,N´- Metilenebis(acrilamida)	-39.73
Fosfato de etileneglicol metacrilato desprotonado	-37.99
Ácido acrilamido-2-metil-1-propanosulfonico	-33.67
Aminoetil metacrilato	-32.20
Ácido itacónico	-31.42
Ácido itacónico desprotonado	-30.01
1,3,5-Trihidroxilestireno	-29.97
N,N-Dietilamino etilmetacrilato protonado (DEAEM·HCl)	-29.82
Acrilamida	-27.39
N,N- Dietilamino etilmetacrilato (DEAEM)	-27.14
Etileneglicol dimetacrilato (EGDMA)	-25.52
Ácido metacrílico desprotonado	-25.16
N-(3-aminopropil) metacrilamida (APMA)	-24.39
Alilamida	-23.69

Tabla 4.7. *Energías de interacción del ácido cólico con los monómeros incluidos en la biblioteca virtual de monómeros del Silicon Graphics Octane, estimadas aplicando el algoritmo de LEAPFROG.*

Los tres monómeros seleccionados pueden interaccionar con el ácido cólico mediante puentes de hidrógeno. Además, el APMA·HCl puede establecer uniones electrostáticas con el grupo ácido carboxílico.

Para preparar los sistemas imprinted, los monómeros funcionales se copolimerizaron con HEMA y agente reticulante EGDMA en presencia de ácido cólico, que actuó como molécula molde (Figura 4.29). La relación molar fármaco:monómero funcional fue en todos los casos 1:4 (Hiratani y col., 2005b; Alvarez-Lorenzo y col., 2006). La composición de los distintos sistemas se recoge en la Tabla 4.8. También se sintetizaron entramados de la misma composición pero sin ácido cólico, para usarlos como controles no imprinted.

Hidrogel	**DEAEM**		**EGMP**		**APMA·HCl**		**Control**	
	MIP	NIP	MIP	NIP	MIP	NIP	MIP	NIP
Monómero funcional (mg)	272	272	262	262	262	262	0	0
Ácido cólico (mg)	150	0	150	0	150	0	150	0
EGDMA (mg)	2578	2578	2539	2539	2737	2737	3000	3000
DMSO (ml)	3	3	3	3	3	3	3	3
AIBN (mg)	30	30	30	30	30	30	30	30

Tabla 4.8. *Composición de los entramados poliméricos preparados sin (control) o con monómero funcional, en ausencia (NIP) o en presencia (MIP) del ácido cólico (molécula molde).*

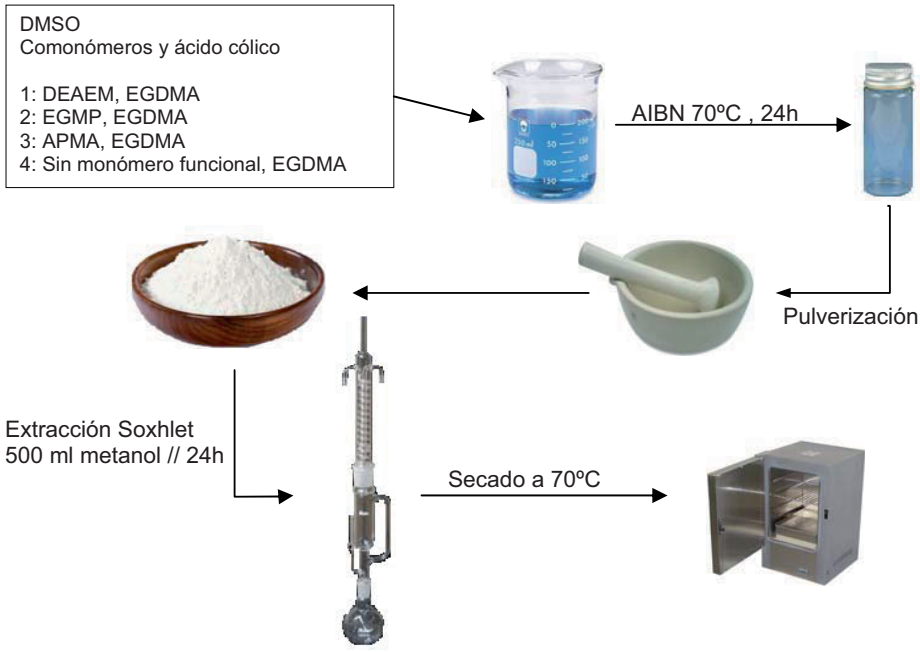

Figura 4.29. *Etapas de la síntesis de los entramados secuestrantes de ácidos biliares.*

Una vez completada la polimerización, que se llevó a cabo a 70ºC durante 24h, los entramados se pulverizaron en un mortero y se separaron por tamización fracciones granulométricas comprendidas entre 32 y 125 μm (Figura 4.30) A continuación, se llevó a cabo la extracción con metanol del ácido cólico contenido en las partículas utilizando un aparato Soxhlet (500 ml, 24 horas). Por último, las partículas se secaron a vacío.

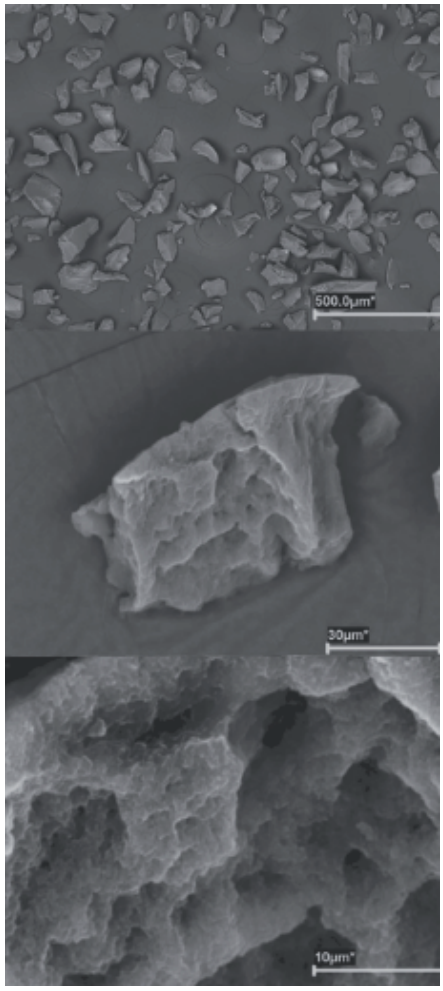

Figura 4.30. *Imágenes SEM de las partículas poliméricas de APMA·HCl.*

Para construir las isotermas de adsorción, se pusieron en contacto porciones de 1,5 mg de cada polímero con 500 µl de disoluciones de colato sódico de concentración comprendida entre 0,1 y 0,5 mM, utilizando viales de ultracentrífuga (Pierce® Centrifuge Column, 0,8 ml). Los sistemas se mantuvieron 12 horas a temperatura ambiente bajo ligera agitación magnética y se sometieron a centrifugación (600 rpm, 2 min). La cantidad de colato sódico no adsorbido se

determinó por espectrofotometría a 389 nm, previa reacción de una muestra de 1 ml con 3 ml de ácido sulfúrico concentrado a 70ºC durante 30 min.

En la Figura 4.31 se presentan las isotermas de adsorción obtenidas con cada uno de los polímeros. La afinidad por el colato sódico se incrementó de manera muy significativa cuando se incorporó monómero funcional al entramado polimérico. Los dos monómeros funcionales con un grupo amina en su estructura, el DEAEM y el APMA, fueron los que comunicaron mayor capacidad de adsorción de colato sódico, en especial cuando éste se encuentra en el medio a baja concentración. Además, el entramado con APMA en su estructura dio lugar a una isoterma en forma de "S". Este perfil es característico de los sistemas en los que la adsorción se produce por mecanismos cooperativos, en los que las moléculas incorporadas inicialmente promueven la incorporación de más moléculas. Este comportamiento también se observó con el colestipol. En el caso particular del APMA, el grupo amino protonado permite el establecimiento de interacciones electrostáticas muy intensas, que hacen posible la captación de la totalidad del colato sódico cuando se encuentra en el medio a concentraciones muy bajas.

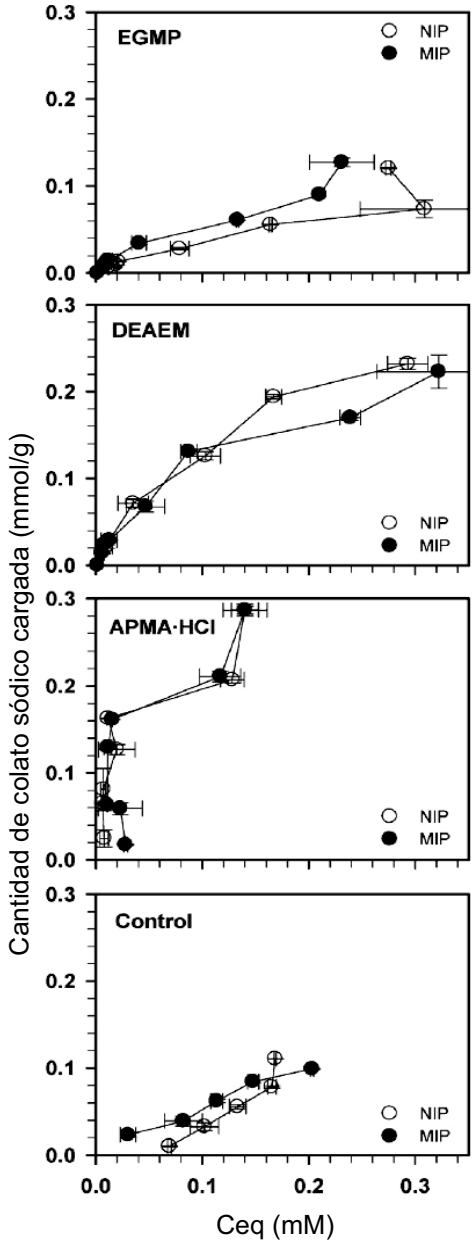

Figura 4.31. *Isotermas de adsorción del colato sódico en agua correspondiente a los polímeros imprinted (MIP) y no imprinted (NIP) preparados con EGMP, DEAEM, APMA·HCl o sin monómero funcional (control).*

Las isotermas de adsorción se ajustaron al modelo de Freundlich con el fin de evaluar la homogeneidad de los puntos de unión y su afinidad por el colato sódico (Garcia-Calzon y Díaz-Garcia, 2007).

$$LogB = m \cdot \log F + \log a \qquad \text{Ec. 4.4}$$

La homogeneidad de los puntos de unión viene dada por el valor del parámetro "*m*" del modelo de Freundlich (Umpleby y col., 2004). Los sistemas control mostraron una mayor homogeneidad de puntos de unión para el colato sódico ("*m*" >1). La presencia de monómero funcional da lugar a entramados con una mayor heterogeneidad de puntos de unión ("*m*" <1). Entre estos últimos, el polímero de APMA fue el que mostró una mayor heterogeneidad en la afinidad.

Todos los entramados poliméricos presentaron un gran número de puntos con baja afinidad. Los entramados sintetizados con EGMP presentaron el número de puntos disponibles para la absorción más bajo y la constante de afinidad menor. En el caso de los polímeros de DEAEM y APMA, no se encontraron diferencias significativas en la afinidad por el colato entre los polímeros sintetizados en presencia y en ausencia de la molécula molde. No obstante, los entramados imprinted sintetizados con APMA mostraron un mayor número de puntos de afinidad alta, lo que prueba el establecimiento de una fuerte interacción entre la molécula molde y el monómero funcional.

A continuación se llevó a cabo un estudio de extracción de colato sódico a partir de un medio acuoso. Para ello, se compactaron 20 mg de cada uno de los polímeros en tubos de filtración de 1 ml y se colocaron en un dispositivo de extracción a vacío. Se hicieron pasar sucesivamente porciones de un 1 ml, hasta un total de 30, de una disolución acuosa de colato sódico 0,2 mM a través de los

polímeros, se recogieron los filtrados de cada porción y se valoró espectrofotométricamente el colato sódico remanente en el filtrado. En la figura 4.32 se muestran las cantidades de colato sódico extraído por cada polímeros y las concentraciones de colato sódico remanentes en el filtrado. Los mejores resultados se obtuvieron cuando se utilizó el polímero con APMA en la extracción, observándose la capacidad de saturación más alta y los niveles de colato sódico remanente más bajos.

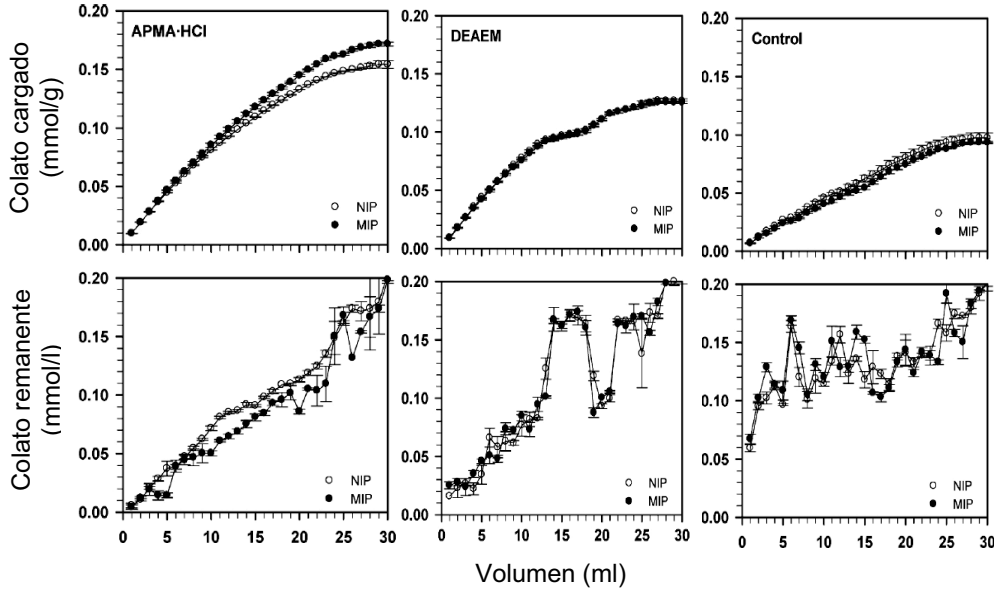

Figura 4.32. *Colato sódico retenido por las partículas poliméricas (grafico superior) y remanente en medio acuoso (gráfico inferior) tras hacer pasar una disolución acuosa de colato sódico a través de entramados con* APMA·HCl, DEAEM y sin monómero funcional (control).

Finalmente, y con el fin de incrementar la capacidad para retener colato sódico se prepararon entramados de APMA·HCl, con un menor grado de reticulación, remplazando parte del agente reticulante por monómero estructural (HEMA) y se

evaluó su comportamiento. La composición de estos entramados se muestra en la tabla 4.9.

Polímero	Ácido Cólico	HEMA	APMA·HCl	EGDMA
APMA·HCl	0 (NIP)- 2,5 (MIP)	0	9,0	91,0
A	0	6,2	9,9	83,9
B	0	12,1	9,7	78,2
C	0	23,3	9,3	67,4
D	0	33,5	8,9	57,5
E	0	43,1	8,6	48,3
F	0 (NIP)- 2,5 (MIP)	60,0	8,3	31,7
G	0 (NIP)- 2,5 (MIP)	92,3	9,2	21,5

Tabla 4.9. *Composición (%mol) de los entramados preparados con APMA·HCl y diferentes grados de reticulación.*

Es previsible que debido al tamaño relativamente grande de la molécula de colato sódico, 17Å de largo y 5,3Å de ancho, los polímeros con un 91% de agente reticulante y, por lo tanto, con una distancia entre los puntos de reticulación de 8,7Å, experimenten impedimentos estéricos para la penetración de colato sódico en su estructura. Disminuyendo el grado de reticulación de los polímeros se consiguió incrementar el rendimiento del proceso (Figura 4.33). En concreto, los polímeros sintetizados con un 31,7% de EGDMA (polímero F, tabla 4.9), capturaron dos veces más colato sódico del medio acuoso que los sintetizados anteriormente. Esta mejora se explica por la mayor facilidad del colato sódico para difundir a través de un entramado con tamaño de malla mayor.

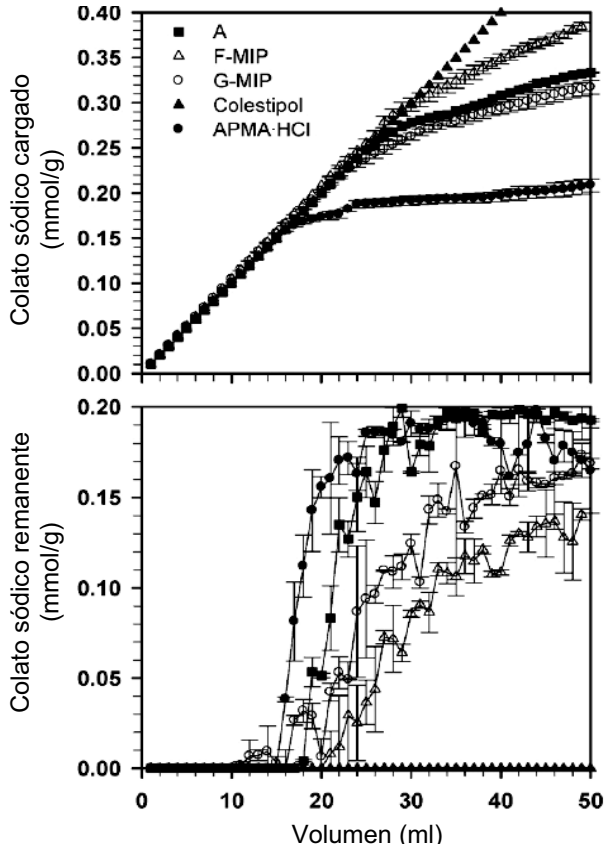

Figura 4.33. *Colato sódico retenido por las partículas poliméricas (grafico superior) y remanente en medio acuoso (gráfico inferior) tras hacer pasar una disolución acuosa de colato sódico a través de entramados de APMA·HCl preparadas con distintos grados de reticulación, así como, a través de gránulos de Colestipol.*

En conclusión, la modelización computacional permitió identificar monómeros funcionales con elevada afinidad por el colato sódico y sirvió de base para sintetizar entramados acrílicos con capacidad para secuestrar colato sódico de un medio acuoso.

4.6. Aplicación de la tecnología de fluidos supercríticos para cargar lentes de contacto comerciales con flurbiprofeno y evaluación del efecto imprinted producido por impregnaciones sucesivas.

El último de los objetivos del trabajo fue evaluar las posibilidades que ofrece la impregnación con fluidos supercríticos como procedimiento de incorporación de fármacos a lentes preformadas y también como técnica de post-imprinting, es decir, de creación de cavidades imprinted en lentes de contacto comerciales preformadas. El procedimiento convencional de moldeado molecular requiere la incorporación del fármaco en el momento de la síntesis de las lentillas y, por lo tanto, cada lentilla se tiene que diseñar para un fármaco concreto. Por ello, resulta de sumo interés la puesta a punto de procedimientos más versátiles que permitan transformar "bajo demanda" lentes comerciales en lentes medicadas con el fármaco que se requiera para una aplicación terapéutica concreta. La solubilización de un fármaco en un fluido en estado supercrítico, capaz de hinchar la estructura de la lente y provocar el reordenamiento de sus cadenas para alojar moléculas, debe dar lugar, una vez que el fluido se retire por despresurización, al depósito de partículas del fármaco en la estructura de la lente. Esto podría constituir un procedimiento rápido de carga de fármacos en lentes comerciales. Una segunda hipótesis de trabajo es que, una vez que se extraiga el fármaco, es posible que la microestructura de la lente quede "marcada" por su presencia, de manera que si vuelve a entrar en contacto con el fármaco, por ejemplo por inmersión en una disolución acuosa, es previsible que lo pueda alojar en una cuantía mayor que una lente que no haya sido sometida previamente a impregnación. De esta manera se obtendría un efecto post-imprinting, es decir, un efecto imprinting en el hidrogel preformado.

Para llevar a cabo el trabajo se eligieron lentes de contacto comerciales Hilafilcon B de Bausch & Lomb (Pure Vision^{TM}, 59% en agua, 8.6 mm curvatura, -8.00 dioptrías, 14 mm Ø) y como fármaco a impregnar el flurbiprofeno, un antiinflamatorio no esteroídico ampliamente utilizado en el tratamiento de procesos inflamatorios oculares comunes y post-quirúrgicos. Este fármaco presenta un solubilidad en agua muy baja ($5 \cdot 10^{-5}$ M ó 12 mg/l; Anderson y Conradi, 1985; Perlovich y col., 2006), que limita la posibilidad de incorporarlo a las lentes de contacto por inmersión en sus disoluciones acuosas. Por el contrario, su solubilidad en $scCO_2$ es mucho mayor: ~160 mg/l y ~510 mg/l a 313 K durante SSI (12 MPa) y SFE (20 MPa). En primer lugar se evaluó la eficacia del procedimiento de impregnación para cargar las lentes con flurbiprofeno y se analizó en qué medida la aplicación de impregnaciones y extracciones sucesivas podría modificar el rendimiento de incorporación del fármaco y su perfil de cesión. A continuación, se determinó la afinidad de las lentes que habían sido impregnadas con flurbiprofeno y extraídas usando $scCO_2$, por otros fármacos estructuralmente relacionados como el ibuprofeno y la dexametasona. De esta manera, fue posible poner de manifiesto la creación de cavidades imprinted para flurbiprofeno. Finalmente, se comprobó que el tratamiento con fluidos supercríticos no había alterado propiedades básicas de las lentes imprescindibles para su utilización como tales dispositivos biomédicos. En la figura 4.34 se muestra la estructura de los fármacos utilizados en el estudio y los monómeros que forman parte de la lentes Hilafilcon B.

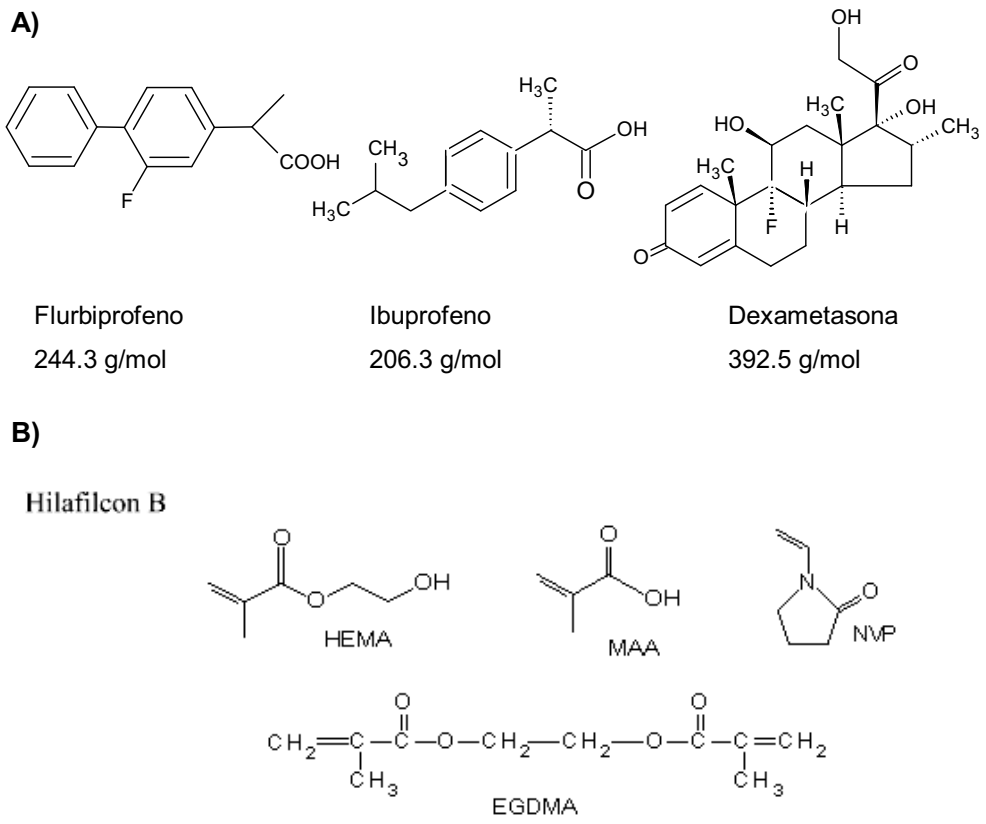

***Figure 4.34**. Estructura de (A) los fármacos y (B) los monómeros constituyentes de las lentes de contacto Hilafilcon B. HEMA: 2-hidroxietil metacrilato; MAA: ácido metacrílico; EGDMA: etilenglicol dimetacrilato; NVP: N-vinilpirrolidona.*

4.6.1. Impregnación/extracción de flurbiprofeno

Se ensayaron dos procedimientos para incorporar flurbiprofeno a lentes Hilafilcon B:

a) impregnación con fluidos supercríticos (SSI), a 40ºC y 12 MPa, en una cámara en la que se disponen 6 lentes de contacto y 3.5 mg de fármaco, seguida de despresurización lenta al cabo de 2.5 horas.

b) inmersión de las lentes en una disolución saturada de fármaco (40 mL, 8 mg/L) durante 2.5-13 horas a 37ºC y bajo agitación (100 rpm).

A continuación, se extrajo el fármaco de las lentes utilizando en el primer caso fluidos supercríticos (SFE, 40ºC, 14 h a 12 MPa y 5 h a 20 MPa) seguido de lavado en agua, y en el segundo, agua (80 mL, 37ºC). Una vez extraídas, las lentes se sometieron de nuevo al proceso de incorporación/extracción de fármaco durante uno ó dos ciclos más, hasta un total de 3 impregnaciones/extracciones (Figura 4.35).

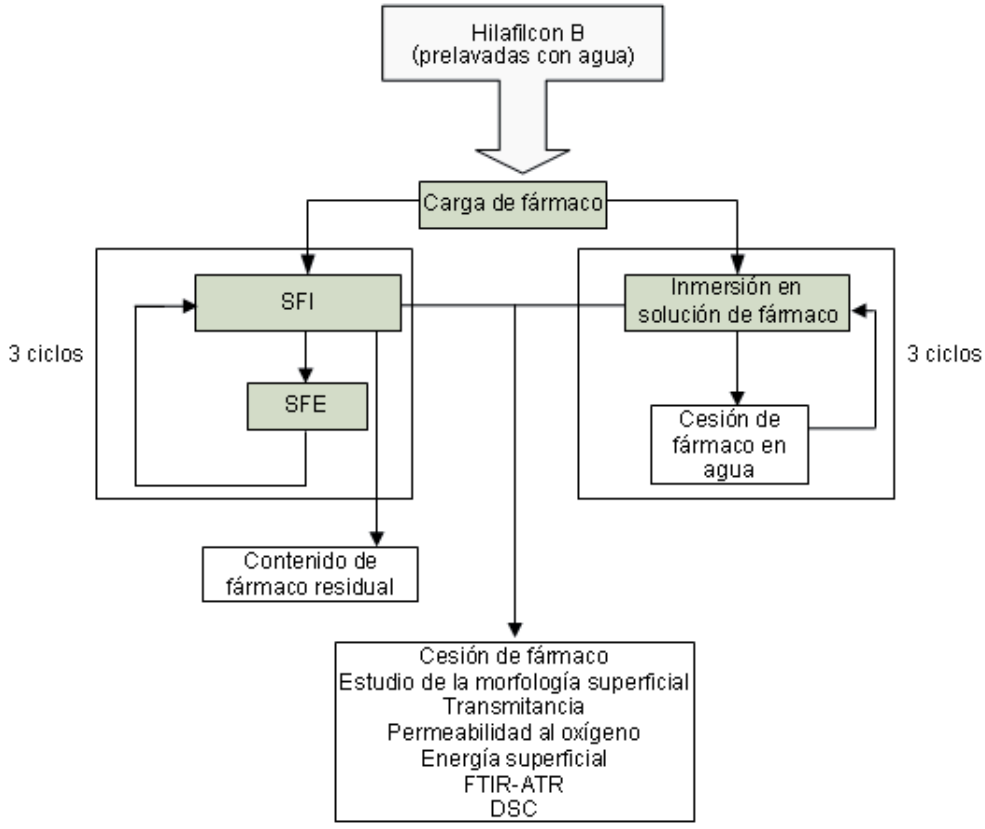

Figure 4.35*.Esquema de la metodología empleada para la impregnación/extración de las lentes de contacto con fármaco.*

Las cantidades de flurbiprofeno incorporadas a las lentes utilizando la tecnología de fluidos supercríticos resultaron ser considerablemente mayores que las que se cargaron por inmersión en una disolución acuosa de fármaco (Figura 4.36). Además, se observó que a diferencia de lo que ocurre con el tratamiento en agua, las lentes sometidas a impregnaciones/extracciones sucesivas con $scCO_2$ incrementan progresivamente su capacidad de carga. Así, con la segunda impregnación se consigue duplicar la cantidad cargada en la primera, y con la tercera impregnación la carga se cuadruplica. De esta manera, se pudieron incorporar hasta 55 mg/g, que equivalen a la dosis de 160 gotas de colirio comercial. En cambio, el tratamiento en agua no permitió superar 1 mg/g, equivalente a 2.5 gotas de colirio. Además, el tratamiento con $scCO_2$ resulta mucho más rápido (en un día se completa cada ciclo de impregnación y extracción) que el convencional en agua, que requiere 4-5 días.

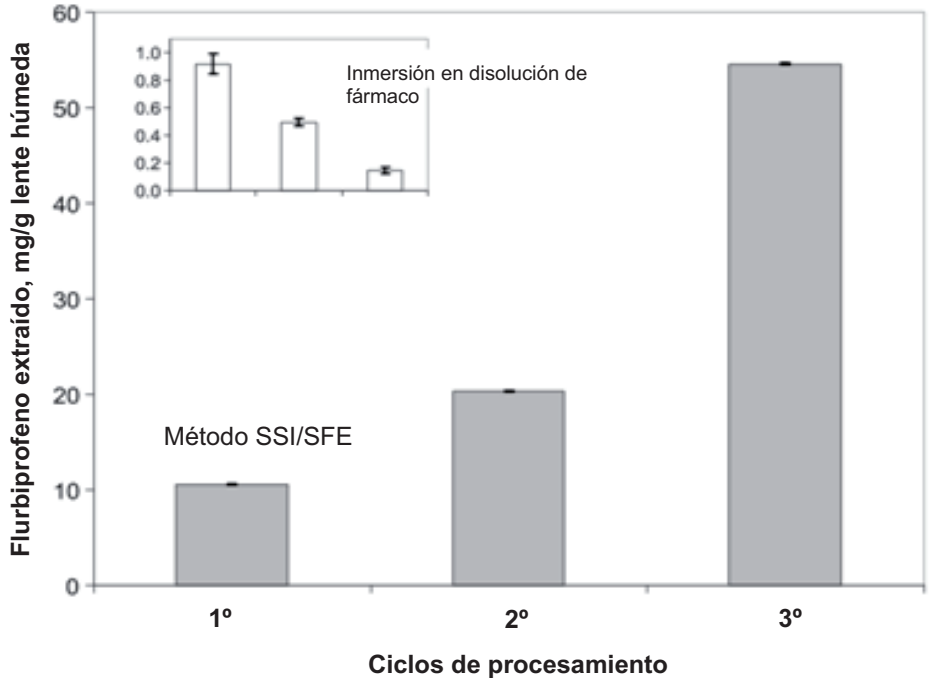

Figura 4.36. *Cantidad de flurbiprofeno extraído a partir de las lentes de contacto tras ciclos consecutivos de carga/extracción, por inmersión en disolución acuosa de fármaco y cesión en agua (gráfico pequeño) o por impregnación y extracción con CO_2 supercrítico.*

El rendimiento superior del tratamiento con fluidos supercríticos se explica por los incrementos que produce el $scCO_2$ en la solubilidad del fármaco y en el hinchamiento del entramado de las lentes de contacto, estos dos aspectos deben facilitar la penetración del fármaco en la estructura de las lentes. Además, las condiciones de SSI se fijaron de manera que el reparto de fármaco entre la lente y el disolvente fuese favorable a la primera. Por otra parte, los comonómeros que constituyen la lente pueden interaccionar por puentes de hidrógeno con las moléculas de fármaco y, especialmente con el átomo de fluor del fármaco, a través del grupo carbonilo. Los incrementos observados en la capacidad de incorporación de fármaco tras ciclos sucesivos indican que el bajo grado de

reticulación de las lentes de contacto permite que las cadenas se reordenen para facilitar el alojamiento del fármaco, y que ese reordenamiento se “memorice” en la lente haciendo posible que las moléculas de fármaco se alojen cada vez en mayor número. Este hecho sugiere la formación de cavidades imprinted de alta afinidad por el fármaco.

Los perfiles de cesión en agua de las lentes cargadas con flurbiprofeno, por cualquiera de los dos procedimientos, se muestran en la figura 4.37. Las lentes procesadas con $scCO_2$ cedieron mayor cantidad de fármaco al aumentar los ciclos de tratamiento, a diferencia de lo que ocurre con las cargadas por inmersión en agua en las que parece producirse una cierta adsorción irreversible que limita tanto la cesión como la recarga. El análisis del porcentaje de fármaco cedido reveló que la velocidad de cesión disminuye al aumentar los ciclos de procesado con $scCO_2$ (Tabla 4.10), lo que refrenda la hipótesis de la formación de cavidades imprinted.

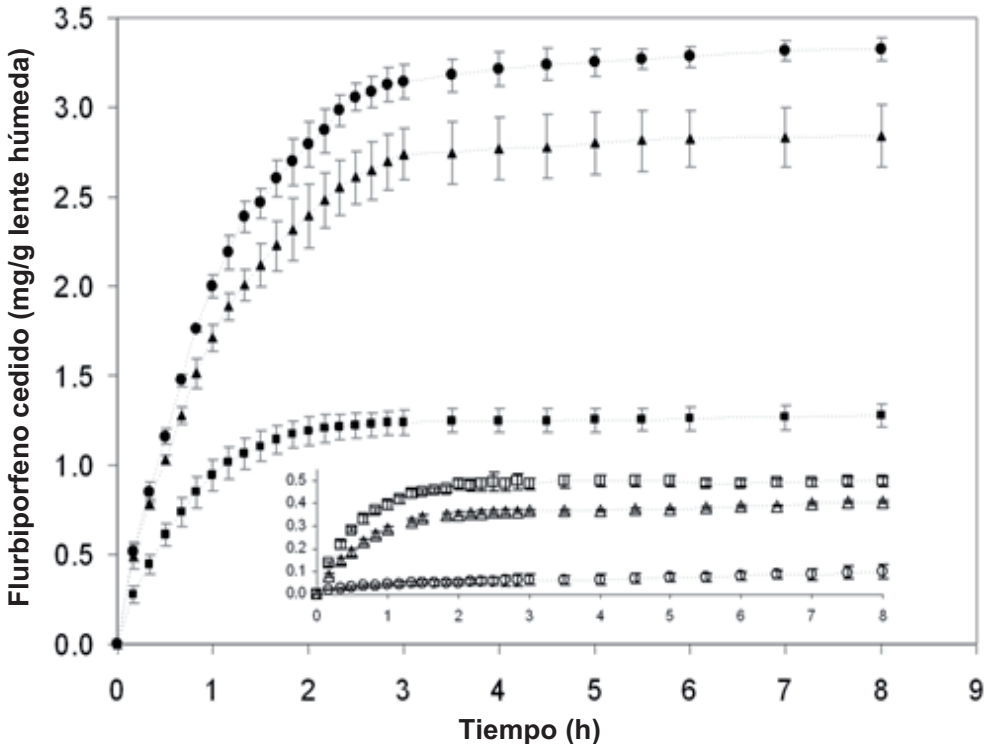

Figura 4.37. *Cinética de cesión de flurbiprofeno en agua a partir de las lentes de contacto Hilafilcon B cargadas mediante inmersión y liberación en agua (gráfico pequeño, símbolos vacíos (□) 1º ciclo; (Δ) 2º ciclo; y (○) 3 ciclo) y mediante impregnación seguida de extracción con CO_2 supercrítico (símbolos llenos: (■) 1º ciclo; (▲) 2 ciclo; y (●) 3º ciclo).*

Ciclos	Impregnación con CO_2 supercrítico				Impregnación en disolución acuosa		
	Cesión (µg/mg de lente húmeda)	Carga	Residual	Fármaco cedido (%)	Cesión (µg/mg de lente húmeda)	Carga	Fármaco cedido (%)
1º	1.28±0.07	10.53	0.013±0.003	11.98	0.498±0.002	0.92±0.07	54.27
2º	2.84±0.18	20.29	0.020±0.002	13.86	0.406±0.004	0.49±0.03	82.39
3º	3.58±0.08	54.54	0.063±0.023	6.48	0.102±0.003	0.147±0.002	69.58

Tabla 4.10*. Flurbiprofen cargado por las lentes de contacto que tras SSI o mediante el método tradicional por inmersión en una solución acuosa de fármaco, y flurbiprofeno cedido en agua expresado como la cantidad total o porcentaje relativo a la cantidad cargada (Valores medios ± desviación estándar).*

4.6.2. Efecto imprinting

Con el fin de dilucidar en qué medida la aplicación de ciclos sucesivos de impregnación/extracción permite crear en las lentes Hilafilcon B cavidades para alojar específicamente flurbiprofeno, se llevó a cabo un estudio de incorporación de éste fármaco, de ibuprofeno y de dexametasona a lentes tratadas y no tratadas. Para ello, se prepararon disoluciones acuosas ($3.3 \cdot 10^{-5}$ M) de cada fármaco y se sumergieron lentes en 20 mL de cada una de ellas durante 14 h. Los resultados obtenidos se muestran en la Figura 4.38.

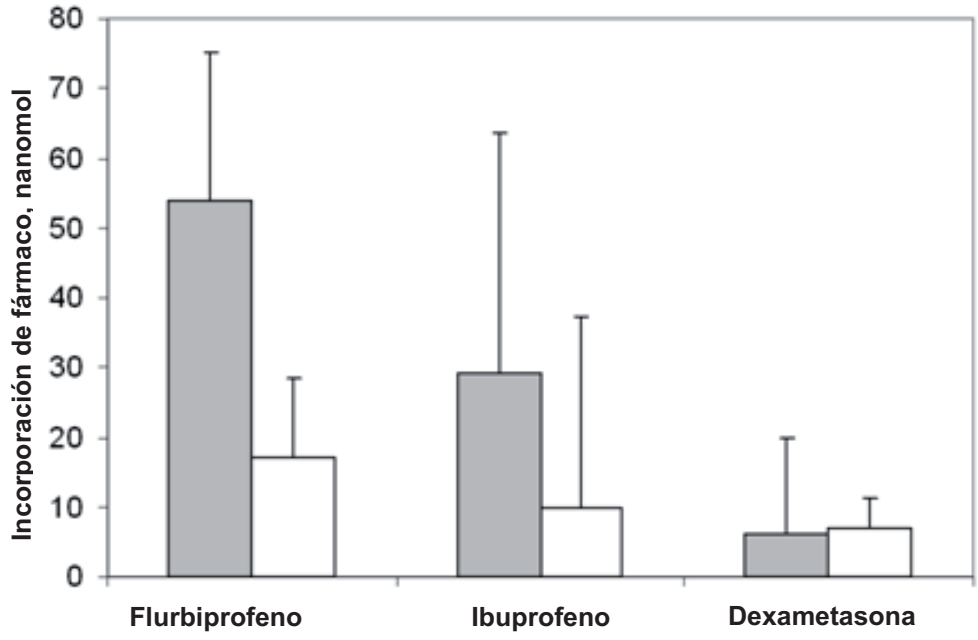

Figura 4.38. *Cantidades de fármaco incorporadas a lentes tras 14 horas de inmersión en disoluciones acuosas* $3.3 \cdot 10^{-5}$ M *de fármaco procesadas con SCF (MIP, ■) y lentes no procesadas/control (NIP, □).*

Las lentes no procesadas presentaron *per se* mayor afinidad por flurbiprofeno que por ibuprofeno y dexametasona. En el caso de las lentes tratadas previamente con flurbiprofeno, la afinidad por este fármaco se incrementó considerablemente, aunque también se observó una mejora en la incorporación de ibuprofeno. Los tamaños moleculares del flurbiprofeno (183.8 cm^3/mol) y del ibuprofeno (182.1 cm^3/mol) son muy similares, y notablemente más pequeños que el de la dexametasona (268.8 cm^3/mol). Por otra parte, tanto el flurbiprofeno como la dexametasona presentan un enlace C-F en su estructura, del que carece el ibuprofeno. Es bien sabido que los grupos carbonilo, presentes en la estructura de las lentes Hilafilcon B, pueden interaccionar fuertemente con el C-F dando lugar a una conformación peculiar en la que el átomo de fluor, muy electronegativo, interacciona perpendicularmente con el grupo carbonilo electrofílico, al tiempo que el enlace C-F se acerca al plano del grupo carbonilo formando un ángulo de 100-140º (Olsen y col., 2003; Paulini y col., 2005; Pagliaro y col., 2005, Hagmann y col., 2008). Estas interacciones, que son muy frecuentes en los procesos de reconocimiento molecular *in vivo*, podrían ser los responsables de la formación de cavidades imprinted en las lentes Hilafilcon B. En el caso de la dexametasona la notable diferencia de tamaño con el flurbiprofeno justifica que su incorporación a la estructura de la lente resulte más difícil.

4.6.3. Propiedades generales de las lentes de contacto

Por último, se comprobó que el tratamiento con fluidos supercríticos no provoca modificaciones significativas en las propiedades de las lentes de contacto desde el punto de vista de su funcionalidad como productos sanitarios. La observación por SEM de las lentes desecadas no reveló cambios en la estructura (Figura 4.39).

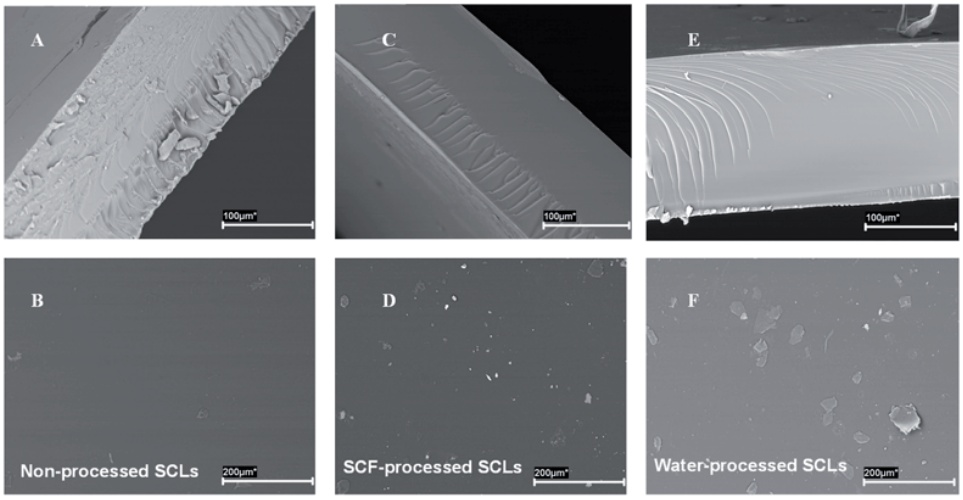

Figura 4.39. *Imágenes de SEM de lentes no procesadas (control), de lentes procesadas con SCF o lentes procesadas con disolución acuosa. Arriba: sección transversal (A, C y E); Abajo: imagen superficial (B, D y F).*

La temperatura de transición vítrea (91-92ºC), el grado de hinchamiento en agua (57.0-57.9%), la transmitancia a 400-900 nm (94-97%), la permeabilidad al oxígeno (14.8 barrer/cm), el ángulo de contacto (63-74º) y la energía superficial de las lentes (26-31 mN/m) tampoco se modificaron.

Por lo tanto, el tratamiento con fluidos supercríticos permite impregnar lentes comerciales Hilafilcon B con flurbiprofeno, regulando tanto la cantidad incorporada como la velocidad de cesión a través de la formación de cavidades imprinted para el fármaco. Un número de ciclos sucesivos de impregnación/extracción da lugar a una reorganización de las cadenas del entramado polimérico, promovida principalmente por la interacción del grupo C-F del fármaco con el carbonilo del polímero. Este tratamiento de post-imprinting no altera las propiedades básicas de las lentes de contacto comerciales.

Conclusiones

5. CONCLUSIONS

The following conclusions can be drawn from the results of the studies carried out to develop medicated SCL and trap systems that are based on hydrogels synthesized applying the molecular imprinting technology:

1.- The isothermal titration microcalorimetry (ITC) provides useful information for the screening of monomers and the identification of the drug/functional monomer ratio. This information enables the rational design of imprinted networks with high affinity for the template molecule. The experiments carried out with norfloxacin and timolol revealed that the imprinted hydrogels synthesized in the presence of the optimum drug/functional monomer ratio combine high ability to load the drug and improved control of drug release, compared to conventional non-imprinted hydrogels.

2.- SCL of poly(hydroxyethyl methacrylate) semi-interpenetrated with the demulcent polyvinylpyrrolidone (PVP) have a high optical clarity and behave as reservoirs that sustain the release of PVP. The molecular weight and proportion of PVP and the content in water enable to tune the friction coefficient of the hydrogels; the interpenetrated and surface protruding PVP chains being as a cushion between the SCL and the ocular surface. The proportion of water in the monomers solution determines the hydrogel microstructure and, particularly, the mean size and size distribution of meso and macropores. Microbiological tests carried out with Pseudomonas aeruginosa and Staphylococcus aureus revealed that hydrogels synthesized from monomers solution with less than 30% water, which have pores below 1 μm, do not allow the penetration of microorganisms. The greater the proportion of water, the higher the likelihood of the entrance of bacteria, as estimated by logistic regression.

3.- The use of computational modeling as screening tool of functional monomers enables to synthesize imprinted networks for the selective capture of bile salts. The computational modeling provided values of interaction energies of cholic acid with a wide range of monomers. Networks prepared with monomers that possess medium-to-low affinity for the template greatly benefit from the application of the molecular imprinting. Tuning the cross-linking degree of networks prepared with high affinity monomers enhanced the yield of trapping.

4.- A procedure for the impregnation with flurbiprofen of commercially available SCL (Hilafilcon B, Bausch & Lomb) using supercritical CO_2 that enhances one order of magnitude the loading without changing the features as medical devices has been implemented. Successive drug impregnation/extraction steps endow the SCL with progressive capability to host the drug and to sustain the release process. These findings are explained by the rearrangements

underwent by the polymeric chains of the SCL when the carbonyl groups interact with the C-F bonds of flurbiprofen. This process is favoured by the swelling and the plasticizing effect of the supercritical CO_2 on the network. The rearrangement leads to cavities that can host the drug in the preformed network, i.e., a post-imprinting effect.

In sum, the results confirm the usefulness of the molecular imprinting technology, supported by analytical and computational tools, for the rational design of polymeric networks that can uptake and control the release of drugs, hydrophilic polymers and active substances. Using this approach, drug/medical device combination products, such as medicated SCL that are imprinted during synthesis or after it, can be obtained. It is also possible to develop traps for the selective capture of biological substances. The microstructure of the imprinted networks determines their performance and remarkably affects the surface roughness, the diffusion of substances through the network, and the interaction with bacteria. .

Bibliografía

6. BIBLIOGRAFÍA

Ahmed, I., Francoeur, M.L., Thombre, A.G., Patton, T.F. The kinetics of timolol in the rabbits lens: implications for ocular drug delivery. Pharm. Res. **6**, 772-778 (1989).

Ahmed, I., Gokhale, R.D., Shah, M.V., Patton, T.F. Physicochemical determinants of drug diffusion across the conjunctiva, sclera, and cornea. J. Pharm. Sci. **76**, 583-586 (1987).

Ali, M., Byrne, M.E. Controlled release of high molecular weight hyaluronic acid from molecularly imprinted hydrogel contact lenses. Pharm. Res. **26**, 714-726 (2009).

Ali, M., Horikawa, S., Venkatesh, S., Saha, J., Pass, S., Hong, J.W., Byrne, M.E. Zero-order therapeutic release from imprinted hydrogel contact lenses within in vitro physiological ocular tear flow. J. Control. Release **124**, 154-162 (2007).

Allender, C.J., Brain, K.R., Heard, C.M. Molecularly imprinted polymers: preparation, biomedical applications and technical challenges. En: Progress in medicinal chemistry, vol. 36; King, F.D., Oxford, A.W., eds. Elsevier, Amsterdam, 1999. Pag. 235-291.

Allender, C.J., Richardson, C., Woodhouse, B., Heard, C.M., Brain, K.R. Pharmaceutical applications for molecularly imprinted polymers. Int. J. Pharm. **195**, 39-43 (2000).

Alonso, M.J. Nanomedicines for overcoming biological barriers. Biomed. Pharmacother. **58**, 168-172 (2004).

Alvarez-Lorenzo, C., Concheiro, A. Intelligent drug delivery systems: polymeric micelles and hydrogels. Mini-Rev. Med. Chem. **8**, 1065-1074 (2008).

Alvarez-Lorenzo, C., Concheiro, A. Molecularly imprinted polymers for drug delivery. J. Chromatogr. B. **804**, 231-245 (2004).

Alvarez-Lorenzo, C., Concheiro, A. Molecularly imprinted gels and nano- and microparticles: manufacture and applications. En: Smart nano and microparticles; Arshady, R., Kono, K., eds. Kentus Books, London, 2005. Pag. 279-336.

Alvarez-Lorenzo, C., Concheiro, A. Molecularly imprinted materials as advanced excipients for drug delivery systems. En: Biotechnology annual review, vol. 12; El-Gewely, M.R., ed. Elsevier, Amsterdam 2006. Pag. 225-268.

Alvarez-Lorenzo, C., Hiratani, H., Gomez-Amoza, J.L., Martinez-Pacheco, R., Souto, C., Concheiro, A. Soft contact lenses capable of sustained delivery of timolol. J. Pharm. Sci. **91**, 2182-2192 (2002).

Alvarez-Lorenzo, C., Moya-Ortega, M.D., Loftsson, T., Concheiro, A., Torres-Labandeira, J.J. Cyclodextrin-based hydrogels. En Cyclodextrins in Pharmaceutics, Cosmetics and Biomedicine: Current and Future Industrial Applications; Bilensoy, E., ed., John Wiley, New York. En prensa, 2010.

Alvarez-Lorenzo, C., Yañez, F., Barreiro-Iglesias, R., Concheiro, A. Imprinted soft contact lenses as norfloxacin delivery systems. J. Control. Release **113**, 236–244 (2006).

Anderson, B.D., Conradi, R.A. Predictive relationships in the water solubility of salts of a nonsteroidal anti-inflammatory drug. J. Pharmacol. Sci. **74**, 815-820 (1985).

Anderson, E.M., Noble, M.L., Garty, S., Maa, H., Bryers, J.D., Shen, T.T., Ratner, B.D. Sustained release of antibiotic from poly(2-hydroxyethyl methacrylate) to prevent blinding infections after cataract surgery. Biomaterials **30**, 5675–5681 (2009).

Anderson, H.S., Karlsson, J.G., Piletsky, S.A., Koch-Schmidt, A.C., Mosbach, K., Nicholls, I.A. Study of the nature of recognition in molecularly imprinted

polymers: influence of monomer-template ratio and sample load on retention and selectivity. J. Chromatogr. A **848**, 39-49 (1999).

Andrade-Vivero, P., Fernandez-Gabriel, E., Alvarez-Lorenzo, C., Concheiro, A. Improving the loading and release of NSAIDs from p-HEMA hydrogels by copolymerization with functionalized monomers. J. Pharm. Sci. **96**, 802-813 (2007).

Aqil, M. Advanced in ophthalmic drug delivery systems. Pharmainfo.net. *http://www.pharmainfo.net/reviews/advances-ophthalmic-drug-delivery-systems-part-ii* [consultada en Junio 2010].

Arggarwal, D., Kaur, I.P. Improved pharmacodynamics of timolol maleate from a mucoadhesive niosomal ophthalmic drug delivery system. Int. J. Pharm. **290**, 155-159 (2005).

Arshady, R., Mosbach, K. Synthesis of substrate-selective polymers by host-guest polymerization. Macromol. Chem. **182**, 687-692 (1981).

Barbu, E., Verestiuc, L., Iancu, M., Jatariu, A., Lungu, A., Tsibouklis, J. Hybrid polymeric hydrogels for ocular drug delivery: nanoparticulate systems from copolymers of acrylic acid-functionalized chitosan and *N*-isopropylacrylamide or 2-hydroxyethyl methacrylate. Nanotechnology **20**, 225108 (2009).

Barr, J. 2004 Annual Report. Contact Lens Spectrum's annual report of major corporate and product developments and events in the contact lens industry in 2004, as well as predictions for 2005. Contact Lens Spectrum (2005). *http://www.clspectrum.com/* [consultada en Junio 2010].

Berkow, R., Beers, M.H., Bogin, R.M., Fletcher, A.J. The Merck manual of medical information. Merck research laboratories, New Jersey, 1997. Pag. 1536.

Bendoriene, J., Vogt, U. Therapeutic use of silicone hydrogel contact lenses in children. Eye Contact Lens **32**, 104-108 (2006).

Bertucco, A., Vetter, G. High pressure process technology: fundamentals and applications. En: Industrial Chemistry Library, vol. 9; Bertucco, A., Vetter, G., eds. Elsevier, Amsterdam, 2001. Pag. 651.

Boatright, J.H., Nickerson, J.M., Moring, A.G., Pardue, M.T. Bile acids in treatment of ocular disease. J. Ocul. Biol. Dis. Inform. **2**, 149–159 (2009).

Boone, A., Hui, A., Jones, L. Uptake and release of dexamethasone phosphate from silicone hydrogel and group I, II, and IV hydrogel contact lenses. Eye Contact Lens **35**, 260-267 (2009).

Bourges, J.L., Bloquel, C., Thomas, A., Froussart, F., Bochot, A., Azan, F., Gurny, R., BenEzra, D., Behar-Cohen, F. Intraocular implants for extended drug delivery: Therapeutic applications. Adv. Drug Deliver. Rev. **58**, 1182-1202 (2006).

Bourlais, C.L., Acar, L., Zia, H., Sado, P.A., Needham, T., Leverge, R. Ophthalmic drug delivery systems. Prog. Retin. Eye Res. **17**, 33-58 (1998).

Braga, M.E.M., Pato, M.T.V., Silva, H.S.R.C., Ferreira, E.I., Gil, M.H., Duarte, C.M.M., De Sousa, H.C. Supercritical solvent impregnation of ophthalmic drugs on chitosan derivatives. J. Supercrit. Fluids **44**, 245-257 (2008a).

Braga, M.E.M., Santos, R.M.S., Seabra, I.J., Facanali, R., Marques, M.O.M., de Sousa, H.C. Fractioned SFE of antioxidants from maritime pine bark. J. Supercrit. Fluids **47**, 37-48 (2008b).

Brown, Z.K., Fryer P.J., Norton, I.T., Bakalis, S., Bridson, R.H. Drying of foods using supercritical carbon dioxide. Investigations with carrot. Innov. Food Sci. Emerg. Technol. **9**, 280-289 (2008).

Budai, L., Hajdú, M., Budai, M., Gróf, P., Béni, S., Noszál, B., Klebovich, I., Antal, I. Gels and liposomes in optimized ocular drug delivery: Studies on ciprofloxacin formulations. Int. J. Pharm. **343**, 34-40 (2007).

Byrne, M.E., Park, K., Peppas, N.A. Molecular imprinting within hydrogels. Adv. Drug Deliver. Rev. **54**, 149-161 (2002).

Calvo, P., Vila-Jato, J.L., Alonso, M.J. Comparative in vitro evaluation of several colloidal systems, nanoparticles, nanocapsules, and nanoemulsions as ocular drug carriers. J. Pharm. Sci. **85**, 530-536 (1996).

Chan, J., El Maghraby, G.M.M., Craig, J.P., Alany, R.G. Phase transition water-in-oil microemulsions as ocular drug delivery systems: In vitro and in vivo evaluation. Int. J. Pharm. **328**, 65-71 (2007).

Chapman, J.M., Cheeks, L., Green, K. Drug-interaction with intraocular lenses of different materials. J. Cataract. Reflact. Surg. **18**, 456-459 (1992).

Chianella, I., Piletsky, S.A., Tothill, I.E., Chen, B., Turner, A.P.F. MIP-based solid phase extraction cartridges combined with MIP-based sensors for the detection of microcystin-LR. Biosens. Bioelectron. **18**, 119-127 (2003).

Chianella, I., Lotierzo, M., Piletsky, S.A., Tothill, I.E., Chen, B., Karim, K., Turner, A.P.F. Rational design of a polymer specific for microcystin-LR using a computational approach. Anal. Chem. **74**, 1288-1293 (2002).

Chow, P.Y.E., Yang, Y.Y. Polymer having interconnected pores for drug delivery method. Patent WO2006/014138A1, 2006.

Civiale, C., Licciardi, M., Cavallaro, G., Giammona, G., Mazzone, M.G. Polyhydroxyethylaspartamide-based micelles for ocular drug delivery. Int. J. Pharm. **378**, 177-186 (2009).

Consejo General Colegios Farmacéuticos, Catálogo de Medicamentos: Oftalmológicos antiinfecciosos, S01AA; Madrid, 2009. Pag. 2725-2732.

Corsini, A., Windler, E., Farnier, M. Colesevelam hydrochloride: usefulness of a specifically engineered bile acid sequestrant for lowering LDL-cholesterol. Eur. J. Cardiovasc. Prev. Rehabil. **16**, 1-9 (2009).

Costa, V.P., Braga, M.E.M., Duarte, C.M.M., Alvarez-Lorenzo, C., Concheiro, A., Gil, M.H., de Sousa, H.C. Anti-glaucoma drug-loaded contact lenses prepared using supercritical solvent impregnation. J. Supercrit. Fluids **53**, 165-173 (2010).

Cunliffe, D., Kirby, A., Alexander, C. Molecularly imprinted drug delivery systems. Adv. Drug Deliver. Rev. **57**, 1836-1853 (2005).

Danion, A., Arsenault, I., Vermette, P. Antibacterial activity of contact lenses bearing surface-inmobilized layers of intact liposomes loaded with levofloxacin. J. Pharm. Sci. **96**, 2350-2363 (2007a).

Danion, A., Brochu, H., Martin, Y., Vermette, P. Fabrication and characterization of contact lenses bearing surface-immobilized layers of intact liposomes. J. Biomed. Mater. Res. Part A **82**, 41-51 (2007b).

Dart, J.K.G., Radford, C.F., Minassian, D., Verma, S., Stapleton, F. Risk factors for microbial keratitis with contemporary contact lenses: a case-control study. Ophthalmology **115**, 1647-1654 (2008).

Davis, J.L., Gilger, B.C., Robinson, M.R. Novel approaches to ocular drug delivery. Curr. Opin. Mol. Ther. **6**, 195-205 (2004).

DeNaeyer, G.W. Exploring the therapeutic applications of contact lenses. Optometry Management, **December**, 11-15 (2008).

Deshpande, A.A., Heller, J., Gurny, R. Bioerodible polymers for ocular delivery. Crit. Rev. Ther. Drug. **15**, 381–420 (1998).

Di Marco, G., Lanza, M., Pieruccini, M. Dynamical mechanical measurements in dry PHEMA and its hydrogels. Nuovo Cim. D **16**, 849–854 (1994).

Diebold, Y., Jarrín, M., Sáez, V., Carvalho, E.L.S., Orea, M., Calonge, M., Seijo, B., Alonso, M.J. Ocular drug delivery by liposome–chitosan nanoparticle complexes (LCS-NP). Biomaterials **28**, 1553-1564 (2007).

Donshik, P.C. Extended wear contact lenses. Ophtalmol. Clin. North Am. **16**, 79-83 (2003).

Dracopoulos, A., Bantseev, V., Sivak, J.G. In vitro uptake and release interaccions of benzylkonium chloride (BAK) by silicon containing and p-HEMA hydrogels contact lens materials. Invest. Ophthalmol. Vis. Sci. **46**, E-Abstract 912 (2005).

Duarte, A.R.C., Simplicio, A.L., Vega-Gonzalez, A., Subra-Paternault, P., Coimbra, P., Gil, M.H., de Sousa, H.C., Duarte, C.M.M. Supercritical fluid impregnation of a biocompatible polymer for ophthalmic drug delivery. J. Supercrit. Fluids **42**, 373-377 (2007).

Duarte, A.R.C., Simplicio, A.L., Vega-Gonzalez, A., Supra-Paternault, P., Coimbra, P., Gil, M.H., Sousa, H.C. de, Duarte, C.M.M. Impregnation of intraocular lens for ophthalmic drug delivery. Curr. Drug Deliv. **5**, 102-107 (2008).

Ebrahim, S., Peyman, G.A., Lee, P.J. Applications of liposomes in ophthalmology. Surv. Ophthalmol. **50**, 167-182 (2005).

FDA, 1994. Premarket notification (510(k)) guidance document for daily wear contact lenses. *http://www.fda.gov/MedicalDevices/DeviceRegulationandGuidance/GuidanceDocuments/ucm080928.htm.* [consultado en Junio 2010].

Felt, O., Einmahl, S., Gurny, R., Furrer, P., Baeyens, V. Polymeric systems for ophthalmic drug delivery. En: Polymeric Biomaterials; Dumitriu, S., ed. Marcel Dekker, New York, 2002. Pag. 377-421.

Filippatos, T.D., Mikhailidis, D.P. Lipid-lowering drugs acting at the level of the gastrointestinal tract. Curr. Pharm. Des. **15**, 490–516 (2009).

Fish, W.P., Ferreira, J., Sheardy, R.D., Snow, N., O'Brien, T. Rational design of an imprinted polymer: maximizing selectivity by optimizing the monomer-template ratio of a cinchonidine MIP, prior to polymerization, using microcalorimetry. J. Liq. Chromatogr. Relat. Technol. **28**, 1-15 (2005).

Fleming, O.S., Kazarian, S.C. Polymer processing with supercritical fluids. En: Supercritical Carbon Dioxide in Polymer Reaction Engineering; Kemmere, M.F., Meyer, T., eds. Wiley-VCH, Weinheim, 2005. Pag. 205–234.

Fleming, O. S., Kazarian, S. G., Bach, E., Shollmeyer, W. Confocal Raman study of PET fibres dyed with supercritical carbon dioxide: dye diffusion and polymer morphology**.** Polymer **46**, 2943-2949 (2005).

Galezowski, X. Sur la place cornéenne dans l´extraction de la catarate et sur les moyens de prévenir la suppuration. Bull. Mem. Soc. Fr. Ophthalmol. **4**, 217-226 (1886).

Garcia-Calzon, J.A., Diaz-Garcia, M.E. Characterization of binding sites in molecularly imprinted polymers. Sens. Actuat. B-Chem. **123**, 1180–1194 (2007).

Gasset, A., Kaufman, H.E. Therapeutic uses of hydrophilic contact lenses . Am. J. Ophthalmol. **69**, 252-259 (1970).

Gaudana, R., Jwala, J., Boddu, S.H.S., Mitra, A.K. Recent perspectives in ocular drug delivery. Pharm. Res. **26**, 1197-1215 (2009).

Gavini, E., Chetoni, P., Cossu, M. PLGA microspheres for the ocular delivery of a peptide drug, vancomycin using emulsification/spray-drying as the preparation method: in vitro/in vivo studies. Eur. J. Pharm. Biopharm. **57**, 207-212 (2004).

Glasson, M.J., Stapleton, F., Keay, L., Willcox, M.D.P. The effect of short term contact lens wear on the tear film and ocular surface characteristics of tolerant and intolerant wearers. Contact Lens Ant. Eye. **29**, 41-47 (2006).

Gong, K., Darr, J.A., Rehman, I.U. Supercritical fluid assisted impregnation of indomethacin into chitosan thermosets for controlled release applications. Int. J. Pharm. **315**, 93–98 (2006).

Guerreiro, A., Soares, A., Piletska, E., Mattiasson, B., Piletsky, S. Preliminary evaluation of new polymer matrix for solid-phase extraction of nonylphenol from water samples. Anal. Chim. Acta **612**, 99–104 (2008).

Gulsen, D., Chauhan, A. Dispersion of microemulsion drops in HEMA hydrogel: a potential ophthalmic drug delivery vehicle. Int. J. Pharm. **292**, 95-117 (2005).

Gulsen, D., Chauhan, A. Effect of water content on transparency, swelling, lidocaine diffusion in p-HEMA gels. J. Memb. Sci. **269**, 35-48 (2006).

Gulsen, D., Chauhan, A. Ophthalmic drug delivery through contact lenses. Invest. Ophthalmol. Vis. Sci. **45**, 2342-2347 (2004).

Gulsen, D., Li, C.C., Chauhan, A. Dispersion of DMPC liposomes in contact lenses for ophthalmic drug delivery. Curr. Eye Res. **30**, 1071-1080 (2005).

Hagmann, W.K. The many roles for fluorine in medicinal chemistry. J. Med. Chem. **51**, 4359-4369 (2008).

Hehl, E.M., Beck, R., Luthard, K., Guthoff, R., Drewelow, B. Improved penetration of aminoglycosides and fluoroquinolones into aqueous humour of patients by mans of Acuvue contact lenses. Eur. J. Clin. Pharmacol. **55**, 317-323 (1999).

Heller, J. Ocular delivery using poly(ortho esters). Adv. Drug Deliver. Rev. **57**, 2053-2062 (2005).

Herrero-Vanrell, R., Fernandez-Carballido, A., Frutos, G., Cadórniga, R. Enhancement of the mydriatic response to tropicamide by bioadhesive polymers. J. Ocul. Pharmacol. Ther. **16**, 419-428 (2000).

Heyrman, T.P., McDermott, M.L., Ubels, J.L., Edelhauser, H.F. Drug uptake and release by a hydrogel intraocular-lens and the human crystalline lens. J. Cataract. Refract. Surg. **15**, 169-175 (1989).

Hillberg, A.L., Brain, K.R., Allender, C.J. Molecular imprinted polymer sensors: implications for therapeutics. Adv. Drug Deliver. Rev. **57**, 1875-1889 (2005).

Hillman, J.S. Management of acute glaucoma with pilocarpine-soaked hydrophilic lens. Br. J. Ophthalmol. **58**, 674-679 (1974).

Hilt, J.Z., Byrne, M.E. Configurational biomimesis in drug delivery: molecular imprinting of biologically significant molecules. Adv. Drug Deliver. Rev. **56**, 1599-1620 (2004).

Hiratani, H., Alvarez-Lorenzo, C. Process for production of hydrogel material enhanced in the intake of drugs and permitting sustained release of drugs. Patent WO03090805, 2003.

Hiratani, H., Alvarez-Lorenzo, C. The nature of backbone monomers determines the performance of imprinted soft contact lenses as timolol drug delivery systems. Biomaterials **25**, 1105-1113 (2004).

Hiratani, H., Alvarez-Lorenzo, C. Timolol uptake and release by imprinted soft contact lenses made of N,N-diethylacrylamide and methacrylic acid. J. Control. Release **83**, 223-230 (2002).

Hiratani, H., Fujiwara, A., Tamiya, Y., Mizutani, Y., Alvarez-Lorenzo, C. Ocular release of timolol from molecularly imprinted soft contact lenses. Biomaterials **26**, 1293-1298 (2005a).

Hiratani, H., Mizutani, Y., Alvarez-Lorenzo, C. Controlling drug release from imprinted hydrogels by modifying the characteristics of the imprinted cavities. Macromol. Biosci. **5**, 728-733 (2005b).

Hiratani, H., Nakajima, T., Yamamoto, K.J. The state and prospect of contact lenses. Jpn. Soc. Biomaterials **20**, 221-227 (2002).

Hou, R., Goldberg, A.C. Lowering low-density lipoprotein cholesterol: statins, ezetimibe, bile acid sequestrants, and combinations: comparative efficacy and safety. Endocr. Metab. Clin. **38**, 79–97 (2009).

Hsiue, G.H., Guu, J.A., Cheng, C.C. Poly(2-hydroxyethyl methacrylate) film as a drug delivery system for pilocarpine. Biomaterials **22**, 1763-1769 (2001).

Hughes, P.M., Olejnik, O., Chang-Lin, J.E., Wilson, C.G. Topical and systemic drug delivery to the posterior segments. Adv. Drug Deliver. Rev. **57**, 2010-2032, (2005)

Hui, A., Boone, A., Jones, L. Uptake and release of Ciprofloxacin-HCl from conventional and silicone hydrogel contact lens materials. Eye Contact Lens **34**, 266-271 (2008).

Hull, D.S., Edelhauser, H.F., Hyndiuk, R.A. Ocular penetration of prednisolone and hydrophilic contact-lens. Arch. Opthalmol. **92**, 413-6 (1974).

Ito, K., Chuang, J., Alvarez-Lorenzo, C., Watanabe, T., Ando, N., Grosberg, A.Y. Multiple point adsorption in a heteropolymer gel and the Tanaka approach to imprinting: experiment and theory. Progr. Polym. Sci. **28**, 1489-1515 (2003).

Jaffe, G.J., Martin, D., Callanan, D., Pearson, P.A., Levy, B., Comstock, T. Fluocinolone acetonide implant (Retisert) for noninfectious posterior uveitis: thirty-four-week results of a multicenter randomized clinical study. Ophthalmology **113**, 1020–1027 (2006).

Jain, M.R. Drug delivery through soft contact-lenses. Br. J. Ophtalmol. **72**, 150-154 (1988).

Johnson, M.E., Murphy, P.J. Changes in the tear film and ocular surface from dry eye syndrome. Prog. Retin. Eye Res. **23**, 449-474 (2004).

Kandimalla, V.B., Ju, H.X. Molecular imprinting: a dynamic technique for diverse applications in analytical chemistry. Anal. Bioanal. Chem. **380**, 587-605 (2004).

Kanpolat, A., Ucakhan O. Therapeutic use of Focus Night & Day contact lenses. Cornea **22**, 726-734 (2003).

Kapoor, Y., Chauhan, A. Ophthalmic delivery of Cyclosporine A from Brij-97 microemulsion and surfactan-laden p-HEMA hydrogels. Int. J. Pharm. **361**, 222-229 (2008).

Kapoor, Y., Thomas, J.C., Tan, G., John, V.T., Chauhan, A. Surfactant-laden soft contact lenses for extended delivery of ophthalmic drugs. Biomaterials **30**, 867-878 (2009).

Karim, K., Breton, F., Rouillon, R., Piletska, E.V., Guerreiro, A., Chianella, I., Piletsky, S.A. How to find effective functional monomers for effective molecularly imprinted polymers?. Adv. Drug Deliver. Rev. **57**, 1795-1808 (2005).

Karlgard, C.C., Jones, L.W., Moresoli, C. Ciprofloxacin interaction with silicon-based and conventional hydrogel contact lenses. Eye Contact Lens **29**, 83-89 (2003).

Karlgard, C.C.S., Wong, N.S., Jones, L.W., Moresoli, C. In vitro uptake and release studies of ocular pharmaceutical agents by silicon-containing and p-HEMA hydrogels contact lens materials. Int. J. Pharm. **257**, 141-151 (2003).

Kaufman, H.E., Uotila, M.H., Gasset, A.R. The medical uses of soft contact lenses. Trans. Am. Acad. Ophthalmol. Otolaryngol. **75**, 361-373 (1971).

Kaur, I.P., Kanwar, M. Ocular preparations: the formulation approach. Drug Dev. Ind. Pharm. **28**, 473-493 (2002).

Kawashima, Y., York, P. Drug delivery applications of supercritical fluid technology. Adv. Drug Deliver. Rev. **60**, 297-298 (2008).

Kazarian, S.G. Polymer processing with supercritical fluids. Polym. Sci. Ser. C **42**, 78-101 (2000).

Kazarian, S.G., Chan, K.L.A. Confocal Raman microscopy of supercritical fluid dyeing of polymers. Analyst **128**, 499-503 (2003).

Kazarian, S.G., Martirosyan, G.G. Spectroscopy of polymer/drug formulations processed with supercritical fluids: in situ ATR-IR and Raman study of impregnation of ibuprofen into PVP. J. Control. Release **232**, 81-90 (2002).

Kearns V.R., Williams R.L. Drug delivery systems for the eye. Expert Rev. Med. Devices **6**, 277-290 (2009).

Kemmere, M.F., Meyer, T. Supercritical carbon dioxide in polymer reaction engineering; Kemmere, M.F., Meyer, T., eds. Wiley-VCH, Weinheim, 2005.

Kikic, F.,Vecchione, F. Supercritical impregnation of polymers. Curr. Opin. Solid St. Mat. Sci. **7**, 399-405 (2003).

Kikic, I., Vecchione, F., Alessi, P., Cortesi, A., Eva, F., Elvassore, N. Polymer plasticization using supercritical carbon dioxide: Experiment and modeling industrial & engineering chemistry research. Ind. Eng. Chem. Res. **42**, 3022-3029 (2003).

Kim, J., Conway, A., Chauhan, A. Extended delivery of ophthalmic drugs by silicone hydrogel contact lenses. Biomaterials **29**, 2259-2269 (2008).

Kim, M.N., Lim, A.H., Yoon, J.S. Antibacterial activity of polymers with norfloxacin moieties against native and norfloxacin-tolerance-induced bacteria. J. Appl. Polym. Sci. **96**, 936-943 (2005).

Kim, S.W., Bae, Y.H., Okano, T. Hydrogels: swelling, drug loading, and release. Pharm. Res. **9**, 283-290 (1992).

Kopecek, J. Hydrogels: From soft contact lenses and implants to self-assembled nanomaterials. J. Pol. Sci. Pol. Chem. **47**, 5929-5946 (2009).

Krejci, L. Therapeutic use of scleral gel contact lenses. Cesk Oftalmol. **27**, 104-109 (1971).

Krejci, L., Brettschneider, I., Praus, R. Comparative study of fluorescein release from various types of therapeutic hydrophilic gel contact lenses. Cesk Oftalmol. **27**, 285-291 (1971).

Krejci, L., Brettschneider, I., Praus, R. Hydrophilic gel contact lenses as a new drug delivery system in ophthalmology and as a therapeutic bandage lenses. Act. Univ. Carol. Med. **21**, 387-96 (1975).

Kuenzler, J.F., McGee, J.A. Contact lens materials. Chem. Ind. **16**, 651-655 (1995).

Kuppermann, B.D., Blumenkranz, M.S., Haller, J.A., Williams, G.A., Weinberg, D.V., Chou, C., Whitcup, S.M. Randomized controlled study of an intravitreous dexamethasone drug delivery system in patients with persistent macular edema. Arch. Ophthalmol. **125**, 309-317 (2007).

Lang, J.C. Ocular drug delivery conventional ocular formulations. Adv. Drug Deliver. Rev. **16**, 39-43 (1995).

Langer, R. Polymeric delivery systems for controlled drug release. Chem. Eng. Commun. **6**, 1-48 (1980).

Lauritsen, K.J., Nguyen, T. Combination products regulation at the FDA. Clin. Pharmacol. Ther. **85**, 468-470 (2009).

Lemp, M.A. Report of the National Eye Institute/Industry workshop on clinical trials in dry eyes. CLAO J. **21**, 221-232 (1995).

Lesher, G.A., Gunderson, G.G. Continuous drug delivery through the use of disposable contact lenses. Optom. Vis. Sci. **70**, 1012-1018 (1993).

Li, C.C., Abrahamson, M., Kapoor, Y., Chauhan, A. Timolol transport from microemulsions trapped in HEMA gels. J. Colloid Interf. Sci. **315**, 297-306 (2007).

Li, C.C., Chauhan, A. Modeling ophtalmic drug delivery by soaked contact lenses. Ind. Eng. Chem. Res. **45**, 3718-3734 (2006).

Li, N., Zhuang, C., Wang, M., Sun, X., Nie, S., Pan, W. Liposome coated with low molecular weight chitosan and its potential use in ocular drug delivery. Int. J. Pharm. **379**, 131-138 (2009).

Li, X., Ciu, Y. Study on synthesis and chloramphenicol release of poly(2-hydroxyethylmethacrylate-co-acrylamide) hydrogels. Chin. J. Chem. Eng. **16**, 640-645 (2008).

Lim, L., Tan, D.T.H., Chan, W.K. Therapeutic use of Bausch & Lomb Pure Vision contact lenses. CLAO J. **27**, 179-185 (2001).

Liu, W., Griffith, M., Li, F. Alginate microsphere-collagen composite hydrogel for ocular drug delivery and implantation. J. Mater. Sci: Mater. Med. **19**, 3365-3371 (2008).

Lloyd, A.W., Faragher, R.G.A., Denyer, S.P. Ocular biomaterials and implants. Biomaterials **22**, 769-785 (2001).

Lord, M.S., Stenzel, M.H., Simmons, A., Milthorpe, B.K. Lysozyme interaction with poly(HEMA)-based hydrogel. Biomaterials **27**, 1341-1345 (2006).

Ludwig, A. The use of mucoadhesive polymers in ocular drug delivery. Adv. Drug Deliver. Rev. **57**, 1595-1639 (2005).

Luque de Castro, M.D., Valcárcel, M., Tena, M.T. Extracción con fluidos supercríticos en el proceso analítico. Reverté, Barcelona, 1993. Pag. 47-51.

Maeda, M., Bartsch, R.A. Molecular and ionic recognition with imprinted polymers: a brief overview. En: Molecular and ionic recognition with imprinted polymers ACS Symposium Series, 703; Bartsch R.A., Maeda, M., eds. American Chemical Society, Washington DC, 1998. Pag. 1-8.

Mainardes, R.M., Urban, M.C.C., Cinto P.O., Khalil, N.M., Chaud, M.V., Evangelista, R.C., Daflon-Gremiao, M.P. Colloidal carriers for ophthalmic drug delivery. Curr. Drug Targets **6**, 363-371 (2005).

Mandeville, W.H., Braunlin, W., Dhal, P., Guo, A., Huval, C., Miller, K., Petersen, J., Polomoscanik, S., Rosenbaum, D., Sacchiero, R., Ward, J., Holmes-Farley, S.R. Three generations of bile acid sequestrants. Mater. Res. Soc. Symp. Proc. **550**, 3–15 (1999).

Marmion, V.J., Jain, M.R. Role of soft contact-lenses and delivery of drugs. Trans. Ophthalmol. Soc. UK **96**, 319-321 (1976).

Martin, R., de Juan, V., Rodriguez, G., Fonseca, S., Martin, S. Contact lens-induced corneal peripheral swelling: Orbscan repeatability. Optom. Vis. Sci. **86**, 340-349 (2009).

Maruyama, K., Yokoi, N., Takehisa, Y., Kinoshita, S. Effect of environmental conditions on tear dynamics in soft contact lens wearers. Invest. Ophthalmol. Vis. Sci. **45**, 2563-2568 (2004).

Matoba, A.Y., McCulley, J.P. The effect of therapeutic soft contact-lenses on antibiotic delivery to the cornea. Ophthalmology **92**, 97-99 (1985).

Mayes, A.G., Whitcombe, M.J. Synthetic strategies for the generation of molecularly imprinted organic polymers. Adv. Drug Deliver. Rev. **57**, 1742-1778 (2005).

Mayol, L., Quaglia, F., Borzacchiello, A., Ambrosio, L., La Rotonda, M.I. A novel poloxamers/hyaluronic acid *in situ* forming hydrogel for drug delivery: Rheological, mucoadhesive and *in vitro* release properties. Eur. J. Pharm. Biopharm. **70**, 199-206 (2008).

Mazuel, C. Norfloxacin. En: Analytical Profiles of Drug Substances and Excipients, vol. 20; Florey, K., ed. Academic Press, London, 1991. Pag. 557-600.

McMahon, T.T., Zadnik, K. Twenty-five years of contact lenses. Cornea **19**, 730-740 (2000).

McStay, D., Al-Obaidi, A.H., Hoskins, R., Quinn, P.J. Raman spectroscopy of molecularly imprinted polymers. J. Opt. A: Pure Appl. Opt. **7**, S340-345 (2005).

Mely, R. Therapeutic and cosmetic indications of Lotrafilcon. A silicone hydrogel extended-wear lenses. Ophthalmologica **218**, 33-38 (2004).

Mika, A.M., Childs, R.F. Acid/base properties of poly(4-vinylpyridine) anchored within microporous membranes. J. Membrane Sci. **152**, 129–140 (1999).

Molinelli, A., O'Mahony, J., Nolan, K., Malcolm R., Smyth, M.R., Jakusch, M., Mizaikoff, B. Analyzing the mechanisms of selectivity in biomimetic self-assemblies via IR and NMR spectroscopy of prepolymerization solutions and molecular dynamics simulations. Anal. Chem. **77**, 5196-5204 (2005).

Momose, T., Ito, N., Kanai, A., Watanabe, Y., Shibata, M. Adsorption of levocabastine eye drops by soft contact lenses and its effects in rabbit eyes. CLAO J. **23**, 96-99 (1997).

Monti, S., Cappelli, C., Bronco, S., Giusti, P., Ciardelli, G. Towards the design of highly selective recognition sites into molecular imprinting polymers: A computational approach. Biosens. Bioelectron. **22**, 153-163 (2006).

Mundada, A.S., Avari, J.G. In situ gelling polymers in ocular drug delivery systems: a review. Crit. Rev. Ther. Drug **26**, 85-118 (2009).

Munoa- Roiz, J.L., Aramendia-Salvador, E. Historia y desarrollo de las lentes de contacto. *http://www.oftalmo.com/publicaciones/lentes/cap2.htm* [consultada en Junio 2010].

Myles, M.E., Neumann, D.M., Hill, J.M. Recent progress in ocular drug delivery for evaluation of several posterior segment disease: emphasis on transcleral iontophoresis. Adv. Drug Deliver. Rev. **57**, 2063-2079 (2005).

Nagarwal, R.C., Kant, S., Singh, P.N., Maiti, P., Pandit, J.K. Polymeric nanoparticulate system: A potential approach for ocular drug delivery. J. Control. Release **136**, 2-13 (2009).

Natu, V., Gil, M.H., Sousa, H.C. de. Supercritical solvent impregnation of poly(ε-caprolactone)/poly(oxyethylene-b-oxypropylene-b-oxyethylene) and poly(ε-caprolactone)/poly(ethylene-vinyl acetate) blends for controlled release applications. J. Supercrit. Fluids **47**, 93-102 (2008).

Nelson, W.L., Fraunfelder, F.T., Sills, J.M., Arrowsmith, J.B., Kuritsky, J.N. Adverse respiratory and cardiovascular events attributed to timolol ophthalmic solution, 1978-1985. Am. J. Ophthalmol. **102**, 606-611 (1986).

Nichols, K.K., Nichols, J.J. The contact lens and tear film laboratory, the Ohio State University College of Optometry. Ocul. Surf. **5**, 259-261 (2007).

Nicolson, P.C.; Vogt, J. Soft contact lens polymers: an evolution. Biomaterials **22**, 3273-3283 (2001).

Novack, G.D. Ophthalmic drug delivery: Development and regulatory considerations. Clin. Pharmacol. Ther. **85**, 539-543 (2009).

O´Mahony, J., Molinelli, A., Nolan, K., Smyth, M.R., Mizaikoff, B. Towards the rational development of molecularly imprinted polymers: ^{1}H NMR studies on hydrophobicity and ion-pair interactions as driving forces for selectivity. Biosens. Bioelectron. **20**, 1884-1893 (2005).

O'Brien T. P., Grinberg, N., Bicker, G., Wyvratt, J., Snow, N.H. Evaluation of the origins of the selectivity of polymers imprinted with a HIV protease inhibitor using infrared spectroscopy and high performance liquid chromatography. Enantiomer **7**, 139-148 (2002).

Oliveira, A.D., D'Azevedo, P.A., Francisco, W. In vitro activity of fluoroquinolones against ocular bacterial isolates in Sao Paulo, Brazil. Cornea **26**, 194-198 (2007).

Olsen, J.A., Banner, D.W., Seiler, P., Obst-Sander, U., D'Arcy, A., Stihle, M., Müller, K., Diederich, F. A fluorine scan of thrombin inhibitors to map the fluorophilicity/fluorophobicity of an enzyme active site: evidence for C-F/C=O interactions. Angew. Chem. Int. Ed. **42**, 2507-2511 (2003).

Pagliaro, M., Ciriminna, R. New fluorinated functional materials. J. Mater. Chem. **15**, 4981-4991 (2005).

Pandit, J.C., Nagyova, B., Bron, A.J., Tiffanny, J.M. Physical properties of stimulated and unstimulated tears. Exp. Eye Res. **68**, 247-253 (1999).

Patrick, M., Mitra, A.K. Overview of ocular drug delivery and iatrogenic ocular cytopathologies. En: Ophthalmic Drug Delivery Systems; Mitra, A.K., ed. Marcel Dekker, New York, 1993. Pag. 1-27.

Paulini, R., Müller, K., Diederich, F. Orthogonal multipolar interactions in structural chemistry and biology. Angew. Chem. Int. Ed. **44**, 1788-1805 (2005).

Pella, D., Singh, R.B., Tomlinson, B., Kong, C.W. Coronany artery disease in developing and newly industrialized countries: A scientific statement of the international college of cardiology. En: Frontiers in Cardiovascular Health, vol. 9; Dhalla, N.S., Chockalingam, A., Berkowitz, H.I., Singal, P.K., eds. Kluwer Academic Publishers, Norwell MA, 2003. Pag. 473–487.

Perlovich, G.L., Kurkov, S.V., Bauer-Brandl, A. The difference between partitioning and distribution from a thermodynamic point of view: NSAIDs as an example. Eur. J. Pharm. Sci. **27**,150-157 (2006).

Peterson, R.C., Wolffsohn, J.S., Nick J., Winterton, L., Lally, J. Clinical performance of daily disposable soft contact lenses using sustained release technology. Contact Lens Ant. Eye **29**, 127-134 (2006).

Piletska, E.V., Piletsky, S.A., Karim, K., Terpetschnig, E., Turner, A. Biotin-specific synthetic receptors prepared using molecular imprinting. Anal. Chim. Acta **504**, 179-183 (2004).

Piletska, E.V., Romero-Guerra, M., Chianella, I., Karim, K., Turner, A.R., Piletsky, S.A. Towards the development of multisensor for drugs of abuse based on molecular imprinted polymers. Anal. Chim. Acta **542**, 111-117 (2005).

Piletsky, S.A., Day, R.M., Chen, B., Subrahmanyam, S., Piletska, Turner, A.P.F. Rational design of MIPs using computational approach. Patent PCT/GB01/00324, 2000.

Piletsky, S.A., Karim, K., Piletska, E.V., Day, C.J., Freebairn, K.W., Legge, C.H., Turner, A.P.F. Recognition of ephedrine enantiomers by molecularly imprinted polymers designed using a computational approach. Analyst **126**, 1826–1830 (2001).

Pinilla-Lozano, I., Larrosa-Poves, J.M., Perez-Olivan, S., Polo-Llorens, V., Izaguirre, L., Navascués, J. Quinolones intraocular penetration depending on therapeutic contact lens wear. Rev. Esp. Contact 1998a. *http://www.oftalmo.com/sec/98-tomo-2/03.htm* [consultado en Junio 2010].

Pinilla-Lozano, I., Polo-Llorens, V., Larrosa-Poves, J.M., Pérez-Oliván, S., Izaguirre, L., Gorricho, J. Medium water content contact lenses ciprofloxacino

saturation: differences between exposure times. Rev. Esp. Contact. 1998b. *http://www.oftalmo.com/sec/98-tomo-2/02.htm* [consultado en Junio 2010].

Pinto-Alphandary, H., Andremont, A., Couvreur, P. Targeted delivery of antibiotics using liposomes and nanoparticles: research and applications. Int. J. Pharm. **13**, 155-168 (2000).

Plazonnet, B., Rathbone, M.J., Hadgraft, J., Roberts, M.S. Ophthalmic drug delivery. En: Modified-release drug delivery technology; Rathbone, M.J., Hadgraft, J., Roberts, M.S., eds. Marcel Dekker, New York, 2003. Pag. 289-313.

Podos, S.M., Becker, Asseff, C.F., Hartstein, J. Pilocarpine therapy with soft contact lenses. Am. J. Ophthalmol. **73**, 336-341 (1972).

Por, Y.P., Mehta, J.S., Chua, J.L.L., Koh, T. Khor, W.B., Fong, A.C.Y., Lim, J.W.K., Heng, W.J., Loh, R.S.K., Lim, L., Tan, D.T.H., Acanthamoeba keratitis associated with contact lens wear in Singapore. Am. J. Ophthalmol. **148**, 7-12, (2009).

Ramström, O., Ansell, R.J. Molecular imprinting technology: challenges and prospects for the future. Chirality **10**, 195-209 (1998).

Reddy, I.K., Ganesan, M.G. Ocular therapeutics and drug delivery: an overview, En: Ocular Therapeutics and Drug Delivery; Reddy, I.K., ed. Technomic, Lancaster PA, 1996. Pag. 3-29.

Refojo, M.F., Leong, F.L. Poly(methylacrylate-co-hydroxyethylacrylate) hydrogel implant material of strength and softness, J. Biomed. Mater. Res. **15**, 497–509 (1981).

Refojo, M.F., Leong, F.L., Chan, I.M., Tolentino, F.I. Absorption and release of antibiotics by a hydrophilic implant for scleral buckling. Retina **3**, 45-49 (1983).

Refojo, M.F.,Yasuda, H. Hydrogels from 2-hydroxyethyl methacrylate and propylene glycol monoacrylate. J. Appl. Polym. Sci. **9**, 2425–2435 (1965).

Robinson, J.R. Ocular drug delivery mechanism of corneal drug transport and mucoadhesive delivery systems. STP Pharma. Sci. **5**, 839-846 (1989).

Romero-Guerra, M., Chianella, I., Piletska, E.V., Karim, K., Turner, A.P.F., Piletsky, S.A. Development of a piezoelectric sensor for the detection of methamphetamine. Analyst **134**,1565–1570 (2009).

Rootman, D.S., Willoughby, R.P.N., Bindlish, R., Avaria, M., Basu, P.K., Krajden, M. Continuous-flow contact lens delivery of gentamicin to rabbit cornea and aqueous-humor. J. Ocul. Pharmacol. **8**, 317-323 (1992).

Rosa dos Santos, J.F., Alvarez-Lorenzo, C., Silva, M., Balsa, L., Couceiro, R., Torres-Labandeira, J.J., Concheiro, A. Soft contact lenses functionalized with pendant cyclodextrins for controlled drug delivery. Biomaterials **30**, 1348-1355 (2009).

Rosa dos Santos, J.F., Couceiro, R., Concheiro, A., Torres-Labandeira, J.J., Alvarez-Lorenzo, C. Poly(hydroxyethyl methacrylate-co-methacrylated-β-

cyclodextrin) hydrogels: Synthesis, cytocompatibility, mechanical properties and drug loading/release properties. Acta Biomater. **4**, 745-755 (2008).

Ruben, M., Watkins, R. Pilocarpine dispensation for soft hydrophilic contact-lens. Br. J. Ophthalmol. **59**, 455-458 (1975).

Rubinstein, M.P. Evans, J.E. Therapeutic contact lenses and eyedrops: is there a problem?. Cont. Lens Anterior Eye **20**, 9-11 (1997).

Russell, D.W. Fifty years of advances in bile acid synthesis and metabolism. J. Lipid Res. **50**, S120–125 (2009).

Sahoo, S.K., Fahima Dilnawaz, F., Krishnakumar, S. Nanotechnology in ocular drug delivery. Drug Discov. Today **13**, 144-151 (2008).

Salz, J.J., Reader, A.L., Schwartz, L.J. Treatment of corneal abrasions with soft contact-lenses and topical diclofenac. J. Refract. Corneal Surg. **10**, 640-646 (1994).

Sander, B., Van Best, J., Johansen, S., Kessel, L., Moldow, B. Fluorescein transport through the blood- aqueous and blood-retinal barriers in diabetic macular edema. Curr. Eye Res. **27**, 247-252 (2003).

Sano, K., Tokoro, T., Imai, Y. A new drug delivery system utilizing piggyback contact lenses. Acta Opthalmol. **74**, 243-248 (1996).

Sato, T., Uchida, R., Tanigawa-Uno, K., Murakami, A. Application of polymer gels containing side-chain phosphate groups to drug-delivery soft contact lens. J. Appl. Polym. Sci. **98**, 731-735 (2005).

Schrader, S., Wedel, T., Moll, R., Geerling, G. Combination of serum eye drops with hydrogels bandage contact lenses in the treatment of persistent epithelial defects. Graefe's Arch. Clin. Exp. Ophthalmol. **244**, 1345-1349 (2006).

Schenker, H.I., Silver, L.H. Long-term intraocular pressure-lowering efficacy and safety of timolol maleate gel-forming solution 0.5% compared with Timoptic XE 0.5% in a 12-months study. Am. J. Ophthalmol. **130**, 145-150 (2000).

Schierholz, J.M., Beuth, J. Implant infections: a haven for opportunistic bacteria. J. Hospital Infection. **49**, 87–93 (2001).

Schwarz, S., Nick, J. Effectiveness of lubricating daily disposable lenses with different additives. Optician **231**, 22-26 (2006).

Seah, S.K.L., Husain, R., Gazzard, G., Lim, M.C.C., Hoh, S.T., Oen, F.T.S., Aung, T. Use of Surodex in phacotrabeculectomy surgery. Am. J. Ophthalmol. **139**, 927-928 (2005).

Sedlacek, J. Possibilities of application of eye drugs with the aid of gel-contact lenses. Cesk Oftalmol. **21**, 509-512 (1965).

Sellergren, B. The non-covalente approach to molecular imprinting. En: Molecularly Imprinted Polymers. Man Made Mimics of Antibodies and their

Applications in Analytical Chemistry; Sellergren, B., ed. Elsevier, Amsterdam, 2001. Pag. 113-184.

Sellergren, B., Hall, A. Fundamental aspects on the synthesis and characterisation of imprinted network polymers. En: Molecularly Imprinted Polymers. Man Made Mimics of Antibodies and their Applications in Analytical Chemistry; Sellergren, B., ed. Elsevier, Amsterdam, 2001. Pag. 21-57.

Shah, C., Raj., S., Foulks, G.N. The evolution in therapeutics contact lenses. Ophthalmol. Clin. North Am. **16**, 95-101 (2003).

Shen, J., Wang, Y., Ping, Q., Xiao, Y., Huang, X. Mucoadhesive effect of thiolated PEG stearate and its modified NLC for ocular drug delivery. J. Control. Release **137**, 217-223 (2009).

Sibrian-Vazquez, M., Spivak, D.A. Improving the strategy and performance of molecularly imprinted polymers using cross-linking functional monomers. J. Org. Chem. **68**, 9604-9611 (2003).

Silbert, J.A. A review of therapeutic agents and contact lens wear. J. Am. Optom. Assoc. **67**, 165-172 (1996).

Silbert, J.A. Therapeutic uses for silicone hydrogels. *http://www.siliconehydrogels.org/editorials/oct_05.asp* [Consultada en Junio 2010].

Singh, C.P., Shah D.O. Surface chemical aspects of ocular drug delivery systems. En: Ocular Therapeutics and Drug Delivery; Reddy, I.K., ed. Technomic, Lancaster PA, 1999. Pag. 31-49.

Sintzel, M.B., Bernatchez, S.F., Tabatabay, C., Gurny, R. Biomaterials in ophthalmic drug delivery. Eur. J. Pharm. Biopharm. **42**, 358-374 (1996).

Smith, J., Safdar, N., Knasinski, V., Simmons, W., Bhavnani, S.M., Ambrose, P.G., Andes, D. Voriconazole therapeutic drug monitoring. Antimicrob. Agents Ch. **50**, 1570-1572 (2006).

Sousa, H.C. de, Gil, M.H.M., Leite, E.O.B., Duarte, C.M.M., Duarte, A.R.C. Method for preparing sustained-release therapeutic ophthalmic articles using compressed fluids for impregnation of drugs. Patent. EP1611877A1, 2006.

Sprincl, L., Kopecek, J., Lim, D. Effect of the structure of poly(glycolmonomethacrylate) gel on the calcification of implants. Calcif. Tissue Res. **13**, 63-72 (1973).

Srivastava, S., Madras, G. Modak, J. Esterification of myristic acid in supercritical carbon dioxide. J. Supercrit. Fluids **27**, 55-64 (2003).

Srividya, B., Cardoza, R.M., Amin, P.D. Sustained ophthalmic delivery ofloxacin from a pH triggered in situ gelling system. J. Control. Release **73**, 205-211 (2001).

Stapleton, F., Keay L,. Katie, E., Naduvilath, T., Dart, J.K.G., Garry, B., Holden, B.A. The incidence of contact lens-related microbial keratitis in Australia, Ophthalmology **115**, 1655-62 (2008).

Steele, C.F. Fitting and management of therapeutic contact lenses. Hospital Optometrist Information series, 2000. *http://www.assoc-optometrists.org/uploaded_files/pdf/fm-tcl-info1.pdf* [Consultada en Junio 2010].

Subrahmanyam, S., Piletsky, S.A., Piletska, E.V., Chen, B., Karim, K., Turner, A.P.F. "Bite-and-Switch" approach using computationally designed molecularly imprinted polymers for sensing of creatinine. Biosens. Bioelectron. **16**, 631–637 (2001).

Sultana, Y., Jha, M.C., Ali, A., Aquil, M. A three-way comparative study on the efficacy of twin sol to gel systems and marketed eye drops of pefloxacin mesylate. J. Ocul. Pharmacol. Ther. **20**, 363-371 (2004).

Sustar, B., Bukovec, N., Bukovec, P. Polymorphism and stability of norfloxacin, 1-ethyl-6-fluoro-1,4-dihydro-4-oxo-7-(1-piperazinil)-3-quinolinocarboxylic acid. J. Therm. Anal. **40**, 475–481 (1993).

Szczotka-Flynn, L. Chemical properties of contact lens rewetters. Contact Lens Spectrum, 2006. *http://www.clspectrum.com/article.aspx?article=13005* [Consultada en Junio 2010].

Tian, X., Iwatsu, M., Kanai, A. Disposable 1-day Acuvue® contact lenses for the delivery of lomefloxacin to rabbits' eyes. CLAO J. **27**, 212-215 (2001a).

Tian, X., Iwatsu, M., Sado, K., Kanai, A. Studies on the uptake and release of fluoroquinolones by disposable contact lenses. CLAO J. **27**, 216-220 (2001b).

Tighe, B. Silicone hydrogel materials: how do they work? En: Silicone hydrogels: The Rebirth of Continuous Wear Contact Lenses; Sweeney, D.F., ed. Butterworth- Heinemann, Oxford, 2000. Pag. 1-27.

Tomlinson, A., Khanal, S. Assessment of tear film dynamics: Quantification approach. Ocul. Surf. **3**, 81-95 (2005).

Turner, A.P.F. Recognition of ephedrine enantiomers by molecularly imprinted polymers designed using a computational approach. Analyst **126**, 1826–1830 (2001).

Uchida, R., Sato, T., Tanigawa, H., Uno, K. Azulene incorporation and release by hydrogel containing methacrylamide propyltrimethylammonium chloride, and its application to soft contact lens. J. Control. Release. **92**, 259-264 (2003).

Umpleby, R.J., Baxter, S.C., Rampey, A.M., Rushton, G.T., Chen, Y., Shimizu, K.D. Characterization of the heterogeneous binding site affinity distributions in molecularly imprinted polymers. J. Chromatogr. B **804**, 141–149 (2004).

Vadnere, M., Amidon, G., Lindenhaum, S., Haslam, J.L. Thermodynamic studies on the gel sol transition of some Pluronic polyols. Int. J. Pharm. **22**, 207-218 (1984).

Vairon, J.P., Yean, L., Meslard, J.C., Bunel, C. Immobilisation reversible sur polymers et liberation controlee: application aun lentilles corneennes reservoirs de medicaments. Actual Chim. **Sep.-Oct.**, 330-335 (1992).

Van Beek, M., Jones, L., Sheardown, H. Hyaluronic acid containing hydrogels for the reduction of protein adsorption. Biomaterials **29**, 780-789 (2008a).

Van Beek, M., Weeks, A., Jones, L., Sheardown, H. Immobilized hyaluronic acid containing model silicone hydrogels reduce protein adsorption. Biomaterials **19**, 1425-1436 (2008b).

Van Nostrum, C.F. Molecular imprinting: a new tool for drug innovation. Drug Discov. Today **2**, 119-124 (2005).

Vandamme, T.F., Brobeck, L. Poly(amidoamine) dendrimers as ophthalmic vehicles for ocular delivery of pilocarpine nitrate and tropicamide. J. Control. Release **102**, 23-38 (2005).

Vandamme, Th.F. Microemulsions as ocular drug delivery systems: recent developments and future challenges, progress in retinal and eye research. Prog. Retin. Eye Res. **21**, 15-34 (2002).

Vandorselaer, T., Youssfi, H., Caspers-Valu, L.E., Dumont, P., Vauthier, L. Treatment of traumatic corneal abrasion with contact lens associated with topical nonsteroid anti-inflammatory drug (NSAID) and antibiotic: a safe, effective, and comfortable solution. J. Fr. Ophthalmol. **24**, 1025-1033 (2001).

Velpandian, T. Intraocular penetration of antimicrobial agents in ophthalmic infections and drug delivery strategies. Expert Opin. Drug Deliv. **6**, 255-270 (2009).

Venkatesh, S., Byrne, M.E., Peppas, N.A., Hilt, J.Z. Applications of biomimetic systems in drug delivery. Expert Opin. Drug Deliv. **2**, 1085-1096 (2005).

Venkatesh, S., Saha, J., Pass, S., Byrne, M.E. Transport and structural analysis of molecular imprinted hydrogels for controlled drug delivery. Eur. J. Pharm. Biopharm. **69**, 852-860 (2008).

Venkatesh, S., Stephen P., Sizemore, S.P., Byrne, M.E. Biomimetic hydrogels for enhanced loading and extended release of ocular therapeutics. Biomaterials **28**, 717-724 (2007).

Verestiuc, L., Nastasescu, O., Barbu, E., Sarvaiya, I., Green, K.L., Tsibouklis, J., Functionalized chitosa/NIPAM (HEMA) hybrid polymer networks as inserts for ocular drug delivery: Synthesis, in vitro assessment, and invivo evaluation; J. Biomed. Mater. Res. A **77**, 726-735 (2006).

Wajs, G., Meslard, J.C. Release of therapeutic agents from contact lenses. Crit. Rev. Ther. Drug **2**, 275-289 (1986).

Waltman, S.R., Kaufman, H.E. Use of hydrophilic contact lenses to increase ocular penetration of topical drugs. Invest. Ophthalmol. **9**, 250-255 (1970).

Warlen, M., Matoba, A., Robinson, N., Gay, C. Ocular delivery of tobramicina with a disposable soft contact lens. Invest. Ophthalmol. Vis. Sci. **33**, Abstract 938 (1992).

Weiner, A.L. Polymeric site-specific pharmacotheraphy. En: Polymeric drug delivery systems for the eye; Domb, A.J., ed. Wiley, Chichester, 1994. Pag. 315-346.

Weissermel, K., Arpe, H.J. Industrial Organic Chemistry, 3rd Ed., Wiley, New York, 1997.

Westesen, K., Bunjes, H., Koch, M.H.J. Physicochemical characterization of lipid nanoparticles and evaluation of their drug loading capacity and sustained release potential, J. Control. Release **48**, 223-236 (1997).

Weyenberg, W., Vermeire, A., Dhondt, M.M.M., Adriaens, E., Kestelyn, P., Remon, J.P., Ludwig, A. Ocular bioerosible minitablets as strategy for the management of microbial keratitis. Invest. Ophthalmol. Vis. Sci. **45**, 3229-3233 (2004).

Willoughby, C.E., Batterbury, M., Kaye, S.B. Collagen corneal shields. Surv. Ophth. Vis. Sci. **47**, 174-182 (2002).

Wilson C.G. Topical drug delivery in the eye. Exp. Eye Res. **78**, 737-743 (2004).

Winterton, L.C., Lally, J.M., Sentell, K.B., Chapoy, L.L. The elution of poly(vinyl alcohol) from a contact lens: the realization of a time release moisturizing agent/artificial tear. J. Biomed. Mater. Res. B **80**, 424-432 (2007).

Witcherle, O., Lim, D. Hydrophilic gels for biological use. Nature **185**, 117-118 (1960).

Wong, T., Ormonde, S., Gamble, G., McGhee, C.N. Severe infective keratitis leading to hospital admission in New Zealand. Br. J. Ophthalmol. **87**, 1103-1108 (2003).

Wulff, G. Molecular imprinting in cross-linked materials with the aid of molecular templates: a way towards artificial antibodies. Angew. Chem. Int. Ed. Engl. **34**, 1812-1832 (1995).

Wulff, G., Biffis, A. Molecularly imprinting with covalent or stoichiometric non-covalent interactions. In: Molecularly Imprinted Polymers. Man Made Mimics of Antibodies and their Applications in Analytical Chemistry; Sellergren, B., ed. Elsevier, Amsterdam, 2001. Pag. 71-111.

Xinming, L., Yingde, C., Lloyd, A.W., Mikhalovsky, S.V., Sandeman, S.R., Howel, C.A., Liewen, L. Polymeric hydrogels for novel contact lens-based ophthalmic drug delivery systems: A review. Contact Lens Anterior Eye **31**, 57-64 (2008).

Xu, J., Li, X., Sun, F. Cyclodextrin-containing hydrogels for contact lenses as a platform for drug incorporation and release. Acta Biomater. **6**, 486-493 (2010).

Yamauchi, A. Soft contact lenses. En: Gels Handbook, vol. 3; Osada, Y., Kajiwara, K., eds. Academic Press, San Diego CA, 2001. Pag. 166-179.

You-Xiong Wang, Y.X., Robertson, J.L., Spillman,W.B., Claus, R.O. Effects of the chemical structure and the surface properties of polymeric biomaterials on their biocompatibility. Pharm. Res. **21**, 1362-1373 (2004).

Zegans, M.E., Becker, H.I., Budzik, J., O´Toole, G. The role of bacterial biofilms in ocular infections. DNA Cell Biol. **21**, 415-420 (2002).

Zhu H., Chauhan, A. A mathematical model for ocular tear and solute balance. Curr. Eye Res. **30**, 841-854 (2005).

Zhu, X.X., Benrebouh, A., Zhang, Y.H., Gouin, S. New polymeric materials from derivatives of bile acids. Polym. Preprints **41**, 1030–1031 (2000).

Zignani, M., Tabatabay, C., Gurny, R. Topical semisolid drug-delivery:kinetics and tolerante of ophthalmic hydrogels. Adv. Drug Deliver. Rev. **16**, 51-60 (1995).

Zimmer, A., Kreuter, J. Microspheres and nanoparticles used in ocular delivery systems. Adv. Drug Deliv. Rev. **16**, 61-73 (1995).

Otras publicaciones relacionadas con el trabajo de la Tesis

7. OTRAS PUBLICACIONES RELACIONAS CON EL TRABAJO DE LA TESIS

7.1. Pluronic and Tetronic copolymers with polyglycolized oils as self emulsifying drug delivery systems

AAPS Pharm. Sci. Tech., 9 (2008), 471- 479.

AAPS PharmSciTech, Vol. 9, No. 2, June 2008 (© 2008)
DOI: 10.1208/s12249-008-9070-8

Research Article

Pluronic and Tetronic Copolymers with Polyglycolyzed Oils as Self-Emulsifying Drug Delivery Systems

Marta Fernandez-Tarrio,[1] Fernando Yañez,[1] Kristof Immesoete,[1] Carmen Alvarez-Lorenzo,[1] and Angel Concheiro[1,2]

Received 20 November 2007; accepted 15 February 2008; published online 14 March 2008

Abstract. The potential of poly(ethylene oxide)-poly(propylene oxide) block copolymers Pluronic® F127 (PF127) and Tetronic® 304 (T304), 904 (T904) and 1307 (T1307) as components of solid self-(micro) emulsifying dosage forms, S(M)EDDS, was evaluated. The dependence of the self-associative properties of Tetronics on pH explained the low ability of the micelles to solubilize griseofulvin at acid pH (sevenfold increase) compared to at alkaline pH (12-fold). Blends of polyglycolyzed glycerides (Labrasol, Labrafac CC, and Labrafil M 1944CS) with each copolymer at two different weight ratios (80:20 and 60:40) were prepared, diluted in water, and characterized in terms of globule size, appearance and griseofulvin solubility. The blends with Labrasol led to microemulsions that are able to increase drug solubility up to 30-fold. SMEDD hard gelatine capsules filled with griseofulvin and Labrasol or Labrasol/copolymer 80:20 showed a remarkable increase in drug solubility and dissolution rate, particularly when T904, T1307 or PF127 was present in the blend. This effect was more remarkable when the volume of the dissolution medium was 200 ml (compared to 900 ml), which can be related to a higher stability of the microemulsion when there is a greater concentration of the copolymer and glyceride in the medium.

KEY WORDS: hydrophobic drugs; poloxamer; poloxamine; polymeric micelles; SMEDDS.

INTRODUCTION

Over the last few years the development of solid self-(micro)emulsifying delivery systems, S(M)EDDS, for poorly-soluble drugs, based on mixtures of surfactants and oils, has been receiving an increasing attention (1–3). Polyoxyethylene sorbitan fatty acid esters (Tween®) or polyglycolyzed glycerides (e.g. Labrasol®) surfactants and modified or hydrolyzed vegetable oils have been shown to be particularly adequate for preparing S(M)EDDS (2,4). Under the temperature and waving conditions of the gastrointestinal tract, SMEDDS can give rise *in situ* to microemulsions with enhanced drug solubility and improved oral absorption (1,5). SMEDDS for oral delivery can be formulated as, among others, soft and hard gelatin capsules (6–8), tablets (9) and pellets (10–12). However, the list of oil/surfactant combinations that provide SMEDDS is still short and important attempts to widen the range of components suitable for this application are happening. Particularly, the use of conventional surfactants at relatively high concentrations is not exempt of adverse reactions and, thus, to find safe alternatives with enough emulsifying capacity is of great practical relevance (2).

Self-assembling amphiphilic copolymers with the ability to form nanoscopic core-shell micelles in aqueous medium have a recognized interest as drug solubilizers and stabilizers in liquid and semisolid drug dosage forms (13–17). Poloxamer (Pluronic®) and poloxamine (Tetronic®) block copolymers, constituted by poly(ethylene oxide) (PEO) and poly(propylene oxide) (PPO), easily spread in water and are commercially available in a wide range of HLB values (18,19). Differently from linear Pluronics, the X-shaped Tetronics, are formed by four PPO-PEO chains bonded to an ethylene diamine central group, which provides pH-responsive micellization properties (20,21). Despite the utility of Pluronics and Tetronics as stabilizers of oily phases (22–24), Pluronics and Tetronics have received minimal (25) or no attention as S(M) EDDS components.

The aim of this work was to explore the possibilities of using Pluronic® F127 (PF127) and Tetronic® 304 (T304), 904 (T904) and 1307 (T1307) as components of S(M)EDDS that also comprise glyceride derivatives. In this way, the evaluation of the effect of the copolymer architecture when the molecular weight and HLB are similar (T1307 and PF127), and of the effect of HLB and molecular weight when the architecture is the same (T304, T904 and T1307) becomes possible. Since the knowledge about Tetronic micellization is still limited (19,20,26,27), this was the issue to be tackled in first place. Secondly, the ability of the copolymers to solubilize griseofulvin [a Class II drug of the BCS (28)] in aqueous media covering a wide range of pH values was evaluated. Afterwards, aqueous dispersions of several mix-

[1] Departamento de Farmacia y Tecnología Farmacéutica, Facultad de Farmacia, Universidad de Santiago de Compostela, 15782, Santiago de Compostela, Spain.
[2] To whom correspondence should be addressed. (e-mail: ffancon@usc.es)

tures of each copolymer with Labrasol®, Labrafac® and Labrafil® were prepared and characterized regarding the size of the droplets and griseofulvin solubilization ability. Hard gelatin capsules were filled with the most efficient glyceride: copolymer mixtures and the ability of the formulations to promote griseofulvin dissolution was evaluated.

MATERIALS AND METHODS

Materials

Tetronic® 304 [$(OE_3OP_4)_2NCH_2CH_2N(OP_4OE_3)_2$], Tetronic® 904 [$(OE_{15}OP_{17})_2NCH_2CH_2N(OP_{17}OE_{15})_2$] and Tetronic® 1307 [$(OE_{72}OP_{23})_2NCH_2CH_2N(OP_{23}OE_{72})_2$] were from BASF, Germany; Pluronic® F127 [$P(EO_{99})$–$P(PO_{69})$–$P(EO_{99})$] and griseofulvin were from Sigma-Aldrich Chemie, Germany. Labrafil® M 1944 CS (mixture of oleic acid 62.65%, linoleic acid 26.7%, palmitic acid 4.74%, and mono- and di-fatty acid esters of PEG-6), Labrasol® [saturated polyglycolysed (PEG-8) caprylic/capric glycerides] and Labrafac® CC (caprylic acid 54.4%, capric acid 44.8%) were from Gattefossé España S.A. Purified water (resistivity> 18.2 MOhm·cm; MilliQ®, Millipore Spain) was obtained by reverse osmosis. All other reagents were of analytical grade.

Methods

Copolymer Dispersions

Potentiometric Titration of Tetronic. Titration of poloxamine copolymers was performed using a pH-meter Crison, model GLP22 (Barcelona, Spain), equipped with a sensor for viscous medium (Ag/AgCl). Hydrochloric acid (0.01 M, 25 ml) was added to 0.01 M Tetronic solutions (25 ml), which were then titrated with 0.01 M sodium hydroxide. The concentrations of the monoprotonated and the diprotonated forms were estimated from the expressions of the dissociation constants K_{a1} and K_{a2} as follows (20):

$$[TH^+] = \frac{[T][H^+]}{K_{a2}} \tag{1}$$

and

$$[TH_2^{2+}] = \frac{[T][H^+]^2}{K_{a2}K_{a1}} \tag{2}$$

The concentration of un-ionized poloxamine molecules is given by:

$$[T] = \frac{[T_{\text{total}}]}{1 + ([H^+]/K_{a2}) + \left([H^+]^2 \Big/ K_{a2}K_{a1}\right)} \left(\frac{V_{\text{initial}}}{V_{\text{initial}} + V_{\text{base}}}\right) \tag{3}$$

where V_{initial} is given by the volume of poloxamine solution and of HCl solution, and V_{base} is the volume of NaOH solution added.

Surface Tension Measurements. Adequate amounts of each copolymer were added to water up to a final concentration of 10^{-2} M and magnetic stirring was applied until complete dissolution. Sets of diluted solutions (10^{-2} to 10^{-7} M) were prepared and left to rest for at least 24 h. Then, the surface tension was measured, in triplicate at 25 °C, using the platinum ring method (Lauda tensiometer/densimeter TD1, Germany).

Dynamic Light Scattering (DLS). The DLS measurements were performed using an ALV-5000F optical system equipped with a CW diode-pump Nd:YAG solid-state laser (400 mW) operated at 532 nm (Coherent Inc., Santa Clara CA, USA). The intensity scale was calibrated against scattering from toluene. Ten percent copolymer solutions were filtered (Millipore® 0.45 μm, Ireland) into the quartz cell (previously washed with condensing acetone vapor) and maintained at 20 °C. The diffusion coefficient was deduced from the standard second-order cumulant analysis of the autocorrelation functions measured at 90° angle. The experiments were

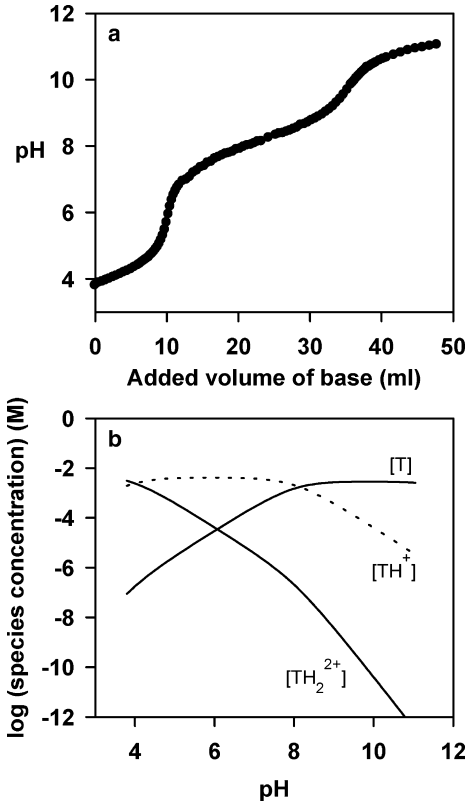

Fig. 1. Potentiometric titration curve obtained for T304 (**a**) and dependence of the concentrations of the non-protonated and protonated forms of T304 as a function of pH (**b**)

Table I. Structural Properties, CMC, and Parameters Used to Characterize the Ability of the Copolymers to Solubilize Griseofulvin

Copolymer	Molecular Weight	HLB[a]	pK_{a1}, pK_{a2}	CMC (mM)	χ	*P* Value	ΔG_s^0 (kJ/mol)
T304	1,650	12–18	4.30; 8.14	5.0	0.012	11.75	−13.26
T904	6,700	12–18	4.03; 7.81	0.3	0.050	3.90	−16.65
T1307	18,000	> 24	4.62; 7.80	0.1	0.045	3.67	−16.40
PF127	12,600	22	–	0.1	0.024	1.16	−14.85

[a] Data taken from the supplier data sheets (35)

carried out in triplicate and the apparent hydrodynamic radius ($r_{h,app}$) of the micelles was calculated from the apparent diffusion coefficients.

Oscillatory Rheometry. The influence of temperature on the storage or elastic (G') and the loss or viscous (G'') moduli of 10% copolymer solutions was recorded in triplicate at 1 rad/s from 20 °C to 60 °C, with a heating rate of 1.5 °C/min, in a Rheolyst AR-1000N rheometer (TA Instruments, UK) equipped with an AR2500 data analyzer, a Peltier plate and a cone geometry (6 cm diameter, 2.1°). An adequate solvent trap was used to prevent evaporation.

Copolymer/Glyceride Systems

Preparation. Glyceride/copolymer 60:40 and 80:20 *w/w* systems were prepared adding 6 g of glyceride and 4 g copolymer to 30.0 ml water, or 8 g of glyceride and 2 g copolymer to 15.0 ml water. Heating (60 °C) and magnetic stirring was applied to enable the complete dispersion of the components. Then, water was added to obtain dispersions with copolymer concentrations of 0.1, 0.5, 1, and 5 mM.

Size of the Droplets. The resultant systems were visually inspected and the size of the drops of internal phase was evaluated using an optical microscope Nikon Optiphot-pol (Japan) connected to an Olympus (Japan) video-camera with a magnification of ×40.

Griseofulvin Solubility Studies. Griseofulvin solubility was evaluated in the copolymer aqueous solutions, in the pure glycerides, and in the aqueous dispersions of glyceride/copolymer mixtures. Four milliliters of each medium were poured in glass ampoules containing 40 mg of griseofulvin. The ampoules were flame-sealed and then tumbled in a water bath for 7 days at 25 °C. The experiments were performed in duplicate. Samples were filtered (0.45 μm cellulose acetate membrane, Albet, Barcelona, Spain) and the concentration of griseofulvin dissolved was quantified at 294 nm (Agilent 8453, Böblingen, Germany), against a blank of copolymer solution of the corresponding concentration, using a calibration curve obtained with griseofulvin solutions in ethanol/water 50:50. The ability of the copolymers to solubilize griseofulvin was evaluated using three descriptors (29):

(a) the molar solubilization capacity, χ, i..e. the number of moles of drug that can be solubilized by one mol of micellar surfactant:

$$\chi = \frac{S_{tot} - S_w}{C_{copol} - CMC} \quad (4)$$

In this equation S_{tot} is the total drug solubility, S_w is the water drug solubility and C_{surf} is the molar concentration of surfactant in solution. Since above CMC the copolymer unimers concentration remains constant and equals to CMC, the surfactant concentration in the micellar form can be estimated as $C_{copol} - CMC$;

(b) the micelle-water partition coefficient, *P*, which is the ratio of drug concentration in the micelle to the drug

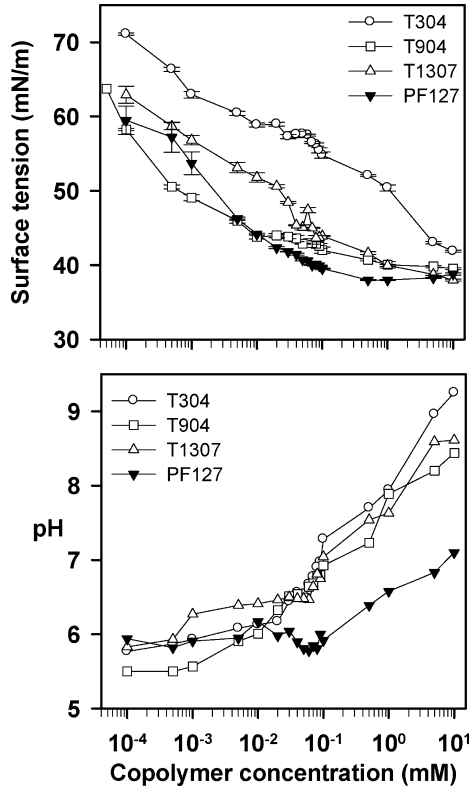

Fig. 2. Dependence of the surface tension and of the pH on the copolymers concentration in water at 25 °C

concentration in water for a particular copolymer concentration:

$$P = \frac{S_{tot} - S_w}{S_w} \quad (5)$$

(c) the standard free energy of solubilization that was estimated from the molar micelle–water partition coefficient, P_M (i.e. P for $C_{copolymer}$=1 M), as follows:

$$\Delta G_s^0 = -RT \ln \frac{\chi(1 - CMC)}{S_w} \quad (6)$$

SMEDDS Capsules

Griseofulvin (1.5 g) was dispersed in Labrasol or Labrasol:copolymer 80:20 mixtures (13.5 g) at 60 °C under stirring, and then 1 ml was injected (needle of 0.8 mm inner diameter) into the body of colorless hard capsules (number 00, Guinama, Valencia, Spain). The amount of griseofulvin in each capsule was 100 mg. Drug release rate was evaluated using a USP 24 type II (Turu Grau, Barcelona, Spain) apparatus at 75 rpm and 37 °C, in 900 ml of pH 7.4 phosphate buffer. At given time intervals, samples (5 ml) were taken and the withdrawn volume replaced by the same volume of fresh dissolution medium. The samples were filtered and, when needed, diluted using ethanol/water 50:50 solution. The concentration of the drug was determined spectrophotometrically (Agilent 8453, Böblingen, Germany) at 294 nm. Additional experiments were carried out in 200 ml of HCl 0.1 M, water or pH 7.4 phosphate buffer in a thermostated beaker (37 °C) under mild stirring (magnetic bar).

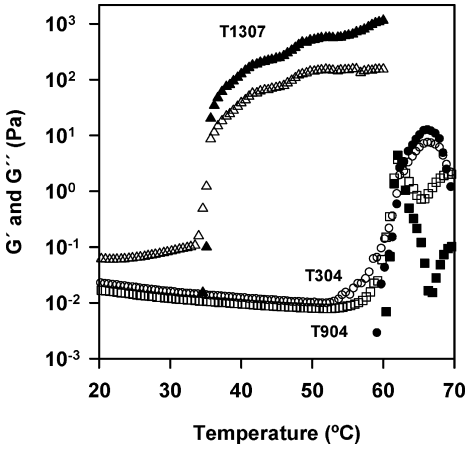

Fig. 3. Effect of temperature on the storage (G', *solid symbols*) and loss (G'', *open symbols*) moduli of 10% Tetronic solutions. Legend as in Fig. 2

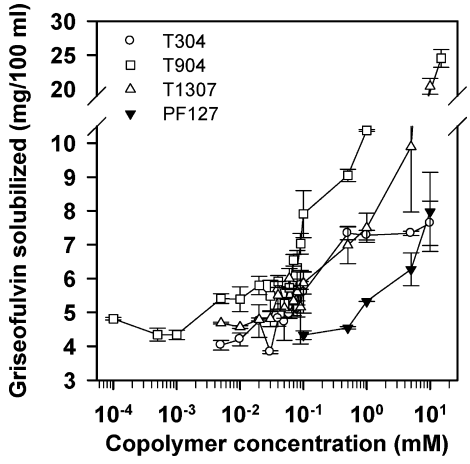

Fig. 4. Griseofulvin solubility in aqueous solutions of the copolymers evaluated

RESULTS AND DISCUSSION

Copolymer Dispersions

The deprotonation–micellization of T904 has been previously found to become more difficult as the pH decreases, shifting the CMC to greater values (21). Proton dissociation of the central ethylene diamine group of Tetronics is a previous condition for micellization; the balance

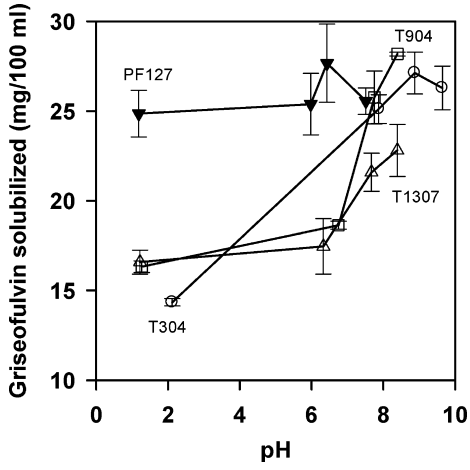

Fig. 5. Griseofulvin solubility in 10% *w/w* copolymer solutions prepared in media of different pH. The copolymer concentrations were 60.6 mM T304, 14.9 mM T904, 5.55 mM T1307, and 0.80 mM PF127. The solubility of griseofulvin was pH-independent (3 mg/100 ml). Legend as in Fig. 2

between the free energy of micellization and the free energy of protonization determining the possibility of micelle formation at pH below pK_a (20). Therefore, the pK_a of T304, T904, and T1307 should be known to be able to understand the self-aggregation and the surface-active properties of the copolymers. The titration profiles showed two inflection points that correspond to dissociation of the each proton of the ethylene diamine group (Fig. 1a). The pK_a values were similar for the three varieties (Table I) and close to the pK_a values previously reported for T701 and T803 (20). At 25 °C, the diprotonated form predominates at pH values below 4 and even up to pH 5.8 the concentration of the diprotonated form is greater than the concentration of the non-protonated form. The mono-protonated form holds the majority in the pH range between pK_{a1} and pK_{a2} (Fig. 1b).

The dependence of the surface tension on the copolymer concentration is shown in Fig. 2. The critical micellar concentration (CMC) of PF127 was 0.1 mM, which is in agreement with the values previously reported for this copolymer (13). The profiles of the Tetronics did not show a clear plateau and the CMC was estimated as the concentration at which a decrease in the slope occurred (Table I). T304 showed the lowest surface activity and the greatest CMC. Since hydrophobic interactions among PO groups are mainly responsible for the self-association in water, the differences in CMC may be explained by differences in the structure of the copolymers (Table I). T304 contains four chains of three EO groups and four PO groups each. T1037 and PF127 have a much greater content in EO and PO groups than T304. T904 occupies an intermediate place. In the case of Pluronics, the greater the content in PO groups, the lower the CMC was. Conversely, an increase in the lengths of the EO blocks elevates the probability of contacts of the PO units with the EO units within the core of the micelles, which decreases the hydrophobicity of the core and results in destabilization of the micelle (13). A similar trend is observed for Tetronics. The pH of the copolymer solutions increased as the concentration in Tetronic rises, which is related to the weak base behavior of the central diamine group (Fig. 2).

DLS analysis of 10% copolymer solutions showed unimodal distributions with a mean hydrodynamic radius of 10 nm for PF127, 4 nm for T904 and T1307, and 0.9 nm for T304. The results confirm that T304 has the weakest self-associative capability owing to the shortest hydrophobic blocks.

At room temperature, all the copolymer solutions at 10% showed a mainly viscous behavior with negligible storage moduli (G' below 10^{-5} Pa). An abrupt rise of G' occurred when the samples were heated; the gel temperature being 35.7 °C for T1307 and 62.4 °C for T304 and T904 (Fig. 3). In general, PPO-PEO block copolymers become less hydrophilic as the temperature rises owing to the progressive dehydration of the blocks. This promotes the formation of more micelles and, eventually, the packing into body centered cubic phase gels (26). The highest values of both moduli occur at the temperature at which the volume fraction of micelles is maximum. At greater temperatures, the dehydration of PPO chains, and even of PEO blocks, causes the polymer to phase separate, and G′ and G″ values to decrease. The differences in the gel temperature among the Tetronic varieties may be again explained by the longer of PPO and PEO segments of T1307 (Table I). Compared to T304 and T904, T1307 has a greater ability to bind water to its structure because T1307 has sufficient EO groups per block for adopting an helicoidal conformation in which interfacial (freezing bound) water may exist (27). Interfacial water is easily lost during the heating process. Additionally, the hydrophobic association requires a minimum number of PO units per block. For a given content in EO groups, the longer the PO block of Pluronics, the lower the gel temperature (30). The preceding reasons explain the low gel temperature of T1307 compared to T904 and T304.

Table II. Griseofulvin Solubility (mg/100 ml) in Clear Aqueous Dispersions of Glyceride/Copolymer Blends

Copolymer	Labrasol/Copolymer		Labrafil/Copolymer		Labrafac/Copolymer	
T304	80:20 *w/w*	60:40*w/w*	80:20*w/w*	60:40*w/w*	80:20*w/w*	60:40*w/w*
0.1 mM	19.58 (0.01)	4.40 (0.87)	2.67 (0.01)	22.26 (0.57)	5.31 (0.28)	6.54 (0.05)
0.5 mM	T	19.46 (0.81)	T	T	10.32 (0.06)	10.21 (0.13)
1 mM	T	19.89 (2.55)	T	T	12.21 (0.75)	21.56 (3.34)
5 mM	T	T	T	T	T	T
T904						
0.1 mM	3.25 (0.12)	3.35 (0.29)	3.14 (0.02)	4.69 (0.25)	7.37 (0.01)	26.44 (1.03)
0.5 mM	5.46 (0.07)	2.67 (0.02)	T	T	13.13 (0.18)	54.75 (6.72)
1 mM	14.25 (0.65)	9.07 (0.70)	T	T	T	T
5 mM	65.60 (5.36)	29.48 (1.24)	PS	PS	PS	PS
T1307						
0.1 mM	T	T	PS	T	T	T
0.5 mM	27.95 (0.49)	36.31 (0.05)	PS	PS	PS	PS
1 mM	34.13 (3.90)	17.55 (2.26)	PS	PS	PS	PS
5 mM	19.18 (3.26)	9.05 (0.20)	W	W	PS	PS
PF127						
0.1 mM	13.71 (0.35)	8.17 (0.03)	T	T	T	T
0.5 mM	24.15 (0.14)	7.97 (0.01)	T	T	T	T
1 mM	13.37 (0.60)	12.61 (0.01)	T	T	T	T
5 mM	T	62.42 (0.71)	T	T	T	PS

Copolymer concentration is indicated in the first column. Mean values and, between brackets, standard deviations
T Turbid, *W* white, *PS* phase separation

Solubilization of Griseofulvin in Copolymer Solutions

Griseofulvin is a representative Class II drug. Griseofulvin absorption from the gastrointestinal tract is variable and incomplete mainly because of the difficulty of achieving in vivo solubility enough to dissolve the commonly used doses (100–250 mg). The pH-independent solubility of griseofulvin makes the evaluation of the incidence of pH on the performance of the formulation as solubilizing system feasible. The solubility of griseofulvin significantly increased in copolymer solutions of concentration above CMC (Fig. 4). Compared to PF127, Tetronics showed an even greater solubilization capability between 0.1 and 10 mM, particularly in the case of T904. The molar solubilization capacity, χ, and the micelle–water partition coefficient, *P*, calculated for a 5 mM copolymer concentration (except for T304 which was 60.6 mM being well above CMC), and the standard free energy of solubilization, ΔG_s^0 , are shown in Table I. The values of this last parameter indicate that the process of incorporation of the drug to the micelles was, in all cases, spontaneous, and that T904 and T1307 have an even greater solubilization capacity of griseofulvin than PF127. To solubilize one mol of griseofulvin, 41 mol of T304, 20.8 mol of T904, 20.4 mol of T1307, or 50 mol of PF127 are required. The ratios obtained are similar or even better than the ratios previously found for other surfactants such as cholate (321 mol), deoxicholate (394 mol), sodium dodecylsulfate (16.7 mol), cetyl trimethyl ammonium bromide (18.2 mol), Tween 80 (62.5 mol), or Cremophor EL (39.2 mol) (31,32). The drug/copolymer molar ratios together with the relatively low CMC of T904, T1307 and PF127 suggest that the evaluated copolymers could act as efficient solubilizer agents, able to form micellar systems resistant to the dilution when entering into contact with biological fluids.

Figure 5 shows the effect of the pH on the solubility of griseofulvin in 10% copolymer solutions. As expected, no influence of pH was observed for PF127 systems since PF127 concentration is well above CMC and the slight effect of salts on the self-aggregation becomes negligible. By contrast, the solubilization performance of Tetronic-based systems was clearly lower at acidic pH than at neutral-alkaline pH. Protonization of the central diamine group makes micellization more difficult and, consequently, there are less micelles available for hosting the drug.

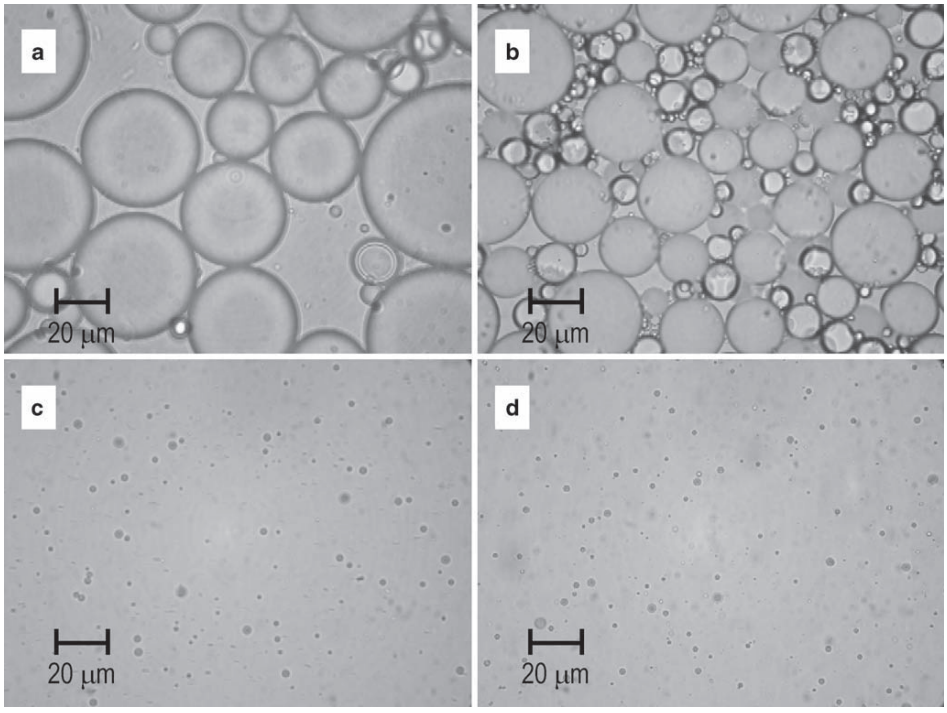

Fig. 6. Optical microscope view (×40) of **a** Labrafac/PF127 (1 mM) 80:20, **b** Labrafac/T1307 (0.5 mM) 80:20, **c** Labrasol:T1307 (1 mM) 60:40, **d** Labrasol:T904 (0.5 mM) 80:20 aqueous dispersions

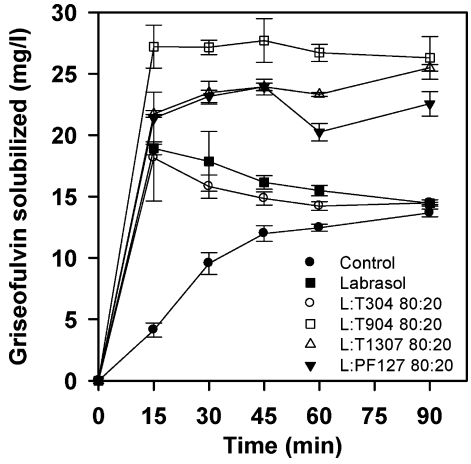

Fig. 7. Griseofulvin release rate in pH 7.4 phosphate buffer (900 ml) from capsules prepared with 100 mg drug and 900 mg excipient (i.e. Labrasol alone or mixed with T304, T904, T1307 or PF127 at a 80:20 weight ratio)

Glyceride/Copolymer Systems

Once the solubilization ability of the copolymers solutions was established, the next step was to evaluate the miscibility with various polyglycolyzed glycerides of different HLB which can act as oily phases or as co-surfactants in microemulsions formulations (33,34). The copolymers and the polyglycolized oils may form together colloidal structures like microemulsions particularly with glycerides of low HLB, such as Labrafil M 1944 CS (HLB 4) or Labrafac CC (HLB 1), or even mixed micelles with Labrasol (HLB 14). Before preparing the dispersions with both components, the solubility of griseofulvin in the pure glycerides (without adding water) was evaluated. Griseofulvin solubility ranged as follows: 248.6 (39.1) mg/100 ml of Labrasol, 85.2 (6.7) mg/100 ml of Labrafil, and 57.0 (5.2) mg/100 ml of Labrafac. Although the solubility was not directly tested in the pure copolymers due to the solid/paste consistency of most Tetronics and Pluronics, the results obtained with the copolymer solutions and the pure glycerides indicate that as a whole the solubility is largely promoted in media with components of intermediate HLB (12–18).

Glyceride/copolymer 80:20 or 60:40 *w/w* mixtures were dispersed in a volume of water adequate to achieve a copolymer concentration ranging between 0.1 and 5 mM (i.e. around or above CMC). The appearance of the systems is reported in Table II. T304 and T904 led to the most homogeneous systems with any glyceride. By contrast, T1307 and PF127, both of much higher HLB (22–24) were only miscible with Labrasol, which is the most hydrophilic glyceride evaluated. The systems that evidenced phase separation, or were off-white or turbid contained droplets of much greater size (20–60 μm) than the clear-translucent systems (<1 μm; Fig. 6). Griseofulvin solubility could only be evaluated in the few mixtures that really provide microemulsions (Table II). In some glyceride/copolymer aqueous dispersions the solubility of griseofulvin was markedly greater than in the copolymer alone solution, although in no case was the solubility observed in the pure glyceride attained.

SMEDD Capsules

To gain an insight into the repercussions of the observed increases in drug solubility on the dissolution rate from a solid dosage form, capsules were prepared containing 100 mg of drug and 900 mg of Labrasol alone or mixed with each copolymer at a 80:20 weight ratio. All mixtures had a viscosity low enough to make the filling of the capsules through the needle of a syringe possible after mixing with the drug and heating at 60 °C. Two different types of dissolution experiments were carried out: (1) the classical test using the type II USP apparatus with 900 ml of buffer phosphate; and (2) a dissolution experiment using 200 ml medium to mimic the solvent volume (a glass of water) that is used in the BCS to estimate if a given amount of drug would have solubility problems when orally administered (28). In the case of the S(M)EDDS, the volume of the medium would be particularly relevant since self-aggregation and formation/stability of microemulsions are greatly conditioned by the volume of the external phase. Although this aspect has not received any adequate attention in previous papers, a better performance of S(M)EDDS when the volume of water is relatively low (as observed in Table II) may be expected.

Figure 7 shows griseofulvin release profiles in 900 ml medium. The presence of glyceride/copolymer 80:20 clearly promotes both dissolution rate and total solubility, despite the

Table III. Griseofulvin Dissolved (mg/l) from Capsules Immersed in 200 ml of Medium (Controls with Griseofulvin Alone Gave 20±0.5 mg/l)

	HCl 0.1 M		Water		pH 7.4 Phosphate Buffer	
Excipient	15 min	45 min	15 min	45 min	15 min	45 min
Labrasol	27.3	20.8	38.2	33.4	22.8	20.1
Labrasol/T304, 80:20	35.9	19.8	53.0	55.6	22.7	18.0
Labrasol/T904, 80:20	43.5	18.5	85.1	79.1	40.4	34.1
Labrasol/T1307, 80:20	77.8	26.3	69.1	77.3	58.2	40.3
Labrasol/PF127, 80:20	77.0	76.9	56.2	69.6	70.2	61.6

Deviations below 5%

copolymer concentration (0.016 mM PF127, 0.121 mM T304, 0.030 mM T904, and 0.011 mM T1307) being well below CMC, even when the content of the capsule is totally dispersed in the release medium. The most efficient system was the mixture containing T904. Capsules prepared with T1307 or PF127 had a slightly slower release rate which could be related to the gelation process of the copolymer/glyceride mixture when enters into contact with the medium at 37 °C. The other glyceride/copolymer capsules showed the maximum amount dissolved between 15–30 min, and then a more or less marked decrease in dissolved griseofulvin was observed. This phenomenon can be explained as follows: once the content of the capsule is wetted, a relatively high local concentration in glyceride and copolymer promotes self-association and formation of a microemulsion; then a micro-enviroment propitious for dissolving griseofulvin is created. As the system progressively dilutes in the bulk of the dissolution medium, some colloidal structures would disintegrate, releasing griseofulvin to water and causing a partial precipitation of the drug initially dissolved. The more stable the colloidal nanostructure (systems containing T904, T1307 or PF127), the less the precipitation.

Table III summarizes the results of the dissolution experiments carried out in 200 ml medium. In general, greater drug solubility values are attained using this volume than 900 ml, which indicates that the volume of the medium is a critical variable when evaluating the performance of S(M) EDDS. The general criteria applied to drug dissolution from solid dosage forms, exclusively based on drug solubility (searching for sink conditions), should be revised when evaluating a S(M)EDDS.

A clear effect of both pH and time was also observed. The lower the pH was, the lower the solubilization capability of Tetronic-containing capsules and the greater the instability of the colloidal system. Samples were taken at 15 min after beginning the experiment and observed under light microscope. In the case of capsules containing T304 and T904 (with low molecular weight and short PPO blocks) no colloidal structures could be observed in HCl 0.1 M, which explains that the drug solubility was similar to the value obtained without excipients. By contrast, in water or in pH 7.4 buffer the enhancement in solubility promoted by the glyceride/copolymer mixtures became evident. This effect was more remarkable in water since the Tetronics can provide a relatively more alkaline microenvironment than the buffer (as shown in Fig. 2), reducing the protonization of the central diamine group and enhancing the stability of the colloidal system. Observation of the release medium under optical microscope evidenced the formation of droplets of similar size to the droplets pictured in Fig. 6c,d. The pH-sensitiveness of the self-associative properties of Tetronics may be an advantage for some drugs that are unstable at acidic pH or that may cause untoward reactions if a fast dissolution in the stomach occurs.

CONCLUSIONS

Tetronic micellar systems are more, or at least equally, efficient to dissolve griseofulvin in water or alkaline medium than the micelles of Pluronic F127 or several other conventional surfactants. If adequate proportions and dilutions are used, T304, T904, T1307 and PF127 mixed with polyglycolyzed glycerides form clear or translucent colloidal systems in aqueous medium. SMEDDS capsules containing blends of Tetronic or Pluronic with Labrasol notably enhance griseofulvin solubility and dissolution rate, particularly when the volume of medium is equivalent to a glass of water, which should be taken with a solid oral dosage form. The results obtained also highlight the relevance of the pH of the medium on the performance of Tetronic-based SMEDDS.

ACKNOWLEDGMENTS

This work was financed by the Ministerio de Educación y Ciencia (SAF2005–01930) FEDER, and Xunta de Galicia (PGI DIT05BTF203011PR; equipment grant PGIDT01PX1203014IF), Spain. F. Yañez thanks MEC for a FPI fellowship. The authors thanks BASF Corporation for providing samples of Tetronic® varieties and to Gattefossé España S.A. for providing samples of polyglycolized glycerides.

REFERENCES

1. C. W. Pouton. Formulation of poorly water-soluble drugs for oral administration: Physicochemical and physiological issues and the lipid formulation classification system. *Eur. J. Pharm Sci.* **29**:278–287 (2006).
2. R. N. Gursoy, and S. Benita. Self-emulsifying drug delivery systems (SMEDDS) for improved oral delivery of liphophilic drugs. *Biomed. Pharmacother.* **58**:173–182 (2004).
3. F. S. Nielsen, E. Gibault, H. Ljusberg-Wahren, L. Arleth, J. S. Pedersen, and A. Müllertz. Characterization of prototype self-nanoemulsifying formulations of lipophilic compounds. *J. Pharm. Sci.* **96**:876–892 (2007).
4. R. G. Strickley. Solubilizing excipients in oral and injectable formulations. *Pharm. Res.* **21**:201–230 (2004).
5. W. Wu, Y. Wang, and L. Que. Enhanced bioavailability of silymarin by self-microemulsifying drug delivery system. *Eur. J. Pharm. Biopharm.* **63**:288–294 (2006).
6. E. I. Taha, S. Al-Saidan, A. M. Samy, and M. A. Khan. Preparation and *in vitro* characterization of self-nanoemulsified drug delivery system (SNEDDS) of all-trans-retinol acetate. *Int. J. Pharm.* **285**:109–119 (2004).
7. J. Y. Hong, J. K. Kim, Y. K. Song, J. S. Park, and C. K. Kim. A new self-emulsifying formulation of itraconazole with improved dissolution and oral absorption. *J. Control Release*. **110**:332–338 (2006).
8. A. A. Date, and M. S. Nagarsenker. Design and evaluation of self-nanoemulsifying drug delivery systems (SNEDDS) for cefpodoxime proxetil. *Int. J. Pharm.* **329**:166–172 (2007).
9. S. Nazzal, and M. A. Khan. Controlled release of a self-emulsifying formulation from a tablet dosage form: Stability assessment and optimization of some processing parameters. *Int. J. Pharm.* **315**:110–121 (2006).
10. J. M. Newton, M. R. Pinto, and F. Podczeck. The preparation of pellets containing a surfactant or a mixture of mono- and di-glycerides by extrusion/spheronization. *Eur. J. Pharm. Sci.* **30**:333–342 (2007).
11. A. Abdalla, and K. Mäder. Preparation and characterization of a self-emulsifying pellet formulation. *Eur. J. Pharm. Biopharm.* **66**:220–226 (2007).
12. M. Serratoni, M. Newton, S. Booth, and A. Clarke. Controlled drug release from pellets containing water-insoluble drugs dissolved in a self-emulsifying system. *Eur. J. Pharm. Biopharm.* **65**:94–98 (2007).
13. A. V. Kabanov, E. V. Batrakova, and V. Y. Alakhov. Pluronic® block copolymers for overcoming drug resistance in cancer. *Adv. Drug Del. Rev.* **54**:759–779 (2002).

14. S. R. Croy, and G. S. Kwon. Polymeric micelles for drug delivery. *Curr. Pharm. Des.* **12**:4669–4684 (2006).
15. M. F. Francis, M. Christea, and F. M. Winnik. Polymeric micelles for oral drug delivery: Why and how. *Pure Appl. Chem.* **76**:1321–1335 (2004).
16. M. H. Dufresne, D. Le Garrec, V. Sant, J. C. Leroux, and M. Ranger. Preparation and characterization of water-soluble pH-sensitive nanocarriers for drug delivery. *Int. J. Pharm.* **277**:81–90 (2004).
17. V. P. Torchilin. Block copolymer micelles as a solution for drug delivery problems. *Expert Opin. Ther. Patents*. **15**:63–75 (2005).
18. G. Dumortier, J. L. Grossiord, F. Agnely, and J. C. Chaumeil. A review of poloxamer 407 pharmaceutical and pharmacological characteristics. *Pharm. Res.* **23**:2709–2728 (2006).
19. D. A. Chiappetta, and A. Sosnik. Poly(ethylene oxide)–poly (propylene oxide) block copolymer micelles as drug delivery agents: Improved hydrosolubility, stability and bioavailability of drugs. *Eur. J. Pharm. Biopharm.* **66**:303–317 (2007).
20. J. Dong, J. K. Armstrong, B. Z. Chowdhry, and S. A. Leharne. Themodynamic modelling of the effect of pH upon aggregation transitions in aqueous solutions of the poloxamine T701. *Thermochim. Acta*. **417**:201–206 (2004).
21. C. Alvarez-Lorenzo, J. Gonzalez-Lopez, M. Fernandez-Tarrio, I. Sandez-Macho, and A. Concheiro. Tetronic micellization, gelation and drug solubilization: Influence of pH and ionic strength. *Eur. J. Pharm. Biopharm.* **66**:244–252 (2007).
22. L. Olivieri, M. Seiller, L. Bromberg, M. Besnard, T. N. Duong, and J. L. Grossiord. Optimization of a thermally reversible W/O/W multiple emulsion for shear-induced drug release. *J. Control Release*. **88**:401–412 (2003).
23. C. R. E. Mansur, S. P. Barboza, G. Gonzales, and E. F. Lucas. Pluronic and tetronic polyols: study of their properties and performance in the destabilization of emulsions formed in the petroleum industry. *J. Colloid Interf. Sci.* **271**:232–240 (2004).
24. F. Tirnaksiz, and O. Kalsin. A topical w/o/w multiple emulsions prepared with Tetronic 908 as a hydrophilic surfactant: Formulation, characterization and release study. *J. Pharm. Pharmaceut. Sci.* **8**:299–315 (2005).
25. J. Y. Hong, J. K. Kim, Y. K. Song, J. S. Park, and C. K. Kim. A new self-emulsifying formulation of itraconazole with improved dissolution and oral absorption. *J. Control. Release*. **110**:332–338 (2006).
26. C. Perreur, J. P. Habas, J. Peyrelasse, J. François, and A. Lapp. Rheological and small-angle neutron scattering studies of aqueous solutions of branched PEO-PPO-PEO copolymers, Part 1. *Physical Rev. E.* **63**:031505 (2001).
27. M. Fernandez-Tarrio, C. Alvarez-Lorenzo, and A. Concheiro. Calorimetric approach to tetronic/water interactions. *J. Thermal. Anal. Calor.* **87**:171–178 (2007).
28. R. Takano, K. Sugano, A. Higashida, Y. Hayashi, M. Machida, Y. Aso, and S. Yamashita. Oral absorption of poorly water-soluble drugs: computer simulation of fraction absorbed in humans from a miniscale dissolution test. *Pharm. Res.* **23**:1144–1156 (2006).
29. C. O. Rangel-Yagui, A. Pessoa Jr., and L. C. T. Costa Tavares. Micellar solubilization of drugs. *J. Pharm. Pharmaceut. Sci.* **8**:147–163 (2005).
30. P. Alexandridis, J. F. Holzwarth, and T. A. Hatton. A correlation for the estimation of critical micellization concentrations and temperatures of polyols in aqueous-solutions. *J. Am. Oil Chem. Soc.* **72**:823–826 (1995).
31. A. Balakrishnari, B. D. Rege, G. Amidon, and J. E. Polli. Surfactant-mediated dissolution: contribution of solubility enhancement and relatively low micelle diffusivity. *J. Pharm. Sci.* **93**:2064–2075 (2004).
32. N. R. Calafato, and G. Pico. Griseofulvin and ketoconazole solubilization by bile salts studied using fluorescence spectroscopy. *Colloid. Surface B.* **47**:198–204 (2006).
33. M. Devani, M. Ashford, and D. Q. M. Craig. The emulsification and solubilization properties of polyglycolysed oils in self-emulsifying formulations. *J. Pharm. Pharmacol.* **56**:307–316 (2004).
34. Z. Hu, R. Tawa, T. Konishi, N. Shibata, and K. Takada. A novel emulsifier, Labrasol, enhances gastrointestinal absorption of gentamicin. *Life Sci.* **69**:2899–2910 (2001).
35. BASF, technical literature. Available at: http://www.basf.com/performancechemical/. Accessed October 22, 2007.

SUMMARY

Soft contact lenses (SCL) have gained interest in the last years as platforms for the sustained release of drugs and therapeutic macromolecules for the management of pathologies affecting the anterior segment of the eye. Nevertheless, the development of drug/SCL combination products demands improvements in the ability of the SCL to host drugs and to control the release. The present Thesis deals with the evaluation of the molecular imprinting technology, supported on analytical and computational tools, for the rational design of hydrogels with improved performance as delivery systems of drugs, hydrophilic polymers and other active substances. Applying this technology, medicated SCL were prepared by adding the active substance during the synthesis (imprinted networks) or by successive drug impregnation/extraction of preformed SCL using supercritical fluids (post-imprinted networks). Trap systems for the selective capture of bile salts have been also prepared. The results obtained clearly indicate that the functional monomer/active substance molar ratio in the reaction medium determines the structure of the imprinted cavities and their aptitude for regulating the release process. The micropore structure of the networks, which depends on the proportion of water in the polymerization medium, influences the surface roughness, the friction coefficient, the drug diffusion, and the interaction with bacteria.